SWELLING BEHAVIOUR OF UNSATURATED FINE GRAINED SOILS

BY

KEVIN O'CONNOR

A thesis submitted for the degree of
Doctor of Philosophy

Geotechnical Engineering Research Centre
City University
London

June 1994

TABLE OF CONTENTS

LIST OF TABLES

CHAPTER 2

CHAPTER 3

CHAPTER 4

CHAPTER 5

LIST OF FIGURES

CHAPTER 2

CHAPTER 3

CHAPTER 4

CHAPTER 5

CHAPTER 6

ACKNOWLEDGEMENTS

This research was inspired by Dr. Ian Symons who had a great interest in the problems related to earth retaining structures. I would hope this work matches his expectations and standards.

The project was funded by the Science and Engineering Research Council and the Transport Research Laboratory.

I am most grateful to my supervisor Dr. Neil Taylor for his suggestions and assistance throughout the project and during the preparation of the manuscript.

Thanks go to Professor John Atkinson and the whole of the *Geotechnical Engineering* Research Centre at City University who contributed in different ways to this work. I thank in particular Dr. Matthew Coop for his advice in the laboratory as well as for his friendship. Mr. Keith Osborne, Mr. Lloyd Martyka and Mr. Harvey Skinner gave me invaluable technical support and humour.

Useful contributions have been given by Dr. D. Carder and Mr. M. Ryley from Transport Research Laboratory who also provided the soils used in the experimental work.

I want to address special thanks to Teresa Cuccovillo whose encouragement and observations throughout the research have been so important for me.

A big thank goes to my family and friends who provided the fundamental emotional funding: Bride and John O'Connor, Maureen, Vish, Joseph, Andy, Simon and Amanda.

Finally I would like to thank Federico for having inspired my acknowledgements.

DECLARATION

I grant powers of discretion to the University Librarian to allow this thesis to be copied in whole or part without further reference to me. This permission covers only single copies for study purposes subject to normal conditions of acknowledgement.

ABSTRACT

The aim of this research was to investigate the swelling behaviour of unsaturated fine grained soils by means of various laboratory tests such as a 100 mm stress path triaxial cell and a computer controlled oedometer. Centrifuge modelling was used as a link between the laboratory tests performed and an existing prototype experimental wall.

Three types of soils with different plasticity have been tested simulating the boundary conditions that act on a soil element behind a stiff wall. Therefore the laboratory equipment was designed or modified to enable the measurement of the swelling pressure of the soil under conditions of lateral confinement.

The results show that the swelling behaviour of these soils is controlled by the testing conditions imposed on the soil as well as the initial state of the soil as described by dry density and water content. Suction measurements made using the filter paper method, showed that dry density and water content can be used instead of specific volume and suction when defining the state of an unsaturated soil.

The results from the centrifuge model tests, in which soil was compacted behind a stiff instrumented wall, showed that measurements of lateral stress change on the model wall were consistent with the swelling behaviour observed in the laboratory tests as well as in a previous full scale prototype test.

Analysis of the experimental data indicated a possible method of extending the current specification set in the United Kingdom (Manual of Contract Documents for Highway Works, 1991) for the use of fine grained soils as backfill material near to structures.

LIST OF SYMBOLS

A	Activity
D	Drainage path length
G_s	Specific gravity of soil
H	Relative humidity
K_a	Coefficient of active earth pressure
K_o	Coefficient of lateral earth pressure at rest
K_p	Coefficient of passive earth pressure
K_r	Coefficient of earth pressure at rest for unloading
LI	Liquidity index
LL	Liquid limit
M	Slope of critical state line
M_*	Aspect ratio of yield surface in q vs. p space
M_r	Molecular mass of water
N_s	Specific volume at reference state (suction dependent)
N_p	Number of passes of plant during compaction
PI	Plasticity index
PL	Plastic limit
R	Universal gas constant
R_s	Radius of curvature of meniscus
S_r	Saturation ratio
T	Absolute temperature
T_s	Surface tension of water meniscus
V_a	Air voids ratio
V_{water}	Volume of water
V_{voids}	Volume of voids
t	Time
e	Void ratio
g	Acceleration due to gravity
h_c	Capillary rise
k	Coefficient of permeability

m_v	Coefficient of volume compressibility
p	Mean total stress $\frac{1}{3}(\sigma_1+\sigma_2+\sigma_3)$
p'	Mean net stress (for unsaturated soil = p - u_a)
p'	Mean net stress (for saturated soil = p - u)
q	Deviator stress
r	Radius of capillary tube
u	Pore pressure (saturated soil)
u_a	Pore air pressure
u_w	Pore water pressure
(u_a-u_w), s	Matrix suction
v	Specific volume
v_w	Specific water volume
w	Water content
w_{fp}	Filter paper water content
Γ	Specific volume of saturated soil at critical state with p' = 1 kPa
Γ_{sw}	Specific volume of unsaturated soil at critical state with p' = 1 kPa related to Γ by saturation ratio
Ψ	Total suction
α	Contact angle of meniscus with side of tube
ρ	Bulk density
ρ_s	Density of soil particles
ρ_w	Density of water
ρ_d	Dry density
ρ_{dmax}	Maximum dry density
ρ_{dmin}	Minimum dry density
κ	Slope of unloading−reloading line in v:ln p' plane
λ	Slope of normal compression line in v:ln p' plane
σ'	Effective stress
σ	Total stress
σ_1, σ_2, σ_3	Principal stresses
σ_v	Vertical stress
σ_h	Horizontal stress
σ_{vm}	Maximum vertical stress

σ_{hm}	Maximum horizontal stress
ϕ	Angle of internal friction
ϕ'	Effective angle of internal friction
ϕ^b	Effective angle of internal friction with respect to suction
τ	Shear stress
ν	Poissons ratio
π	Osmotic suction
χ	Chi factor

1. INTRODUCTION

1.1 OBJECTIVES OF RESEARCH

The construction of earth retaining walls associated with large structures such as bridge abutments often require the use of substantial quantities of backfill. In these circumstances the cost of the completed retaining structures is a significant percentage of the final cost of the whole scheme. In the majority of construction projects where earthworks are involved it is common practice to reject fine grained and clayey soils as backfill material and replace them with coarser granular backfill. The higher strength and stiffness, the reduced potential to swell as well as the ease of compaction and the free drainage properties of granular soils are the main factors that make them preferable as backfill. However, the practice of using high quality granular fill is becoming more and more costly as the availability of such fill reduces and the costs of transport increase.

In the light of the increasing costs, engineering interest is being directed towards other materials. A costing study (Naish, 1988) indicated that substantial reductions in the cost of backfill could be made by utilising some of the fine grained soils at present classed as unsuitable. Despite the possible savings, there is understandable caution when using fine grained soils as fill adjacent to structures since case studies have shown the consequences resulting from the incorrect estimation of the soil behaviour. Mawditt (1989) for instance, reported a case study where a 9 m high bridge abutment showed signs of premature deterioration shortly after commissioning. In situ measurements showed that the abutment had moved outwards by approximately 100 mm and that high horizontal stresses had developed behind the wall. In this case London Clay taken from deep excavations (about 30 m) had been used to backfill the abutment. After investigations it was concluded that the high lateral pressures and related movement of the wall were due to the dissipation of the high suction present in the clay as water was absorbed after construction and the soil swelled.

When considering the use of fine grained soils as backfill one of the main concerns of the design engineer is the behaviour of the soil during both the construction and design life of the structure. Fine grained soils that have the potential to swell can produce significant volumetric changes resulting from inundation. If the structure confines the soil the resulting restriction of the volume changes will give rise to increases in the boundary stresses, this, if designed for may compromise the stability and serviceability of the structure. These considerations

have highlighted the need to investigate more thoroughly the swelling behaviour of fine grained soil behind retaining structures.

Standard design methods for retaining walls rely on soil mechanics theory in which the soil is assumed to be either fully saturated or dry. When compaction is involved, as in the case of backfill materials, the act of compaction on the soil creates an unsaturated soil mass consisting of three phases; soil particles, water and air. This alters significantly the mechanical behaviour of the soil both in the short and long term. Even if much research has been directed towards the study of the mechanics of unsaturated soil, only recently have consistent frameworks been proposed. This has left engineers using factors of safety that, as well as assuring the integrity of the structure, also compensate for the lack of full understanding of the response of the soil.

The development of swelling pressure on a retaining wall is related to the boundary conditions of the retained soil. The greater the confinement of soil the higher is the swelling pressure developed. The boundary conditions that were chosen for this project represents one of the worst conditions that could be imposed, that is the compaction of fill behind a stiff retaining wall which has a high degree of confinement.

A number of different areas of soil mechanics have been relevant for the purposes of the research, these are: the structure and mechanics of unsaturated soils, effects of compaction on soil behaviour and earth pressures related to compaction and subsequent swelling of fine grained soils. The objectives of the research were:

- To develop different laboratory techniques for the measurement of swelling pressure under different boundary conditions and to compare these techniques with full scale tests and centrifuge modelling.

- To investigate the dependence of the swelling pressure developed by compacted unsaturated soils on factors such as plasticity, dry density and water content of the soil.

- To examine the swelling pressure of the backfill behind a stiff retaining wall through centrifuge model tests which reproduce the conditions that a prototype wall may face.

- To examine wether the experimental results could support an extension to the current specification limits imposed for the compaction of fine grained clayey soils adjacent to structures.

The research also augmented the pilot scale studies on different fills compacted behind retaining walls undertaken by the Transport Research Laboratory (TRL).

The experiments have been conducted on three types of fine grained soils of which only one falls within the current specification: Brickearth (just inside the acceptable plasticity limits of the current specification), Wadhurst Clay (of intermediate plasticity, just outside the acceptability limits) and London Clay (a high plasticity soil). Choosing one soil within the specification provided a reference when comparing the swelling behaviour of the other two soils and interpreting the specification.

The apparatus used for the experiments were:

- A modified 100 mm triaxial stress path cell. This was a computer controlled apparatus which investigated swelling under boundary conditions of constant vertical stress and zero lateral strain.

- A modified oedometer. In this apparatus, the sample was restrained laterally by the confining ring and vertically by a stiff load cell which was used to measure the swelling pressure on water inundation.

- A computer controlled oedometer. This apparatus provided the same boundary conditions as for the triaxial stress path cell, but the (lateral) swelling pressure was not measured. The tests were relatively easy to perform and gave information on the swelling movements due to inundation.

- A conventional triaxial cell. The undrained shear strength of the compacted soils was measured to give some indication of their trafficability.

- A geotechnical centrifuge. Centrifuge tests were undertaken of fill compacted behind model retaining walls. This simulated to some extent the TRL pilot scale studies and provided a link between the laboratory tests and a practical application.

1.2 STRUCTURE OF THESIS

The first part of this thesis considers those topics of soil mechanics which are relevant to the study and form the background to the research project. In the second part the experimental work performed is described in depth with an emphasis on the procedures adopted in the sample preparation and test methods. The presentation of the results, analysis and discussion critically examine the data obtained from which the conclusions and implications are drawn.

The following is a brief preview of the topics considered in the various chapters:

Chapter 2 provides the background to the thesis. The topic of unsaturated soil is introduced and the aspects of behaviour relevant to the development of swelling pressure described. This is followed by a review of previous fundamental research undertaken into the study of the mechanical behaviour of unsaturated soils. The effect of soil compaction on the lateral earth pressure exerted on retaining walls is considered and the definition of swelling pressure is discussed. The final section of this chapter examines the specification currently existing for the compaction of clayey backfill (MCHW1, 1991) and the major factors influencing it.

Chapter 3 covers the experimental work performed in the laboratory both in terms of developments of laboratory apparatus and in terms of testing procedures. A significant section is dedicated to the performance of the instrumentation and data acquisition systems in order to establish the quality of the measurements taken during the experiments. Chapter 4 describes the basic principles governing centrifuge modelling and its application within the geotechnical engineering research outlined. The design of the instrumented model retaining wall used and the testing procedures are described.

Chapter 5 presents the results obtained from testing the three soil types in the different laboratory apparatus and the centrifuge. Chapter 6 contains the analysis and discussion of the results. The approach in this chapter was to examine the swelling pressure developed by the three different soils individually, relating the results to the various tests performed. The experimental data are analysed in terms of dry density, swelling pressure, water content (normalised with respect to the plastic limit, PL) and plasticity index (PI). The behaviour of the three different soil types are compared and the results are interpreted, where possible, within a framework for unsaturated soils through the use of suction measurements.

Chapter 7 presents the conclusions and implications of the analysis and proposes recommendations for the possible widening of the current specification (MCHW1, 1991) used for classifying materials suitable for backfilling adjacent to structures. Also some recommendations for improvements in experimentation are given.

2. BACKGROUND

2.1 INTRODUCTION

The research undertaken uses fine grained soils in an unsaturated compacted state and investigates the influence of soil properties, such as water content, dry density and plasticity, on the swelling pressure developed behind a stiff retaining wall as the soil becomes inundated with water. Several areas of geotechnical engineering are relevant to the mechanics of this problem and they can be grouped as follows:

- The structure of unsaturated soils, i.e. the differences between saturated and unsaturated soils and the additional factors that need to be considered when using a material that has three phases (soil, water and air).

- The mechanics of unsaturated soils, i.e. the development of a framework which describes the volumetric and shear behaviour of unsaturated soils.

- Earth pressures, i.e. the development and application of earth pressure calculations both in saturated and unsaturated soils.

- Compaction, i.e. the different aspects of soil compaction and their influence on the mechanical behaviour of the soil mass formed.

2.2 SATURATED AND UNSATURATED SOIL

Soil is an aggregate of mineral grains in which the void spaces are filled with fluid, usually water and/or air. The presence of dissolved impurities (such as dissolved salts) can alter the physio−chemical nature of the water and its interaction with the soil. A state of equilibrium between the water and air phases exists, this governs the amount of air that can be dissolved in the water. As well as being dependent on external factors such as ambient pressure this state of equilibrium is also affected by the soil particles whose small size and large surface area allow the formation of menisci which create suctions. Therefore the general mechanical properties of any particular sample of soil are dependent on the proportions of the soil, water

and air present as well as the soil itself.

The definitions of saturated and unsaturated soil commonly refer to the proportions of the solid liquid and gas in a mass of soil. Figure 2.1 shows how the percentages of the three phases in a soil changes as a sample that is saturated with air (dry) becomes a sample saturated with water. The soil that exists between these two extremes of saturation is known as unsaturated.

A useful parameter for describing the state of a soil related to its phases is known as the Saturation Ratio (S_r). This expresses the percentage of the volume of water in the soil sample to that occupied by the total voids.

$$S_r\ (\ \%\ ) = \frac{V_{water}}{V_{voids}} \times 100 \qquad 2.1$$

A soil consisting of only soil and air has a saturation ratio of 0 % whereas a soil consisting of only solids and water has a saturation ratio of 100 %. The category of unsaturated soils (0 % < S_r < 100 %) can be further divided depending on the proportions of the three phases present (Wroth and Houlsby, 1985). With the saturation ratio below approximately 80 % the gas phase in the soil is generally continuous throughout the soil and the water phase is discontinuous. At saturation ratios above approximately 90 % the gas becomes occluded forming bubbles in the now continuous water phase. Between these two states a transition zone exists where the air and water both exist in a continuous form. A convenient representation showing the variation of the three phases is a triangular diagram as in Figure 2.2. The three apexes of the triangle represent 100 % of the phase indicated and the opposite side of each apex represents the 0 % of the phase. The triangle shows all the theoretically possible combinations of the three phases soil, water and air. The shaded area represents those soils that are typically encountered in geotechnical engineering. This may be subdivided further into two categories saturated soils, where the saturation ratio is greater than 98 % and unsaturated soils which constitutes the remainder of the area.

2.3 THE COMPOSITION OF CLAY

Clay particles consist of platelets whose surfaces are negatively charged. To maintain chemical equilibrium cations in the soil water such as sodium (Na^+), calcium (Ca^{2+}) or magnesium (Mg^{2+}) are attracted to the surface of the platelets. The concentration of these cations is higher nearer the surface of the platelet than in the body of the pore fluid. Any diffusion of the cations is prevented by the electrostatic attraction of the clay surface. The surface of the platelet where the positively charged cations are held is called the diffuse double layer. The outer surface of the diffuse double layer has a positive charge and maintains an electrical equilibrium by attracting water molecules (which are electrostatically polarised). As more water molecules are attracted to the diffuse double layer, the clay platelets are forced further apart until a new state of equilibrium is reached with the ambient stress levels. This increased distance between the clay platelets is observed on a macroscopic scale as an increase in the volume occupied by the soil.

The same process is reversible so that if water leaves the pore fluid by, for example, evaporation an imbalance in the electrostatic equilibrium is created. Water molecules that were once attracted to the diffuse double layer become free and leave in the form of vapour. Reduction in the water molecules attracted to the diffuse double layer allows the platelets to move closer together resulting in a decrease in volume. The diffuse double layer then remains with a positive charge (due to the cations) until other water molecules (or anions) are attracted to it.

The various clay mineral types have different degrees of expansion which are dependent on the constituent atoms in the clay crystal lattice. The kaolinite group of minerals generally have low expansive properties, illites show some expansion characteristics and montmorillonites (smectites) are highly expansive. Figure 2.3 shows a comparative study of the expansive properties of montmorillonite and kaolinite (Grim, 1962). All of the samples were restrained laterally and allowed to expand vertically under a constant stress of 7 kPa (1 psi). It can be seen that different proportions of the mineral can affect the amount of volume change that the soil undergoes on inundation.

The pore water chemistry itself can also have a large effect on the magnitude of volume change and swelling behaviour of a soil. The type and concentration of the cations present in the soil water affects the adsorption of water and consequent swelling. For example the

presence of calcium or magnesium ions in the pore water produces less swelling of the soil than when sodium ions are present.

2.4 CLAY MINERALOGY RELATED TO ENGINEERING PROPERTIES

The engineering properties of soils are dependent upon the particle size, shape, surface area, stress history as well as the mineral composition. It is not possible to classify all soils or clays in such a way that their mechanical behaviour can be predicted solely on the basis of the clay mineral composition. However a knowledge of the clay minerals and their effects will become more important as soils with higher clay contents are used more widely in engineering.

2.4.1 Index Tests

The index tests as proposed by Atterberg were adapted for use in soil mechanics by Casagrande (1947) and are still used as a convenient way of expressing the properties of soils containing clay minerals. The tests provide a determination of the water content of the soil at arbitrary but established boundaries. These boundaries describe the change in the condition of clayey soil as its water content varies. The water content at which the soil changes from being a slurry (with a negligible strength) to a material which has some resistance to deformation is called the liquid limit. As the water content continues to reduce the stiffness of the soil increases until a point is reached where the soil no longer behaves as a plastic material but begins to behave in a brittle manner, this point is defined as the plastic limit (Head, 1984) The definitions and methods used for the determination of the index properties are fully defined in the current specification (B.S. 1377 part 4).

The plastic limit (PL) is defined as the minimum water content at which the soil can be deformed plastically by rolling into a 3 mm thick thread. The definition of the liquid limit (LL) used in the United Kingdom is the water content of the soil at which a standard 80 g 30° cone will penetrate the sample of soil for a displacement of 20 mm when dropped under its own weight. Plasticity index (PI) is the difference between the liquid limit (LL) and plastic limit (PL) and is the range of moisture contents over which the soil remains in a plastic state.

$$PI = LL - PL \qquad 2.2$$

The liquidity index (LI) of a soil is defined as the ratio of the water content (w) minus the plastic limit (PL) all divided by the plastic index (PI). The expression for liquidity index is:

$$LI = \frac{w - PL}{PI} \qquad 2.3$$

It is a way of expressing the natural water content of a soil or clay in relation to its plastic and liquid limit.

The plasticity characteristics of a soil are related to the amount of clay sized particles present. A relevant parameter that reflects the amount of clay minerals present in the soil is known as Activity (A) (Skempton, 1953). In general, a soil with a high activity number has a relatively high water holding capacity and a low permeability; the converse is true for a soil with a low activity.

$$\text{Activity (A)} = \frac{\text{Plasticity Index}}{\%\text{ by weight of clay} < 2\mu m} \qquad 2.4$$

It is possible to interpret empirically the Atterberg limits in terms of the interaction of the water molecules with the clay particles. At low moisture contents water molecules are adsorbed to the surface of the clay particles and held in a tight, well orientated pattern. Insufficient water is available and the molecules are not sufficiently free to lubricate the soil particles. As the water content of the soil increases the layers of water adsorbed to the diffuse double layer increase. The outermost layers are less attracted and are able to move more freely and lubricate the movement of the clay particles under the application of a small load. In this case the plastic limit can be interpreted as the water content at which the surface of the particles can adsorb just slightly more water than can be held in a rigid condition. In a similar way the addition of further water to obtain the liquid limit can be interpreted as the water content at which the clay particles are still able to retain a sufficiently strong attraction to the water molecules. This prevents the soil from losing rigidity and becoming dispersed within the water.

Although the liquid and plastic limit values are based on empirical tests they may be related to more fundamental properties such as shear strength (Skempton and Northey, 1953), angle of friction (Mitchell, 1976) and compressibility (Wroth and Wood, 1978). For example, Figure 2.4 shows the relationship between liquidity index and shear strength for several

remoulded clays (Skempton and Northey, 1953). As the water content of the soil moves from the Plastic Limit to the Liquid Limit the strength and stiffness of the soil decreases.

2.5 SUCTION

Soil suction has been defined in a number of ways. Early definitions by Schofield (1935) and Aitchison (1961) regarded soil suction as a "pressure deficiency" in the pore water of a soil, expressing either "qualitatively or quantitatively the actual potential adsorption or imbibition of water by soil". At an International Conference (Pore Pressure and Suction in Soils, 1961) organised to discuss pore pressure and suction in soils there was disagreement regarding the definitions that should be used to describe suction in soils. In the formal discussions Aitchison and Bishop (1961) suggested that suction could be considered as the difference between the pore air pressure (u_a) and the pore water pressure (u_w), that is ($u_a - u_w$). Their definition of suction considered that the soil was an inert medium that did not interact with the pore fluid and that the suctions developed were due only to capillary effects. As discussed in Section 2.3 the physio–chemical behaviour of clays are affected by the chemistry of the pore water. The presence of dissolved ions in the pore water give rise to what is called osmotic suctions. In reality it is the two components, matrix and osmotic suction that contribute to the total suction of a soil. The work in this thesis has been performed using distilled water so any possible contribution by the osmotic suction is constant. Therefore any reference to suction will refer to the matrix suction.

2.5.1 Matrix suction

Matrix suction results from the capillary effect in the voids between the soil particles. In a soil the distance between the particles (i.e. pore size) determines the height above the water table to which the soil will remain saturated. This can be explained by examining the capillary rise in a glass tube. If a glass tube is placed in a container of water the surface tension of the water causes a capillary rise as shown in Figure 2.5. If the surface tension of the water meniscus (T_s) acts at an angle α to the side of the tube then, by resolving the forces in a vertical direction the resultant force due to the surface tension of the meniscus ($2\pi r\ T_s \cos \alpha$) is able to support a column of water with a height h_c .

$$\text{surface tension} = \text{column weight}$$

$$2 \pi r T_s \cos \alpha = \pi r^2 h_c \rho_w g \qquad 2.5$$

$$\Longrightarrow \qquad T_s = \frac{R_s h_c \rho_w g}{2}$$

where

T_s	is the surface tension of the water
α	is the angle of contact between water and tube
r	is the radius of the capillary tube
h_c	is the capillary rise
g	is the acceleration due to gravity
R_s	is the radius of curvature of meniscus ($r/\cos\alpha$)

The smaller the radius of the tube the higher the capillary rise. To maintain equilibrium with the free surface of water which is at atmospheric pressure the column of water in the tube is under a negative water pressure. At the top of the column the water pressure $u_w = -\rho_w g h_c$ is equal to the atmospheric pressure, u_a. This then relates the matrix suction $(u_a - u_w)$ to the capillary rise, i.e.

$$(u_a - u_w) = - \rho_w g h_c \qquad 2.6$$

Then by substituting equation 2.5 into equation 2.6 the matrix suction $(u_a - u_w)$ can be expressed as a function of the radius of curvature of the meniscus and the surface tension of the water.

$$(u_a - u_w) = \frac{2T_s}{R_s} \qquad 2.7$$

The radius of curvature of the meniscus (R_s) is related to the radius of the tube and can be used to represent the pore radius in a soil. The smaller the pore radius in the soil the greater the matrix suction of the soil and analogous capillary rise. Figure 2.6 depicts a profile through a soil stratum in which the water table shows where the water is at atmospheric pressure. The greater the distance from the water table the smaller the radius of the meniscus, the higher the matrix suction.

2.5.2 Osmotic suction

The difference in the concentration of water molecules between the diffuse double layer in a clay mineral (Section 2.3) and the surrounding pore fluid produces an osmotic pressure. Any deficit in the equilibrium of this system results in an osmotic suction (π).

2.5.3 Total suction

It is accepted that matrix suction is a fundamental component of the mechanical behaviour of unsaturated soils (Alonso, Gens and Hight, 1987). It is known that the chemical composition of the soil water has a direct effect on the interaction of the dissolved ions and clay minerals. The effects on the mechanical properties of soil due to ion concentration in the soil water has been observed both in saturated soils and unsaturated soils (Edil and Motan, 1984). Therefore the inclusion of osmotic suction in the formation of total suction equation allows for situations when the solute types and concentration are different. A general equation for suction may be written as:

$$\Psi = (u_a - u_w) + \pi \qquad 2.8$$

where

Ψ	is the total suction
$(u_a - u_w)$	is the matrix suction
π	is the osmotic suction

2.5.4 The Measurement of suction

Several methods exist for the measurement of suctions in soil. This section briefly outlines some of the methods used for the measurement of total and matrix and osmotic suctions.

Psychrometer – The total suction of a soil can be found by measuring the relative humidity

in the voids inside or near to the soil. The relationship between the relative humidity and the total soil suction was given by Richards (1965).

$$\Psi = \frac{R\,T}{g\,M_r} \log_e H \qquad 2.9$$

Where

Ψ	is the total suction (kPa).
R	is the universal gas constant (8.31432 J mol^{-1} K^{-1}).
T	is the absolute temperature (K).
M_r	is the molecular mass of water (18.06 kg $kmol^{-1}$).
H	is the relative humidity.

When in equilibrium at constant temperature only the relative humidity remains unknown in the above equation, so by measuring the relative humidity it is possible to obtain a value for the value of total suction. The method proposed by Richards (1965) used a device known as a Psychrometer that was able to measure the relative humidity of the soil. A Psychrometer works by the heating and cooling of a thermocouple which is made from two different metals. If one end of the thermocouple junction is cooled relative to the other side an emf is produced and a voltage may be measured (Seebeck effect). The opposite will occur when a current is passed through the thermocouple, i.e. one side of the metal junction will cool relative to the other (Peltier effect). These two physical effects are analogous to the temperature difference between a wet and dry bulb thermometers used for measuring relative humidity. By passing a current through the thermocouple the temperature of one of the junctions drops and vapour from the atmosphere condenses on the junction. When the current is turned off the condensed water begins to evaporate and produces an emf. After the maximum rate of cooling has been passed the emf output drops and the temperature equilibrium between the thermocouple and its surroundings is re-established. The calibration of the psychrometers is performed by measuring the output voltage from the device when suspended above a salt solution (such as NaCl or KCl) that at different concentrations and temperatures has a known osmotic suction (Campbell and Gardner, 1971). In the sealed calibration chamber the total suction will be equivalent to the osmotic suction. The range of total suction measurement that is possible is from 0 to approximately 7000 kPa in calibration (Brown and Cartos, 1982) where as in actual soil measurements the suctions have been recorded up to 4000 kPa for compacted silty sand (Daniel, Hamilton and Olsen, 1981).

Tensiometer – The matrix suction of a soil may be measured by a tensiometer, this consists of a sealed tube that is made from a high air entry porous stone. The inside of the sealed tube is filled deaired water and connected to a pressure meter. When the tube is placed in contact with the soil the suction exerted draws the water through the porous stone creating a negative pressure in the water. At equilibrium the water in the tensiometer will have the same suction as soil. The range over which the tensiometer works is dependent on the cavitation pressure of the water within the device, this can be taken as a suction approximately 90 kPa at atmospheric pressure.

Thermal conductivity sensors – By measuring the thermal conductivity of a porous block it is possible to obtain an indirect measure of the matrix suction. This sensor consists of two elements, a heating resistor (which generates the heat field) and a temperature sensing element (whose output is temperature dependent). Both elements are encased in one porous ceramic medium. The thermal conductivity of the porous block is dependent on the amount of water present, the higher the water content the greater the thermal conductivity and the lower the temperature of the sensing element. That is the change in temperature is inversely proportional to the water content of the block. The amount of water present within the block is itself dependent on the matrix suction applied to the block by the soil. Calibration of the sensor is performed by subjecting the sensor to different suctions (e.g. by using the pressure plate apparatus) and measuring the thermal conductivity. The ranges of suctions that have been measured during calibrations were in the range of 0 to 200 kPa (Lee and Fredlund, 1984).

Axis Translation – Axis translation is a laboratory technique that enables the measurement of matrix suctions. The method of increasing (translating) the axes of reference for the pore water pressure from atmospheric to a higher pressure overcomes the problems of cavitation in the pore water. Hilf (1956) showed that the matrix suction in a soil was unaffected by increasing the surrounding air pressure. This method has been used to measure and control matrix suction in unsaturated soils. For example Sivakumar (1993) used the axis translation technique to increase the pore air pressure and total stress in triaxial tests performed on compacted Kaolin. This method prevented the water in the testing system from cavitating whilst still enabling the measurement of the matrix suction (by subtracting the pore water pressure from the pore air pressure).

Filter paper method – This indirect method of suction measurement was originally used in

agricultural science as a simple method for measuring soil suction (Gardner, 1937). More recent studies have applied this technique in geotechnical engineering. As described by Chandler and Gutierrez (1986) pieces of filter paper are placed in contact with the soil and sealed in a container. Over a period of between five and seven days the moisture in the filter paper and soil will come into equilibrium. By carefully weighing the pieces of filter paper and calculating their moisture contents it is possible to correlate the moisture content of the filter paper with a equivalent matrix suction. If the filter papers are not allowed to contact the soil during the equilibration then the suction value calculated is equivalent to the total suction of the soil. One of the standard filter papers used for this test is Whatman's No. 42, a high quality ash less filter paper which has a consistent calibration curve. As for the psychrometer the calibration of the filter paper can be performed using standard salt solutions which have known suctions. Other techniques are used such as pressure plates (a method using axis translation techniques) or oedometer tests (where samples of clay were over consolidated to known effective stresses) from which the suction of the soil could be related to the filter paper water content. The calibrations performed by a number of authors (Chandler and Gutierrez, 1986; Chandler, Crilly and Montgomery−Smith (1992)) have shown there to be two calibration curves which depend on the moisture content of the filter paper. The calibration curves for Whatman's No. 42 paper are shown in Figure 2.7, the relationship between the water content of the filter paper and the suction is as follows,

$$\log_{10} \text{suction} = \begin{cases} 4.84 - 0.0622\, w_{fp} & 15\ \% \le w_{fp} \le 47\ \% \\ 6.05 - 2.48 \log w_{fp} & 47\ \% < w_{fp} \end{cases} \qquad 2.10$$

where w_{fp} is the water content of the filter paper (%)

A reason for the difference in the calibration curves was proposed by Miller and M^{c}Queen, (1978) who associated the lower moisture content of the filter paper with the capillary forces exerted by the water within the filter paper, whereas at higher moisture contents the water was considered to be held in an adsorbed water film in the paper.

2.6 DEFINITION OF SWELLING

The swelling of compacted clay fills involves two processes which occur simultaneously. Micro−scale swelling involves the hydration of clay mineral platelets, and macro−scale

swelling which is concerned with the relief of high suctions in the capillaries during wetting. Both can cause volume change and associated changes in effective stress.

The term swelling pressure has been used by many researchers in many different ways, and the definition is often dependent in some way on the test method. Brackley (1975) stated that swelling pressure could be defined as the pressure required to hold the soil at constant volume when water was added. He gave three different methods for determining the swelling pressure. Each method satisfied his definition of swelling pressure but each produced considerably different values.

The three methods are the consolidation test, the equilibrium of void ratios and the constant volume test. Each method will be briefly described:

Method 1: consolidation test – The specimen with a known initial thickness and dry density is placed in a consolidometer and allowed under a seating pressure to swell on the addition of water until equilibrium is reached. Subsequently incremental loads are added and the specimen is allowed to consolidate. The percentage volume change is plotted against the log of the pressure on the specimen. The point at which the curve intersects the zero volume change line is the swelling pressure. This test results in an upper bound for the swelling pressure.

Method 2: equilibrium of void ratios – Four to five samples with identical thickness, initial moisture content and dry density are placed in oedometers under the same seating pressure. The loads on the different specimens are increased to different values and allowed to equilibrate. Water is then added to the samples which are allowed to swell or compress until equilibrium is again established. These equilibrium positions are used to obtain (by interpolation) the load under which the sample does not undergo volume change on saturation. Brackley (1975) suggested that this method followed the probable stress path that the soil may undergo in the field where after construction the clay may not be exposed to water for several months and after wetting a long time may elapse before equilibrium is reached. This test gives a lower bound to the swelling pressure.

Method 3: constant volume method – After placing in the consolidometer and adding water, the swelling of the specimen was controlled by the addition or subtraction of loads so that there was neither swelling or compression whilst maintaining a constant volume. The manual

control of this test proved difficult; the loading path was such that there was always some swelling and small variations in volume could not be avoided. At near equilibrium the addition of a small weight made the sample compress and cross the zero volume change line. This intersection represents the swelling pressure and gave a median value compared to the other two methods.

Figure 2.8 shows the results from tests performed on Black Cotton soil (PL = 60 %, LL = 98 %) by Sridharan et al. (1986) using the 3 methods discussed by Brackley (1975). The three methods produced very different results. Method 1 was allowed to swell fully prior to consolidation and provided an upper bound for the swelling pressure of the soil. Method 2 had the merit of following the probable stress path that the soil may undergo in the field, as discussed above. The method produced the lowest value of swelling pressure but three separate samples were required. The last method (Method 3) produced an intermediate swelling pressure value by maintaining a small volume change during the inundation.

Using method 2, the equilibrium of void ratios, Ryley (1988) investigated the swelling pressure developed by two clays of different plasticity. One of the clays used in these tests (London Clay) was also used in a pilot scale retaining wall facility (Symons, Clayton and Darley, 1989). A comparison of the swelling pressures was made and it was shown that the pressures developed in the wall were higher that those seen in the oedometer tests. Ryley (1988) concluded that such laboratory tests are more suited for comparing different materials rather than giving absolute predictions of the pressures likely to be developed behind a rigid structure.

Johnson (1989) observed that the magnitude of the swelling pressure depended on the degree of confinement of the soil with the greater degree of confinement leading to increased swell pressure. Table 2.1 shows the various definitions of swelling pressure in decreasing order of confinement. This observation would suggest that the difference between the swelling pressures measured in the pilot scale retaining wall facility (Symons, Clayton and Darley, 1989) and the laboratory tests (Ryley 1988) could be explained by the differences in the boundary conditions of the soil. The lower swelling pressures reported by Ryley (1988) would suggest that factors such as a lower degree of confinement as well as frictional effects between the soil and the apparatus could account for the reduction in the measured swelling pressure.

2.7 EFFECTIVE STRESS IN UNSATURATED SOILS

Terzaghi's principle of effective stress (Terzaghi, 1936) states that any change of stress, such as compression, distortion and strength only occur when there are changes in the effective stress. The fundamental equation states that the effective stress (σ') is the difference between the total stress (σ) and the pore water pressure (u), i.e.;

$$\sigma' = \sigma - u \qquad 2.11$$

It has been excepted that this equation can be used in the calculation of stresses in dry or fully saturated soils. For unsaturated soils where there are the three phases of soil, water and air, Terzaghi's equation no longer produced accurate results. This led to a development by Bishop (1959) where the effective stress equation was modified. In unsaturated soil the pore pressure has two components, pore water pressure (u_w) and pore air pressure (u_a). The relationship was formulated as follows;

$$\sigma' = \sigma - u_a + \chi(u_a - u_w) \qquad 2.12$$

The additional parameter χ, was dependent upon the soil type and its saturation. For saturated soils the value of χ was unity and for dry soils χ was zero.

The validity of this form of the effective stress equation was investigated further by a number of researchers. Bishop, Alpan, Blight and Donald (1960) tested pairs of identical samples in saturated and unsaturated conditions and concluded that χ could be estimated from shear tests by assuming that c' and ϕ' in Equation 2.13 were independent of the degree of saturation, from this some values of were obtained.

$$\tau = c' + \sigma' \tan\phi' \qquad 2.13$$

The following year Bishop and Donald (1961) published the results from triaxial shear tests on a silt. In these tests, the cell pressure (σ_r), pore water pressure (u_w) and pore air (u_a) pressure could be measured and controlled independently. This allowed σ_r, u_a and u_w to be controlled so that any of the variables ($\sigma_r - u_a$), ($\sigma_r - u_w$) and ($u_a - u_w$) could be kept constant during shearing. By showing that the stress–strain curves were not affected when the variables were kept constant Bishop and Donald concluded that the form of the equation proposed by Bishop in 1959 (Equation 2.12) was correct.

Jennings and Burland, (1962) questioned the assumptions made by Bishop's equation. They argued that when the degree of saturation fell below a critical value Equation 2.12 did not provide a relationship between volume change and effective stress. This critical degree of saturation depended on the grain size characteristics of the soil i.e. for coarse granular soils the critical degree of saturation was around 20 %, whereas for a clayey soil the critical degree of saturation was near 85 %.

Coleman (1962) suggested that in order to reduce the total stresses to effective stresses it was important to use the pore air pressure as a base from which the axial stress, radial stress and pore water pressure could be measured. The axial stress would become $(\sigma_a - u_a)$, the radial stress would become $(\sigma_r - u_a)$, and the pore water pressure would become $(u_w - u_a)$. This idea of separating the effects of the stress state variables was acknowledged by Bishop and Blight (1963) who published evidence that re-evaluated the effective stress equation (Equation 2.12). They proposed a modified stress state equation comprising two components $(\sigma - u_a)$ and $(u_a - u_w)$ as;

$$\sigma' = \sigma - u_a + f\,(u_a - u_w) \qquad 2.14$$

By plotting the data in terms of e, $(\sigma - u_a)$ and $(u_a - u_w)$ it was possible to represent the volumetric changes of the soil. An example of such a plot is shown in Figure 2.9. These results were re-analysed by Burland (1964) who was able to demonstrate that a single effective stress concept was invalid for volume change behaviour.

Matyas and Radhakrishna (1968) performed tests on a soil containing a mixture of kaolin and flint. Two series of consolidation tests were performed under conditions of either isotropic or K_o conditions with different values of suction. Relationships between void ratio (e), mean net stress $(p - u_a)$ and suction $(u_a - u_w)$ showed that depending on the value of the mean net stress, the soil when wetted would either swell or collapse. Also by plotting the degree of saturation (S_r) against the mean net stress $(p - u_a)$ and suction $(u_a - u_w)$ a surface was produced which demonstrated that as the suction was reduced to zero the saturation ratio approached 100 %. Figure 2.10 shows the proposed state surfaces in e, $(p - u_a)$ and $(u_a - u_w)$ space and S_r, $(p - u_a)$ and $(u_a - u_w)$. Matyas and Radhakrishna (1968) noted that the hysteresis observed in the wetting and drying as well as loading and unloading paths could not be explained in terms of any one single equation without a reference to the state of the soil.

The difficulty in the acceptance of these relationships lay in the idea that the description of the state of stress in a soil should only be related to considerations of force equilibrium without involving any soil parameters. Equation 2.12 proposed by Bishop (1959) needed to incorporate a soil parameter so that a single effective stress variable could be formed. Later experimental evidence would show that there was more than one independent stress state variable

Fredlund and Morgenstern (1977) proposed the use of two independent stress state variables. Considering the soil as a multi−phase continuum in which the soil was considered as a chemically inert solid they performed a theoretical analysis and produced three possible combinations of the stress state variables that could be used to describe the state of stress in a unsaturated soil. The possible combinations were: $(\sigma - u_a)$ and $(u_a - u_w)$ or, $(\sigma - u_w)$ and $(u_a - u_w)$ or, $(\sigma - u_a)$ and $(\sigma - u_w)$. Using these combinations of stress state variables Fredlund, Morgenstern and Widger (1978) suggested the following relationship for the shear strength of an unsaturated soil using the stress state variables $(\sigma - u_a)$ and $(u_a - u_w)$:

$$\tau = c' + (\sigma - u_a) \tan \phi' + (u_a - u_w) \tan \phi^b \qquad 2.15$$

where

τ	is the shear strength.
c'	is the cohesion with respect to the effective stress.
ϕ'	is the angle of friction with respect to the effective stress.
ϕ^b	is the angle of friction with respect to the suction.

By plotting the data with the axes of shear strength (τ), suction $(u_a - u_w)$, and net stress $(\sigma - u_a)$ it was possible to form a failure envelope in three dimensions (Figure 2.11). Experimental work by Escario and Saez (1986) showed that there was a non−linearity in the shear strength at failure with respect to the suction i.e. the value of ϕ^b was not a constant. This is evident in Figure 2.12 where the results from direct shear tests on an unsaturated clay show the linearity of ϕ with mean normal stress and the non−linearity of ϕ^b with suction.

The inability to link volume changes to stress changes prevented the development of a coherent framework from which a constitutive model could be developed. However since 1990 a number of frameworks have been proposed and are still the focus of research.

Toll (1990) performed a series of experiments on a compacted gravel and proposed a framework that would explain the shear behaviour in terms of total stresses and suctions. The samples were sheared under conditions of constant water content. The model was based on two stress state variables: suction ($u_a - u_w$) and net stress ($\sigma - u_a$) which in terms of the stress invariants q and p become mean normal stress ($p - u_a$). The degree of saturation (S_r) was included as a parameter to represent the soil state.

$$q = M_a (p - u_a) + M_w (u_a - u_w) \qquad 2.16$$

$$v = \Gamma_{aw} - \lambda_a \ln (p - u_a) - \lambda_w \ln (u_a - u_w) \qquad 2.17$$

The parameters M_a (total stress ratio) and M_w (suction ratio) were variants of the saturated critical state parameter M (= q/p') which depended on the degree of saturation of the soil (S_r) as shown in Figure 2.13. Toll (1990) described the way in which M_a and M_w approached a single value M_s (saturated stress ratio) at a high degree of saturation. Likewise λ_a and λ_w were variants of the slope of the critical state line (λ) for saturated soils and also depended on S_r in a similar way. The relationship between M_a, M_w, λ_a, λ_w and S_r was derived by a regression technique. The intercept Γ_{aw} was related directly to Γ, the intercept of the critical state line at p' = 1 kPa, by S_r. The complete framework could be represented in terms of the stress state variables q, ($p - u_a$), ($u_a - u_w$) and the volumetric variables v and S_r, Figure 2.14 shows the critical state surfaces for the gravel.

Wheeler (1990) re-analysed the data from the tests performed by Toll (1990) and suggested an alternative form for the critical state relationship. Wheeler agreed that the framework provided a way of explaining the behaviour of unsaturated soil. However he argued that when using the five state variables (q, $p - u_a$, $u_a - u_w$, v and S_r) it would be difficult to determine the values of q and v at the critical state because it would not be possible to predict the value of the saturation ratio during the test. This would mean that the values of M_a, M_w, λ_a, λ_w and Γ_{aw} would not be known. The alternative framework proposed by Wheeler determined the

shear and volumetric behaviour without using the saturation ratio as a variable. The form of the proposed relationships were;

$$q = M (p - u_a) + f (u_a - u_w) \qquad 2.18$$

$$v_w = \Gamma - \lambda \ln (p - u_a) + f (u_a - u_w) \qquad 2.19$$

By using a cubic function of the suction ($u_a - u_w$) the predictions of critical state values for the deviator stress were found to be more accurate than the equation proposed by Toll (1990) in Equation 2.16. For volumetric behaviour, Wheeler (1990) defined the specific water volume (v_w) which was directly related to the water content (w) and specific gravity (G_s) by:

$$v_w = w G_s + 1 \qquad 2.20$$

The difficulty that Wheeler (1990) noted was that Equations 2.16 and 2.17 were unable to give information on the specific volume (v) of the soil at the critical state and therefore the volume change of the soil during shearing could not be predicted.

A constitutive mathematical model was proposed by Alonso, Gens and Josa (1990) which represented the behaviour of partially saturated soils. The model was able to account for stiffness changes and reproduce the irreversible behaviour of the soil during both swelling and collapse as a result of changes in suction. The variables involved in the framework were mean net stress $p' = (p - u_a)$, deviator stress (q), suction ($u_a - u_w$) and specific volume (v). The specific volume had a linear relationship with the mean net stress. The formulation of the model was based on isotropic stress states. On loading and unloading the soil behaves elastically according to:

$$dv = - \kappa \frac{dp}{p} \qquad 2.21$$

where κ is an elastic stiffness parameter for changes in mean net stress (This was assumed to be a constant to ensure that the elastic part of the model was conservative).

and volumetric changes being given by:

$$v = N_{(s)} - \lambda_{(s)} \ln \frac{p}{p^c} \qquad 2.22$$

where

p is the mean net stress $= \frac{1}{3}(\sigma_1 + \sigma_2 + \sigma_3) - u_a$

p^c is a reference state where the specific volume, $v = N_{(s)}$.

$\lambda_{(s)}$ is a stiffness parameter for changes in the mean net stress for virgin states of the soil (dependent on suction).

Figure 2.15 shows one of the prominent features of the model, the loading collapse (LC) yield curve. Plotted in suction vs. p' space the loading collapse yield curve separates the elastic regions of the soil behaviour from the plastic regions. This figure shows the increase in p' with constant suction. Elastic behaviour is observed until the stress path reaches the yield curve. Thereafter irrecoverable plastic straining occurs and the yield surface moves out. If the suction is increased (at a constant p') another yield surface can be reached (the suction increase yield (SI) curve) where irrecoverable plastic strains also occur. This is shown in Figure 2.16.

The model is also able to show volumetric changes as the suction is decreased. Figure 2.17 shows two samples of soil (A and B) both with the same initial suction but under different mean effective net stresses (p'_1 and p'_2 respectively). As the suction in sample A is reduced elastic swelling occurs until zero suction is approached at A'. For sample B, elastic swelling occurs until the yield surface is reached at B'. After reaching this yield surface irrecoverable plastic compression occurs. This change in suction also relates to the volumetric changes of the sample. As sample A undergoes a reduction in suction at constant p'_1 the volume of the sample increases whereas for sample B the same reduction in the suction under a higher mean effective net stress p'_2 initially increases in volume until the yield surface is reached (B') and then reduces in volume as the soil compresses.

For non−isotropic stress states the yield conditions could be viewed in q, p', s space. For a given suction the yield surface could be described by an ellipse exhibiting isotropic

hardening. Under saturated conditions the model conformed with modified Cam–Clay. The equation for the ellipse in the planes of constant suction is given by:

$$q^2 - M^2 (p' + p_s')(p_o' - p') = 0 \qquad 2.23$$

where

p_s' is the value of p' at q = 0.

p_o' is the isotropic pre–consolidation stress.

M is the slope of the critical state line.

Figure 2.18 shows the three dimensional view of the yield surfaces in q,p and s space. Examining sections of constant suction as in Figure 2.19 it is easier to identify the yield surfaces.

Wheeler and Sivakumar (1992) and Sivakumar (1993) used experimental data obtained using a controlled suction triaxial stress path cell on samples of compacted kaolin to support their framework for unsaturated soil. The framework considered five state variables: mean net stress $p' = \frac{1}{3}(\sigma_1 + 2\sigma_3) - u_a$, deviator stress, $q = (\sigma_1 - \sigma_3)$, suction $s = (u_a - u_w)$, specific volume (v) and water content (w). Using axis translation techniques (Hilf, 1956) to keep pore water pressures above atmospheric pressure, samples were consolidated to the same effective net stress and then sheared in three different ways while keeping the suction and radial stress constant. The three types of shearing tests were:

fully drained	–	q increases as u_a and u_w were held constant.
constant v	–	u_a and u_w increased by equal amounts to keep v constant.
constant p'	–	u_a and u_w increased by equal amounts to keep p' constant.

Figure 2.20 shows the paths followed by the samples moving from the normal consolidation line to the critical state lines. Tests were performed at two different values of suctions from which Wheeler and Sivakumar (1992) identified critical state lines for each suction value. The work proved to be generally consistent with that of Alonso et al. (1990) although, as Figure 2.21 shows, at the higher value of suction tested the critical state line in terms of v and p' (p' plotted on a logarithmic scale) was found to be concave upwards rather than convex as in the model of Alonso et al. (1990). The idea of including water content as a state variable was not conclusively proved and a plot of the water content against mean net stress (Figure 2.22) showed no significant trend due to the scatter of the data.

In 1993 new evidence reported by Wheeler and Sivakumar (1993) demonstrated that water content was not a state variable. A new development to the framework proposed the existence of a section of state boundary surface that linked a normal compression "hyper−line" to a critical state "hyper−line". Hyper−lines in this case were used to describe equations that were capable of representing states of a soil that could exist in a four dimensional mathematical space. The implications of this were that it would be possible to represent isotropic normal compression and critical state each by two equations that related the four state variables. The equations took the form:

Normal consolidation Hyperline	Critical state Hyperline	
$q = 0$	$q = M_{(s)}\, p + \mu_{(s)}$	2.24
$v = N_{(s)} - \lambda_{(s)} \ln\left(\frac{p}{p_{at}}\right)$	$v = \Gamma_{(s)} - \psi_{(s)} \ln\left(\frac{p}{p_{at}}\right)$	

where $M_{(s)}, \mu_{(s)}$, $\Gamma_{(s)}$, $\psi_{(s)}$, $N_{(s)}$ and $\lambda_{(s)}$ were all functions of suction derived from the experimental data.

Within the proposed state boundary hyper−surface the soil behaviour was assumed to be elastic. As in the model from Alonso et al. (1990) the elastic swelling index (κ) was assumed to be independent of suction. Figure 2.23 shows an elliptical yield surface for a constant suction. The yield curve in the q−p plane forms the top surface of an elastic wall which corresponds to the intersection (in the v−p plane) of a swelling line moving from the normal compression hyper−line to the critical state hyper line.

The equation of the ellipse is given by:

$$q^2 = M_*^2 \, (p_o - p)(p + p_o - 2\, p_x) \qquad 2.25$$

where

p	is the mean net stress = $\frac{1}{3}(\sigma_1 + \sigma_2 + \sigma_3) - u_a$
p_o and p_x	are found from the intersections of the swelling line with the isotropic normal compression and the critical state lines
M_*	is the aspect ratio of the ellipse

Since the ellipse passing between points A and B does not arrive at the origin of the q p plane

the intersection point aspect ratio (M_*) is used. It is a function of suction and size of the yield curve.

$$M_* = \left(\frac{M_{(s)}\, p_x + \mu_{(s)}}{p_o - p_x} \right) \qquad 2.26$$

With this formulation of the framework, Wheeler and Sivakumar (1993) used the values of the experimentally determined parameters that were dependent on suction ($\lambda_{(s)}$, $N_{(s)}$, $\mu_{(s)}$, $\psi_{(s)}$, and $\Gamma_{(s)}$) to make predictions of the expected stress paths to be followed. Figure 2.24 shows the close agreement obtained in q−v and v−p space between the predicted and actual test data. In q−p space the correspondence between the paths is not very close though the start and end points are in agreement.

2.8 EFFECTS OF FABRIC IN COMPACTED SOILS

Lambe (1958) put forward a theory that the fabric of a compacted clay changed with moisture content. When soil was compacted at a water content dry of the optimum the clay particles would form a "flocculated" fabric (without orientation of the particles), whereas if the clay was compacted wetter than the optimum moisture content a "dispersed" fabric (particles having an orientation) would result. The idea, illustrated in Figure 2.25, formed the basis of a thorough investigation into the fabric and strength characteristics of compacted clays performed by Seed and Chan (1959). A simplified model proposed by Brackley (1975) considered unsaturated clay soils existing as packets of soil particles, with each packet being completely saturated and the inter−packet voids being filled with air (Figure 2.26). This meant that the soil mass was unsaturated whereas the individual soil packets were saturated. By assuming that the packets were saturated, Brackley (1975) developed the idea that the total volume change of the soil mass would be due to the summation of the effects of swelling or compression of the packets and their shear behaviour.

From observations of electron micrographs of natural soils M^{c}Gown and Collins (1975) proposed a classification system for identifying the different types of collapsible and expansive soils. They observed that soil microfabric could be classified using three basic forms: "elementary particle arrangements" − where groups of clay platelets are joined together to form elementary particles, "particle assemblages" − where the elementary particles are

arranged in aggregations or matrices with other larger sand or silt grains and finally "pore spaces". The arrangement and proportions of these three forms were indicative of the type of behaviour of the soil. Figure 2.27 illustrates the types of microfabric observed.

2.8.1 Fabric and compaction method

The influence of the method of compaction on unsaturated soils was investigated by Seed and Chan (1959). Tests were performed on two soils: a sandy clay and a silty clay. Two different methods of compaction were used in the experiments to achieve the required dry densities: static compaction, where a direct load was applied to the soil using an hydraulic ram and kneading compaction, where the soil was kneaded into the mould. Both methods remoulded the soil but in different ways. With static compaction remnants of the original fabric were retained whereas kneading compaction destroyed the original soil fabric.

Samples with the same dry density were prepared using both methods. While maintaining a constant sample volume, water was added and the soil was allowed to swell. For the samples that were compacted at moisture contents less than the optimum water content the swelling pressures observed were similar. However for the soils compacted wet of the optimum moisture content there were significant differences in the values of swelling pressure between the two methods (Figure 2.28).

This difference in the swelling behaviour arising from the two compaction methods was investigated further. Samples were prepared with a constant moisture content (greater than optimum) whilst the dry density was varied. For the two soils tested the swelling pressure measurements showed that for the same initial dry density the statically compacted soil consistently produced higher swelling pressures (Figure 2.29).

The method of compaction was also seen to influence the shear behaviour of the compacted soil. Figure 2.30 shows the variation in the deviator stress with axial strain for quick undrained triaxial tests on samples of silty clay. The samples were prepared by either static or kneading compaction to similar dry densities but at water contents dry and wet of the optimum water content. The samples that were compacted dry of the optimum moisture content produced similar stress−strain behaviour achieving the same failure stress. However the samples with a comparable dry density but with a water content above the optimum water

content produced different stress–strain responses. At these higher moisture contents the deviator stress at failure was lower, as would be expected, but there was a significant difference in the stiffness response of the soil. The sample prepared by kneading compaction showed that during shearing a constant stiffness was maintained compared with the strain hardening exhibited by the statically compacted samples during shearing. The failure strength was found to be approximately equal in both cases.

Seed and Chan (1959) postulated that the difference in stiffness was due to the method of compaction i.e. dry of the optimum water content both samples (prepared by kneading or static compaction) produced a "flocculated" fabric whereas wet of the optimum water content only the statically compacted samples produced a "flocculated" fabric, the kneaded samples producing a "dispersive" fabric.

2.8.2 Permeability of compacted clay fills

For a saturated soil the permeability is a function of the void ratio and for an unsaturated soil the permeability is affected additionally by the degree of saturation. The permeability of a soil which is initially saturated will reduce as the saturation ratio decreases since the water present in the pore spaces is replaced gradually by air, so increasing the flow path through which the permeating water must travel. When the saturation ratio decreases sufficiently a point will be reached where the water phase becomes discontinuous ($S_r < 80$ %) and water flow cannot continue. Lambe (1958) related the hydraulic conductivity of a compacted clay to the orientation of the soil particles which had either a "flocculated" or "dispersed" structure (Figure 2.31). Another theory was proposed by Olsen (1962) where he suggested that flow of water in a compacted clay would occur in the spaces between the clods of the clay rather than through the clods of clay. In a dry compacted clay fill the interclod voids would be larger therefore the hydraulic conductivity would be higher whereas in a soil compacted with a higher moisture content the interclod voids would be smaller and the hydraulic conductivity less.

Benson and Daniel (1991) performed tests to measure the hydraulic conductivity of samples of compacted clay. The samples were prepared from clods of different sizes (19 mm and 4.8 mm). The results showed that clod size had a significant influence on the hydraulic conductivity of the compacted soils. For the samples compacted dry of the optimum the

hydraulic conductivity of the samples prepared with small clods were up to six orders of magnitudes less than the samples prepared with large clods. The hydraulic conductivity of the specimens compacted wet of optimum did not depend on the clod size since complete remoulding of the clods had occurred. This can be seen in Figure 2.32 which show the hydraulic conductivity related to the standard and modified compaction curves. Benson and Daniel (1991) also interpreted the results in terms of initial dry unit weight and indicated that the conductivity decreased as the initial water content increased Figure 2.33. For the four different samples of the compacted soils tested by Benson and Daniel (1991) the hydraulic conductivity for moisture contents greater than 19 % showed to have a permeability less than two magnitudes different, this can be explained by the similar dry density and water content of the samples as shown by the dry density water content relationship in Figure 2.32.

2.9 COMPACTION: DEFINITIONS AND INFLUENCES

A definition of compaction was introduced by the Road Research Laboratory in a widely used reference book on soil mechanics for road engineers (Road Research Laboratory, 1952):

> " Soil compaction is the process whereby soil particles are constrained to pack more closely together through a reduction in air voids, generally by mechanical means. "

The compaction of soil produces a material which has a greater shear strength and at the same time it reduces the propensity for settlement and deformation as well as its permeability to water. To use soil as an engineering material it is necessary to understand the factors which can affect its integrity both in the short and long term. The factors that are of the greatest influence in the compaction of soil are:

- the soil characteristics – grading, plasticity etc.
- the moisture content of the soil
- the volume of the soil compacted
- the amount of energy used to compact the soil.

2.9.1 Definitions

The measurements used to define quantitatively the compaction of soil are: bulk density (ρ), dry density (ρ_d), voids ratio (e) and air voids (V_a). The relationships define the proportions of solid, water and air within the soil. Useful definitions are as follows:

Bulk density (ρ) – is the ratio of the mass of a given volume of soil to the volume that the soil occupies. Units are Mg/m^3.

Dry density (ρ_d) – is the ratio of the mass of solid particles in the given volume of soil to the volume that the soil occupies. Units are Mg/m^3.

Void ratio (e) – is the ratio of the volume of voids in the sample (water and air) to the volume of solids. This term is dimensionless.

Air Voids (V_a) – is the ratio of the volume of air in the sample to the total volume of the sample and is usually expressed as a percentage. The method of calculation air voids defined in the British Standard (BS 1377 pt 4) is as follows. The term is dimensionless.

$$V_a = \left(1 - \frac{\rho_d}{\rho_s} - \frac{\rho_d . w}{100 . \rho_w} \right) * 100 \ \% \qquad 2.27$$

where

V_a is the air voids ratio (%)

ρ_w is the density of water (Mg/m^3)

ρ_s is the density of the soil particles (Mg/m^3); $\rho_s = \rho_w \times G_s$

ρ_d is the dry density of the soil (Mg/m^3)

w is the water content (%)

G_s is the specific gravity of the soil

2.9.2 Influence of soil type

For the input of a standard compactive effort the highest dry densities are achieved by soils having little or no plasticity, for example, sands and gravels. For these types of soil greater densities are achievable when the soil is well graded, rather than poorly graded. The soils which exhibit plasticity due to the presence of silt and clay particles are able to retain more water the lower the achievable dry density for the same compactive effort. Figure 2.34 shows the compaction curves (using the standard 2.5 kg rammer test) for a wide variety of soils ranging from crushed limestone to high plasticity clay. The difference between the soils used in this project is also revealed in their compaction curves (Section 5.1.2).

2.9.3 Influence of moisture content

The presence of water in soils has a large effect on the strength of the soil. As water is added to a sand the achievable dry density for a standard compaction will increase until an optimum water content is reached after which the achievable dry density reduces (Figure 2.35). This peak in the dry density results from the way in which the water forms menisci between the particles of sand creating a negative pore water pressure (suction). At water contents drier than the optimum the higher suctions result in an increased effective stress within the soil, making its shear strength greater and compaction harder. As more water is added the suction within the soil decreases and higher densities are achieved. At water contents greater than the optimum high the suctions are reduced and during compaction the pore water develops positive pore water pressures which, unless they dissipate quickly, prevent the soil from becoming denser. The same effects are observed in soils containing silt or clay however because the particles are smaller (with larger surface areas) the suctions are much higher so for the same water content these soils will have lower dry densities following compaction. Increasing the water content above the optimum produces a reduction in the dry density. This reduction is due to the generation of excess water pressures in the soil water which are unable to dissipate sufficiently fast to allow further compaction. Figure 2.36 shows work performed by Lewis (1959) where samples of clay were tested in unconfined compression to give a value of the undrained shear strength at different values of moisture content and dry density. The results revealed that as the water content was increased both the dry density and shear strength of the soil reduced.

2.9.4 Influence of volume compacted

As the thickness of the layer which is being compacted increases there is a variation of shear stresses exerted by the compactor throughout the layer this results in a variation of the density of the soil with depth. In order to achieve a more uniform distribution of dry density the soil mass can be compacted in smaller layers (Figure 2.37). The effects of layer thickness was demonstrated by Parsons (1992) who interpreted results from a previous study, where it was shown that an increase in the depth of fill produced a lower dry density for the same compactive effort (Figure 2.38). The soil in this experiment was a high plasticity clay compacted in a standard way by an 8 tonne roller.

2.9.5 Influences of compactive energy

The energy used in compacting a soil is directly related to the achievable dry density. Generally as the compaction energy input into a soil mass increases there will be a greater reduction in the air voids of the soil and a higher dry density will be achieved. The required amount of energy required can be applied by successive applications of a load such as a weight dropping from a fixed distance or a roller passing over the surface of the soil. After each application of the load the dry density of the soil mass increases. During the compaction process the stresses imposed by the roller can be seen to increase as the successive passes reduce the thickness of the top layer of soil and reducing the area of contact that the roller has with the soil (Figure 2.39). At the surface of the compacted layer the shear stress applied can exceed the maximum shear strength of the soil and over stressing can occur resulting in a decrease in density. Figure 2.40 shows the change in the density observed when compacting a granular soil with standard weight machine and an excessively heavy machine for the same granular soil.

2.10 EARTH PRESSURES DUE TO COMPACTION

During the construction of retaining walls it is common practice to construct the wall prior to the placing of fill material. It is necessary to compact the fill behind the wall to produce a dense material which has high strength and low compressibility. The earth pressure analyses performed by Coulomb and Rankine assumed that the retaining wall is created within the soil.

No consideration was given to effects that the construction of the wall and the compaction of the backfill would have on the magnitude of wall stresses.

Granular material is normally chosen for this purpose as it can be easily compacted to achieve high densities and strengths whilst maintaining a high permeability thus preventing the build up of water pressures. Other materials having a higher clay or silt content can also be used however additional increases in the lateral pressure may occur after construction as the lower permeability fill becomes wetter.

During the compaction process the forces exerted by the compaction plant increase both the vertical and horizontal pressure within the soil. For granular soil the shearing resistance between the particles can be overcome by the application of dynamic loading. For clayey soils dynamic methods are inefficient in overcoming the undrained shear strength of the soil and static loading is preferable.

2.10.1 Compaction in a granular soil

Broms (1971) and later Ingold (1979) developed theories that could explain and predict the mechanism for compaction of a granular soil. Broms plotted the stress path for an element of soil behind a retaining wall at different depths. By assuming that no lateral yield was occurring during compaction (only true for an infinitely long and wide roller) the horizontal stress could be estimated using the coefficient earth pressure at rest $\sigma'_h = K_o . \sigma'_v$.

Figure 2.41 shows the stress path followed by an element of soil at a shallow depth below the ground surface during compaction by a roller. From an initial stress state (assumed to be $\sigma'_{h1} = K_o . \sigma'_{v1}$) the infinitely long and wide roller passes over the fill and increases the vertical stress to σ'_{v2} and horizontal stress to σ'_{h2} when it moves away the vertical stress decreases. The horizontal stress is assumed to remain constant ($\sigma'_{h2} = \sigma'_{v2}$) until the vertical stress has decreased below a critical value after this point the horizontal pressures are assumed to reduce linearly with the vertical stress (i.e. $\sigma'_h = K_r . \sigma'_v$) until the initial vertical stress value (σ'_{v1}) is achieved. The value of K_r is called the coefficient of earth pressure at rest for unloading and as Broms noted was dependent on the angle of friction of the soil and could be taken as $1/K_o$. The final horizontal stress (σ'_{h3}) remains higher then the initial horizontal stress. For an element of soil deeper behind the wall the initial and final vertical stresses are

higher but the effect of the stress from the roller will be decreased. When the roller is unloaded the maximum horizontal (σ'_{h3}) load is maintained.

The stress path followed by an element can be extended to the compaction of a layer. Figure 2.42 shows the lateral pressure distribution used by Broms (1971). Before the roller is applied to the fill the lateral earth pressure is assumed to be $\sigma'_h (= K_o . \sigma'_v)$. On the application of the roller the horizontal stress rises to a maximum σ'_{hm} $(= K_o . \sigma'_{vm})$. On removing the roller the material below a critical depth (where the stress state after compaction returns to the to the initial stress value) retains its horizontal stress whereas the material above undergoes a horizontal stress reduction according to ($\sigma'_h = K_r . \sigma'_v$). The residual horizontal pressure distribution is then shown by the shaded area of Figure 2.42. If several layers are compacted then a stress distribution such as in Figure 2.43 is formed. This can be simplified by assuming that the compaction is performed in thin layers so that the locus of the maximum lateral earth pressure produces a straight line as indicated in Figure 2.44.

A similar analysis used by Ingold (1979) assumed that because the soil would strain a small amount horizontally under the load of the roller the resulting horizontal stress would not be as high as $K_o . \sigma'_{vm}$. Approximations made in the calculation of the vertical stress increase caused by the roller allowed a simple method for calculating the maximum horizontal pressure (Figure 2.45).

2.10.2 Compaction in a clayey soil

A demonstration of the way in which compaction of a soil occurs in a clayey soil was described by Clayton and Symons (1992). A sample of loose soil was placed in an hydraulic oedometer and subjected to a number of cycles of increasing vertical stress. The diameter of the soil was maintained constant by the application of a variable radial pressure. As the vertical stress increased and decreased the sample was gradually compacted. Graphs of undrained shear strength vs. total vertical stress showed that strength of the soil increased as the vertical stress and density were increased. The residual lateral stress (measured when the vertical total stress was reduced to zero) was observed to increase in magnitude evident in the graph showing the vertical and lateral total stresses after each loading stage (Figure 2.46).

The hypothesis put forward by Clayton and Symons (1992) for predicting the lateral earth

pressures after compaction assumed that the wall was rigid and that friction on the wall was negligible. The variation of the horizontal stress was formed by integrating the Boussinesq solution for a point load on an incompressible elastic half space. The two curves shown in Figure 2.47 represent the horizontal stress calculated in this way by using two undrained shear strength values 50 kPa and 400 kPa. An undrained shear strength of 50 kPa was considered as the lower limit of trafficability (Farrar and Darley, 1975) below which the soil is too weak to support the compaction plant. The upper value of undrained shear strength, 400 kPa was used because the authors considered that the use of soils with undrained shear strengths in excess of 400 kPa would be unlikely. The vertical lines in Figure 2.47 are the limits on the horizontal stress which are influenced by the undrained shear strength of the soil and the overburden ($\gamma z + 2Cu$). Clayton and Symons (1992) assumed that the maximum residual horizontal stress after compaction would be less than twice Cu. Since the depth of fill to be compacted is usually small the controlling factor was the undrained shear strength of 2Cu. From this method of analysis it was possible to determine the maximum thickness of layer that could be compacted depending on the undrained shear strength of the soil. For a soil with an undrained shear strength of 50 kPa the maximum depth for optimum compaction was approximately 90 mm whereas for a soil with an undrained shear strength of 400 kPa the maximum depth was approximately 25 mm. The practical problems associated with using such a thin layer of soil would create major increases in the time taken and costs for any backfilling operation but also increase any potential for the development of larger swelling pressures that may develop in the drier soil. It would be envisaged that wetter soils (with lower shear strength) would be used to facilitate the use of thicker layers in the compaction.

2.10.3 Hysteretic model for compaction

A predictive model for evaluating earth pressures due to compaction was developed around the hysteretic nature of soil compaction (Duncan and Seed, 1986). This computer based method used correlations of different parameters with the angle of internal friction (ϕ). These correlations included relationship between K_o and ϕ for normally consolidated soils (Jaky, 1944), the relationship between K_o and ϕ for over consolidated soils (Mayne and Kulhawy, 1982) and the parameters α and β from the studies of Duncan and Seed (1986). The elastic stress calculations used in the computer program required a relationship between the internal angle of friction (ϕ) and the Poission's ratio (ν). The assumptions made for this

equation regarded that:

- the state of stress in a compacted fill would lie between an at−rest and failure condition.

- there was a valid relationship between K_o and ν in the at−rest condition.

- at failure the Poission's ratio (ν) = 0.5.

The equation used to relate ν and ϕ was as follows:

$$\nu = \frac{4 - 3\sin\phi}{8 - 4\sin\phi} \qquad 2.28$$

The program (called EPCOMP2) followed the hysteretic changes in the stresses in the compacted fill through many cycles of placement and compaction. The results from this method were shown by Duncan and Seed (1986) to agree with field measurements.

Using this program a number of charts were developed that simplified the evaluation of the induced pressures due to compaction (Duncan, Williams, Sehn and Seed, 1991). Charts were prepared for both granular and cohesive soils considering the various cases involved in the compaction process i.e., plant type and mass, roller thickness, distance of roller from the wall, the height of the layer to be compacted and the internal angle of friction (ϕ). Figure 2.48 shows a typical chart relating the lateral pressure after compaction with the depth of the compacted layer for different magnitudes of load. These values of lateral pressure were calculated for a single roller length (7 ft), a fixed distance between wall and roller (0.5 ft), a known thickness of compacted soil (0.5 ft) and an angle of friction of 35°. Because of the many variables involved in the loading cases it was not possible to represent all of the combinations on a single graph so the values from the chart could be multiplied by factors that would adjust the earth pressure to give a corrected value.

The chart shows two types of curve. The first shows the earth pressures for different loading cases for cohesive soil (dashed) and granular soils (solid) and secondly for the variations in the earth pressure at rest expressed in terms of $K_o\gamma$. The lateral earth pressure is estimated by following the line representing the loading case of interest until it intersects the appropriate line corresponding to the value of $K_o\gamma$. The value of lateral pressure after compaction can

then be read and adjustment factors are then applied.

This method of computing the lateral earth pressure after compaction was compared to compaction studies performed by the Transport Research Laboratory (Section 2.13). The first comparison was made to an instrumented retaining wall that was backfilled with sand (Carder, Pocock and Murray, 1977). The agreement between the values calculated and actually measured are very good (Figure 2.49). The range of lateral earth pressures calculated using the full computer model (EPCOMP2), the design charts and the measured earth pressures agree well with the measured values. A further comparison was made with a second study performed in the same retaining wall facility where silty clay was used for the backfilling material (Carder, Murray and Krawczyk, 1980). The analyses performed proved to be less conclusive (Figure 2.49). The direct computer analysis again predicted values of lateral earth pressure within the range of the experimental data, however the values calculated using the charts and tables were unable to apply a correction factor to the value of ϕ_u (13°) because it lay outside the assumed range for ϕ ($25° \leq \phi \leq 40°$) in the adjustment tables. The values used in the comparison were the drained strength parameters found by Carder et al. (1980), ($c' = 0$ and $\phi' = 37°$). The resulting comparison proved unsuccessful since the actual earth pressures measured were taken soon after the completion of the compaction when the soil was still in an undrained state.

2.11 RESEARCH INTO LATERAL EARTH PRESSURES DUE TO COMPACTION

Between 1977 and 1989 a programme of research was undertaken at the Department of Transport Research Laboratory to investigate soil structure interaction. The chosen subject for this analysis was the stress−strain behaviour of retaining walls when using different backfilling materials. To avoid any scale effects apparent when using small scale models (when tested at 1 g) the pilot scale retaining wall was constructed at a large scale. This allowed standard methods of placement to be used in the compaction of the backfill. The experimental wall was constructed in a reinforced concrete trough where the soil could be placed between a moveable metal retaining wall and a fixed concrete wall Figure 2.50. The metal wall consisted of three 2 m^2 articulated steel panels which were connected to a jacking system. The centre panel was instrumented to record the changes in the lateral pressure and displacements. In the opposite wall were located other pressures cells so that is was possible to measure the lateral pressures developed during compaction, Figure 2.51 shows the location

of the pressure cells.

A fundamental part of this work was the choice and use of pressure cells which were required to measure the lateral earth pressures. An earlier study (Carder and Krawczyk, 1975) examined the behaviour of three types of pressure cells which could be located in the wall at the interface between the soil and the wall. The pressure cells used were, a hydraulic cell, a strain gauged cell and a pneumatic cell. The hydraulic cell consisted of a flexible steel diaphragm (adjacent to the soil) confining a water filled chamber which was connected to an electrical pressure transducer, changes in the water pressure related to the pressure on the wall. The strain gauged cell consisted of a stress transducer connected to an enlarged top plate which was in contact with the soil but free to move laterally. The pneumatic cell was of a similar construction to the hydraulic cell however air pressure was used as the cell fluid. The soil pressure was measured by increasing the flow of air through the cell to slightly inflate the stainless steel diaphragm until contact was made with the soil. When a small but constant rate of flow was achieved the air pressure necessary for this corresponded to the soil pressure acting on the soil. For all of the cell tested the friction was minimised by the use of a thin layer of grease between two sheets of rubber placed between the cells an the soil. The study compared the behaviour of the three types of cell under a known applied pressure. The results indicated that the testing procedure as well as the method of compaction affected the output from the cells, it was concluded that it was possible to use the cells for measuring earth pressures provided that calibration procedures closely simulated the in situ conditions and corrections were applied to the data (to compensate for the effects of the layers of rubber and grease between the wall and the load cell). The large range of horizontal earth pressure measured in the cells reflect firstly, the difficulty in the measurement of earth pressures arising for the compaction of soil and secondly, the compliance of the load cell and their compressible covering of rubber and grease.

2.11.1 Lateral Earth Pressures in Sandy Soil

The first use of the retaining wall facility to measure the stress−strain behaviour of a compacted sand backfill (Carder, Pocock and Murray, 1977). The soil chosen for the experiment was an uniformly graded, washed sand which had an optimum moisture content for compaction of 10 %. A 1.3 Mg vibrating roller was used to compact the soil in layers. After completing each layer measurements of displacements and pressures were taken from

all the instruments. During the test it was possible to move the metal wall and induce passive or active failure in the soil. The results showed that the residual earth pressures present after compaction were significantly higher than would be expected from the self weight alone of the soil. However, providing that the wall had sufficient flexibility (with small movements < 4 mm) there would be a reduction of lateral stress of up to 70 % allowing the pressure on the wall to reduce to the active pressure conditions Figure 2.52. Therefore it was confirmed that it was justifiable to design retaining walls when this type of fill was placed using the calculated value for active earth pressure.

2.11.2 Lateral Earth Pressures in silty clay

The following investigation using the retaining wall facility examined the development of the soil pressures produced from a silty clay (Carder, Murray and Krawczyk, 1980). The soil had a plastic limit of 17 % and liquid limit of 42.5 % and was placed at the limit of the current specification for use as a backfill material (Section 2.14). The change in soil type from a free draining sand to a silty clay introduced additional factors that affected the lateral stress. The lower permeability of the silty soil reduced the ability of the soil to dissipate the excess pore pressures developed during compaction. In addition to the pressure cells described above piezometers were installed to measure the pore water pressure. The additional data allowed the calculation of the effective stress state within the soil. The soil was compacted in layers of 125 mm thick using a smooth wheeled roller weighing 3.25 Mg. At the end of the construction the top of the soil was covered with plastic sheeting to prevent moisture loss. Like the compacted sand in the previous experiment the lateral pressures after compaction were seen to be significantly higher than those calculated. However in contrast there was a gradual decrease in the lateral thrust on the wall over a period of three months (Figure 2.53). This was attributed to the decrease in the pore pressures as the excess pore pressures dissipated. At the end of this period the rate of decrease had fallen and the distribution of stress had approached the K_o condition.

2.11.3 Lateral Earth Pressures in Clayey Soil

In 1989 a further investigation was commissioned to study the compaction and swelling pressures developed by a clayey fill (Symons, Clayton and Darley, 1989). The specifications

that were currently operative (Department of Transport, 1986) classified the soil chosen for the study (London Clay: LL = 78 %, PL = 29 %, G_s = 2.78) as unsuitable for backfilling to structures. The specification recognised the fact that there was no established method for estimating compaction pressures and stress–strain behaviour for this type of fill. The work aimed to asses the magnitude and effects of volume changes that could occur after construction. The soil was excavated from a borrow pit from a depth of between 2 m and 5 m, transported to the test facility where it was compacted in layers of 125 mm using a 7 Mg self propelled vibrating roller. The dry density of the soil was found to vary between 1.46 Mg/m^3 (nuclear gauge) to 1.42 Mg/m^3 (sand replacement method) with the air void ratios respectively 6 % and 8 %. Triaxial compression tests performed on 38 mm undisturbed samples gave a strength envelope defined by c' = 15 kN/m^2 and ϕ' = 19^o, and an undrained shear strength of 125 kN/m^2. After compaction the fill was covered with plastic sheets to prevent moisture loss. Over a period of 40 days there was a gradual reduction in the lateral pressure measured on the retaining wall (Figure 2.54) and after this time water could be introduced into the fill to investigate the problem of swelling of the backfill. To accelerate the swelling process vertical sand drains were drilled into clay and kept filled with water. The total lateral thrust on the metal retaining wall increased rapidly from an initial thrust of 95 kN to a maximum of 265 kN in 180 days, (Figure 2.55). From this point there was a gradual reduction in the thrust reaching a minimum of 200 kN after 500 days. Measurements of surface movements occurring during the inundation are shown in Figure 2.56; a heave of up to 128 mm was recorded. The highest rate of heave occurred during the first 250 days of the swelling. 700 days after the compaction was completed piezometer readings indicated that the pore water pressure had reduced towards zero. The test was terminated and samples were taken for undrained triaxial compression tests and moisture content tests. It was found that the greatest changes in the moisture content occurred near the surface of the soil which was reflected in the lower shear strengths obtained in this region (Figure 2.57).

2.12 COMPACTION SPECIFICATIONS

Compaction specifications can either specify the method by which the soil must be compacted (method specification) or the final requirements that the fill must have in terms of density or air voids. The specification referred to in this thesis is taken from the Earthworks section of the Manual of Contract Documents for Highway Works (1991).

2.12.1 Method specification

Method specifications state the exact method to be applied for compaction, i.e. the type of compacting plant (weight, dimensions of compacting area), the thickness of the layer of soil and the number of passes that the compacting plant has to pass over the area. This type of specification was based on extensive investigations into compaction performed at the Transport Research Laboratory over many years. It was aimed at allowing contractors to choose from a variety of compaction plant and then by using reference charts it would be possible to understand quickly the thickness of each layer and the number of passes required for a satisfactory compaction of the particular type of soil. In the preparation of the tables it was necessary to choose the condition of the soil that would provide some margin of safety. This was achieved by using a moisture content for each soil that would be in the lower range of moisture contents for the natural soil. At these lower moisture contents compaction would be more difficult, however by using sufficient energy it would be possible to achieve a minimum of 10 % air voids in the soil. In actual field compaction using the soil in a condition wetter than this minimum would produce a greater degree of compaction.

Table 2.2 shows an portion of the current specification that refers to the method of compaction required for the different soil types, where N is the minimum number of passes that the compactor has to perform over each point, D is the maximum depth of the layer and N# is the number of passes to be applied over the soil when the materials are to be used near to the surface. The of N# value indicated has to be doubled when materials such as general granular fill (Class 1A or 1B) or general cohesive fill (Class 2A, 2B, 2C and 2D) are used.

2.12.2 End product specification

End product specification defines the final state of the compacted soil, which is normally expressed in terms of dry density or a density relative to a standard method of density determination. However because the dry density achievable is also dependent on the material used, other factors such as air voids ratio need to be specified. The most common methods used in end product specification are: relative compaction, relative density and air voids.

Relative compaction expresses the required field dry density as a percentage of the maximum dry density as determined by a recognised standard e.g. 2.5 kg Proctor compaction test.

Normally, for the 2.5 kg Proctor compaction test the required value of the relative compaction is between 90 and 100 % of the maximum density. Specifications using relative density are used for granular soils like sands and gravels. The in situ dry density is compared to the maximum and minimum achievable dry densities as determined in the laboratory. The maximum dry density is found by compacting saturated sand into the mould using vibration whereas the minimum dry density is found by pouring dry sand into the container. Relative density is calculated as follows in terms of dry density;

$$\text{Relative density (\%)} = \frac{\rho_{dmax}(\rho_d - \rho_{dmin})}{\rho_d(\rho_{dmax} - \rho_{dmin})} * 100 \qquad 2.29$$

where:

ρ_d is in situ dry density

ρ_{dmax} is maximum dry density

ρ_{dmin} is minimum dry density

Using the air voids ratio is commonly used as an end product specification in conjunction with dry density. For soil that is to be used as general fill a minimum air voids ratio of 10 % is required whereas for special applications 5 % is the minimum. Table 2.3 shows the specification selection requirements for selective cohesive fill (class 7A).

2.13 CURRENT SPECIFICATION FOR COMPACTION OF CLAYEY BACKFILL

At present the various types of materials for use in backfilling and compaction behind road structures are given in the "Specification for Highway Works", published by the Department of Transport (1991).

The specifications are intended to assist the engineer in the selection of soil used for earthworks.. All possible types of material that may be found on site or imported are classified. For each material a general description, typical use and permitted constituents is given. Soil properties are required to lie within certain limits to be acceptable for the different methods of compaction.

Table 6/1 of the "Specification for Highway Works" lists the acceptable materials for use as backfill. Two basic types of material can be used which are defined in the specification as

cohesive and granular. The type of fill relevant to this project is selected cohesive fill that would be used as backfill adjacent to structures. From Table 6/1 this is defined as a Class 7A material. The range of acceptable material properties are;

- Grading: 100 % to pass 75 mm sieve and 15 – 100 % to pass 63 μm sieve.
- Moisture content: limits set by engineer.
- Moisture condition value (a value which correlates density and compactive effort to the moisture content of the soil and enables an assessment of the suitability of the soil for use as backfill): limits set by engineer.
- Undrained shear strength parameters: limits set by engineer.
- Effective angle of internal friction and cohesion: limits set by engineer.
- Liquid limit: not to exceed 45 %
- Plasticity index: not to exceed 25 %

The method of compaction for this type of material requires the end product to be at least 100 % of the maximum dry density as defined by the Proctor compaction test with a 2.5 kg rammer (BS1377, Part 4) or not more than 5 % air voids, whichever gives the lower dry density at the field moisture content.

There are limits to the placement water contents of fill that can be used in practice. The upper limit is determined by the trafficability of the soil. A fill moisture content that is too far in excess of the plastic limit will lead to difficulties when using compaction plant. The lower limit of the water content is determined by the acceptable percentage of air voids present when the soil is compacted to 100 % of the maximum dry density. If a very dry soil is compacted until it reaches the 100 % of maximum dry density line, the air voids may be in excess of 10 %. Wetting of a soil in this state may lead to a collapse of the soil structure. It would be possible to compact this dry soil to a density greater than the 100 % of the Proctor density value in order to reduce the air voids. However, a large input of energy would be required which may cause damage to the retaining structure immediately or in the long term. Furthermore excessive swelling pressures could develop as the material became wetter and started to swell. Compaction curves with the current specification limits are shown in Figure 5.2 for the three soils tested.

The upper and lower acceptability limits of moisture content are related to the plasticity of the soil as determined in the Atterberg limit test. For Class 7A material the moisture content

limits have to be specified by the Engineer, however for the purposes of this report, the lower limit on moisture content will be taken as PL−4 % (a value used for Class 2A − wet cohesive material) and the upper limit taken as 1.2 PL %, a moisture content at which clayey soil has sufficient strength for acceptable trafficability (Parsons, 1992).

2.14 SUMMARY

Historically the development of soil mechanics has been focused on saturated soils where the pores are filled with one fluid, either water or air. Concepts such as Terzaghi's principle of effective stress have been used as a basis from which frame works that are able to describe the behaviour of the soil have been formulated. For example the development of the critical state soil mechanics framework developed by Schofield and Wroth (1968) based on Terzaghi's principle of effective stress using the results from tests performed on reconstituted saturated soils.

In reality a large proportion of the soils encountered in the engineering environment are unsaturated and their behaviour differs from predictions made using the existing saturated of dry soil mechanics framework. The suctions that exist in the soil arise from the capillary effect of the water in the pores (matrix suction) and from the clay minerals in the soil (osmotic suction). The combined effect of these two suctions produces what is referred to as total suction. The presence of suction in the soil alters the mechanical behaviour of the soil and it is necessary to measure the suctions to fully describe its behaviour.

Many researchers have tried to modify and or extend the existing effective stress principle to account for these observed differences. Early work was unable to link directly observed volume changes with the shear behaviour of the soil. Notable contributions have been made by: Bishop et al. 1959 − 1963 for the development of one modified effective stress equation which incorporated a factor (χ) to account for the degree of saturation of the soil; Fredlund et al. 1977 − 1982 for producing a relationship for the shear strength of an unsaturated soil based on the extended Mohr−Coulomb failure criteria; and Matyas and Radhakrishna (1968) who by treating the applied stress and suction as two independent variables were able to represent the volumetric behaviour of the soil by surfaces relating stress state, void ratio, suction and saturation ratio. Between 1986 and 1993 the most significant steps have been taken to unify the volumetric and shear behaviour of unsaturated soil Alonso et al. (1985 −

1993) and Wheeler et al. (1990 – 1993) have proposed frameworks in which the behaviour of unsaturated soils can now be predicted in terms of volumetric and shear behaviour.

To use fine grained unsaturated soils as engineered fill it is important to understand the important issues when compacting; soil type, placement conditions, compacted volume as well as method and energy of compaction determine pressures exerted onto adjacent structures, the density, permeability and strength of the final product.

These issues have, and continue to be the focus of research work since the understanding of the fundamental mechanics of unsaturated soil and the more problem orientated research move towards a common understanding and approach to analysis and prediction of unsaturated soils. The work in this thesis hopefully moves in this direction.

3. LABORATORY APPARATUS AND PROCEDURES

3.1 INTRODUCTION

The laboratory tests were carried out using four different types of apparatus. Of these only one was a standard piece of equipment whereas the other three were either modified or newly designed. With the different pieces of apparatus it was possible to examine the differences the development of swelling pressure with respect to the confinement of the soil. If correlations were successful it would be possible to use the more robust modified oedometer apparatus (with greater confinement) as an instrument from which it would be possible to correlate the results with the more rigorous 100 mm stress path cell whose confinement conditions could represent more accurately the confinement conditions of the soil when placed. This would provide an ability to achieve rapid test results from a relatively simple piece of apparatus which could be reliably linked to an accurate measure of the expected swelling pressure

In this Chapter a description of the fundamental components of each piece of apparatus will be given, followed by any modifications made and by the procedures adopted during the tests. The main piece of apparatus used was a modified computer controlled triaxial cell in which different stress paths could be applied to soil samples of 100 mm in diameter and up to 200 mm in length. The second piece of apparatus used was an oedometer cell in which the movement of the top platen was restricted. A load cell was used to measure the change in vertical stress when water was added to the sample. The third piece of apparatus used was a computer controlled shear box which was adapted to measure the volumetric changes of samples maintained under a condition of zero lateral strain and subjected to different but constant vertical stresses as they were wetted. Finally a standard 38 mm triaxial cell was used to measure strength in a quick triaxial test. The accuracy of the measurements is discussed together with the calibration procedures adopted for the various transducers.

3.2 CHOICE OF SOIL

One of the main objectives of this research as described in Chapter 1 was to investigate the swelling pressure developed by compacted fine grained backfill behind stiff retaining walls and then to examine the results with reference to the current specification limits (MCHW1, 1991) used for the compaction of fine grained clayey soils adjacent to structures. The soils

selected for use in the experimental work were chosen carefully so as to firstly, maximise the range of possible soils that could be used as backfill to structures and secondly to augment previous compaction and swelling studies.

The soils selected were:

- Brickearth - a brown silty clay with LL = 78 % and PL = 28 %
- Wadhurst Clay - a beige coloured clay with LL = 57 % and PL = 24 %
- London Clay - a grey coloured clay with LL = 38 % and PL = 18 %

Of these soils only the Brickearth was within the acceptable limits of the specification (LL $\leq$ 45% and Plasticity Index $\leq$ 25 %). The Wadhurst Clay was a soil of an intermediate plasticity just outside the acceptable specification limits whereas the London Clay was a high plasticity soil well outside the specification. The Brickearth and London Clay had both been used in previous experimental studies both in laboratory testing (Ryley, 1988) and also full scale compaction and swelling studies (Carder et. al. 1988, Symons et. al 1989) and their use in this research provided an ideal opportunity for comparison.

3.3 SAMPLE PREPARATION

Sample preparation was a very important part of the testing procedure. It was critical that the method of soil preparation and compaction method chosen would result in consistent, uniform samples. In practice clayey backfill material is excavated from a borrow pit and recompacted in location at a water content similar to its natural in situ water content. The study of the compaction of soil contained in Chapter 2 highlighted the large influence that the compaction process has on the behaviour of the final mass of soil. For the experiments performed in this thesis the soil preparation and placement method chosen did not copy any typical techniques used in the field. However, the process was a well controlled standardised procedure that could produce consistent samples on a small scale.

The general method of preparation was to produce small lumps of soil at a known and controlled moisture content and to remould these into a container by applying a load. For this project, soil samples were prepared with different initial water contents ranging from PL − 4 to about 1.2 PL where PL is the plastic limit of the soil (Section 2.15). To ensure

the repeatability of the samples a careful study of each process in the preparation was made.

Soil was initially air dried and crushed using a jack hammer. This was then sieved and the fraction retained between 10 mm and 5 mm sieves was kept and dried further in an oven at 60 °C. To achieve the desired moisture content, distilled water was sprayed at intervals onto the soil over a period of several hours. This enabled the water to penetrate the granules and achieve equilibrium. By controlling the ratio of water to soil granules, it was possible to produce samples of different water contents. The soil was then compacted into a U100 tube, 400 mm in length, which provided a sufficiently large specimen from which soil samples could be prepared for all the different types of laboratory tests undertaken for each particular compaction condition.

The compactive effort for remoulding the soil granules in the U100 preparation tube was provided by an hydraulic ram powered by compressed air. It was possible to control the stress applied to the soil by varying the supply air pressure. The soil was compacted in several layers to avoid the presence of a large density gradient in the sample (Section 2.11.4). By adding to the tube a known mass of soil and applying the stress for a fixed period of time it was possible to achieve a consistent layer thickness. It was necessary to experiment with the amount of soil compacted and applied stress, in order to obtain an air voids ratio of not more than 5 % as required by the specification (Section 2.13). The surface between each layer was scarified using a toothed disk to prevent the formation of horizontal planes or discontinuities within the sample.

Once the soil had been compacted in the tube it could be extruded and the following samples prepared;

- one 200 × 100 mm diameter sample for the swelling tests in the 100 mm diameter stress path cell.

- three 76 × 38 mm diameter samples for the strength correlation tests in the 38 mm diameter stress path cell.

- one 19 × 76 mm diameter sample for the modified oedometer tests.

3.4 THE 100 mm TRIAXIAL CELL

Modifications to the existing 100 mm cell and its control program allowed the measurement and control of radial strains in the soil sample. The sample, consisting of compacted soil, was allowed free access to water while being subjected to a constant axial stress and any potential radial straining was prevented by control of the cell pressure. The boundary conditions applied in these tests were chosen to simulate the boundary conditions that an element of soil would experience behind a stiff retaining wall. The change in cell pressure necessary to keep the sample with a constant diameter corresponded to the swelling pressure of the soil.

3.4.1 General arrangement

Based on the original hydraulic triaxial cell described by Bishop and Wesley (1975), Atkinson et al. (1985) developed a large size computer controlled triaxial stress path apparatus suitable for testing soil samples of up to 200 mm in length and 100 mm in diameter. The triaxial cell is computer controlled so that different stress paths can be applied to the sample.

Figure 3.1 shows a schematic diagram of the standard 100 mm hydraulic triaxial cell. The soil sample sits on a pedestal at the central axis of the apparatus. Three tension bars, spaced at an angle of 120° surround the sample. Their purpose is to connect the base of the main pressure vessel to a top plate through which a submersible load cell passes O−ring seals on the top and bottom plates ensure that the pressure within the vessel is maintained. The pedestal sits on a column that passes through the base of the pressure vessel into a rubber rolling bellofram which seals the cell. Linear bearings placed around the column allow free, low friction, vertical movement whilst maintaining the centrality of the pedestal. The base of the column passes through another bellofram seal into a lower sealed pressure chamber. By controlling the pressure in the lower axial pressure chamber it is possible to control the stress transmitted to the sample in the upper chamber. The internal load cell is fixed onto a metal rod that passes through two O−ring seals. The rod then screws internally into a threaded ring which allows the internal load cell to be raised or lowered.

The apparatus is provided with three pressure control units that vary the pressure in the cell, the pressure in the axial ram, and the back pressure applied to the sample. The input air pressure is supplied by a centralised screw type air compressor that can deliver a maximum

air pressure of 800 kPa. The pressure reaching the hydraulic cell is regulated by the computer system that controls the electro-manostats via relay switches and stepper motors. If an increase or decrease in pressure is required the computer system converts the required change in pressure to a number of pulses that are sent to the relay switches. The conversion factor between the pulses supplied and the change in pressure is dependent upon the gear box of the stepping motor in the electro-manostat. A typical value of conversion is that one pulse produces a change of 0.5 kPa in the electro-manostat. Air/water interfaces transfer the controlled air pressures leaving the electro-manostats to water pressures that then act in the cell and on the axial ram. The air/water interfaces consist of sealed cylinders in which water is pressurised by the air delivered by the manostats. Air pressure enters at the top of the cylinder which then forces water out through a pipe at the base of the cylinder.

3.4.2 Instrumentation

The axial load is measured using a 10 kN internal load cell supplied by Wykeham Farrance and based on an original Surrey University design. Because the load cell is mounted inside the cell the deviatoric force measurements are not affected by the frictional errors that external load cells suffer. The pressure of the cell water is measured by means of a Druck pressure transducer inserted directly into the base of the cell. The measurement of pore pressure is made using another Druck transducer connected to the base of the sample. Both transducers work in a pressure range 0 to 1000 kPa. The axial strain is measured externally using a resistive displacement transducer manufactured by MPE Ltd with a nominal stroke of 25 mm. As the sample deforms axially the transducer measures the relative displacement between the top of the cell that is firmly connected to the top of the sample and the axial ram which acts at the base of the sample. A transducer measures the displacement of the internal piston of the volume gauge allowing the calculation of the volumetric strains of the sample (this method of volume measurement is only useful for saturated soils). The compliance of the triaxial cell and transducers (displacement and load) may cause significant errors in measurements taken. To account for the variation in the load cell stress−strain response a steel sample was subjected to a similar stress path as followed by the soil and the test data obtained were corrected.

All of the above transducers are operated with an 8 Volt DC supply and are connected along with the computer and pressure regulators to a 240 Volt AC uninterruptable power supply.

In the event of a loss of electricity supply the uninterruptable power supply is able to maintain the power to the apparatus for up to 10 minutes allowing sufficient time for the emergency electricity generators to start.

Figure 3.2 shows a schematic diagram of the system used. The computer, a BBC model B computer, both monitors and controls the system through a Spectra Micro-ms interface unit, manufactured by Intercole Systems Ltd. This communicates with the computer via a RS423 serial link. The BBC system is fully described by Clinton (1987). Basically the interface unit provides an analogue to digital conversion of the signal received from all the transducers. The Spectra Micro-ms works with a 12 bit analogue to digital converter over a full scale range of $\pm$ 10.24 volts. The system auto-scales the output voltage from the transducers over eleven ranges in order to select the scale that best matches the signal. Since auto-ranging is applied the resolution of the output from the transducers is not constant along their working range. The best resolution is achieved when the transducer is positioned as close as possible to the electrical zero.

3.4.3 Modifications to 100 mm Cell and control program

For the purposes of the experiments that were performed in the 100 mm stress path cell it was necessary to be able to keep the sample under constant axial stress and zero radial strain during its inundation with water.

In the standard configuration of the triaxial cell described above, the radial strain is calculated using axial and volumetric strain measurements and also assuming that the sample remains

as a right circular cylinder during the test. For a saturated sample (having a saturation ratio, $S_r > 98$ %), the current diameter of the sample D_c is calculated using the following equation:

$$D_c = D_i \sqrt{\frac{1 - \epsilon_v}{1 - \epsilon_a}} \qquad 3.30$$

where

D_i is the initial diameter

ϵ_v is the current volumetric strain

ϵ_a is the current axial strain

This calculated radial strain then may be used to control the cell pressure to maintain the diameter of the sample. This procedure is only satisfactory for fully saturated samples and where internal local axial strain measurements are made. For the unsaturated soils used in this project it was not possible to measure volumetric strains using the standard method. The major difficulty was the fact that the soil samples to be tested would have saturation ratios much less than 98 % and any volumetric measurements would suffer considerable errors. Therefore alternative methods were investigated to measure radial strains in the samples.

Two new types of device were chosen for the internal radial strain measurement; submersible displacement transducers and proximity sensors (Figure 3.3). By using two different devices a comparison and evaluation could be made between them for future use with other triaxial systems.

The displacement transducers used were miniature submersible LVDT (Linear Variable Differential Transformer) type displacement transducers. They consist of a primary coil and two identical secondary coils, axially spaced and wound on a cylindrical coil former. A rod shaped magnetic core is positioned centrally inside the coil and provides a preferred path for the magnetic flux linking the coils. Any movement in the magnetic core produces a change in magnetic flux and a variation in the output which is measured and calibrated for displacement. When the core is symmetrically placed (electrically) with respect to the two secondary coils, equal voltages are induced in the two coils. If the two coils are connected in opposite phase the resultant voltage tends to a zero value. By setting the transducers at this "null point" the greatest resolution in the measurement is achieved from the analogue to

digital convertor. The transducers have been specially sealed to permit their use in the electrically hostile under water environment.

The LVDT's were connected to a conditioning module which provided the AC input to the transducer and rectified the output to DC which was suitable for the control and logging system. This type of LVDT has a free armature that is kept in contact with the sample by the use of a spring and a bearing pad. The bearing pad prevented the armature from pushing into the specimen and giving a false output. The three transducers are attached to a perspex ring which surrounds the sample. Each transducer is separated by an angle of 120°.

The proximity sensors are displacement transducers that are able to measure relative displacement between the sensor and a target without touching the target. They measure displacement by use of induction. An alternating current flows through the sensor coil generating an electromagnetic field which radiates out from the sensor. As a conductive target enters this field, a current flows on the target and a secondary electromagnetic field is induced in the sensor. The induced current has an opposite sense which then reduces the intensity of the of the original field. The opposing electromagnetic field results in an impedance variation in the sensor coil.

The sensor coil makes up one arm of a balanced bridge network. As the target changes position within the sensor field, the bridge network senses the impedance variations in the sensor coil and passes the information on to a signal conditioning electronics for conversion to an analogue voltage. This voltage is directly proportional to target displacement. The magnitude of the analogue output is dependent on the relative position of the target within the sensors electromagnetic field the further the sensor is from the target the higher the analogue output. The three proximity sensors are mounted in a similar fashion to the LVDT's, that is at an angle of 120° to each other on a perspex ring.

For the sensors to perform correctly a conductive target is necessary, for this a sheet of aluminium foil was wrapped around the sample prior to the latex membrane being positioned over the sample. Since target material, shape, thickness, etc., influence output it is necessary to statically calibrate the system with the specific target to be used. This is achieved by sticking a piece of the same foil on a moulded piece of perspex with the same curvature as the sample and attaching it to the calibrating device. To avoid problems with the layer of foil preventing the soil from swelling, incisions were made in the foil thus reducing its strength.

These modifications to the cell allowed a highly accurate measurement of radial strains and an equivalently accurate control of the radial deformation. As the sample was flooded with water, swelling in the radial direction was measured. Any differences in diameter detected by the control system could then be compensated by changes in the cell pressure in order to maintain the required zero lateral strain. These changes in cell pressure then correspond to the swelling pressure of the soil.

The BBC computer and the control program were altered in a number of ways. The control codes for the Micro-ms analogue to digital converter were changed so that the extra channels needed for radial strain monitoring could be scanned. The original six channels monitored (axial load, cell pressure, pore pressure, axial strain, volume strain and power supply) were increased to twelve channels to include the six additional displacement transducers. Because of the additional channels and consequent extra demand on the computer memory the storage capacity of the computer was extended by connecting an additional parallel processing unit.

A number of methods for the control of the radial strains were tried but the most satisfactory technique was found to be having the control system actively controlling the radial strain from the start of the test rather than setting limits above or below which the control system would be activated. Readings from the two levels of radial displacement transducers were taken and the average calculated. This reduced the potential for errors due to non-uniform distortion of the soil sample. If three successive averages over the 20 second control interval indicated a consistent increase or decrease in radial strain then the computer either decreased or increased the cell pressure in steps of 0.5 kPa.

The most suitable method chosen for introducing water to the sample was a method that simulated the conditions present behind a retaining wall. For an element of compacted soil behind a retaining wall a reasonable assumption for the ingress of water is that water flows slowly into the soil subjected to a hydrostatic head. This has been achieved by means of a raised water tank that supplies a small (approximately 10 kPa), but constant head of pressure. This supplied water through a central drain allowing it to be absorbed gradually by the soil, ensuring that uniform swelling would occur (Figure 3.4). This drain, a 17 mm diameter porous metal pipe, could be firmly push fitted into a 17 mm diameter hole that had been drilled axially through the sample. The pore size of the material used in this test was nominally 5 microns. At either end of the sample the porous metal pipe was attached to a stainless steel spigot also 17 mm in diameter which had a hole drilled through it. The spigots

fitted into sealed receiving holes located in the top and bottom platens. This method enabled the sample to swell radially along its length whilst still allowing axial straining to occur. The shear resistance developed axially along the soil−pipe interface was not expected to effect the radial straining of the soil sample however the amount by which the soil could strain axially would be reduced. Therefore any measurements of axial strain would only be used as indicative of a trend and not used directly for analysis.

The existing volume gauge was disconnected and replaced by drainage leads that were connected to the base pedestal and the top platen. These allowed water simultaneously to enter the top and the bottom of the sample and also prevented any airlocks from forming. Figure 3.5 shows a schematic diagram of the modifications made to the 100 mm cell and the testing conditions applied during the inundation of the sample.

3.4.4 Set−up procedure for 100 mm samples

Readings from the load cell and pressure transducers were zeroed with the cell filled only with water. This action offsets the effects of buoyancy of the load cell and the static head of the water in the cell. The drainage passages at the base of the cell were flushed through with distilled water to remove any debris from the passages avoiding blockages. Silicone grease was then applied along the sides of the base pedestal and the top platen forming a water tight seal when the latex membrane was fitted .

Before the sample was extruded a 17 mm diameter hole was drilled axially through the sample, and a steel rod inserted to prevent the hole from distorting during extrusion. Once removed from the preparation tube, the sample was cut and trimmed in a soil lathe until the required sample length and diameter was obtained. Two sample sizes were tested, either, 100 mm diameter and 200 mm length or 100 mm diameter and 100 mm length. The pieces of soil removed during trimming were used for obtaining a value of the initial soil water content. After accurately weighing the sample and measuring its dimensions the porous metal pipe was inserted until the metal spigots protruded equally from both ends. The sample was then placed on the base pedestal with the lower spigot locating into a hole sealed by O−rings . The top platen with a similar receiving hole was then placed on top of the sample. A sheet of tin foil, needed for the proximity sensors was wrapped around the sample and kept in place using two small elastic bands. A latex rubber membrane that has been presoaked in water for

24 hours, was placed around the sample. Rubber O−rings were used to seal the membrane against the base pedestal and top platen.

The rings needed to hold the radial transducers were located so that when the transducers were fixed in position they would be located respectively at 1/3 and 2/3 of the total height of the sample. The transducers were then clamped to the perspex rings using fixing screws, the three LVDTs on one ring and the three proximity transducers on the other ring. The initial radial position of the transducers relative to the sample was dependent on the testing requirements. Normally the transducers were arranged so that at the end of the first stage of the test (isotropic compression to 50 kPa) the movement of the sample would bring the transducers towards the point of electrical zero or "null point" before the start of the second, swelling stage. The purpose for arriving at the electrical "null point" is that the auto-scaling analogue to digital converter is able to apply the small output voltage to a large scale thus obtaining the greatest resolution of the readings. An alternative method used was to modify the electrical zero in the amplifier since it had been proved that this did not change the calibration constants of the transducers. For the samples that were 100 mm diameter and 100 mm in height only one level of transducers (LVDT) were used and placed at 1/2 of the total height.

After the top drainage leads were connected to the top cap the outside of the cell is bolted into position and the cell is filled with water and the first stage of the test could begin.

3.4.5 Testing procedure

During the first stage the total stresses on the soil sample were increased isotropically from approximately 2 kPa to 50 kPa. This pressure notionally represented the overburden stress experienced by an element of soil at a point between 2 - 3 m deep behind a retaining wall. All of the sample drainage valves were kept open during this stage to keep the sample in a fully drained condition. The final isotropic state was held constant for a period of between 10 to 24 hours prior to starting the flooding stage to allow for the equalisation of stresses.

At the start of the flooding stage both the axial and radial strains were re-zeroed. The control requirements of the test were also changed, the axial stress was kept constant at 50 kPa and the average radial strain was kept at zero by increasing or decreasing the radial stress. The

valves that connected the constant head tank to the sample were opened and water was allowed to come into contact with the soil. Stand pipes were fitted to the open ends of the drainage valves enabling the water to flush out any air locks from the drainage passages and also maintain a head of water above the sample. All the relevant stresses and strains were logged at specified intervals during the test and stored on computer disk as well as paper.

The test was deemed to have finished when no further increase in cell pressure (swelling pressure) occurred and the rate of axial strain was constant. After the control program was stopped the axial ram was fixed in position and the pressure in the cell released. On removing the sample, the dimensions and weight of the sample were taken. A number of moisture content samples were cut from the soil sample to verify that a uniform distribution of moisture content had been reached through the sample.

3.5 MODIFIED OEDOMETER

In this apparatus, radial straining of the soil sample was prevented by a conventional stiff oedometer ring. Changes in vertical stress were measured using a load cell. The test was designed to provide a simple measure of swelling pressure and the results could be related to those from the more complicated 100 mm stress path cell tests.

3.5.1 General arrangement

The design requirements of this piece of equipment necessitated a rugged design that could, if required, be used as a site piece of equipment. The frame consisted of two pieces of steel each 250 mm long, 250 mm wide and 10 mm thick. The pieces of steel were separated a distance of 200 mm by three 20 mm diameter steel rods (Figure 3.6). The rods were arranged in a triangular pattern, sufficiently spaced to allow easy access for the oedometer cell. The base plate of the frame had a spigot fixed so that the oedometer cell could always be located in the same position. A load cell was attached through the top plate by a reverse screw threaded shaft which allowed it to be raised or lowered on to the sample. The load cell used was a 230 kg capacity miniature load cell manufactured by RDP Ltd. It was powered using an 8 Volt DC supply and the output is logged using a BBC model B computer and a Spectra Micro-ms analogue to digital converter as used for the 100 mm triaxial cell.

3.5.2 Testing procedure

For each test a standard oedometer sample was trimmed, weighed and then positioned in the oedometer cell with dry porous discs above and below. After placing the oedometer cell in the frame the load cell was lowered until the sample was under a small seating pressure ($\approx$ 5 kPa). The seating pressure was used to ensure that the soil, porous stone and load cell were in full contact prior to wetting. This also removed any looseness in the fit of the threaded ring system. After 5 minutes distilled water was added to the cell until the sample was covered. The resulting swelling pressure was logged until no further change of swelling pressure was monitored. The sample was quickly removed from the oedometer cell and the final moisture content taken.

3.6 COMPUTER CONTROLLED OEDOMETER

Complementary to the modified oedometer and 100 mm triaxial cell the computer controlled oedometer was used to examine the behaviour of the soil at a wider range of initial dry densities as well as under different initial confining pressures.

3.6.1 General arrangement

These oedometer tests were performed in computer controlled shear box that was adapted for use as an oedometer. This apparatus allowed both the measurement and control of the vertical stress and strain. The control of the vertical stress was achieved by a computer which regulated the air pressure acting in a pneumatic piston fixed to the end of the lever arm (Figure 3.7). A 10 kN Wykeham Farrance load cell connected to the point of action of the lever provided the reaction to the soil sample. Vertical displacements were measured using a displacement transducer (manufactured by MPE Ltd.). The computer controlling the test was a IBM compatible computer with a 286 processor. Analogue to digital conversion was performed by an interface card manufactured by CIL Electronics Ltd. This interface card had a 16 bit base resolution, for each channel only one gain could be selected either $\pm$ 10 Volts, $\pm$ 1 Volts, or, $\pm$ 100 microVolts. No auto-ranging facility was present on the card so the resolution was constant unless operated by the software.

3.6.2 Testing procedure

Each sample was placed in a standard oedometer cell and then transferred to the computer controlled apparatus. As with the 100 mm triaxial cell the computer controlled oedometer had boundary conditions of constant vertical stress and zero radial strain, however changes in lateral stress were not measured.

Two types of experiment were undertaken. The first series of experiments investigated the influence that the initial dry density had on the change of volume of the soil during wetting. A number of samples with the same initial moisture content were compacted to different initial dry densities. The samples were then compressed to the same initial vertical stress of 50 kPa, then, while keeping the vertical stress constant, the change in axial strain was measured during inundation with water.

The second series of experiments used soil samples that were prepared, again with a constant initial moisture content but with similar initial dry densities. These samples were compressed to different initial vertical stresses (in a range from 25 kPa to 400 kPa) prior to wetting. This series of experiments investigated the effects of different initial vertical stress on the volumetric changes of the sample.

3.7 38 mm TRIAXIAL CELL

The tests performed were conventional undrained triaxial compression tests and were used to determine the value of shear strength of the compacted fill to give information regarding its trafficability.

3.7.1 General arrangement

This piece of equipment is manufactured by Wykeham Farrance Ltd and is frequently found in most commercial soil testing laboratories. The tests performed were the conventional undrained triaxial compression tests. Each sample was fitted between rigid end caps, covered with a latex membrane and was then placed inside a perspex cell which was filled with water.

Water pressure was applied to the sample using a compressed air supply via an air/water interface. The control of the cell pressure was performed manually. The sample was loaded axially through the reaction with a ram bearing on the top cap as the cell was driven upwards by a motor. The axial load on the sample is shown by a calibrated proving ring fitted externally to the pressurised cell. This apparatus was not instrumented so the measurements of axial load and axial strain were recorded manually.

3.7.2 Testing procedure

Three 38 mm sample tubes were taken from the 100 mm diameter preparation tube. After extrusion the sample was trimmed to a length of 76 mm and then weighed. The sample was placed on the base pedestal and sealed from the cell fluid by a latex membrane and O-rings. The cell was filled with water and a confining pressure applied. The cell was then driven upwards by a motor and gear box and the axial load on the sample recorded at predetermined strain intervals. This quick undrained compression test was performed at three different confining pressures. No pore pressure measurements were taken since the samples are unsaturated. This simple fairly rapid compression test provided an easy and quick method for determining a value of shear strength for the remoulded samples.

3.8 FILTER PAPER SUCTION MEASUREMENTS

A small number of filter paper suction measurements were performed on compacted samples of Wadhurst Clay. As described earlier (Section 2.5.4) this method of suction measurement is an inexpensive but useful method for determining the suctions (matrix or total) within the soil. The suction measurements from these tests were be able to give a useful indication of the suction within the soil. This helped with the analysis of the test results within the frameworks proposed by Alonso et al. (1990) and Wheeler et al. (1993) where the suction of the soil is taken as one of the stress state variables (Section 2.7).

3.8.1 Testing Procedure

The soil granules prepared to water contents of between 15 % and 21 % and were allowed to equilibrate. For each water content four samples were compacted to the same initial dry density using the same method as in Section 3.2. The samples of soil were each 76 mm in diameter and 19 mm high were then arranged in a column. Between each sample a single piece of filter paper (Whatman's No. 42: circular filter paper, 70 mm diameter) was placed. Each piece of filter paper was taken directly from the package using a pair of tweezers to avoid the possibility of crushing the filter paper or adding grease and sweat from the fingers. The soil column was then placed in an air tight container and allowed to equilibrate at a constant temperature of 20 $\pm$ 1 °C. The time necessary for equilibration was important, less than 5 days did not allow the soil and filter paper to come into full equilibrium, whereas more than 10 days allowed the possible growth of bacteria and fungi that could effect the weighing process. Some authors have suggested the use of fungicides to pretreat the papers (Fawcett and Collis-George, 1967) while other authors have not observed any difference between the treated and untreated papers (Chandler and Gutierrez, 1986). In these experiments no treatment of the filter paper was performed. After an equilibration period of 7 days the sample of soil was dismantled and the filter papers recovered and placed quickly into pre-weighed sealable polythene bags. Care was taken to ensure that any particles of soil adhering to the filter paper were removed. Each bag with filter paper was weighed to an accuracy of 0.0001 g (using an analytical balance). The filter papers were removed from the bags and dried in an oven at 105 $\pm$ 1°C, when dry the filter papers were replaced into the same bags and reweighed. Knowing the masses of the wet and dry filter paper it was then possible to calculate the water content of the filter paper and derive by using the relevant calibration curve (Equation 2.10) a value of matrix suction in the soil.

3.9 CALIBRATION, RESOLUTION, ERRORS AND ACCURACY

The function of a transducer is to sense change in its physical environment such as pressure or displacement. The measuring device must be capable of faithfully and accurately detecting any changes that occur in the measured quantity. The calibration of such an instrument relates the output from that instrument to some reference standard. To obtain the best performance from any instrument it is very important to understand the principles by which the instrument functions, its basic characteristics and the errors which influence the measurement of the

reading. Without an understanding or appreciation of these factors the reliability of the data acquired using such transducers should be questioned. It is also important to understand the relative magnitudes and hence importance of the various factors influencing the behaviour of the measurement system. For example, errors in a system caused by noise only begin to affect the accuracy of the system when the magnitude of the noise exceeds the resolution of the system. Below this point of minimum resolution no changes in the output can be detected. The accuracy and resolution of each transducer have been assessed and summarised in Table 3.1.

3.9.1 Calibration

For the calibration of the displacement transducers a micrometer that can be read to the nearest 0.01 mm is generally suitable. The displacement transducer is fitted in a stiff frame with the armature connected to the micrometer. Any adjustment to the micrometer produces a change in output from the device. A new calibrating device was designed and built for the calibration of the submersible miniature LVDTs and the proximity sensors.

The basic methods for calibrating force and pressure transducers are basically the same. The standard calibrating device that has been used is a hydraulically operated dead weight tester (manufactured by Budenburg Ltd.). A dead-weight tester consists of two cylinders of known area linked together by a reservoir. Known loads are placed on one of the cylinders on a precision fitting piston whilst the sensor to be calibrated is connected to the other cylinder. The fluid pressure in the reservoir is increased until the force is large enough to just lift the piston-weight combination. As the piston floats the force exerted by the piston-weight combination is the same as the force experienced by the transducer.

In all calibration procedures it is advisable to take readings both in the ascending and descending order. This procedure will normally reveal losses due to friction, hysteresis and other form of non-linearity present in the system. The calibration procedures of the single transducers have been described in detail elsewhere (Lau, 1988). The instruments were recalibrated every 3 - 4 months to validate the performance of each device.

3.9.2 Resolution

The resolution of an instrument can be defined as the smallest change in input that produces a detectable change in the output. It is observed when the input to an instrument is gradually increased from an initial value and no change in output can be seen until a certain input value is exceeded. The resolution depends on the amplification applied to the output voltage, the number of bits on which the analogue to digital conversion and the calibration constant. The Spectra Micro-ms uses a 12 Bit analogue to digital converter that has a full range of $\pm$ 10.24 Volts. The system auto-scales the input voltage over eleven ranges before choosing the scale that best fits the signal the maximum resolution achievable is 4.88 microVolts/Bit. The CIL interface card used for the computer controlled oedometer has a base resolution of 16 Bits where only one gain can be selected for each channel (either: $\pm$ 10 Volts, $\pm$ 1 Volt or $\pm$ 100 microVolts). The maximum resolution obtainable when using the smallest scale is 3.05 microVolts/Bit.

3.9.3 Error

The difference between the measured value and the true value is termed the error of the measurement. The error of a measurement results from the combination of a number of individual errors. By understanding how the individual errors arise, corrections to the final data may be made thereby increasing the overall accuracy of the measurement. The major causes of errors in measurement are:

- Interference (noise) - electrical, electromagnetic and electrostatic pick-up in the measuring system which can superimpose large variations in the output signal. It is important to isolate the measuring system from any external influences such as generators and shield the components from interfering with each other. When measuring small output voltages the errors caused by noise becomes the major factor affecting the measurements. Increasing the output voltage increases the resolution of the reading and depending on where the noise is generated in the electrical system, it may decrease the noise.

- Zero Drift - this represents a variation in the output with time under constant conditions input. It is caused by changes in the ambient conditions of pressure and

temperature or ageing of the electrical components. The zero drift of the load or pressure transducers can be assessed by comparing the variation between the readings corresponding to the zero conditions at the beginning and end of the test.

3.9.4 Accuracy and Precision

The accuracy of a measurement can be defined as the closeness with which the reading approaches an accepted standard value. Accuracy is a relative term influenced by static error, drift, reproducibility and non-linearity. In any experiment the accuracy is numerically equal to the referred error value, i.e. the degree of error in the final result. The accuracy is determined by calibrating under certain operation conditions and is expressed as a percentage at a certain point of the scale. For a complete system the accuracy is dependent upon the individual accuracies of the sensing element and the manipulating device. The overall accuracy can be determined by summing up the accuracy limits of the individual components i.e. if $\pm a_1$, $\pm a_2$, and $\pm a_3$ are the accuracy limits then overall accuracy (A) is expressed as $A = \pm (a_1 + a_2 + a_3)$. In practice it is not probable that all the elements of the system will have the greatest static error at the same time so to account for this the root mean square accuracy is often specified, this is expressed as $A = \sqrt{(a_1^2 + a_2^2 + a_3^2)}$.

The precision of an instrument is the closeness with which individual measurements are distributed about their mean value. It is a measure of the scatter of the set of readings among themselves. It includes the uncertainty in the reading due to random errors and the resolution of the instrument, however it gives no information relating to accuracy. The precision of an instrument is found by calculating the mean value of the scatter of the individual measurements

3.9.5 Linearity

To enable more accurate data gathering and reduction most transducers are designed to produce a linear relationship between the input and output. The closeness of a calibration curve to a specified straight line is known as the linearity of the transducer. The linearity of the instrument is expressed as the maximum deviation of the output curve from the best-fit straight line, the value of linearity is given as a percentage of the full scale. In order to avoid

misleading statements the range to which the linearity refers to should be stated.

3.9.6 Hysteresis

The hysteresis of a transducer is the maximum difference between the output readings obtained during a calibration cycle. When a device, e.g. a load cell is loaded and unloaded the non-coincidence of values obtained from the increasing and decreasing measurements is called hysteresis. This is due to frictional losses in the system or some mechanical backlash in gears or linkages. In a similar way the hysteresis for the displacement transducers can be evaluated by performing a calibration cycle of increasing and decreasing displacements.

4. CENTRIFUGE MODELLING

4.1 INTRODUCTION

Tests performed in stress path cells provide the ability to study the behaviour of single elements of soil. The stress path followed can be chosen to replicate the conditions that the soil in the prototype situation is believed to be under. By repeating similar tests under different stress paths it is possible to build up a picture of the soil behaviour at different horizons in the soil. However, it is important to understand what, if any, are the limitations of such laboratory tests when compared to the behaviour of soil in the prototype structures. Therefore to confirm if the single element tests are a valid method for comparison and prediction it is often necessary to perform experiments at a large scale so that the overall behaviour of the soil mass can be observed. The requirements for large scale testing greatly increases the costs of any testing program and may limit the type and number of tests performed. Centrifuge modelling offers an efficient and economical method of understanding the behaviour of soil as part of large structures and has been used as a link between the laboratory and prototype tests performed.

A series of centrifuge model tests was designed to study the development of swelling pressure on idealised retaining walls. Since the distribution and subsequent dissipation of pore pressures would not necessarily be uniform with depth, it was important to investigate any stress redistribution that occurred and to correlate the development of swelling pressures on model walls with those determined from the single element tests.

4.2 MODELLING AND CENTRIFUGE TESTING

Modelling is used in all aspects of engineering and is used for the study of real or envisaged situations. The degree of similarity between the prototype and the model determines how well the model is able to replicate the situation. Scaling laws relate the model to the prototype. They do not just refer to the dimensions of the model but must relate to the prototype scale all of the significant aspects of the model, soil type, permeability, boundary conditions, etc. To establish the correct scaling relationships dimensional analysis is used. Although this method neither produces analytical solutions to or reveals the mechanisms by

which the model responds it does give information about the form of the mathematical relationship connecting the relevant variables in prototype and model.

A useful example for explaining the use of modelling is to consider an element of soil in the ground. At any point in a stratum of soil the behaviour of an element of soil is determined by stress state, stress history, effective stress, the nature of the soil and the flow of water. Modelling these factors at a small scale within the laboratory environment does not generally produce similitude between model and prototype. The major difficulty with modelling soil at small scale in a laboratory is the need to model the induced stresses due to the self weight of the soil. Consider a sample of soil that is required to model a prototype situation of a normally consolidated soil with a unit weight of 18 kN/m^3 and a stratum thickness of 10 m. The total vertical stress at any depth is given by

$$\sigma = \gamma z \qquad 4.1$$

where σ is the total stress.
γ is the unit weight (= soil mass$\times$g).
z is the depth below the soil surface.

At the base of the stratum the total vertical stress is easily found to be 180 kPa. Now to perform a model test at a scale smaller than the prototype it is necessary to scale the dimensions in the problem. So instead of having a 10 m stratum a model depth of 100 mm could be used; this gives a scale of 1:100. At this smaller scale the total stress at the base of the model would only by 1.8 kPa (= 18 kN/m^3 $\times$ 100 mm) which does not model the prototype stress distribution.

To achieve the correct effective stress profile the acceleration field can be increased so instead of performing the model test under an acceleration field of 1$\times$g (Earth's gravity g = 9.81 ms^{-2}) the acceleration is increased so that unit weight of the soil is greater by a factor of n. To increase the acceleration field acting on the soil a centrifuge is used. The rotation of the centrifuge creates a radial acceleration field relative to the central axis, however relative to the soil a vertical acceleration field is created. This increases the self weight stress of the soil.

By choosing the appropriate model scale and associated acceleration field factor it is possible to replicate the prototype stress distribution in a scale model. Figure 4.1 shows the

comparison in the stress distribution of the prototype with the a scale model at $1 \times g$ and $n \times g$, where the scale factor, $n = 100$. It is possible to change both scale factor and model dimensions and still obtain the same effective stress profile, e.g. if the model was 250 mm high then to obtain a effective stress at the base of the model of 180 kPa a scaling factor of $n = 40$ would be required. Further use of dimensional analysis is able to produce scaling factors relating other frequently used quantities; these are listed in Table 4.1. It is not always feasible to reproduce all of the features of a large scale prototype within a model, so it is necessary then to assess the relevant scaling factors and determine which are the most relevant to a particular problem being investigated. In some cases it is also possible to choose some of the properties of the model so that when scaled model successfully represents the prototype. For example when modelling liquefaction in sands under dynamic loading there are conflicts between the two independently derived scale factors for time. Dynamic events within the soil have a scale factor of $1/n$ whereas time dependent diffusion has a scale factor of $1/n^2$. In this case by increasing the viscosity of the pore fluid of the model by a factor of n, the scale factors for time both become $1/n$ and the model is able to maintain similarity with the prototype.

The reliability of a model can be verified by comparison with the behaviour of a prototype. This may not always be possible since the prototype structure may not exist. An alternative technique is applied where the internal consistency of the model is tested against similar models which have different scales but representing the same prototype, this method is known as "modelling of models". Figure 4.2 shows the relationships between a model length and the scale factor in terms of acceleration ratio. As the dimensions of the model decrease the scale factor increases to maintain similarity between model and prototype. From this it is possible to assess the accuracy and limitations of the models before extrapolating their behaviour to the prototype.

When modelling unsaturated soils it is also necessary to consider the effect that increasing the gravity field will have on the matrix suction existing in the soil. For soils the increase in the gravity field increases the self weight stresses in the pore water held in the menisci between the constitutive particles of the soil. When the self weight stress from the water is greater than the existing matrix suction water leaves the menisci between the particles and moves down towards the saturated layer. This process continues until the water in the menisci between the soil particles of the unsaturated zone forms a sufficiently small radius so that the matrix suction developed is able to balance the increase in the self weight stress. This effect becomes

more evident as the size of the particles present in the soil increase (Takada, 1991). The flow of water through unsaturated fine grained soils was examined by Cooke and Mitchell (1991). Water containing chemical tracers was added to a column of unsaturated silty sand and was allowed to permeate downwards from the surface. The migration of the water could be monitored at various time intervals as it penetrated the soil. A comparison of the centrifuge model with both prototype and computer models showed agreement in the change in water content with depth as well as the time taken to reach equilibrium. Cooke and Mitchell concluded that for fine grained unsaturated soils centrifuge modelling was able to model the flow of water through the soils.

The possibility of using centrifuge modelling to study the swelling of clay was examined by Frydman and Weisberg (1991). Scale centrifuge and prototype models were tested to examine the process of swelling of a compacted clay in a cylindrical container. The results of the study indicated that centrifuge modelling could be used in the determination of the magnitude of the swelling pressure realised at equilibrium as long as care was taken to reduce the friction between the model container and the walls which was a significant factor which could influence the swelling process.

The centrifuge used for this project was an Acutronic 661, with a hinged platform located 1.8 m from the centre of rotation. The package, which contains the model, sits on the platform and this is balanced by a moveable counterweight located at the other end of the rotor. As the test is started the platform carrying the package swings outwards towards the horizontal (Figure 4.3). The radial acceleration field generated which acts radially relative to the axis of rotation is combined with the vertical gravitational acceleration of earth's gravity to produce a net acceleration field which always acts vertically with respect to the model.

Since the acceleration of a body rotating around an axis is related to its distance from the centre of rotation there is an effect on the stress distribution through the soil. Schofield (1980) reported that the error in the stress distribution due to the variation in the gravity field could be minimised by choosing an appropriate radius at which to calculate the scale factor for the model. By designing the model such that the stresses correspond to the prototype at ⅔ the depth of the model (Figure 4.4) the error between under−stress and over−stress in the model

is minimised. The error between the prototype and model can be expressed as:

$$\text{error } (\%) = \frac{h}{2\pi R} * 100 \qquad 4.2$$

where

h	is the height of the model.
$2\pi R$	is the circumference of rotation

So the higher the model (h) the larger is the discrepancy, in the stress distribution for most centrifuges this error is less than 3 %. For the Acutronic 661 and a model height of 160 mm the error is $\approx$ 1.4 %.

Events that involve diffusion depend on the permeability of the soil (which is a soil property and independent of acceleration) and the square of the drainage path length. Under high gravity fields the linear dimension of drainage path length is scaled by a factor n but since the diffusion process is a function of the square of the drainage path then the scaling factor is n^2. This implies that the swelling pressures obtained in a centrifuge experiment at 38 g lasting for 3 days on a model wall 160 mm high represents the development of swelling pressures on a 6 m high prototype retaining wall over a period of 12 years.

4.3 CENTRIFUGE CONTROL AND COMMAND SYSTEM

The centrifuge is powered by a 25 kW electric motor which through a 5:1 reducing gearbox is able to provide centrifuge speeds up 350 R.P.M. Packages weighing 200 kg can be tested at the maximum acceleration of 200$\times$g; larger payloads (up to a maximum of 400 kg) can be tested at reduced accelerations.

The centrifuge is situated within a reinforced bunker which is isolated by an armoured door during testing. One of the most important parts of the centrifuge system are the safety systems which are able to detect any problems in the system and if necessary stop the centrifuge from operating. The most likely source of danger when using the centrifuge is when the machine rotates out of balance. This arises when the counter weight is not correctly positioned to balance the inertial radial forces of the model package. If sensors detect an out-of-balance force of more than 20 kN the control system stops the centrifuge. To avoid this occurring

every part of the test package is weighed and its distance from the axis of rotation determined. A relatively simple calculation then determines the required position of the counter weight which then can be positioned. Often during a test the weight of the package can change as water enters or leaves the soil. This affects the balance of the rotor arm and may, if the change is sufficiently great, cause the safety mechanism to operate. If this change in weight may be a significant problem further balance equations are made knowing the initial weight and the expected final weight, this can result in the machine being starting out of balance and then during the test regaining balance due to the loss or gain of water.

The in−flight control and the acquisition of data from the model is performed through the use of hydraulic and electrical slip rings. The slip rings are located at the top of the centrifuge, one part of the device rotates with the centrifuge while the other remains fixed to the outer shell. In the hydraulic slip ring water flowing into the space between the rotating and non-rotating part of the slip ring passes through ports on the inner rotating spindle and into pipes which travel along the rotor arm towards the package. The electrical slip ring operate in a similar way however the connection between the rotating and non-rotating parts is made using carbon brushes (fixed) which bear on rotating metal alloy commutators. In the present configuration of the centrifuge there are 5 hydraulic and 100 electrical slip ring interfaces available.

Data acquisition is performed using an IBM compatible computer containing a Burr-Brown PCI-20001-C-2A analogue to digital interface carrier board with two PCI-20001-5M-1 expansion modules, this gives a total number of 40 channels of which 32 are operational. The 12 bit analogue to digital convertor produces a resolution of 4.8 mV/Bit for the input voltage range of $\pm$ 10 Volts; this can be improved by the use of amplifiers. There are three sets of signal amplifiers, one on the centrifuge package, one before the analogue to digital card and the final located on the PCI-20001-C-2A. The amplification of the output signal in the junction box on the package boosts the signal before the slip rings which helps to minimise the noise in the signal. Between the slip ring and the analogue to digital conversion unit there is a low pass filter with selectable frequency of 0.1 or 1 kHz.

The output from the PCI-20001-C-2A is directed into a software package called LABTECH NOTEBOOK, which as well as capturing the data output from the analogue to digital board is also able to show a real time display of the data acquired in both graphical and digital formats.

4.4 GENERAL MODEL ARRANGEMENT

The basic approach to the centrifuge model was to create a stiff retaining wall that was able to measure the change in thrust exerted by a compacted soil that was during inundation. The model was made in a centrifuge strong box with internal dimensions of 550 mm long, 200 mm wide and 400 mm high. The wall comprised 4 stiff horizontal segments, each segment (40 mm high and 200 mm wide) was supported by 3 load cells which were connected to a rigid support. Figure 4.5 shows the configuration of the model.

An important feature of the model was the design of the wall segments (Figure 4.6). The base of each segment had a low friction teflon strip inserted to minimise the inter-segmental friction. To avoid the wall segments becoming jammed during the installation and testing the width of each segment was 2 mm shorter that the width of the strong box and a bevel was cut on the edge of each segment. The gaps between the wall and the side of the wall segment were then filled with a silicon grease to prevent the entry of water or soil. The miniature load cells used were custom built by Saxeway Ltd. They were designed to so that it would be possible to fit all twelve load cells in the space between the wall and its support.

4.5 TESTING PROCEDURE

For a period of twenty four hours the load cells were connected to the power supply so that they could warm up to their running temperature and reduce any errors involving temperature drift. The wall was constructed by bolting each of the three load cells into the segment and then fixing the segment to the support. When all four segments had been completed the support and wall were placed into the strong box and fixed in place with bolts. Prior to the compaction of the soil wall segments were supported by two pieces of metal that were placed vertically between the support and the segments. Using additional bolts these supports were used to brace the wall segments during compaction and prevent the load cells from being damaged by any stray blows. The soil was then compacted behind the retaining wall in layers of approximately 20 mm by allowing a 2 kg weight to fall a distance of 0.5 m onto a square plate 36 cm^2; each location was subjected to 10 blows. This process would generally last between 2½ to 3 hours.

Preliminary tests had shown that the wetting of the clay would require a long time so to speed up the wetting process vertical drains were installed in the compacted soil. After compaction a square grid of wick drains (spaced at 25 mm centres) were inserted into the soil to reduce the drainage path lengths and speed up the swelling process. The top surface of the soil was covered with a sheet of filter paper to prevent the possibility of cracking in the top surface of the clay during the test.

The test required that there was a constant and freely available water supply to the top of the soil to supply the clay with water. A network of perforated plastic pipes was laid on the surface and was connected via the hydraulic slip ring to the main water supply. The control of the water flowing into the model was achieved by using a needle valve. An over flow pipe was installed to ensure that the water level could never rise to the top of the wall and wet the load cells. Following this, four displacement transducers were connected to a metal plate and positioned above the soil for the measurement of the heave during the wetting. On the tips of each displacement transducer armature a circular pad was placed which prevented the armature from embedding in to the soil during the inundation process. A later modification to the model was the installation of displacement transducers to measure the horizontal and vertical movement of the wall segments. Figure 4.7 shows a view of the final configuration of the of the model prior to testing.

The weight of the package was checked for the final time and the counter weight adjusted to the correct location. After loading the package on the swinging platform the transducers and water supply were connected to the relevant junctions and data logging commenced. The aerodynamic shroud surrounding the centrifuge was closed and locked remotely from the control room. The centrifuge speed was increased to give the required acceleration field. When the test speed had been reached and the transducer outputs were stable, the water supply was turned on. The data from the 21 transducers were displayed in both analogue and digital forms using LABTECH NOTEBOOK.

Each test would last until no further significant change in load on the wall segments was observed. At this point the water supply was turned off and the centrifuge stopped. The package was then removed from the centrifuge and re-weighed before being dismantled so that moisture content profiles could be taken down through the soil.

5. RESULTS

The results of the tests carried out during the research project are presented. Three different soils: London Clay, Wadhurst Clay and Brickearth were tested in a wide variety of apparatus. In excess of 170 individual tests were performed under different conditions of initial water content and dry density.

In the first section, the results of the preliminary tests such as index testing and grading are described. The main results are then presented as follows: for each piece of apparatus used, typical results and their analysis are shown for each soil, which is followed by a synthesis of all the data obtained. Finally, the results from the three soils are correlated and analysed together. Summaries of the experimental data are given in Tables 5.1 to 5.17.

5.1 PRELIMINARY TESTS

The engineering properties of soils are controlled by a number of factors such as particle size distribution, non-clay mineral composition, organic material and geological history. However for the majority of soils the mechanical properties of soils are largely determined by the finest 20 % of the constituent grains for the soils used, that is the clay and fine silt fractions. The preliminary tests aimed to classify the soils within the existing standard methods and quantify their properties.

The preliminary tests performed were: index testing, specific gravity determination and particle size distribution. These provided standard data for the soils which could be used in subsequent analysis. The tests also provided an opportunity to ensure that methods of mixing and drying employed in the sample preparation did not affect the properties of the soil.

5.1.1 Index tests and activity

Liquid and Plastic Limit tests were performed on all the soils in accordance with BS 1377 part 4. As discussed in Section 2.4.1 the index tests although based on simple empirical tests can be correlated with more fundamental properties such as shear strength (Skempton and

Northey, 1953) and compressibility (Wroth and Wood, 1978). The Liquid and Plastic Limits are the water contents at which the soil changes its mechanical behaviour. The definitions and methods used are fully defined in the current specification (BS 1377 part 4). Previous research into the use of index tests (Sherwood and Ryley, 1968) has shown that these tests are subject to variability. Sherwood and Ryley (1968) sent samples of the same soil to different laboratories for the determination of the Liquid Limit. The imprecision in the results were attributed to defects in the apparatus such as damaged cones as well as operator induced errors. Since in this research later analysis would use the index tests to establish correlations in the behaviour of the soil several determinations of the Liquid and Plastic Limit were performed using carefully checked apparatus and different but experienced operators. The results from these tests are detailed in Table 5.1.

The particle size distributions for the three soils are shown in Figure 5.1. Wet sieving was used to separate the soil into its size fractions. Any soil passing the finest mesh (0.063 mm) was subjected to a sedimentation test to determine the distribution down to a particle size of 0.002 mm. The values for activity are given in Table 5.2. The particle size data for Wadhurst Clay shown in Figure 5.1 identifies two separate distributions; one for the "as dug" material prior to any testing is shown as the dashed line and the solid line shows the particle size distribution for the soil after the testing program was completed. The difference between the curves can be attributed to the breaking of the soil particles as a result of the many cycles of wetting, drying and crushing used in the preparation of the samples. This change in particle size which was less then 0.002 mm did not significantly alter the activity value of the soil. For the Wadhurst Clay the initial Activity was 0.45 which changed to 0.48 after testing. Although the percentage change is very small it can be considered as an exceptionally high value that would not occur if the soil had not been recycled so many times No "as dug" material was available for the London Clay and Brickearth soils to allow a similar comparison although a similar result may be anticipated.

5.1.2 Compaction

The three soils were subjected to a standard compaction test using a 2.5 kg rammer (BS 1377 Part 4 1990). The curves produced give a measure of the variation of the achievable dry density for the standard compactive effort as the moisture content of the soil changes (Figure 5.2). The shaded area on each graph defines the acceptable states for compaction of

fine grained clayey soil when used as fill adjacent to structures (Section 2.13). Studies into the compaction of various soils (Parsons, 1992) indicate that the maximum achievable dry density (for the same compactive effort) is inversely proportional to plasticity index, this is demonstrated by the compaction curves of the soils used in the experiments. London Clay with the highest plasticity index (PI = 50 %) has the lowest maximum dry density in the Proctor compaction test where as the Brickearth (PI = 20 %) has the highest maximum dry density.

The method of compaction used in the preparation of the samples for the tests differed from the standard Proctor compaction method (Section 3.3.2). Figure 5.3 shows the variation of dry density with moisture content normalised with respect to the plastic limits of the three soils tested. The values are compared with the maximum dry density as determined by the Proctor compaction test. Also plotted are the lines showing the percentage of air voids for the different combinations of dry density and moisture content. The densities achieved at water contents below W/PL = 0.9 were observed to be higher than the 2.5 kg Proctor maximum compaction value which was a result of using greater compactive effort in the preparation of the samples than for the Proctor test. The specification requirements for the compaction of these types of clayey fill (Section 2.15) as well as limiting the placement water contents also controls the final air voids (and hence the dry density) in the soil. For both the London Clay and the Wadhurst Clay the majority of the samples prepared for the range of moisture contents tested had an air voids ratios of less then 5 % (the maximum specified air voids). However for the Brickearth, as the moisture content was reduced, there was a notable deviation away from the 5 % air voids ratio line, which can be explained by examining the achieved dry density and water content. The dry densities achieved with the Brickearth samples were higher than either the Wadhurst Clay and London Clay for the same value of W/PL. As the water content was reduced the data began to move away from the 5 % air voids line suggesting that the soil was on the dry side of the optimum compaction moisture content (for that compactive effort) so the achievable dry density began to reduce.

5.2 TYPICAL RESULTS

5.2.1 100 mm triaxial cell

These tests performed were designed to investigate the stress/strain behaviour of an element of compacted unsaturated soil behind a stiff retaining wall during inundation with water. The boundary conditions chosen for the experiment represented the confinement experienced by an element of soil in such a situation. During the inundation of the sample lateral strains (i.e. radial strain for the cylindrical soil sample) were kept to zero whilst allowing axial straining under a constant vertical stress.

During the ingress of water the boundary conditions of the sample were controlled such that there was no change in the radial strain whilst axial straining was allowed to take place, during this process a constant total axial stress of 50 kPa was maintained on the sample. Figures 5.4 to 5.6 show the data from typical tests performed in the 100 mm triaxial cell on the three soil types. Figures 5.4 (a) to 5.4 (d) relates to a sample of London Clay (test number LC-9), Figures 5.5 (a) to 5.5 (d) relates to a sample of Wadhurst Clay (test number WA-1) and Figures 5.6 (a) to 5.6 (d) relates to a sample of Brickearth (test number BE-5). The initial conditions of the sample, that is water content, dry density etc. are given in the Tables 5.3 to 5.14. Figure 5.4 (a) shows the variation of radial stress with time and Figure 5.4 (b) shows the corresponding variation of radial strain with time for the soils. The variation of axial stress and axial strain with time are shown in Figures 5.4 (c) and 5.4 (d) respectively. This pattern is repeated in Figures 5.5 and 5.6 for the Wadhurst Clay and the Brickearth.

The isotropic compression to 50 kPa caused a decease in the diameter of the samples. Both the initial density and moisture content of the soil influenced the amount of compression: high initial water contents and low dry densities produced greater strains than drier denser soils. This compression continued during the resting period (with radial and axial stress constant) though the rate of compression reduced. The length of resting period was between 10 and 24 hours and depended on the reduction in the strain rate to approximately half of its initial value.

After the resting period, the radial strains were zeroed and water was allowed to enter the sample. As the water started to be absorbed by the soil there was a rapid increase in the radial

stress. This is reflected in Figures 5.4 (a), 5.5 (a) and 5.6 (a) which, after the resting period show the increase in radial stress. Because the sample was prevented from swelling radially any increase in volume only occurred in the axial direction. Figures 5.4 (b), 5.5 (b) and 5.6 (b) show that while the axial stress was maintained constant at 50 kPa the axial strain became more negative as the sample elongated. After reaching a peak value, the radial stress decreased towards a constant lower value. During the swelling stage the radial deformations were always controlled to within $\pm$ 0.0025 mm of the starting point, this is equivalent to 0.005 % for the 100 mm diameter samples used.

The suctions existing within the soil due to the compaction and initial water content were reduced as water was absorbed. The boundary conditions imposed by the test of a zero change in the radial strain was achieved by adjusting the cell pressure which was equivalent to the swelling pressure that would be observed in the soil. The only direction in which volumetric changes were allowed was in the axial direction. As the test progressed the cell pressure reduced in order to maintain zero radial strain. This reduction can be attributed to the softening of the soil in conjunction with the boundary conditions of the test. As the soil became wetter a general softening of the sample occurred and this coupled with the ability of the sample to strain axially tended to relieve the swelling pressures and the axial straining continued throughout the test as water was absorbed and the volume of the sample increased. This process of axial extension and reduction of radial stress (with constant, zero radial deformation) would have continued until the sample would reach a state of equilibrium where no further water entered the sample and volume changes ceased.

5.2.2 Modified oedometer

The experiments performed in this apparatus had a higher degree of confinement than the 100 mm triaxial cell. Radial movement was prevented by the presence of the stiff oedometer ring and axial movement was restricted by the reaction of the load cell against the top platen.

When the oedometer cell was flooded with water there was a rapid increase in the vertical pressure as the soil tried to expand against the stiff confinement (Figures 5.7 to 5.9). The vertical swelling pressure increased to a maximum value but did not reduce with time. This reflected the stiff boundary restraint which prevented any change in volume of the sample.

5.2.3 Computer controlled oedometer

These tests were used to examine the volumetric behaviour of the soil. The boundary conditions were the same as for the 100 mm stress path cell i.e. constant vertical stress and zero radial strain during wetting. However as the oedometer ring was not instrumented with radial stress transducers the direct measurement of swelling pressure was not possible. The soil was compressed to a chosen vertical stress and then, while maintaining the vertical stress constant, the change in axial strain was measured as water was added.

The behaviour of the soil was found to be influenced by the dry density and imposed vertical stress. In the first series of tests samples were prepared to a similar initial density and water content. The samples were then compressed to different vertical stresses at which point they were inundated with water. The second series of tests examined the behaviour of samples that were prepared with different initial dry densities but the same water contents. These were then compressed to the same vertical stress of 50 kPa and then flooded. The vertical stress of 50 kPa was chosen to be the same stress as for the experiments performed in the 100 mm triaxial cell.

Test profiles in terms of vertical stresses and strains for these experiments are shown in Figures 5.10, 5.11 and 5.12. In all of the samples compression was observed during the application of the initial vertical stress ramp. The stress ramps were applied at different rates to achieve the required stress within one hour. On inundation volumetric changes of the sample occurred due either to swelling or collapse of the soil (depending on stress state and suction). The standard convention for strains is used, i.e., negative strains indicate expansion whereas positive strains indicate compression. For all the soils the largest strains experienced were seen in the samples that were inundated at lower vertical stresses and produced swelling. As the imposed vertical stress was increased the resulting amount of swelling was reduced. By increasing the vertical stress sufficiently it was possible to cause a positive (compressive) vertical strain on wetting. This was observed for a sample of London Clay that was compressed to 400 kPa prior to inundation (Figure 5.10). When water was added, a rapid increase in the vertical strain occurred which is usually referred to as collapse compression.

The difference in the swelling and collapse behaviour is illustrated in Figures 5.13 and 5.14. Here two samples of London Clay (L56 and L57) were compressed to two different vertical stresses (100 kPa and 400 kPa) prior to inundation. The two stress rates applied during the

compression stage were 100 kPa/hour and 400 kPa/hour but produced an almost identical change in vertical strain of 1.1 % when the required axial stress was reached. At the end of the compression stage both samples had the same dry density. With the addition of water, sample L56 began to swell and sample L57 underwent collapse compression.

The second series of experiments were performed on samples which had similar initial dry densities but different initial water contents. The samples were then compressed to a pre-inundation vertical stress of 50 kPa. When water was added the volumetric strains were measured (Figure 5.15). Although Figure 5.15 shows that the soil behaved in a similar manner, the range of dry densities tested was narrow and if samples of lower density were tested then collapse compression would have been observed.

5.2.4 38 mm Triaxial cell

A typical response of the samples when subjected to undrained compression is given in Figures 5.16, 5.17 and 5.18. After approximately 10 % axial strain the peak shear strength was reached and a rupture plane formed in the sample. An analysis of the failure plane revealed that its surface was not smooth but had some undulations, possibly a remnant of the clods of soil that had not been totally remoulded during compaction.

5.2.5 Filter paper suction tests

For each of the samples of Wadhurst Clay three matrix suction measurements were made. The suctions were calculated using the filter paper calibration curves shown in Figure 2.7 which represented the following equations:

$$\log \text{ suction} = \begin{cases} 4.84 - 0.0622\, w_{fp} & 15\ \% \le w_{fp} \le 47\ \% \\ 6.05 - 2.48 \log w_{fp} & 47\ \% < w_{fp} \end{cases} \qquad 2.10$$

The relationships between the value of suction (calculated using the above relationship with the filter paper water content) and the state of the soil samples are given in Figure 5.19. The relationships between suction, dry density and water content (in terms of plastic limit) are shown. It can be seen that as the water content of the soil is reduced so the matrix suction of

the soil increases (with dry density constant). Likewise with water content constant the suction would increase with the dry density.

5.2.6 Centrifuge model tests

The centrifuge model tests were performed to simulate to some extent the pilot scale studies that had been previously undertaken at the Transport and Road Research Laboratory (Carder et al., 1977 and 1980; Symons et al., 1989) and provide a link between the laboratory tests and a practical application.

The limitations of space within the centrifuge box (see Section 4.4) required that specially designed miniature load cells had to be used. During the initial tests spurious output from the load cells were attributed to mechanical problems in the wall such as over tightening of the fixing nuts or the interference of the wall segments with the side of the container. However as these possible problems were eliminated it became clear that the some of the irregularities were originating in the load cells.

By investigating carefully the characteristics and output from each load cell it was discovered that a number of problems were causing the errors. The load cells were manufactured using silicon strain gauges which were attached to the core of the load cell over which a metal shroud was tightly fitted (see Figure 4.6). The strain gauges initially had not been temperature compensated due to the lack of space within the load cell. Subsequent modifications provided external temperature compensation which improved the stability of the output, though a minimum of 12 hours were required to ensure that the load cells had reached a stable operating temperature.

The load cells were manufactured to have the same length though there was found to be a some variation in the actual lengths. The average length of the load cell was 14.97 ± 0.12 mm. Due to the variance in the length of the load cells unwanted stresses were created in the wall. At the end of each load cell the contact area between the bearing plate of each load cell and the wall segment allowed the wall segments to develop bending moments during installation and fixing. The implication of this was that when the wall was constructed and each segment was bolted to the support frame there was the possibility that some of the three load cells would be placed into tension because of the difference in the length. This

major problem was alleviated to some extent by carefully choosing and placing the load cells used in each segment of the wall so as to minimise the difference in their lengths. Despite this there was always some pre-tensioning of the load cells when the wall was assembled and for this reason it was possible only to measure the changes in the pressure on the wall.

During the compaction of the clay the model wall was supported as it was considered necessary to protect the load cells from any excessive force that could damage them. This was achieved by tightening screws in the support panel which would prevent any movement and protect the load cells from any shock loading. After compaction the screws were released and the load were able to measure the change in pressure on the wall.

The various stages in the assembly of the wall, compaction of the clay and the inundation of the soil are shown in Figure 5.20a. These data show all of output from the three load cells used in the top section of the wall during a centrifuge test on London Clay (CLC3). The traces from each of the load cells show the difficulties associated with the processing of the data from each test. An initial inspection of the data is unable to separate the behaviour of the soil from the stresses imposed by the inconsistency in the dimensions of the load cells and their pre-tensioning. Only by carefully recording all of the actions performed during the preparation of the model and the test itself was it possible to associate changes in the output of the load cells with either the mechanical changes in the wall or the behaviour of the soil.

The recording of data was started towards the end of the warming up period of the load cells. To construct each segment of the wall the load cells were disconnected from the power supply, the jump in the output of approximately 5 kN was not a real load but due only to the disconnection. When the wall segment was inserted into the supporting frame and the retaining nuts tightened the differences in the load cell outputs reflected the strains induced resulting from the differences in the dimensions of the load cells. For this section of wall the load cell that was placed in the greatest tension was the upper of the three load cells. The use of the metal spacer to support the wall during the compaction introduced greater tension in the load cells. As the compaction of the soil reached the top segment of the wall there was an increase in the loads. As with all of the segments of the wall the loads in the load cells reduced slightly during the night before the test was to start. This was similar to the effects seen by Carder et al., (1980) where also the load on a retaining wall reduced over a period of three months (Section 2.13.2). Carder et al., (1980) attributed this reduction in stress on the wall as being to the reduction of the excess pore pressures in the soil. Although the soil

type and time scale are different to the retaining wall models a similar relaxation of the stresses and redistribution of the suctions may explain the reduction in the loads. A further reduction in the loads on the load cells occurred after the removal of the spacers. When test was started and the soil inundated with water the soil began to swell and the loads on the load cells increased. During the swelling period there was a sudden step in the measured load; this was due to an electrical fault and was also registered by the transducers in the model that were not related to the measurement of the load on the wall. This step was removed during the data processing as it did not relate to a physical change in the load cells.

Figure 5.20b shows the variation of stress with depth before inundation. The stress acting on each section of the wall could be calculated by dividing the total load acting on each panel (derived from the output from the three load cells) by the area of the section. Previous studies on compaction from Carder et al. (1977), reported in Section 2.11.1, had shown that wall stresses after compaction were greater than an idealised (K_o) stress distribution. The variation shown in Figure 5.20b could not be attributed to any soil behaviour. The negative values of stress observed at 60 and 80 mm below the soil surface could also not be explained in terms of soil behaviour and subsequent investigations revealed that they were due to unavoidable wall stresses induced during the preparation of the model. The use of the horizontal stress in this form would lead to an inaccurate assessment of the swelling pressures. The difficulty was overcome by essentially considering as zero these stresses prior to swelling so that the monitored swelling pressure represented the change in the horizontal stress on the wall. Figure 5.21 shows the development of load in one segment of the wall. The output from the three load cells is converted into stress in Figure 5.22. Repeating this process for all four sections of the wall, it was possible to create a picture of the variation of the swelling pressure with time for all the wall sections (Figure 5.23a). For the test shown in Figure 5.23a (CLC3), the first and second section of the wall both showed an increase to a maximum pressure during the first 10 hours of testing, followed by subsequent reduction. The third and fourth sections both showed an increase of the pressure up to a maximum value after 15 hours, but with no subsequent reduction. The fact that the second section showed a significantly lower change in stress than the other three sections, was explained as being an effect of the initial stresses induced in the wall during the assembly of the model (Figure 5.20b). From this variation of swelling pressure with time it was possible to build up a profile of the variation of swelling pressure behind the wall at different times, as shown in Figure 5.23a for the test CLC3. The peak stress can be seen to occur at different times behind the wall: in section 1 after 5 hrs, in section 2 after 10 hrs, in section 3 after 20 hrs and in

section 4 after 40 hrs. Profiles of change in horizontal stress with depth at different time intervals are shown in Figure 5.23b.

Before the start of the test spot heights of the surface of the soil were taken which were then used to calculate the volume of soil mass. These were compared with after−test measurements (Figure 5.24) to reveal the change in height of the sample. Measurements of the surface displacement of the compacted soil during the test showed that there was uniform rate of swelling of the soil both along the length of the wall and behind the wall as Figure 5.25 shows. In the first 30 minutes of the test the LVDTs recorded an apparent settlement of the surface of the soil, which was caused by the wetting and softening of the filter paper placed on the surface of the soil.

At the end of the test samples of soil were taken from three points behind the wall. At each location samples were taken at ten different levels down through the soil mass. Water content profiles were taken down through the soil at three different points behind the wall (Figure 5.26). They all showed an increase in the water content but with a non−uniform distribution with depth.

In the later tests modifications were made to the wall to allow the measurement of the movement of the wall panels. Figure 5.27 features the wall movements recorded for a centrifuge test performed using Wadhurst Clay (test CWA3). The changes that took place reflect the horizontal movements of all four segments and the vertical movement of the top segment. In the first few minutes of the experiment the movement observed was attributed to the wall moving down within the box as a result of the increase in its self weight as the centrifuge package was accelerated to the running speed. As the confined soil began to swell little movement was experienced horizontally (approximately 0.005 mm). Vertical movement of the top segment of wall showed that despite a low friction teflon coating on the panel the still existed a degree of soil - wall friction remained. Overall the data confirmed that there were no excessive wall movements that could act to relieve any stresses.

6. ANALYSIS AND DISCUSSION

6.1 INTRODUCTION

Presented in this chapter is the analysis and discussion of the thesis. It will cover the approach taken to the project, the results from the experimental work and the subsequent implications. The aim of the project was to investigate the swelling behaviour of compacted unsaturated fills and to determine the factors controlling the swelling pressures developed by the soils used as fills. The context in which the work was undertaken was that of a study of the pressures developed on a stiff wall retaining compacted clayey fill which subsequently absorbed water and underwent swelling. The project has also addressed the possibility of modifying the current specification (MCHW1, 1991) to include a wider spectrum of clayey soils as fill to structures.

For the tests to be relevant to the prototype situations the confinement conditions imposed needed to simulate the boundary conditions and in situ stresses acting on the soil. The choice of using a stiff retaining wall provided a means of studying the swelling behaviour in one of the most unfavourable conditions due to the high confinement imposed on the soil. In fact, the lack of flexibility in the wall resulted in the development behind the wall of large lateral swelling pressures (under zero lateral strain) and significant vertical strains (under a constant overburden stress). As had been seen from previous studies (Carder et al., 1980), wall flexibility resulted in loss of stress on the wall so that a stiff wall would develop the largest possible stress due to swelling.

The three soils chosen were typical examples of the soils that may be found in the South-East of Britain. The plasticity index of the soils gave an indication of the differences in their swelling behaviour: 20 % for the Brickearth, 33 % for the Wadhurst Clay and 50 % for the London Clay. A testing program was undertaken on these soils, from which it was possible to compare a soil currently compliant with backfilling specifications (Brickearth) to soils whose plasticity indexes were higher than currently permitted (Wadhurst Clay and London Clay). The tests were performed to investigate whether or not the placement water content could be exceeded, whilst obtaining values of swelling pressure similar to those exhibited by the soil when this conformed to the specifications. The maximum limit of 5 % air voids required by the specification was kept as a target value in order to limit the potential for

settlements of the end product. In some cases this value was exceeded to extend the ranges of swelling pressure observed during the tests.

The behaviour of these different clays will be examined to establish the factors controlling the swelling behaviour in terms of the initial state of the soil and the testing method.

6.2 COMPARISON OF RESULTS FROM THE 100 mm STRESS PATH TRIAXIAL CELL AND THE MODIFIED OEDOMETER

The experiments performed in the 100 mm stress path triaxial cell and modified oedometer were aimed at comparing and contrasting the differences in the swelling response of compacted fine grained soils when wetted under different conditions of confinement. The 100 mm stress path cell had boundary conditions that would simulate the conditions experienced by an element of soil behind a stiff retaining wall at a depth from 2 to 2.5 m. The stress path followed was an isotropic compression to 50 kPa after which the soil was inundated from a central drain. Conditions of zero radial strain were maintained by increasing or decreasing the radial stress while free axial straining was allowed under a constant axial stress of 50 kPa. In contrast, in the modified oedometer the sample was restrained both radially (by the oedometer ring) and vertically (by a stiff load cell). On inundation the load cell was used to register any increase in the vertical stress.

From the tests in the two different apparatus, it was hoped to be able to correlate the results and establish a relationship between them.

When examining the dependence of swelling pressure on soil type, dry density, and moisture content it is important to define the swelling pressure and the conditions under which it was measured. There have been a number of different approaches to the measurement and definition of swelling pressure (Section 2.6). However all of the approaches fundamentally link the volume and stress changes in the soil by using the boundary conditions applied to the sample. Understanding the influences of these boundary conditions makes possible the interpretation of results with respect to full scale situations. The basis of soil swelling is the potential that the soil has to absorb water and increase in volume. The amount by which the soil can increase in volume depends on the type of soil, the availability of water and the degree of confinement at the sample boundaries. As water passes into a compacted soil

volume change occurs. If the soil is in a loose state it will compress (collapse), if the soil is in a dense state it will expand (swell). When the soil swells whilst volumetric expansion is restricted, there will be an increase in the stress at the boundary. This boundary stress will continue to increase as long as the suction is able to draw water into the soil. Any movement occurring at the boundary reduces the pressure at that boundary. The following example will illustrate this point.

Two identical cylinders of soil are prepared to the same initial water content and dry density. One of these cylinders is then placed into a well fitting porous steel container. When both samples are placed in a humidity controlled room and exposed to the same increase in humidity their stress strain behaviour will be different. The unconfined sample will absorb water and an increase in volume will occur. The confined sample will absorb water but will not be able to change volume, the stress on the boundary will increase up to the point at which there is equilibrium between the suctions, which are attracting water into the soil, and the confining forces exerted by the container. This example of a totally confined sample is reflected in the conditions set by the modified oedometer. The typical results shown in Figure 5.7 indicate that the swelling pressure increases to a maximum and remains constant. By changing the flexibility of the boundary conditions it is possible to control the volume and stress changes of the soil. From the above statements it would be possible to expect that the modified oedometer, having a higher degree of confinement, would produce a higher swelling pressure than the 100 mm stress path cell where the soil was allowed to expand axially.

In Figure 6.1 the total swelling pressure in the 100 mm stress path cell has been plotted against the total swelling pressure measured in the modified oedometer for samples which were tested in the two apparatus at similar initial dry densities and water contents. The graph uses data from all the soils tested. The swelling pressures of the London and Wadhurst Clay in the modified oedometer are higher than those from the 100 mm cell; the opposite case is shown by some of the Brickearth samples. An alternative way of comparing the results from the two different apparatus can be that which refers to the net swelling pressure.

Measurement of the total swelling pressure is able to give a complete view of the stress changes in a wall. This has the advantage of showing the actual stresses acting on the wall and, as such, is able to measure the variation in the stresses due to the compaction as well as those due to inundation. When deducting the initial pre-wetting stress it is possible to define a net swelling pressure. For instance when a sample is under a stress of 50 kPa, as in

the 100 mm cell, the change in the boundary stress from the pressure of 50 kPa on wetting would give the net swelling pressure. This net swelling pressure excludes the effects of compaction and burial and only represents the stress changes that occur due to the inundation. In the oedometer the net swelling pressure is obtained by subtracting the offset of the load cell when this is placed on the sample immediately before wetting. The use of net swelling pressures can be useful when it is necessary to exclude the effects due to compaction and only consider the swelling behaviour of the soil, for example when comparing the effects due to different testing methods or boundary conditions. Therefore in the analysis of the results net swelling pressures will be considered.

In Figure 6.2 the net swelling pressure from the modified oedometer and the 100 mm cell has been plotted for samples at similar initial dry densities and water contents. For both the London Clay and Wadhurst Clay samples considered, Figure 6.2 shows that the swelling pressures measured in the modified oedometer were higher (approximately double) than those measured in the 100 mm cell, as would be expected from the greater confinement imposed by the oedometer. The use of net instead of total swelling pressure produces also a better defined correlation between the results. For those samples of Brickearth which could be directly compared, the correspondence between the two values of swelling pressure measured by the different tests is closer and the explanation for this will be given in Section 6.3.

6.3 DEPENDENCE OF SWELLING PRESSURE ON DRY DENSITY AND WATER CONTENT

In order to assess the factors controlling swelling pressure samples of Brickearth, London Clay and Wadhurst Clay were tested in both the modified oedometer and 100 mm stress path triaxial cell at different values of initial dry density and water content. For each soil the initial states of the samples are plotted on axes of dry density and water content, for both the modified oedometer and the 100 mm triaxial stress path cell (Figures 6.3 to 6.8). Also shown in the graphs are lines of constant air void ratios. The values of dry density and water content were varied to give an air void ratio generally less than 5 % (to conform with the current specification (MCHW1, 1991), though some tests were conducted on samples with air void ratios up to 15 % to cover a wider range of soil behaviour. In the graphs every point is labelled with the net swelling pressure measured during the test. The results from the tests performed in the 100 mm triaxial stress path cell and modified oedometer have been separated

since, as discussed above, the swelling pressures measured were not only determined by the initial state but also by the boundary conditions applied by the two testing methods.

For one of the 100 mm samples of London Clay, as indicated in Figure 6.7, a negative value of net swelling pressure was measured. This result was interpreted as the soil, at this particular initial state with a relatively high water content, was unable to continue to withstand the initial confining stress of 50 kPa on inundation. As the boundary conditions were controlled to prevent positive or negative radial strains, the radial stress decreased below the initial value of 50 kPa in order to maintain the constant diameter of the soil. This behaviour can be associated with a collapse compression.

The aim of plotting the data in this way was to assess the possibility of establishing a qualitative relationship between swelling pressure dry density and water content. This was achieved by grouping the data into ranges depending on the value of the swelling pressure. The range of variation of the swelling pressure for each band was chosen to include a minimum of two points and generally corresponds to 50 kPa. The upper and lower limit of the bands are shown by the contours drawn in Figures 6.9 to 6.14.

In Figure 6.11, which refers to samples of Wadhurst Clay tested in the 100 mm cell, the lower band was extended to 100 kPa, since otherwise the range from 0 to 50 kPa would have included two samples which had swelling pressures of 64 and 105 kPa. In the same way the lower bound in Figure 6.14, referring to samples of London Clay tested in the modified oedometer, has been extended to account for a set of three points for which swelling pressures between 60 and 70 kPa were measured. In this way it was possible to achieve a shape consistent with the majority of the contours.

For the three clays the contours show consistent trends which are independent of the different boundary conditions applied in the 100 mm cell and in the modified oedometer. For a constant initial water content the contours show that the value of swelling pressure tends to increase as the dry density increases. In the same way for a constant value of dry density the contours show that the swelling pressure tends to decrease as the water content increases. Thus initial dry density and water content appear to be the key soil parameters which control the potential of the soils to swell.

Although the contours show similar trends, they do not overlap when a comparison is made

between the results obtained from the two different apparatus on the same soil. This reflects the fact that swelling pressure is not only a function of the initial dry density and water content but it is also dependent on the confining boundary conditions. The contours drawn for the 100 mm triaxial tests and for the modified oedometer tests can be compared for each soil tested and for similar values of initial dry density and water content. For Wadhurst Clay and London Clay (Figures 6.11 to 6.14) the comparison confirms that the swelling pressures measured in the oedometer tests were higher than those observed in the 100 mm cell; this was also demonstrated in Figure 6.2. For Brickearth Figure 6.2 suggests that there is not a significant difference between the results from the two apparatus but this does not seem to be shown when comparing the contours. Figure 6.2 was constructed by comparing the swelling pressure from the two different apparatus for samples at similar initial dry density and water content. When the contours are considered the comparison is made for swelling pressures measured over a wide range of water contents and dry densities. As it can be seen from Figures 6.9 and 6.10, the contours for the modified oedometer are steeper than those for the 100 mm cell so that similar values of swelling pressures would be obtained only in a narrow band of water content and dry density. Otherwise the contours show higher swelling pressures in the case of the modified oedometer and this conforms to what has been generally found for the other two clays as a consequence of the higher degree of confinement existing in this apparatus.

6.4 DRY DENSITY AND WATER CONTENT AS STATE VARIABLES : THE EXAMPLE OF WADHURST CLAY

Since compacted soil is unsaturated its behaviour cannot be described completely by only the three variables (q, v, and p') defining the state of a saturated soil. The recent frameworks developed to describe the mechanics of unsaturated soils were presented in Chapter 2. Toll (1990) determined that five state parameters are necessary to fix the state of such soils: deviator stress (q), mean normal stress ($p - u_a$), specific volume (v), suction ($u_a - u_w$) and saturation ratio (S_r). Alonso et al. (1990) considered only four of these parameters to be independent, thereby eliminating the saturation ratio.

When performing laboratory experiments on unsaturated soils, it is difficult to control and measure suction without making substantial modifications to the apparatus and control programs. So in order to by−pass this problem and keep the experimental conditions as

simple as possible, an alternative method to control indirectly suction was considered. The basic idea consisted of trying to relate suction to easily measurable soil parameters such as water content, dry density and saturation ratio, i.e.

$$\text{Suction} = f\ (\ w\ ,\ \rho_d\ ,\ S_r\ ) \qquad 6.1$$

In fact, among these variables S_r is supernumerary since it is dependent on dry density and water content according to the following relationship:

$$S_r = \frac{w}{\frac{\rho_w}{\rho_d} - \frac{1}{G_s}} \qquad 6.2$$

This gives,

$$\text{Suction} = f\ (\ w\ ,\ \rho_d\ ) \qquad 6.3$$

The measurements of suction were performed on samples of Wadhurst Clay using the filter paper method (Section 5.2.5), in order to investigate whether or not suction could be experimentally related to dry density and water content. If a relationship existed, then Equation 6.3 would be validated.

Before analysing the results obtained some considerations regarding the use of the filter paper method need to be made. One of the difficulties of measuring suction with the filter paper method is the contact that the filter paper has with the soil. If the filter paper is in contact with the soil then the suction measurement is that of the matrix suction, but if the filter paper is kept remote from the soil then the suction measurement would be that of the total suction. When considering a compacted soil (where the air void ratio of the soil is greater than zero), it is likely that in any particular cross-section of the sample chosen for the measurement of suction, air voids will be present. If the filter paper is then placed on this plane and the suction value calculated, it is necessary to understand what the suction value measured represents. If the percentage of air voids is very low then it would be reasonable to consider the suction value calculated as representing the matrix suction. Likewise if the percentage of air voids is very large with a small amount of the soil making contact with the filter paper then the suction measurement could be reasonably linked with the total suction. Since the

samples of Wadhurst Clay tested all had air void ratios less than 15 %, so at a section through the soil the filter paper would be in contact with the soil particles and water over 85 % of its area. Therefore suction measured by the filter paper was assumed to be the matrix suction.

Figure 5.19 shows that suction decreases as water content increases and dry density decreases. The values of suction, dry density, and water content (in terms of w/PL) were normalised in two ways: firstly with respect to the dry density and secondly with respect to the water content of the soil. In the development of the equations the water content has been divided by the plastic limit to allow possible future correlations with soils of different plasticities. Both of the normalised relationships are plotted. The results are plotted in Figure 6.15 where suction and dry density have been made non-dimensional dividing them respectively by a reference pressure p_o (p_o = 1 atm) and by the density of water (ρ_w = 1 Mg/m^3). When normalising with respect to dry density the equation of the best fit line is given by:

$$\log_{10}\left(\frac{s/p_o}{\rho_d/\rho_w}\right) = \log_{10}\left(\frac{w/PL}{\rho_d/\rho_w}\right)^{-4.28} - 0.7 \qquad 6.4$$

and when normalising with respect to the water content (w/PL) the equation of the best fit line is given by:

$$\log_{10}\left(\frac{s/p_o}{w/PL}\right) = \log_{10}\left(\frac{\rho_d/\rho_w}{w/PL}\right)^{+5.28} - 0.7 \qquad 6.5$$

Expanding equations 6.4 and 6.5 shows that they are equivalent and as such they can be rearranged to represent suction in the following way:

$$\log_{10}\left(\frac{s}{p_o}\right) = 5.28\ \log_{10}\left(\frac{\rho_d}{\rho_w}\right) - 4.28\ \log_{10}\left(\frac{w}{PL}\right) - 0.7 \qquad 6.6$$

Within the range of dry densities and water contents considered in the experiments on Wadhurst Clay Equation 6.6 allows the definition of suction as a function of dry density and water content. This result shows that, under the above conditions, controlling the dry density and water content of the soil is equivalent to controlling two of the state variables governing the behaviour of unsaturated soils usually expressed in the literature in terms of specific

volume and suction.

The values of dry density and water content obtained from samples of Wadhurst Clay on which filter paper measurements were made are plotted in Figures 6.16 and 6.17 which refer respectively to tests performed in the 100 mm cell and in the modified oedometer. In the same figures the values of suction are indicated. For a similar dry density a decrease in water content could be related to an increase in suction, this can be seen in Figure 5.19 where the relationship between water content and matrix suction (for similar dry densities) is not linear. Likewise, for soils of similar water content an increase in the dry density also resulted in an increased value of suction.

The association of values of suction with values of swelling pressures measured for samples of similar initial dry density and water content in both the 100 mm cell and modified oedometer is shown in Figure 6.18. In both cases the swelling pressure tends to increase as the suction increases. This trend would have been expected since suction and swelling pressure have been shown to be dependent on dry density and water content in the same manner (suction and swelling pressure both increase as dry density increases and water content decreases). Although at low swelling pressures the data points seem to align, at higher swelling pressures the increase in suction seems to be more rapid. This is the case for both the 100 mm and modified oedometer. However a better definition of the relationship between matrix suction and swelling pressure would require future testing at intermediate values of suction and swelling pressure

The dependence of suction on dry density and water content has not been investigated for London Clay and Brickearth. However the fact of being able to identify bands of variation of swelling pressures for these two soils by controlling the initial dry density and water content of the samples, suggests that within each band suction did not have a significant independent effect on the swelling pressure. Therefore dry density and water content proved to be effective in controlling, together with the stresses, the state of these unsaturated soils.

6.5 METHOD OF COMPACTION

Standard methods of compaction involved some form of compaction plant passing over the soil until a required standard, either in terms of method or end product specification

(Section 2.12), is achieved. The compaction of an element of soil behind a retaining wall as well as increasing the soil density, creates residual lateral stresses which remain in the soil after the compaction plant has passed (Clayton and Symons, 1992). In this project the method chosen for the compaction of the soil (Section 3.2), although not an exact replication of any standard compaction process, was a repeatable method that was able to provide samples of soil that were consistent in fabric and density.

The horizontal stress distribution after compaction has been observed to be significantly different from K_o or isotropic conditions (Broms, 1971 and Carder et al., 1980). In the 100 mm stress path triaxial cell the isotropic compression used for the initial loading path of the samples did not attempt to replicate the development of stresses due to compaction, but solely provided a confining stress that could be applied to the soil prior to inundation.

6.6 THE USE OF THE COMPUTER CONTROLLED OEDOMETER TO STUDY VOLUMETRIC CHANGES

A large number of tests were performed in the computer-controlled oedometer. The tests were complementary to those undertaken in the 100 mm stress path cell and were able to study the volumetric behaviour of the soil over a wide range of moisture contents, dry densities and confining stresses. The boundary conditions in the computer controlled oedometer were the same as the 100 mm stress path cell. After the initial compression the vertical stress was maintained constant (allowing vertical straining) and the radial strain was always zero due to the confinement of the oedometer ring; no measurement was made of the change in radial stress.

By examining the relationship between the dry density and the vertical strain it was possible to collate the data from all of the tests performed. Figure 6.19 illustrates the way in which volumetric strains can be controlled either by imposing different vertical stresses or changing the initial dry density of the soil. The initial points for all the soils lie on the zero vertical strain line; they are the values of the dry density of the samples after the initial compression. The end points indicate both the change in dry density and change in vertical strain for each sample. The lines that join the initial and final points are not stress paths followed during the test but only serve to identify the corresponding initial and final points for every test. The end point for each test has the vertical confining stress indicated. It is possible to extrapolate lines

of constant pressure by joining the end points of the tests. Figures 6.20 and 6.21 show lines of constant vertical stress for London Clay and Wadhurst Clay. When there is only one result at a particular pressure, the dotted line has been drawn to indicate tentatively the assumed relationship.

The study of the volumetric changes in a compacted soil provides a knowledge that can be applied to the control of the soil when used as an engineering material. The appropriate dry density or confining stress necessary for the control of volumetric strains can be determined in two ways. The first method can be explained by examining Figure 6.21 (Wadhurst Clay). It can be seen that for tests performed under an initial vertical stress of 50 kPa there will be an initial dry density for which the soil will not undergo any net volumetric straining (i.e. change in volumetric strain after inundation). For the Wadhurst Clay the initial dry density necessary to give a net volumetric strain of zero (with a water content of 20.3 %) would lie between 1.57 and 1.59 Mg/m^3, since densities below 1.57 Mg/m^3 result in compression and densities above 1.59 Mg/m^3 result in swelling. The condition of zero volumetric change can be seen with sample W24 in Figure 6.21 (indicated by the letter D). This sample started swelling from a water content of 20.3 % and a dry density of 1.58 Mg/m^3 and reached a final water content of 26.6 % and a dry density of 1.52 Mg/m^3. As in the case of sample D the zero net compressive strain is accompanied by a decrease in the dry density and an increase in water content which both determine a decrease in suction. From Equation 6.6 it is possible to calculate the variation of matrix suction from an initial value of 458 kPa to a final value of 117 kPa. Under a vertical stress of 100 kPa the volumetric change was limited to a swelling of less that 1 % of its original height.

The second method uses the applied vertical stress to determine the dry density of the soil required to minimise the volumetric strains. Figure 6.20 shows results from tests performed on London Clay over a wide range of dry densities and under different vertical stresses. The results indicate that for a soil with a dry density of 1.55 Mg/m^3 and a water content of 21.8 %, it would be necessary to apply a vertical stress of 300 kPa to obtain a zero net volumetric strain.

With the above methods it is necessary to appreciate that increasing the vertical confining stress to control the volumetric strain of the soil during inundation may lead to the development of increased lateral stresses. However by referring to the results from the other measurements of swelling pressure (such as the 100 mm stress path cell or modified

oedometer) it is possible to obtain a value for the lateral stress for the soil in this condition.

6.7 THE INTERPRETATION OF TEST RESULTS WITHIN A FRAMEWORK OF UNSATURATED SOIL BEHAVIOUR

Equation 6.6 now makes possible the calculation of suction within a soil if the dry density and water content are known. This is an indirect method using a relationship between the suction in the filter paper and the state of the soil. The tests performed as part of this research were primarily aimed at investigating the swelling pressure developed in compacted fill. With the configuration used for the apparatus, the water content changes that occurred during the inundation stage could not be measured. This means that by using Equation 6.6 the changes in suction of the soil could be only calculated either at stages at constant water content or when direct measurements of water content were taken, that is at the beginning or end of the test. This means that it has not been possible to obtain information regarding the change in the suction of the soil samples during testing. Figure 6.22 shows the variation of specific volume and suction with vertical stress for some of the computer controlled oedometer tests performed on Wadhurst Clay. The calculation of the specific volume comes directly from the test data whereas the calculation of the suction has been made using Equation 6.6. The boundary conditions of the test were such that the vertical stress on the sample was kept at a constant value during inundation. So, although it was not possible to determine the change in suction, it was possible to obtain a value of the suction at the end of the test when the soil had reached equilibrium. In each graph the dotted line joins the end of the compression stage with the end of the test.

Under compression the suction of the samples increases slightly; after inundation there is a decrease in suction and an associated increase in specific volume. For samples with the same initial densities and water contents it can be seen that the imposition of a larger vertical stress reduces the dissipation of suction and the change in dry density.

All of the Wadhurst Clay samples tested in the computer controlled oedometer exhibited swelling on inundation. With regard to the other soils the lack of suction measurements prevents the direct calculation of values of suction. It is reasonable, however, to expect that for London Clay and Brickearth the relationship between dry density, water content and suction would remain with the same fundamental form as Equation 6.6 but with different

values for the constants. However a comparison with London Clay would be useful to show the variation of suction when collapse of the soil occurs. For the purposes of this analysis the calculation of the suction for London Clay has been carried out using the same constants as determined for Wadhurst Clay. This allows to show qualitatively the variation of suction during the test and irrespective of its actual value. Figure 6.23 shows the behaviour of two samples of London Clay when tested in the computer controlled oedometer. Both of the samples started at similar specific volumes and were loaded vertically to stresses of 100 and 400 kPa and then inundated. Calculations of suction estimated using Equation 6.6 showed that both samples underwent an increase in suction during compression but on inundation the sample having the lower vertical stress of 100 kPa showed an increase in the specific volume as the suction decreased, whereas the sample that had been compressed to a vertical stress of 400 kPa displayed an increase in volume as the suction decreased.

With these examples it is possible to represent the behaviour of the soil tested in the computer controlled oedometer in terms of the framework for unsaturated soil proposed by Alonso et al. (1980). As described in Section 2.7 this framework supports the existence of yield surfaces which separated the zones of elastic and plastic soil behaviour. These yield surfaces can be reached by varying the loads and suction of the soil. Figure 6.24 shows the path that would be followed by two different soil samples (A and B) during loading and inundation. Since no measurements of radial stress were made in the computer controlled oedometer the mean effective normal stress, used in the model proposed by Alonso et al. (1980), will be replaced by the vertical stress.

During compaction the soil will reach a state to which a certain yield surface would correspond. This surface is the yield surface that the sample would reach after being unloaded during preparation and then sufficiently compressed during testing. The example of two soil samples (A and B) with an initial state after preparation within this yield surface is illustrated in Figure 6.24. The samples have the same value of specific volume and suction at this zero vertical stress. During the compression stage of the test both samples show a decrease in specific volume (and consequent increase in suction) as the vertical stress is increased. If for one of the samples (B) the suction and vertical stress are increased beyond the yield surface a new yield surface is created. On wetting the suction of both samples reduces. The sample which in the first stage of the test was compressed to the lower vertical stress (path A) would undergo an increase in specific volume, whereas the sample which was compressed to the higher vertical stress (path B) would undergo a decrease in specific volume. During

inundation the path followed by sample A would remain within the Load Collapse yield surface that corresponded to the state of the soil after preparation and only swelling would occur in this case. Likewise, for path B the compression to the higher stress would push both the Load Collapse and Suction Increase curves beyond the original yield surface. When the sample is wetted under constant vertical stress collapse of the soil occurs and large plastic strains develop. A complete interpretation of this behaviour of the soil within a framework for unsaturated soils would require tests over a wide range of specific volumes, vertical stresses and suctions.

6.8 COMPARISON OF THE CENTRIFUGE TESTS WITH LABORATORY EXPERIMENTS

The research performed in the 100 mm stress path triaxial cell was directed at analysing the behaviour of an element of compacted soil under similar conditions as would exist behind a stiff retaining wall. When comparing the results from the 100 mm stress path cell with those from the centrifuge it is necessary to consider the swelling pressures developed for similar vertical stresses. In all of the tests performed in the 100 mm cell a constant vertical total stress of 50 kPa was applied to the sample during inundation. This stress would correspond to an equivalent depth behind the retaining wall which could be determined by knowledge of the bulk unit weight of the soil. The range of depth represented by the 100 mm stress path cell tests was between 2.3 and 2.7 m. For the soils tested in the centrifuge the depth equivalent to a vertical stress of 50 kPa was found to correspond to the second section of the model wall, which was located between 40 and 80 mm below the soil surface (1.5 to 3 m at the prototype scale). For example the centrifuge test CLC3 which is shown in Figure 6.27a as having a maximum swelling pressure of 60 kPa has been extracted from Figure 5.23b. The initial bulk unit weight of the soil (2.021 Mg/m^3) was used to calculate the depth at which the pressure of 50 kPa would occur, this depth (2.5 m) coincided with the second segment of the wall in the centrifuge model. Figures 6.25a, 6.26a and 6.27a show the maximum swelling pressures measured in the centrifuge tests and those measured in the 100 mm stress path triaxial tests for the other soils.

The swelling pressure measurements from the centrifuge tests generally fall within the swelling pressure boundaries identified for the 100 mm cell tests. This indicates that the swelling pressures measured in the centrifuge and those measured in the 100 mm stress path

cell are comparable when similar dry density, water content and confining stress are considered.

The comparison of the swelling pressures from the centrifuge and the modified oedometer has been attempted by looking at the maximum swelling pressure developed in the centrifuge at various depths. A typical outcome is shown in Figures 6.25b, 6.26b, 6.27b for the three different soils. As can be seen, only two out of eight points fall within the same range of swelling pressure determined by the oedometer, all the others are generally lower than the values determined in the oedometer at similar initial water contents and dry densities. Similar results have been found at other depths. The reason for such a poor comparison can be explained by the fact that in the oedometer the volumetric changes are prevented and the confining stress is not known.

6.9 COMPARISON OF THE CENTRIFUGE TESTS WITH THE PILOT SCALE STUDY

The centrifuge tests have proved a useful tool for the analysis of the swelling behaviour of compacted soil. Despite the difficulties encountered with the load cells (Section 5.2.6) the data from the tests were able to confirm the applicability of centrifuge testing to unsaturated soils. The justification for such a statement can be seen when comparisons are made between the prototype and scale model studies performed. The London Clay used for the tests in this thesis was taken from the same stock pile of soil as was used in a full scale retaining wall test performed at the Transport Research Laboratory (Symons et al. 1989) it was possible to compare the mechanical behaviour of the soil without needing to consider the differences in the soil type. Therefore the data gained from the experiments performed in the retaining wall facility at the Transport Research Laboratory (Section 2.10.2) provide a means of comparing the behaviour of soil when compacted behind a retaining wall.

As described earlier the prototype retaining wall was designed to measure the load on a section of wall that was 2 m wide and extended 2 m below the surface of the soil. The centrifuge model comprised four sections of instrumented wall each section 40 mm high, which at the testing speed represented a height of 1.5 m, giving a total wall height of 6 m. The variation of lateral thrust with time, shown in Figure 2.55 can be converted into lateral pressure by dividing the value of thrust by the area of the wall. Figure 6.28 presents a

comparison of the upper sections of two centrifuge model tests (CLC3 and CLC4) compared with the prototype retaining wall. The scaling of the x-axis is presented in days; this is the true scale for the prototype wall and the scaled time for the centrifuge tests (as described in Section 4.2 the scaling factor $1:38^2$ was used to convert the experimental time for the model wall to an equivalent time for the prototype).

The most obvious similarity between the centrifuge models and the prototype wall is that the variation of pressure on the wall with time follows a similar pattern. At the commencement of inundation there is a rapid rise in the swelling pressure which decreases after reaching a peak. The peak pressures for the centrifuge tests CLC3 and CLC4 are higher than the peak for the prototype due to the different conditions of dry density and moisture content of the soil prior to wetting (as shown in Figure 6.28).

In terms of volumetric changes the vertical movement of the surface of the soil in the centrifuge showed a more consistent rate of heave when compared to the prototype wall. The events that occurred during and after construction of the prototype wall affected the thrust on the wall as well as the surface movements of the soil, as it can be seen in Figures 2.55 and 2.56.

Using the centrifuge model it is possible to estimate the time necessary for the soil to cease swelling. The rate of heave of the soil in the centrifuge test (taken from CLC3) reduced from 0.157 mm/hour after 6 hours from the time of inundation to 0.044 mm/hour after 70 hours after inundation. These values correspond to full scale rates of 0.036 m/year after 1 year and of 0.01 m/year after 11 years. An extrapolation of these data was attempted using curve fitting techniques and is shown in Figure 6.29. A second degree polynomial fit would suggest that the heave would reach a maximum of 7.7 mm ($\equiv$ 0.289 m) after 160 hours ($\equiv$ 26 years). This would infer that 73 % of the final swelling might occur within the first 80 hours ($\equiv$ 13 years).

The importance of the drainage conditions is shown in Figure 6.30, where a centrifuge test (CLC2) and a test from the prototype wall on London Clay are compared. Both started with broadly similar initial conditions of water content and dry density. In the centrifuge test vertical drains were not used whereas for the prototype experimental wall sand drains were used to increase the rate of inundation of the soil. The swelling response of the clay with time can be seen to be significantly different. The experiment on the prototype wall showed a rapid

rise in swelling pressure over the first 100 days, whereas the centrifuge test displayed a much slower development of swelling pressure equivalent to a period of more than 8 years. The effects of using drains to speed up the swelling process has been observed in the field. Blight and De Wet (1965) compared the surface movements of two areas of unsaturated silty clay which were flooded. One area had vertical drains spaced every 3 m, the other area had no drains inserted. Figure 6.31 shows a marked difference in the measured surface movements between the two areas. The maximum value of heave in the untouched soil took place approximately 4 years after the maximum heave was observed in the area that had drains.

6.10 COMPARISON OF CENTRIFUGE RESULTS WITH COMPUTER CONTROLLED OEDOMETER TESTS

Some of the Wadhurst Clay prepared for the centrifuge model test (CWA3) was used to perform three computer controlled oedometer tests. The three oedometer samples used for this comparison were taken during the preparation of the centrifuge model by driving oedometer rings into the compacted soil. This was able to produce samples which had same initial water content and dry density as the centrifuge test. Calculations for the total stress at the mid-points of each section of the wall were made and the samples were compressed to these initial stresses in the computer controlled oedometer. The samples were inundated and the vertical strain was measured under the constant vertical stress. As discussed previously (Section 6.5), the increase in the overburden pressure was able to limit the amount of swelling (Figure 6.32).

Figure 6.33 shows a comparison of the initial and final water contents of samples taken from the centrifuge tests and the computer controlled oedometer. The soil in the centrifuge model and the soil in the computer controlled oedometer started from an initial water content of 18 %. At the end of the tests samples were taken to determine the final water contents. The final water content profile for the centrifuge model shows that water was absorbed by the soil at all levels, more being absorbed at the surface than at lower levels (35 % near the surface of the soil, decreasing to 20 % at the base).

This pattern of moisture content change with depth compares with the final distribution of water content in the prototype wall tested at the Transport Research Laboratory (Figure 2.57). The samples tested in the computer controlled oedometer under various vertical stresses show

a different distribution of water content with depth. Of the three samples tested only the upper sample had the same final moisture content as the centrifuge model, the remaining two samples had water contents up to 3 % higher than the corresponding water contents from the centrifuge test. The difference in the final moisture contents can be explained by examining the differences in the hydraulic boundary conditions of the two different tests. Since the samples of soil in the oedometer came from the sample of soil as used in the centrifuge it would be expected that under an equivalent pressure the coefficients of permeably (k) and compressibility (m_v) would be the same. Therefore by using the equation for 1 dimensional consolidation it is possible to compare the effects of the drainage paths in the two experiments. The time taken for one dimensional consolidation or swelling (t) is given by:

$$t = \frac{D^2 m_v \gamma_w}{k} \qquad 6.7$$

where

D is the drainage path length

k is the coefficient of permeability

m_v is the coefficient of volume compressibility

For the oedometer the drainage conditions can be easily described as being from the top and bottom of the sample. The oedometer samples were 19 mm high which would give a drainage path length of 19/2 mm In the centrifuge two conditions of drainage existed; vertical wick drains as well as top and bottom drainage. The vertical wick drains were spaced at 25.4 mm centres giving a drainage path length of 25.4/2 mm where as the drainage path length for the top and bottom of the sample was 160/2 mm. By considering the two conditions separately it is possible to compare the time necessary for swelling to occur by relating the relevant drainage paths this has been achieved by rearranging Equation 6.7 for each case and dividing to give the time for swelling in terms of the drainage path length.

$$t_{centrifuge} = t_{oedometer} \left(\frac{D_{centrifuge}}{D_{oedometer}} \right)^2 \qquad 6.8$$

If the vertical wick drains are considered the comparative time taken for swelling is given by

$$t_{centrifuge} = t_{oedometer} \left(\frac{25.4 / 2}{19 / 2} \right)^2 \qquad 6.9$$

resulting in a comparative swelling time of,

$$t_{centrifuge} = 1.8\ t_{oedometer} \qquad 6.10$$

If drainage occurred from the top and bottom of the model then the time for swelling would be given by

$$t_{centrifuge} = t_{oedometer} \left(\frac{160 / 2}{19 / 2} \right)^2 \qquad 6.11$$

giving a comparative swelling time of,

$$t_{centrifuge} = 70\ t_{oedometer} \qquad 6.12$$

From Figure 6.32 an extrapolation of the time necessary for equilibrium to be reached can be taken as 30 hours, if this value is then substituted into Equations 6.10 and 6.12 it is possible to obtain an estimate for the time necessary for the centrifuge sample to reach equilibrium. With the vertical wick only drains a 30 hour oedometer test would require 54 hours running time in the centrifuge where as with only top and bottom drainage a running time of 2100 hours would be necessary.

The centrifuge test CWA3 was stopped prematurely after approximately 17 hours due to electrical fault in a junction box. This event prevented the soil from reaching an equilibrium condition and resulted in the discrepancy between the water content of the soil with depth as shown in Figure 6.33. The similarity in the water contents for the upper section of the wall can be explained by the combined drainage conditions of both vertical and horizontal drains contributing to a reduction in the time necessary for complete swelling.

6.11 APPLICATION OF RESULTS TO CURRENT SPECIFICATION

One of the aims of this research was to investigate the possibility of widening the range of acceptable soils that could be used as backfill material to structures. It has been shown that there are combinations of dry density, water content and initial stress state which would minimise the development of swelling pressures. The current specification, described in Section 2.13 of Chapter 2 limits the soil type which can be used and controls the density and water content of the compacted soil. The choice of the soil type is determined by a plasticity index not greater than 45 % and a liquid limit not greater than 25 %, therefore prescribing a plastic limit less than or equal to 25 %. The additional requirement on dry density and water content is expressed in terms of air void ratio for which a limit of 5 % is set. Because of its similarity with the conditions existing for an element of soil behind a stiff retaining wall, the results from the 100 mm stress path cell will be used to examine the possibility of widening the current specification (MCHW1, 1991).

Of the three soils tested in this research only one of these (Brickearth) was acceptable for use as fill to structures according to the current specification (MCHW1, 1991, Section 2.13). The upper limit of placement water content is set by the trafficability of the soil and the lower limit of water content is set by the potential that the soil has to swell. By examining the data obtained for Brickearth it is possible to see the full implications of the results.

Figure 6.34 shows the initial conditions of the compacted Brickearth with the associated values of swelling pressure measured after inundation. The swelling pressure boundaries as developed in Section 6.3 are indicated as well as the lower limit for placement water content of the soil accepted by the specification (PL−4). Despite the scatter of the data a reasonable interpolation indicates that a maximum swelling pressure of 50 kPa might be measured while still satisfying the specification. If this value can be deemed to be acceptable then this value can be used to examine the lower limit of the other soils.

For London Clay (Figure 6.35) we can see that in order to obtain a maximum swelling pressure of 50 kPa a minimum water content of 28 % (1×PL) would be required. This limit in conjunction with the limit on trafficability would provide a range, albeit a small range of water content at which the soil could be compacted and which tests indicate will result in low swelling pressure, that is less than apparently allowed by the current specification.

For Wadhurst Clay a similar conclusion could be drawn however the scatter of the data create difficulties when trying to be specific. Figure 6.38 shows a tentative if somewhat conservative interpolation giving a minimum water content of 23 % (PL−1).

On the Basis of the above soils with higher plasticity indices could be used if the placement condition were altered such that the swelling pressure on adjacent structures could be kept to a value less than or equal to the swelling pressure developed by soils which are currently acceptable.

6.12 SUMMARY

The swelling pressure developed by unsaturated compacted clayey soils has been measured by using different pieces of apparatus and the importance of evaluating similarity between prototype and model (whether single element or centrifuge) has been discussed.

The testing methods provide information on the swelling behaviour, in terms of stresses in the 100 mm stress path cell and modified oedometer and in terms of volumetric response in the computer controlled oedometer.

The study of volumetric behaviour has enabled the formulation of an approach that could be used in the control of excessive expansion of compacted unsaturated soil. This has been achieved by controlling either placement density or overburden stress and it has been demonstrated how volumetric changes of the soil can be minimised. However it has been recognised that this method of control of soil volume may lead to additional stresses on adjacent structures.

7. CONCLUSIONS

7.1 EXPERIMENTAL WORK

The study of the swelling behaviour of unsaturated fine grained soils has required the development of various pieces of equipment able to provide data from different testing conditions. All the experiments were designed to represent the conditions of zero lateral strain which apply to swelling soil placed behind a stiff retaining wall. The research considered the case of a stiff retaining wall in order to provide an upper limit to the swelling pressure. Samples of compacted unsaturated fine grained soil were inundated with water during the experiments and their volumetric and stress response were investigated.

In the 100 mm stress path cell the confining pressure was adjusted in order to maintain a zero radial strain condition, while the vertical stress was kept constant and the sample inundated. The change in the horizontal stress occurring as a result of the inundation has been considered as the swelling pressure of the sample. The test provides values of the swelling pressure for an element of soil at a given depth whilst allowing volumetric change. Since the samples were unsaturated, the measurement of volume change required the implementation of a new technique consisting of accurate radial strain measurements.

For more flexible walls a decrease in the magnitude of the swelling pressure developed can be expected. In the development of the 100 mm stress path cell the possibility of accounting for such a condition has been considered. In fact, in order to simulate a greater flexibility in the wall the control program can be modified to allow for various degrees of horizontal straining to occur.

The modified oedometer imposes boundary conditions of zero horizontal and vertical strain, and is able to measure the vertical stress developed by the sample during inundation. The computer controlled oedometer can be used in a similar manner to the 100 mm stress path cell to measure the volume changes experienced by an element of soil during inundation at a given depth, maintaining a constant vertical stress.

Centrifuge tests were performed on a model representing a stiff wall retaining unsaturated compacted soil. The model was instrumented with load cells and displacement transducers to

observe the swelling response with time and depth. The results were compared with those from the laboratory tests and provide a means to relate some aspects of the behaviour of compacted unsaturated soils observed in the laboratory to the behaviour observed in tests performed on a prototype wall at the Transport Research Laboratory.

Swelling pressure can be regarded as a total change in pressure on the structure (total swelling pressure) or as a net change in pressure when referred to the initial post compaction stresses (net swelling pressure). In the laboratory tests both the absolute and net changes in pressure could be obtained. In the centrifuge tests only the net pressures could be obtained. As discussed in Section 6.2 it was considered more reasonable and useful to refer to the net value, since this can be taken into account as an additional component to the lateral stress distribution induced by the compaction and the self weight of the soil.

7.2 DEPENDENCE OF THE SWELLING BEHAVIOUR OF FINE GRAINED SOIL ON THE INITIAL STATE

The experimental work has been carried out on three different fine grained soils with varying plasticity: Brickearth, Wadhurst Clay and London Clay. Several tests to measure the swelling pressure were performed in the 100 mm cell and modified oedometer on samples having varying initial water contents and dry densities. Although in the two apparatus the samples were subjected to different boundary conditions, the results showed consistent trends of the variation of the swelling pressure with initial values of water content and dry density. The values of swelling pressure were found to increase as the dry density increased and the water content decreased. Bands of variation of swelling pressures with initial water content and dry density were defined (Section 6.3).

For Wadhurst Clay it was found that dry density and water content can be sufficient to define the state of the soil, provided that the values of the applied stresses are known. This was shown by performing filter paper suction measurements which could be quantitatively related to water content and dry density (Section 6.4).

In order to generalise this result similar tests would need to be performed on a large number of different unsaturated fine grained soils. The implication following from the validation of the result from Wadhurst Clay would be that two easily measurable variables, such as dry

density and water content, could replace suction and specific volume when defining the state of unsaturated soils. The suction measurements on Wadhurst Clay were found to be useful in interpreting the observed behaviour within the most recent frameworks on unsaturated soils (Section 6.7)

7.3 COMPARISON OF SWELLING PRESSURE FROM LABORATORY, CENTRIFUGE AND PILOT SCALE TESTS

The tests performed in the 100 mm stress path triaxial cell and in the modified oedometer although imposing the same radial boundary conditions imposed different vertical boundary conditions to the samples when measuring the swelling pressure. In the first case the vertical stress was controlled and the sample was allowed to strain axially; in the second case the lateral stress was not known and the sample was prevented from straining axially. As discussed in Section 6.2, the difference in the boundary conditions was reflected in the swelling response of the soil.

Despite the fact that the modified oedometer did not allow the control and knowledge of the boundary stresses acting on the sample, the experiments were performed to assess wether this simple test could substitute the more complex tests in the 100 mm cell through possible correlations between their results. However the number of samples tested at similar water contents and dry densities in the two different apparatus were not sufficient to establish a quantitative correlation. It was generally indicated that higher swelling pressures were obtained in the modified oedometer due to the greater degree of confinement. In order to be able to make any reliable correlations a substantial number of additional tests would be required. These tests should include observations of swelling pressures in both the 100 mm cell and modified oedometer over an extended range of densities, water contents and pressures.

The maximum swelling pressures measured in the 100 mm cell under a given vertical stress (50 kPa) were found to be similar to those measured in the centrifuge tests, provided that the comparison was made between the section of the model wall at a depth equivalent to the vertical stress applied in the 100 mm cell (Section 6.8), i.e, at a depth equivalent to 50 kPa The results indicate that the boundary conditions of soil compacted behind a stiff retaining wall was successfully simulated by single element tests in the 100 mm triaxial cell.

In the upper sections of the wall the maximum swelling pressure did not correspond to the swelling pressures at equilibrium since as water entered the soil volumetric straining and softening occurred, relieving these pressures. At greater depths behind the wall the maximum swelling did correspond to the maximum swelling pressure in measured in the tests however as discussed earlier this may be as a result of insufficient test time for equilibrium at depth to be achieved.

A relationship between swelling pressure and depth in the centrifuge tests could not be found. Had the tests in the 100 mm stress path triaxial cell been conducted for different vertical stresses, a comparison with the centrifuge test would have required the increase of the efficiency of the drains so that the availability of water to the deeper layers in the centrifuge would be comparable to that existing in the triaxial cell. Tests performed in the computer controlled oedometer on the same soil as used in one of the centrifuge tests, showed that after wetting the final water contents for various vertical stresses were higher than those measured in the model, especially for the lower layers (Section 6.10).

The computer controlled oedometer provided a swelling response in terms of volumetric strains which can be regarded as an upper limit, since the soil in this condition was able to undergo the maximum possible increase in water content for the imposed vertical stress level. In this case the lateral stresses were not known and the sample was constrained volumetrically.
The qualitative response of swelling pressure with time in the centrifuge tests was found to be similar to the pilot scale retaining wall experiment performed by Symons et al. (1989) at the Transport Research Laboratory. This comparison also emphasised the important role played by the drainage conditions on the development of swelling pressures in the soil. In order for the centrifuge to be able to simulate the in situ swelling response behind a stiff retaining wall, care has to be taken to ensure that similar drainage conditions are achieved.

7.4 PRACTICAL IMPLICATIONS OF THE RESEARCH

The use of fine grained fill is beneficial in two main ways, economic and environmental. The costs of removing unsuitable soil and importing expensive granular fill are greatly reduced if locally available fill is used. The environmental savings come from the potential reduction

in extraction of the dwindling deposits of granular material and the reduction in construction traffic onto and off the site, often on minor roads.

There are a number of points that must be considered before using such fill:

The construction application - To assess the difficulties associated with using compacted fills, it is necessary to understand the application for which they will be used. If fine grained soils are used as fill material in areas behind structures that will not be used for some time, then the fill may be compacted to a low density and low moisture content. Any subsequent possibility of developing large swelling pressures on wetting would then be avoided since in this state it is more likely that collapse compression would occur. However, in situations such as the approach roads to bridge abutments, substantial settlements may result and where the road passes over areas of compacted fill, more rigorous control of the density of the compacted soil is necessary. Any swelling may cause deformations of the road surface or detrimental increases in the stresses acting on earth retaining structures.

The properties of the soil - Like other engineering fill materials fine grained soil when used as fill needs to have consistent properties so that its behaviour can be predicted and controlled. As with granular material, regular testing of the soil should be made to guard against any variations that may affect its swelling potential. When using these fills the strict control of moisture content and dry density after compaction are crucial. As has been demonstrated in this study a decrease of $2-3$ % in the moisture content can lead to a major increase in swelling pressure.

One of the implications of this research has been to indicate a possible way of widening the current specification (MCHW1, 1991) relating to the compaction of fine grained soils adjacent to structures. It has been shown that soils with a higher plasticity than currently accepted could possibly be used as fill to structures if the water content at compaction is carefully controlled so that swelling pressures are comparable to those of lower plasticity soils which conform with the current specification.

7.5 LIMITATIONS AND FUTURE WORK

The tests in the 100 mm triaxial stress path cell have considered only a single value of the vertical stress applied to the samples. Additional tests at different values of vertical stress should be performed to provide a wider picture of the swelling behaviour of the soil with depth. These results could then be compared to the results from the existing centrifuge model tests and the computer controlled oedometer.

The experimental work has been focused on the post compaction changes of lateral stress in unsaturated soil as inundation occurs and has provided useful information on the swelling behaviour of compacted soils. However, as discussed in Section 2.9, both the method and type of compaction influence the behaviour of unsaturated soils. A useful extension of this work would be to examine the effects that compaction methods have on the development of the swelling pressure in these situations. This would include the type of compaction as well as the size of the of compacted soil granules.

After the compaction of fill behind a retaining wall, time may elapse prior to the inundation of the soil. During this period the suctions in the soil may redistribute and as was observed in the prototype retaining wall facility studied by Carder et al. (1980), the horizontal stress on the wall was seen to reduce. This reduction in stress with time should be investigated to examine the effect that a resting period would have on the development of swelling pressures.

With regard to the measurement of suction further tests may be performed over a wider range of suctions and on different soils, together with comparative tests using other methods of suction measurements. In this way it can be assessed wether it is possible to generalise the result obtained for Wadhurst Clay to other fine grained soils.

Examining the soil behaviour under the boundary conditions imposed by a stiff retaining wall has provided an upper limit to the swelling pressure that can be used for design. A study into the swelling behaviour of more flexible walls would provide less conservative values of the swelling pressure and support any proposed changes in engineering practice. The study of the swelling behaviour of unsaturated soils behind more flexible walls could be investigated using the 100 mm stress path cell. Changes made to the control program could easily simulate flexibility in the wall and would allow various degrees of horizontal straining to occur. Correlations with a centrifuge model wall would confirm any findings.

In order to ensure that the proposed method to widen the specification limits is valid it is recommended that swelling pressure tests should be undertaken on a variety of different soils with plasticity indices in the range of 20 % to 50 %. These tests should be undertaken at different water contents, dry densities and ideally different initial confining stresses.

7.6 SUMMARY

- It has been demonstrated that the swelling pressure developed in unsaturated compacted soils is dependent on: type of the soil, initial water content, initial dry density, confining stress and testing conditions. By controlling these factors it is possible to limit both volumetric and stress changes within the soil.

- Swelling pressure has been found to increase as initial dry density increases and water content decreases.

- The filter paper technique provides a simple but powerful method of measuring the soil suction. The tests performed in this research on one of the soils has been used as a basis for the development of a relationship between suction, current water content and dry density.

- The installation of internal radial strain measurements into the 100 mm stress path cell has provided a useful and accurate method for measurements of volumetric changes in unsaturated soil samples. With a few additional modifications and the use of the filter paper suction measurements this system could be used for further studies on the fundamental behaviour of unsaturated soils.

- Centrifuge modelling of unsaturated soil compacted behind stiff retaining walls has shown to be consistent with a prototype model as well with the 100 mm triaxial stress path cell. The future use of centrifuge modelling in the study of unsaturated soils will be useful in the validation of results obtained from laboratory based experiments on single element tests.

- The work demonstrates that it may be possible to extend the current specification

limits and to include fine grained soils as backfill to structures provided that the placement water content and degree of compaction are carefully controlled so as to limit the development of excessive swelling pressures.

REFERENCES

Aitchison, G.D. (1961). Relationships of moisture stress and effective stress functions in unsaturated soils. Proc. Conference on Pore Pressure and Suction in Soils. ISMFE.

Aitchison, G.D. and Bishop, A.W. (1961). Discussion. Proc. Conference on Pore Pressure and Suction in Soils. ISMFE. Butterworths.

Alonso, E.E., Gens, A. and Hight, D.W. (1987). General Report - Special Problem Soils. 9th ECSMFE, Dublin, vol 3. pp. 1087–1146.

Alonso, E.E., Gens, A. and Josa, A. (1990). A constitutive model for partially saturated soils. Geotechique, vol. 40, no. 3, pp. 405–430.

Atkinson, J.H. Evans, J.S. and Scott, C.R. (1985). Developments in micro computer controlled stress path testing equipment for the measurement of soil parameter. Ground Engineering, vol. 18, no. 1, pp. 15–22.

Benson, C.H. and Daniel, D.E. (1991). Influence of clods on hydraulic conductivity of compacted clay. Journal of Geotechnical Engineering. ASCE, vol. 116, no. 8, pp 1231–1248.

Bishop, A.W. (1959). The principle of effective stress. A lecture in Oslo (1955). Printed in Tek. Ukeblad, no. 39, pp. 859–863.

Bishop, A.W. and Blight, G.E. (1963). Some aspects of effective stress in saturated soils and partly saturated soils. Geotechnique, vol. 13, no. 3, pp. 177–197.

Bishop, A.W. and Wesley, L..D. (1975). A hydraulic triaxial apparatus for controlled stress path testing. Geotechnique, vol. 25, no. 4, pp. 675–670.

Bishop, A.W., Alpan, I., Blight, G.E. and Donald, I.B. (1960). Factors controlling the strength of partly saturated cohesive soils. Proceedings ASCE conference on Shear strength of cohesive soils, Boulder, Colorado. pp. 503−531.

Bishop, I.W. and Donald, I.B. (1961). The experimental study of partly saturated soils in the triaxial apparatus. Proceedings 5th International Conference of Soil Mechanics and Foundation Engineering. Paris, vol. 1, pp. 13−21.

Blight, G.E. and De Wet, J.A. (1965). The acceleration of heave by flooding. A symposium in print. Moisture Equilibria and Moisture Changes in Soils Beneath Covered Areas. Butterworths, Australia. pp 89 − 92.

Brackley, I.J.A. (1975). A model of unsaturated clay structure and its application to swell behaviour. 6th Regional conference for Africa on Soil Mechanics and Foundation Engineering, Durban, South Africa.

Broms, B. (1971). Lateral earth pressures due to compaction of cohesionless soils. Proceedings of the 4th Conference on Soil Mechanics, Budapest. pp. 373−384.

Brown, R.W. and Cartos, D.L. (1982). A calibration model for screen caged Peltier thermocouple psychrometers. U.S. Department of Agriculture, Research Paper INT−293, July.

Burland, J.B. (1964). Effective stress in partially saturated soils. Geotechnique, vol. 14, pp. 64−68.

Campbell, G.S. and Gardner, W.H. (1971). Psychrometric measurement of soil potential: temperature and bulk density effects. Soil Science Society of America. Vol. 35, pp. 8−12.

Carder, D.R. and Krawczyk, J.V. (1975). Performance of cells designed to measure soil pressure on earth retaining structures. Department of Transport. Transport and Road Research Laboratory, LR 689, Crowthorne.

Carder, D.R., Murray, R.T. and Krawczyk, J.V. (1980). Earth pressures against an experimental retaining wall backfilled with silty clay. Department of Transport. Transport and Road Research Laboratory, LR 946, Crowthorne.

Carder, D.R., Pocock, R.G. and Murray, R.T. (1977). Lateral stress measurements with sand backfill. Department of Transport. Transport and Road Research Laboratory, LR 766, Crowthorne.

Casagrande, A. (1947). Classification and identification of soils. Proceedings of the American Society of Civil Engineers, vol. 73.

Chandler, R.J. and Gutierrez, C.I. (1986). The filter paper method of suction measurement. Geotechnique, vol. 36, pp. 265–268.

Chandler, R.J., Crilly, M.S. and Montgomery-Smith, G. (1992). A low cost method of assessing clay desiccation for low rise buildings. Proceedings of the Institution of Civil Engineers, Civil Engineering, vol. 92, no. 2, pp. 82–89.

Clayton, C.R.I. and Symons, I.F. (1992). The pressure of compacted fills on retaining walls. Geotechnique, vol. 42, no. 1, pp. 127–130.

Clinton, D.B. (1987). The determination of soil parameters from stress path tests. PhD thesis, City University, London.

Coleman, J.D. (1962). Stress-strain relations for partly saturated soil. (correspondence), Geotechnique, vol. 12, no. 4, pp. 348–350.

Cooke, A.B. and Mitchell, R.J. (1991). Evaluation of contaminant transport in partially saturated soils. Centrifuge 1991, edited by Ko, Balkema, Rotterdam.

Daniel, D.E., Hamilton, J.M. and Olsen, R.E. (1981). Suitability of thermocouple psychrometers for studying moisture movement in unsaturated soils. Permeability and Ground water Contaminant Transport, ASTM STP 746.

Department of Transport (1986). Specification for highway works. 6th edition. HMSO.

Duncan, J.M. and Seed, R.B. (1986). Compaction induced earth pressures under K_o conditions. Journal of Geotechnical Engineering. ASCE, vol. 112, part 1.

Duncan, J.M., Williams, G.W., Sehn, A.L. and Seed R.B. (1991). Estimation of earth pressures due to compaction. Journal of Geotechnical Engineering. ASCE, vol, 119, no. 12, pp. 1833–1847.

Edil, T.B. and Motan, E.S. (1984). Laboratory evaluation of soil suction components. Geotechnical Testing Journal Vol. 7, No. 4, pp. 173–181.

Escario V. and Saez J. (1986). The shear strength of partly saturated soils. Geotechnique, Technical note, Vol 36, pp 453 - 456.

Farrar, D.M. and Darley, P. (1975). The operation of earth moving plant on wet fill. Department of Transport. Transport and Road Research Laboratory, LR 668. Crowthorne.

Fawcett, R.G. and Collis–George, N. (1967). A filter paper method for determining the moisture characteristics of soil. Australian Journal of Experimental Agriculture and Animal Husbandry, vol. 7, pp 162–167.

Fredlund D.G. Morgenstern N.R.and Widger R.A. (1978). The shear strength of unsaturated soils. Canadian Geotechnical Journal. Vol 15, Nr 3, pp 313 - 321.

Fredlund, D.G. and Morgenstern, N.R. (1977). Stress state variables for unsaturated soils. Journal of the Geotechnical Engineering Division. Proceedings of the ASCE, vol. 103, no. GT5.

Frydman, S. and Weisberg, E. (1991). A study of centrifuge modelling of swelling clay. Centrifuge '91. Balkema, Rotterdam.

Grim, R.E. (1962). Applied Clay Mineralogy. London McGraw-Hill.

Head, K.H. (1984). Manual of soil laboratory testing. Volume 1: Soil classification and compaction tests. London, Pentech Press.

Hilf, J.W. (1956). An investigation into the poe water pressure in compacted cohesive soils. Technical Memorandum no. 654, U.S. Department of Interior Bureau of Reclamation, Denver.

Ingold, T.S. (1979). The effects of compaction on retaining walls. Geotechnique, vol. 29, no. 3, pp 265−283.

Jaky, J. (1944). The coefficient of earth pressure at rest. Journal of the Society of Hungarian Architects and Engineers. pp. 355−358.

Jennings, J.E. and Burland, J.B. (1962). Limitations to the use of effective stresses in partially saturated soils. Geotechnique, vol. 12, no. 2, pp. 125−144.

Johnson, L.D. (1989). Horizontal and vertical swell pressures from a triaxial test: a feasibility study. Geotechnical Testing Journal, GTJODJ, vol. 12, no. 1, March, pp. 302−311.

Jones, R.H. and Greenwood, J.R. (1993). Relationship testing for acceptability assessment of cohesive soils. Proceedings of the conference of Engineered Fills, Newcastle Upon Tyne, UK. Thomas Telford. Ltd. pp 302−311.

Lambe, T.W. (1958). The structure of compacted clay. Journal of soil mechanics and Foundation Engineering. ASCE, vol. 84, no. 2, pp. 1−35.

Lau, W.H. (1988). The behaviour of clay in simple shear and triaxial tests. PhD thesis. City University, London.

Lee, L.J. and Fredlund, D.G. (1984). Measurement of soil suction using the MCS 6000 sensor. Proceedings of the 5th International Conference on Expansive Soils. Adelaide, Australia, pp. 50−54.

Lewis, W.A. (1959). Investigation of the performance of pneumatic-tyred rollers in the compaction of soil. Road Research Laboratory. Technical Paper no. 45. HMSO.

Manual of Contract Documents for Highway Works (1991). Volume 1, Specification for Highway Works, December 1991, HMSO, London.

Matyas, E.L. and Radhakrishna, H.S. (1968). Volume change characteristics of partially saturated soils. Geotechnique, vol. 18, pp. 432–438.

Mawditt, J.M. (1989). Conventional retaining walls: pilot and full scale studies. Contribution to a discussion. Ground Engineering Group. Proceedings of the Institution of Civil Engineers. no. 86, Part 1, pp. 973–994.

Mayne, P.W. and Kulhawy, F.H. (1982). K_o- OCR relationships in soil. Journal of Geotechnical Engineering. ASCE. vol. 108, part 6, pp. 851–872.

M^{c}Gown, A. and Collins K. (1975). The microfabrics of some expansive and collapsing soils. Proceedings of the 5th Pan American Conference on Soil Mechanics and Foundation Engineering. Buenos Aires. Vol 1. pp 323 - 332.

MCHW1 (1991). Manual of contract documents for highway works. vol. 1, Specification for highway works, HMSO, London.

Miller, R.F. and M^{c}Queen, I.S. (1978). Moisture relations in Rangelands, Western United States. Proceedings of the 1st International Rangeland Congress, 1978, pp. 318–321.

Mitchell, J.K. (1976). Fundamentals of soil behaviour. New York. J. Wiley and sons.

Naish, N.G. (1988). A cost survey of backfill around bridge abutments and retaining walls in South-East England. Department of Transport, TRRL, Contractor Report 112, Crowthorne.

Olsen, H.W. (1962). Hydraulic flow through saturated clays. Clay Mineralogy, vol. 9, no. 2, pp. 131–161.

Parsons, A.W. (1992). Compaction of soils and granular materials: A review of research performed at the Transport Research Laboratory. HMSO. London.

Pore Pressure and Suction in Soils, (1961). International conference organised by ISSMFE, Butterworths, London.

Richards, B.G. (1965). Measurements of the free energy of soil moisture by the psychrometric technique using thermistors. Moisture Equilibria and Moisture Changes in Soils Beneath Covered Areas. A symposium in print. Australia, Butterworths.

Road Research Laboratory (1952). Soil mechanics for road engineers. HMSO. London. Chapter 9.

Ryley, M.D. (1988). The swelling Behaviour of clay fill. Working Paper GE/4/88. Transport and Road Research Laboratory, Crowthorne.

Schofield A.N. and Wroth C.P. (1968). Critical State Soil Mechanics. Mc Graw-Hill Book Company. London, 1968.

Schofield, A.N. (1935). The pF of the water in soil. Trans. 3rd International Congress of Soil Science, vol. 12, pp. 37–48.

Schofield, A.N. (1980). Cambridge geotechnical centrifuge operations. Geotechnique, vol. 30, pp. 227–268.

Seed, H.B. and Chan, C.K. (1959). Structure and strength characteristics of compacted clays. Proceedings ASCE, no. SM5, pp. 87–127.

Sherwood, P.T. (1970). The reproducibility of the results of soil classification and compaction tests. Report LR 339. Road Research Laboratory (Transport Research Laboratory), Crowthorne, Berkshire.

Sivakumar, V. (1993). A critical state framework for unsaturated soils. PhD Thesis. University of Sheffield.

Skempton, A.W. and Northey, R.D. (1953). The sensitivity of clays. Geotechnique, vol. 3, pp. 30–53.

Skempton, A.W. (1953). The colloidal "Activity" of clay. Proceedings 3rd International Conference on Soil Mechanics, vol. 1, pp. 33–62.

Skempton, A.W. and Northey, R.D. (1953). The sensitivity of clays. Geotechnique, vol. 3, pp. 30–55.

Sridharan, A., Sreepada, R. and Sivapullaiah, P.V. (1986). Swelling pressure of clays. Geotechnical Testing Journal, vol. 9, no. 1, pp. 24–33.

Symons, I.F., Clayton, C.R.I. and Darley, P. (1989). Earth pressures against an experimental wall backfilled with heavy clay. Department of Transport. Transport and Road Research Laboratory, RR 192. Crowthorne.

Takada, N. (1991). An introduction to centrifuge model testing. Developments in Geotechnical Aspects of Embankments, Excavations and buried Structures. Balkema, Rotterdam.

Terzaghi, K. (1936). The shearing resistance of saturated soil and the angle between the planes of shear. Proceedings 1st International conference Soil Mechanics and Foundation Engineering, vol. 1, pp. 54–56, Harvard, Mass.

Toll, D.G. (1990). A framework for unsaturated soil behaviour. Geotechnique, vol. 40, no. 1, pp. 31–44.

Wheeler, S.J. (1990). An alternative framework for unsaturated soil behaviour. Geotechnique, vol. 41, no. 2, pp. 257–261.

Wheeler, S.J. and Sivakumar, V. (1992). Critical state concept for unsaturated soil. Proceedings for 7th International Conference on Expansive soils. Dallas, pp. 167–172.

Wheeler, S.J. and Sivakumar, V. (1993). A state boundary for unsaturated soil. Proceedings of Conference on Engineered Fills. Newcastle Upon Tyne, UK, Thomas Telford Ltd., pp. 66–77.

Wroth, C.P. and Houlsby, G.T. (1985). Soil Mechanics: Property characterisation and analysis procedure. Proc 11th ICSMFE, San Francisco, vol. 1, pp. 1–55.

Wroth, C.P. and Wood, D.M. (1978). The correlation of index properties with some basic engineering properties of soils. Canadian Geotechnical Journal, vol. 15, no. 2, pp. 137–145.

Method	Definition	Remark
A [ASTM D4546]	pressure required to bring soil back to the original volume after the soil is allowed to swell completely without surcharge (except for a small seating pressure)	may lead to larger swell pressures because the method incorporates hysteresis that tends to overcome specimen disturbance
B	pressure applied to the soil so that neither swell or compression takes place on inundation; a specimen may be confined and pressure inferred from deflection of the confining vessel	a null test in which measured swell pressures are influenced by apparatus stiffness; apparatus of higher stiffness leads to less expansion on swelling; large swell pressures can be relieved with small specimen expansion; therefore stiffer apparatus can provide improved control over one-dimensional changes and can lead to improved measurements of swell pressure
C [ASTM D4546]	pressure necessary to permit no change in volume upon inundation when initially under applied pressure equal to the overburden pressure; various loads are applied to the soil after inundation to maintain no volume change	must be corrected for specimen disturbance; one dimensional consoildometer swell tests are influenced by lateral skin friction especially in tests conducted on stiff clays or shales
D	pressure required for preventing volume expansion in soil in contact with water; various loads are applied to the soil after inundation to maintain no volume change	requires correction of swell pressure similar to method C above but a standard correction procedure is not available

Table 2.1 Definitions of swelling pressure (after Johnson 1989).

TABLE 6/4 : Method Compaction for Earthworks Materials : Plant and Methods (Method 1 to Method 6)
(This Table is to be read in conjunction with sub-Clause 612.10)

Type of Compaction Plant	Ref No.	Category	Method 1		Method 2		Method 3		Method 4		Method 5	Method 6		
			D	N#	D	N#	D	N#	D	N	D N	N for D = 110 mm	N for D = 150 mm	N for D = 250 mm
Smooth wheeled roller (or vibratory roller operating without vibration)		Mass per metre width of roll:												
	1	over 2100 kg up to 2700 kg	125	8	125	10	125	10*	175	4	unsuitable	unsuitable	unsuitable	unsuitable
	2	over 2700 up to 5400 kg	125	6	125	8	125	8*	200	4	unsuitable	16	unsuitable	unsuitable
	3	over 5400 kg	150	4	150	8	unsuitable		300	4	unsuitable	8	16	unsuitable
Grid roller		Mass per metre width of roll:												
	1	over 2700 kg up to 5400 kg	150	10	unsuitable		150	10	250	4	unsuitable	unsuitable	unsuitable	unsuitable
	2	over 5400 kg up to 8000 kg	150	8	125	12	unsuitable		325	4	unsuitable	20	unsuitable	unsuitable
	3	over 8000 kg	150	4	150	12	unsuitable		400	4	unsuitable	12	20	unsuitable
Tamping roller		Mass per metre width of roll:												
	1	over 4000 kg	225	4	150	12	250	4	350	4	unsuitable	12	20	unsuitable
Pneumatic-tyred roller		Mass per wheel:												
	1	over 1000 kg up to 1500 kg	125	6	unsuitable		150	10*	240	4	unsuitable	unsuitable	unsuitable	unsuitable
	2	over 1500 kg up to 2000 kg	150	5	unsuitable		unsuitable		300	4	unsuitable	unsuitable	unsuitable	unsuitable
	3	over 2000 kg up to 2500 kg	175	4	125	12	unsuitable		350	4	unsuitable	unsuitable	unsuitable	unsuitable
	4	over 2500 kg up to 4000 kg	225	4	125	10	unsuitable		400	4	unsuitable	unsuitable	unsuitable	unsuitable
	5	over 4000 kg up to 6000 kg	300	4	125	10	unsuitable		unsuitable		unsuitable	12	unsuitable	unsuitable
	6	over 6000 kg up to 8000 kg	350	4	150	8	unsuitable		unsuitable		unsuitable	12	unsuitable	unsuitable
	7	over 8000 kg up to 12000 kg	400	4	150	8	unsuitable		unsuitable		unsuitable	10	16	unsuitable
	8	over 12000 kg	450	4	175	6	unsuitable		unsuitable		unsuitable	8	12	unsuitable
Vibratory roller		Mass per metre width of a vibratory roll:												
	1	over 270 kg up to 1500 kg	unsuitable		75	16	150	16	unsuitable		unsuitable	unsuitable	unsuitable	unsuitable
	2	over 450 kg up to 700 kg	unsuitable		75	12	150	12	unsuitable		unsuitable	unsuitable	unsuitable	unsuitable
	3	over 700 kg up to 1300 kg	100	12	125	10	150	6	125	10	unsuitable	16	unsuitable	unsuitable
	4	over 1300 kg up to 1800 kg	125	8	150	8	200	10*	175	4	unsuitable	6	16	unsuitable
	5	over 1500 kg up to 2300 kg	150	4	150	4	225	12*	unsuitable		unsuitable	4	6	12
	6	over 2300 kg up to 2900 kg	175	4	175	4	250	10*	unsuitable		400 5	3	5	11
	7	over 2900 kg up to 3600 kg	200	4	200	4	275	8*	unsuitable		500 5	3	5	10
	8	over 3600 kg up to 4300 kg	225	4	225	4	300	8*	unsuitable		600 5	2	4	8
	9	over 4300 kg up to 5000 kg	250	4	250	4	300	6*	unsuitable		700 5	2	4	7
	10	over 5000 kg	275	4	275	4	300	4	unsuitable		800 5	2	3	6
Vibrating plate compactor		Mass per m^2 of base plate												
	1	over 580 kg up to 1100 kg	unsuitable		unsuitable		75	6	unsuitable		unsuitable	unsuitable	unsuitable	unsuitable
	2	over 1100 kg up to 1200 kg	unsuitable		75	10	100	8	75	10	unsuitable	unsuitable	unsuitable	unsuitable
	3	over 1200 kg up to 1400 kg	unsuitable		75	6	150	6	150	8	unsuitable	unsuitable	unsuitable	unsuitable
	4	over 1400 kg up to 1800 kg	100	6	125	6	150	4	unsuitable		unsuitable	8	unsuitable	unsuitable
	5	over 1800 kg up to 2100 kg	150	6	150	5	200	4	unsuitable		unsuitable	5	8	unsuitable
	6	over 2100 kg	200	6	200	5	250	4	unsuitable		unsuitable	3	6	12

Table 2.2 Sample of method specification (Manual of Contract Documents for Highway works 1991).

TABLE 6/1 : Acceptable Earthworks Materials: Classification and Compaction Requirements (See Footnotes) *(continued)*

Class				General Material Description	Typical Use	Permitted Constituents (All Subject to Requirements of Clause 601 and Appendix 6/1)	Material Properties Required for Acceptability (In Addition to Requirements on Use of Fill Materials in Clause 601 and Testing in Clause 631)				Compaction Requirements in Clause 612	Class		
							Property (See Exceptions in Previous Column)	Defined and Tested in Accordance With:	Acceptable Limits Within: Lower	Upper				
SELECTED COHESIVE FILL	7	A	—	Selected cohesive material	Fill to structures	Any material, or combination of materials, other than argillaceous rock and materials designated as Class 3 in the Contract. If chalk is used it shall form 100% of constituents (Properties i and iii shall not apply to chalk)	(i) grading	BS 1377: Part 2	Tab 6/2	Tab 6/2	End product: 100% of maximum dry density of BS 1377: Part 4 (2.5 kg rammer method) or a dry density corresponding to 5% air voids at field mc whichever is lower	7	A	—
							(ii) mc	BS 1377: Part 2	App 6/1	App 6/1				
							(iii) MCV	Clause 632	App 6/1	App 6/1				
							(iv) undrained shear parameters (c and u)	Clause 633	App 6/1	App 6/1				
							(v) effective angle of internal friction (o') and effective cohesion (c')	Clause 636	App 6/1	App 6/1				
							(vi) SMC of chalk	Clause 634	App 6/1	App 6/1				
							(vii) liquid limit	BS 1377 Part 2	--	45				
							(viii) plasticity index	BS 1377 Part 2	—	25				

Table 2.3 End product specification for selective cohesive material. (Manual of contract Documents for Highway Works 1991).

Transducer Type	Model	Working Range	Resolution	Typical calibration constant	Non Linearity % of full scale	Thermal Sensitivity % of full scale per °C	hysteresis % of full scale	System Noise	Overall Accuracy
Displacement	RDP [DCT 1000]	50 mm	0.002 mm	0.145 mV/ mm	0.5	0.01	0.04	0.005 mm	0.005 mm ± 0.05 % of full scale
	MPE	25 mm	0.002 mm	0.575 mV/ mm	0.45	0.02	0.05	0.006 mm	0.006 mm ± 0.45 % of full scale
	Slumberger [DG5]	10 mm	0.001 mm	3.1 mV/ mm	0.3	0.005	0.2	0.008 mm	0.008 mm ± 0.36 % of full scale
	RDP [D5 - 200W]	7 mm	1.4×10^{-5} mm	350 mV/ mm	0.25	0.01	0.04	0.0007 mm	0.0007 mm ± 0.048 % of full scale
	Kamen [KD 4000-6UI]	5 mm	1.3×10^{-4} mm	374 mV/ mm	0.03	0.02	0.06	0.0012 mm	0.0012 mm ± 0.07 % of full scale
Load	Wykemham Farrance [WF 17100]	10 kN	0.05 N	1.618 mV/ kN	0.5	0.05	0.4	3.7 N	3.7 N ± 0.64 % of full scale
		3 kN	0.05 N	1.3 mV/ kN				3 N	3 N ± 0.64 % of full scale
	Saxeway	2.5 kN	0.1 N	1.25 mV/ kN	0.36	0.06	0.47	3.9 N	3.9 N ± 0.6 % of full scale
Pressure	Druck	1000 kPa	0.06 kPa	0.081 mV/ kPa	0.4	0.07	0.2	0.4 kPa	0.4 kPa ± 0.45 % of full scale

Table 3.1 Accuracy and resolution of transducers.

PARAMETER	SCALE FACTOR (prototype : model)
Acceleration	1:n
Length	1:1/n
Density	1:1
Strain	1:1
Permeability	1:1
Time - related to inertial effects	$1:1/n^2$

Table 4.1 Scaling factors used in centrifuge testing.

	LONDON CLAY		WADHURST CLAY		BRICKEARTH	
	Liquid Limit %	Plastic Limit %	Liquid Limit %	Plastic Limit %	Liquid Limit %	Plastic Limit %
TEST VALUE	77.8	26.7	55.8	23.7	39.1	18.4
	77.3	28.8	57.3	24.9	37.4	17.5
	79.5	27.6	57.9	25.1	38.7	18
	-	28.5	56.6	23.5	-	17.3
AVERAGE	78.2	27.9	56.9	24.3	38.4	17.8
VALUE USED	78	28	57	24	38	18

Table 5.1 Index tests of three soils tested.

	SPECIFIC GRAVITY	ACTIVITY
LONDON CLAY	2.78	0.5
WADHURST CLAY	2.7	0.45
BRICKEARTH	2.72	0.13

Table 5.2 Activity and specific gravity of soils tested.

BRICKEARTH 100mm stress path	initial wet density Mg/m^3	final wet density Mg/m^3	initial dry density Mg/m^3	final dry density Mg/m^3	initial water content (w) %	initial w/PL -	final water content (w) %	final w/PL -	initial air voids %	final air voids %	initial void ratio %	final void ratio %	total swelling pressure kPa	net swelling pressure kPa
BE1 #	2.212	-	1.919	-	15.240	0.847	-	-	0.19	-	0.417	-	63	13
BE2	2.058	2.127	1.844	1.826	11.620	0.646	16.50	0.917	10.79	2.75	0.475	0.490	97	47
BE2A	2.049	2.078	1.847	1.812	10.930	0.607	14.63	0.813	11.89	6.85	0.472	0.501	109	59
BE3	2.145	2.210	1.889	1.921	13.520	0.751	15.06	0.837	5.00	0.46	0.440	0.416	70	20
BE4	2.118	2.139	1.780	1.802	18.960	1.053	18.71	1.039	0.81	0.04	0.528	0.509	65	15
BE5 #	2.199	-	2.008	-	9.500	0.528	-	-	7.10	-	0.355	-	181	131
BE6	2.159	2.178	1.919	1.906	12.540	0.697	14.27	0.793	5.40	2.73	0.418	0.427	157	107
BE7	2.180	2.194	1.954	1.936	11.550	0.642	13.30	0.739	5.58	3.06	0.392	0.405	223	173
BE8	2.240	2.235	1.986	1.965	12.800	0.711	13.74	0.763	1.58	0.78	0.370	0.384	128	78
BE9	2.232	2.241	2.008	1.980	11.120	0.618	12.74	0.708	3.83	1.98	0.354	0.374	270	220
BE10 #	2.156	-	1.960	-	10.010	0.556	-	-	8.32	-	0.388	-	175	125

 # test incomplete, some measurements not taken.

Table 5.3 Brickearth 100 mm stress path cell data.

BRICKEARTH modified oedometer	initial wet density Mg/m^3	final wet density Mg/m^3	initial dry density Mg/m^3	final dry density Mg/m^3	initial water content (w) %	initial w/PL -	final water content %	final w/PL -	initial air voids %	final air voids %	initial void ratio %	final void ratio %	total swelling pressure kPa	net swelling pressure kPa
BE1-O1	2.175	2.180	1.887	1.887	15.26	0.848	15.55	0.864	1.81	1.28	0.441	0.441	10	8
BE1-O2	2.183	2.187	1.892	1.896	15.36	0.853	15.39	0.855	1.38	1.14	0.438	0.435	16	12
BE1-O3	2.190	2.197	1.902	1.899	15.14	0.841	15.72	0.873	1.28	0.34	0.430	0.432	11	2
BE2-O1	2.150	2.186	1.916	1.911	12.25	0.681	14.37	0.798	6.11	2.28	0.420	0.423	28	24
BE2-O2	2.180	2.222	1.942	1.934	12.26	0.681	14.91	0.828	4.80	0.07	0.401	0.406	28	20
BE3-O1	2.133	2.154	1.875	1.870	13.80	0.767	15.20	0.844	5.21	2.85	0.451	0.455	24	18
BE3-O2	2.132	2.157	1.868	1.867	14.16	0.787	15.54	0.863	4.89	2.35	0.456	0.457	20	16
BE3-O3	2.158	2.181	1.893	1.891	14.00	0.778	15.33	0.852	3.89	1.49	0.437	0.438	23	20
BE4-O1	2.062	2.070	1.729	1.701	19.27	1.071	21.75	1.208	3.13	0.49	0.573	0.599	5	2
BE4-O2	2.111	2.124	1.781	1.812	18.48	1.027	17.25	0.958	1.59	2.15	0.527	0.501	6	2
BE4-O3	2.109	2.117	1.778	1.780	18.59	1.033	18.92	1.051	1.55	0.86	0.529	0.528	5	3
BE6-O1	2.157	2.199	1.924	1.917	12.10	0.672	14.72	0.818	5.96	1.33	0.413	0.419	21	18
BE7-O1	2.103	2.183	1.902	1.901	10.53	0.585	14.82	0.823	10.02	1.94	0.430	0.431	80	75
BE7-O2	2.111	2.176	1.917	1.904	10.14	0.563	14.28	0.793	10.10	2.83	0.419	0.429	69	64
BE8-O1	2.203	2.217	1.961	1.948	12.36	0.687	13.80	0.767	3.69	1.51	0.387	0.396	40	34
BE8-O2	2.232	2.244	1.978	1.978	12.82	0.712	13.47	0.748	1.91	0.65	0.375	0.375	43	40
BE8-O3	2.225	2.244	1.976	1.971	12.57	0.698	13.82	0.768	2.49	0.29	0.376	0.380	49	44
BE9-O1	2.156	2.224	1.964	1.960	9.79	0.544	13.46	0.748	8.57	1.54	0.385	0.388	118	111
BE9-O2	2.157	2.225	1.963	1.967	9.86	0.548	13.08	0.727	8.47	1.94	0.386	0.383	96	85
BE10-07	2.116	2.215	1.931	1.926	9.58	0.532	15.05	0.836	10.50	0.22	0.408	0.412	117	107
BE10-O6	2.189	2.258	2.017	1.990	8.50	0.473	13.45	0.747	8.67	0.06	0.349	0.367	145	136
BE10-O4 +	2.171	2.250	1.980	1.973	9.61	0.534	14.02	0.779	8.16	-	0.373	0.378	157	147

+ value of final air voids senstive to measurement of final height, negative value indicates error in measurement.

Table 5.4 Brickearth modified oedometer test data.

BRICKEARTH 38mm triaxial	initial wet density Mg/m^3	initial dry density Mg/m^3	initial water content (w) %	initial w/PL -	initial air voids %	initial void ratio	cell pressure kPa	shear strength kPa
BE1	2.206	1.915	15.18	0.843	0.517	0.420	100	678.3
BE1	2.196	1.908	15.07	0.837	1.097	0.426	200	659.6
BE1	2.196	1.916	14.61	0.812	1.575	0.420	350	604
BE2	2.253	2.012	11.95	0.664	1.978	0.352	100	845
BE2	2.239	2.002	11.86	0.659	2.673	0.359	200	1064
BE2	2.254	2.016	11.80	0.656	2.080	0.349	100	846
BE3	2.198	1.926	14.08	0.782	2.054	0.412	200	486
BE3	2.185	1.908	14.52	0.807	2.141	0.425	100	419
BE3	2.202	1.929	14.15	0.786	1.777	0.410	250	521
BE4	2.106	1.767	19.18	1.066	1.119	0.539	100	16
BE4	2.093	1.758	19.08	1.060	1.830	0.547	100	16

Table 5.5 Brickearth 38 mm triaxial test data.

		vertical stress kPa	vertical strain %	water content %	w/PL -	dry density Mg/m^3	air voids %	net vertical strain %
b51	initial	0	0	11.65	0.65	1.7641	14.59	
b51	after compression	50	0.536	11.65	0.65	1.7689	14.36	0
b51	final	50	0.435	18.25	1.01	1.7527	3.57	-0.101
b52	initial	0	0	11.05	0.61	1.7434	11.86	0
b52	after compression	50	0.682	11.05	0.61	1.856	11.26	0
b52	final	50	0.441	16.37	0.91	1.8262	2.96	-0.241
b53	initial	0	0	11.69	0.65	1.7591	14.77	
b53	after compression	50	1.703	11.69	0.65	1.8227	11.68	0
b53	final	50	1.515	18.12	1.01	1.77	2.85	-0.188
b61	initial	0	0	12.58	0.7	1.6679	17.7	
b61	after compression	25	0.28	12.58	0.7	1.7298	14.64	0
b61	final	25	-0.099	19.75	1.1	1.6638	5.97	-0.379
b62	initial	0	0	11.9	0.66	1.8798	8.52	
b62	after compression	50	0.443	11.9	0.66	1.9083	7.13	0
b62	final	50	0.322	17.32	0.96	1.777	3.89	-0.121
b63	initial	0	0	11.9	0.66	1.7712	13.81	
b63	after compression	100	0.443	11.9	0.66	1.7979	12.51	0
b63	final	100	0.561	17.9	0.99	1.7704	3.22	0.118
b64	initial	0	0	11.31	0.63	1.7586	15.46	
b64	after compression	75	0.706	11.31	0.63	1.7804	14.41	0
b64	final	75	0.902	17.69	0.98	1.7554	4.41	0.196

Table 5.6 Brickearth computer controlled oedometer test data.

WADHURST CLAY 100mm stress path	initial wet density Mg/m^3	final wet density Mg/m^3	initial dry density Mg/m^3	final dry density Mg/m^3	initial water content (w) %	initial w/PL -	final water content (w) %	final w/PL -	initial air voids %	final air voids %	initial void ratio %	final void ratio %	total swelling pressure kPa	net swelling pressure kPa
WA1	2.044	2.016	1.664	1.623	22.84	0.921	24.23	0.977	0.39	0.58	0.623	0.664	114	64
WA2	2.071	2.020	1.713	1.625	20.92	0.844	24.30	0.980	0.72	0.31	0.576	0.661	155	105
WA3 #	2.154	-	1.861	-	15.70	0.633	-	-	1.84	-	0.451	-	275	225
WA4 +	2.135	2.060	1.838	1.655	16.15	0.651	24.45	0.986	2.25	-	0.469	0.631	325	275
WA5 #	2.084	-	1.723	-	20.92	0.844	20.92	0.844	0.12	-	0.567	-	65	15
WA6	2.091	2.037	1.738	1.650	20.30	0.819	23.43	0.945	0.32	0.20	0.553	0.636	91	41
WA8	2.015	1.975	1.631	1.559	23.50	0.948	26.68	1.076	1.25	0.67	0.655	0.732	69	19
WA9 #	2.076	-	1.811	-	14.63	0.590	-	-	6.42	-	0.491	-	100	50

+ value of final air voids sensitive to measurement of final sample height, negative value indicates error in measurment.
 # test incomplete, some measurements not taken.

Table 5.7 Wadhurst Clay 100 mm stress path cell data.

WADHURST CLAY modified oedometer	initial wet density Mg/m^3	final wet density Mg/m^3	initial dry density Mg/m^3	final dry density Mg/m^3	initial water content (w) %	initial w/PL -	final water content (w) %	final w/PL -	initial air voids %	initial void ratio %	final void ratio %	total swelling pressure kPa	net swelling pressure kPa
WA1-O6 +	2.040	2.064	1.655	1.652	23.28	0.939	24.93	1.005	0.19	0.63	0.635	111	108
WA1-O4 +	2.020	2.049	1.640	1.641	23.16	0.934	24.87	1.003	1.27	0.65	0.645	105	100
WA1-O7 +	2.025	2.052	1.650	1.648	22.73	0.917	24.55	0.990	1.39	0.64	0.639	125	121
WA2-O4 +	2.084	2.115	1.727	1.721	20.71	0.835	22.87	0.922	0.29	0.56	0.569	197	191
WA2-O6 +	2.088	2.113	1.730	1.728	20.64	0.832	22.3	0.899	0.20	0.56	0.563	230	229
WA3-O6 +	2.156	2.206	1.866	1.852	15.56	0.627	19.14	0.772	1.86	0.45	0.458	631	625
WA4-O4 +	2.129	2.180	1.839	1.835	15.76	0.635	18.8	0.758	2.90	0.47	0.471	600	598
WA4-O6 +	2.152	2.200	1.866	1.851	15.32	0.618	18.86	0.760	2.28	0.45	0.458	633	629
WA4-O7 +	2.178	2.225	1.881	1.867	15.79	0.637	19.15	0.772	0.64	0.44	0.446	587	583
WA7-O11	1.865	1.922	1.549	1.505	20.38	0.822	27.69	1.117	11.04	0.74	0.794	79	77
WA7-010	1.785	1.878	1.483	1.445	20.38	0.822	30	1.210	14.85	0.82	0.869	43	41
WA7-O7	1.912	1.962	1.588	1.555	20.38	0.822	26.21	1.057	8.80	0.70	0.737	117	114
WA7-O11A	1.682	1.834	1.397	1.377	20.38	0.822	33.13	1.336	19.78	0.93	0.960	20	16
WA7-O10A	1.800	1.890	1.495	1.468	20.38	0.822	28.7	1.157	14.15	0.81	0.839	55	51
WA8-O10 +	2.009	2.011	1.621	1.595	23.95	0.966	26.06	1.051	1.14	0.67	0.692	56	53
WA8-O11 +	2.016	2.023	1.627	1.617	23.86	0.962	25.15	1.014	0.89	0.66	0.670	70	68

+ value of final air voids sensitive to measurement of final sample height, negative value indicates error in measurment.

Table 5.8 Wadhurst Clay modified oedometer test data.

WADHURST CLAY 38mm Triaxial	initial wet density Mg/m^3	initial dry density Mg/m^3	initial water content (w) %	initial w/PL -	initial air voids %	initial void ratio	cell pressure kPa	shear strength kPa
WA1	2.036	1.664	22.33	0.90	1.196	0.622	100	189
WA1	2.044	1.671	22.29	0.90	0.861	0.616	150	202
WA1	2.056	1.680	22.36	0.90	0.202	0.607	200	187
WA2	2.054	1.677	22.48	0.91	0.166	0.610	50	203
WA2	2.055	1.678	22.5	0.91	0.126	0.610	200	214
WA2	2.057	1.681	22.36	0.90	0.154	0.606	150	213
WA6	2.014	1.755	19.89	0.80	0.116	0.539	100	358
WA6	2.104	1.755	19.88	0.80	0.113	0.538	50	363.5
WA6	2.092	1.745	19.84	0.80	0.730	0.547	75	336
WA8	2.036	1.660	22.65	0.91	0.900	0.626	50	128
WA8	2.005	1.633	22.76	0.92	2.337	0.653	100	143
WA8	2.023	1.649	22.66	0.91	1.555	0.637	100	141

Table 5.9 Wadhurst Clay 38 mm triaxial test data.

		vertical stress kPa	vertical strain %	water content %	w/PL -	dry density Mg/m^3	air voids %	net vertical strain %
W11	initial	0	0	20.3	0.846	1.732	0.69	
W11	after compression	50	0.61	20.3	0.846	1.743	0.08	0
W11	final	50	-6.227	24.66	1.028	1.610	0.66	-6.837
W12	initial	0	0	20.3	0.846	1.717	1.57	
W12	after compression	50	0.41	20.3	0.846	1.724	1.17	0
W12	final	50	-2.916	24.63	1.026	1.620	1.03	-3.326
W13	initial	0	0	20.3	0.846	1.675	3.94	
W13	after compression	50	0.083	20.3	0.846	1.689	3.13	0
W13	final	50	-5.217	26.99	1.125	1.548	0.88	-5.3
W14	initial	0	0	20.3	0.846	1.596	8.51	
W14	after compression	50	0.74	20.3	0.846	1.608	7.83	0
W14	final	50	-2.357	27.56	1.148	1.502	2.99	-3.097
W15	initial	0	0	20.3	0.846	1.555	10.86	
W15	after compression	50	1.68	20.3	0.846	1.581	9.34	0
W15	final	50	3.676	21.15	0.881	1.442	1.68	1.996
W16	initial	0	0	20.3	0.846	1.348	22.69	
W16	after compression	50	1.01	20.3	0.846	1.362	21.9	0
W16	final	50	7.068	21.42	0.893	1.444	1.18	6.058
W17	initial	0	0	20.3	0.846	1.291	25.95	
W17	after compression	50	1.66	20.3	0.846	1.313	24.7	0
W17	final	50	13.013	34.46	1.436	1.410	-0.81	11.353
W21	initial	0	0	20.3	0.846	1.545	11.43	
W21	after compression	25	0.99	20.3	0.846	1.560	10.54	0
W21	final	25	-3.945	30.2	1.258	1.446	2.78	-4.935
W22	initial	0	0	20.3	0.846	1.570	9.99	
W22	after compression	50	0.59	20.3	0.846	1.579	9.46	0
W22	final	50	-2.947	28.55	1.190	1.488	2.41	-3.537
W23	initial	0	0	20.3	0.846	1.568	10.07	
W23	after compression	75	0.65	20.3	0.846	1.579	9.48	0
W23	final	75	-1.596	27.08	1.128	1.510	3.18	-2.246
W24	initial	0	0	20.3	0.846	1.572	9.89	
W24	after compression	100	0.68	20.3	0.846	1.582	9.28	0
W24	final	100	-0.28	26.66	1.111	1.521	3.09	-0.96
W25	initial	0	0	20.3	0.846	1.583	9.26	
W25	after compression	150	1.6	20.3	0.846	1.608	7.78	0
W25	final	150	1.37	27.8	1.158	1.541	1.16	-0.23

Table 5.10 Wadhurst Clay computer controlled oedometer test data.

LONDON CLAY 100mm stress path	initial wet density Mg/m^3	final wet density Mg/m^3	initial dry density Mg/m^3	final dry density Mg/m^3	initial water content (w) %	initial w/PL -	final water content (w) %	final w/PL -	initial air voids %	final air voids %	initial voids ratio	final voids ratio	total swelling pressure kPa	net swelling pressure kPa
LC1	1.867	1.850	1.386	1.352	34.69	1.239	36.84	1.316	2.08	1.59	1.006	1.057	63	13
LC4	1.835	1.828	1.304	1.296	40.68	1.453	41.04	1.466	0.01	0.18	1.131	1.145	44	-6
LC5	1.903	1.911	1.438	1.428	32.29	1.153	33.81	1.208	1.81	0.33	0.933	0.946	72	22
LC6	1.934	1.897	1.483	1.430	30.36	1.084	32.67	1.167	1.61	1.86	0.874	0.944	74	24
LC7	1.876	1.906	1.498	1.465	25.22	0.901	30.1	1.075	8.33	3.18	0.856	0.897	93	43
LC8	2.049	1.938	1.657	1.554	23.69	0.846	27.65	0.988	1.15	1.16	0.678	0.789	145	95
LC9	2.069	2.003	1.691	1.582	22.32	0.797	26.62	0.951	1.41	0.99	0.644	0.757	212	162
LC10	2.051	2.009	1.671	1.587	22.72	0.811	26.54	0.948	1.93	0.78	0.664	0.751	219	169
LC11	1.993	1.945	1.561	1.487	27.63	0.987	30.85	1.102	0.69	0.66	0.780	0.870	109	59

Table 5.11 London Clay 100 mm stress path cell data.

LONDON CLAY modified oedometer	initial wet density Mg/m^3	final wet density Mg/m^3	initial dry density Mg/m^3	final dry density Mg/m^3	initial water content (w) %	initial w/PL -	final water content (w) %	final w/PL -	initial air voids %	final air voids %	initial voids ratio	final voids ratio	total swelling pressure kPa	net swelling pressure kPa
LC2-O1 #	1.824	-	1.358	-	34.25	1.223	-	-	4.61	-	1.047	-	111	100
LC2-O2	1.857	1.872	1.384	1.375	34.17	1.220	36.16	1.291	2.92	0.83	1.008	1.022	45	35
LC2-O3	1.830	1.866	1.362	1.358	34.40	1.229	37.39	1.335	4.17	0.36	1.041	1.047	67	28
LC5-O2	1.845	1.883	1.398	1.391	31.96	1.141	35.41	1.265	5.00	0.71	0.988	0.999	36	35
LC5-O3 +	1.912	1.929	1.452	1.437	31.62	1.129	34.28	1.224	1.83	-0.94	0.914	0.935	42	38
LC6-O1	1.879	1.903	1.434	1.438	31.05	1.109	32.34	1.155	3.92	1.76	0.939	0.933	67	58
LC6-O2	1.881	1.913	1.447	1.449	30.00	1.071	32.08	1.146	4.55	1.42	0.921	0.919	74	70
LC6-O3	1.896	1.927	1.457	1.449	30.11	1.075	32.97	1.178	3.69	0.11	0.907	0.919	69	65
LC7-O1 +	1.987	2.020	1.600	1.592	24.17	0.863	26.86	0.959	3.76	-0.03	0.737	0.746	204	195
LC7-O2 +	2.012	2.047	1.607	1.609	25.19	0.900	27.21	0.972	1.70	-1.68	0.730	0.727	202	200
LC7-O3 +	2.022	2.054	1.625	1.621	24.43	0.873	26.68	0.953	1.83	-1.58	0.711	0.715	211	208
LC8-O2 +	2.050	2.083	1.653	1.653	24.03	0.858	26	0.929	0.81	-2.43	0.682	0.682	232	226
LC11-O1	1.952	1.971	1.513	1.516	29.02	1.036	30	1.071	1.66	0.00	0.837	0.834	43	38
LC11-O2 +	1.959	1.982	1.518	1.521	29.04	1.037	30.32	1.083	1.29	-0.81	0.831	0.828	43	36
LC11-O3 +	1.980	2.004	1.538	1.542	28.72	1.026	30	1.071	0.49	-1.71	0.807	0.803	56	53

+ value of final air voids senstive to measurement of final sample height, negative value indicates error in measurement.

 # test incomplete, some measurements not taken.

Table 5.12 London Clay modified oedometer test data.

LONDON CLAY 38mm triaxial	initial wet density Mg/m^3	initial dry density Mg/m^3	initial water content (w) %	initial w/PL -	initial air voids %	initial voids ratio	cell pressure kPa	shear strength kPa
LC2	1.822	1.360	33.99	1.214	4.842	1.044	100	67.5
LC2	1.890	1.412	33.86	1.209	1.430	0.969	100	64
LC2	1.874	1.402	33.65	1.202	2.404	0.983	100	64
LC3	2.048	1.681	21.84	0.780	2.841	0.654	100	595.7
LC3	2.042	1.673	22.06	0.788	2.929	0.662	100	588
LC3	2.059	1.668	23.48	0.839	0.858	0.667	100	548
LC4	1.729	1.207	43.28	1.546	4.347	1.303	100	21.5
LC4	1.649	1.174	40.5	1.446	10.236	1.368	75	15.5
LC4	1.703	1.197	42.3	1.511	6.331	1.323	50	22
LC5	1.912	1.451	31.76	1.134	1.723	0.916	100	31.76
LC5	1.920	1.456	31.8	1.136	1.293	0.909	75	31.8
LC5	1.909	1.450	31.63	1.130	1.948	0.917	50	31.63
LC6	1.946	1.495	30.16	1.077	1.149	0.860	150	93.8
LC6	1.908	1.469	29.86	1.066	3.292	0.892	100	91.27
LC6	1.932	1.493	29.45	1.052	2.357	0.863	50	64.63
LC7	1.970	1.584	24.37	0.870	4.431	0.755	200	285
LC7	1.940	1.559	24.45	0.873	5.820	0.784	300	229
LC8	2.042	1.643	24.28	0.867	1.024	0.692	100	370
LC8	2.045	1.654	23.6	0.843	1.457	0.681	200	370
LC8	2.056	1.663	23.62	0.844	0.910	0.672	300	367
LC11	1.945	1.511	28.72	1.026	2.268	0.840	100	140
LC11	1.964	1.525	28.82	1.029	1.217	0.823	200	145
LC11	1.965	1.527	28.68	1.024	1.272	0.820	350	153

Table 5.13 London Clay 38 mm triaxial test data.

		vertical stress kPa	vertical strain %	water content %	w/pl	dry density Mg/m^3	air voids %	net vertical strain %
L51	initial	0	0	20.95	0.7482	1.5957	9.17	
L51	after compression	50	0.293	20.95	0.7482	1.6004	8.9	0
L51	final	50	-7.72	31.36	1.1200	1.4686	1.12	-8.013
L52	initial	0	0	21.29	0.7604	1.6139	7.59	
L52	after compression	100	0.514	21.29	0.7604	1.6222	7.11	0
L52	final	100	-4.38	29.42	1.0507	1.5109	1.2	-4.894
L53	initial	0	0	21.73	0.7761	1.5054	13.14	
L53	after compression	150	0.755	21.73	0.7761	1.5169	12.48	0
L53	final	150	-0.737	30.25	1.0804	1.4897	1.35	-1.492
L54	initial	0	0	22.57	0.8061	1.5322	10.31	
L54	after compression	250	1.069	22.57	0.8061	1.5487	9.34	0
L54	final	250	0.43	28.45	1.0161	1.5464	0.39	-0.639
L55	initial	0	0	22.01	0.7861	1.5702	8.96	
L55	after compression	50	0.215	22.01	0.7861	1.5735	8.77	0
L55	final	50	-6.88	31.57	1.1275	1.4643	1.09	-7.095
L56	initial	0	0	21.13	0.7546	1.5515	13.46	
L56	after compression	100	1.111	21.13	0.7546	1.5325	12.49	0
L56	final	100	-1.539	30.9	1.1036	1.4825	0.86	-2.65
L57	initial	0	0	21.64	0.7729	1.513	12.83	
L57	after compression	400	1.147	21.64	0.7729	1.5306	11.82	0
L57	final	400	3.842	27.49	0.9818	1.5725	0.2	2.695
L58	initial	0	0	21.86	0.7807	1.5377	11.07	
L58	after compression	300	0.878	21.86	0.7807	1.5513	10.29	0
L58	final	300	0.93	26.35	0.9411	1.5464	0.53	0.052
L59	initial	0	0	22.03	0.7868	1.5403	10.66	
L59	after compression	275	1.08	22.03	0.7868	1.5571	9.68	0
L59	final	275	1.008	27.49	0.9818	1.5485	0.99	-0.072
L41	initial	0	0	22.21	0.7932	1.5757	8.36	
L41	after compression	50	0.75	22.21	0.7932	1.5869	7.67	0
L41	final	50	-5.798	31.44	1.1229	1.4778	0.38	-6.548
L42	initial	0	0	22.5	0.8036	1.6688	2.42	
L42	after compression	50	0.34	22.5	0.8036	1.6745	2.09	0
L42	final	50	-9.454	29.86	1.0664	1.5174	0.1	-9.794
L43	initial	0	0	23.22	0.8293	1.6084	4.8	
L43	after compression	50	1.99	23.22	0.8293	1.641	2.86	0
L43	final	50	-6.18	30.19	1.0782	1.4891	1.48	-8.17
L45	initial	0	0	22.11	0.7896	1.4749	14.33	
L45	after compression	50	0.4	22.11	0.7896	1.4809	13.99	0
L45	final	50	-4.25	33.64	1.2014	1.445	1.96	-4.65

Table 5.14 London Clay computer controlled oedometer test data.

Centrifuge model tests		initial wet density Mg/m^3	initial moisture content (w) %	initial dry density Mg/m^3	initial w/pl	initial air voids %	initial voids ratio
Wadhurst Clay	CWA1	1.981	15.78	1.711	0.658	9.621	0.578
Wadhurst Clay	CWA2	1.961	18.60	1.654	0.775	7.988	0.633
Wadhurst Clay	CWA3	2.071	18.09	1.754	0.754	3.312	0.539
Wadhurst Clay	CWA4	1.947	23.97	1.570	0.999	4.196	0.719
London Clay	CLC2	1.979	26.57	1.564	0.949	2.203	0.727
London Clay	CLC3	2.021	22.27	1.653	0.795	3.747	0.634
London Clay	CLC4	1.986	21.22	1.638	0.758	6.325	0.648
Brickearth	CBE1	2.103	21.22	1.735	1.179	-0.595	0.556
Brickearth	CBE2	2.174	12.10	1.939	0.672	5.230	0.392

Table 5.15 Centrifuge test data for the three soils tested.

Average water content of two adjacent samples (W/PL) -	Average dry density of two adjacent samples Mg/m^3	Matrix Suction kPa
0.653	1.698	1893
0.653	1.697	2071
0.651	1.659	2597
0.8	1.629	922
0.795	1.625	717
0.786	1.634	743
0.858	1.634	436
0.857	1.629	505
0.85	1.627	440
0.871	1.619	435
0.874	1.629	420
0.871	1.64	4.26
0.618	1.866	3719
0.62	1.859	3806
0.966	1.621	318
0.961	1.619	338

Table 5.16 Suction measurements (Wadhurst Clay).

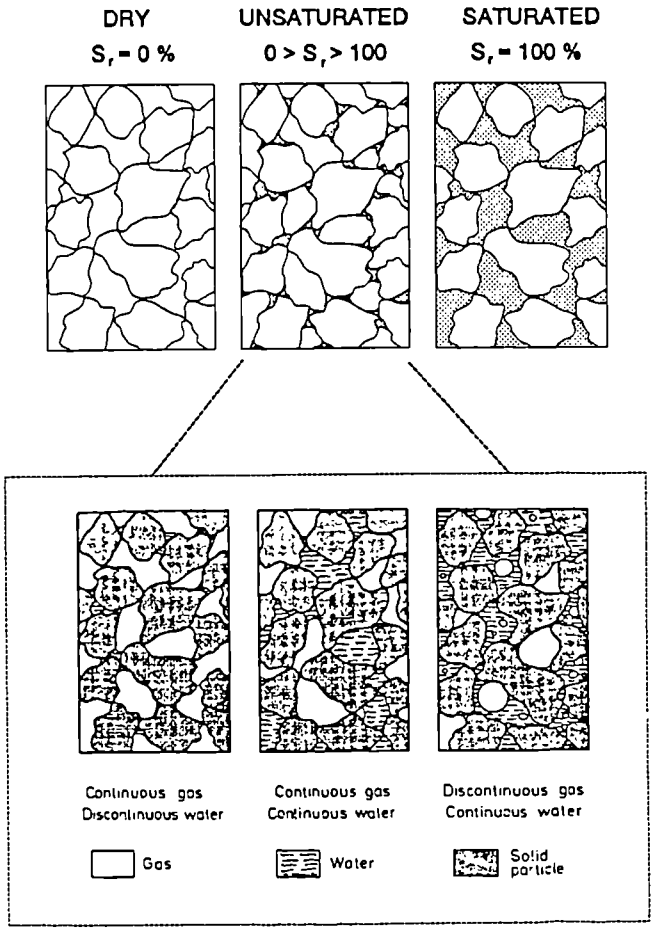

Figure 2.1 Progression from dry to saturated soil (after Wroth and Houlsby, 1985).

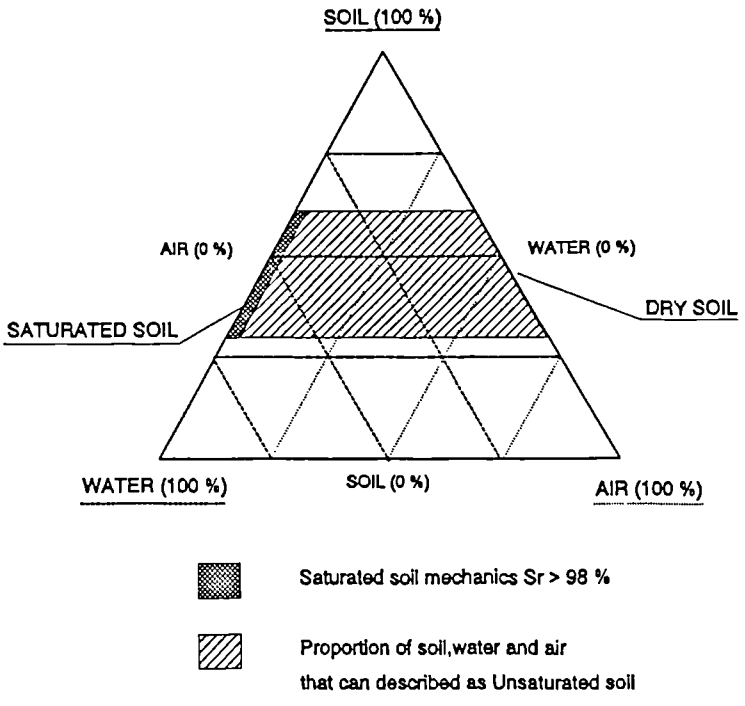

Figure 2.2 Triangular diagram showing combinations of the three phases present in unsaturated soil.

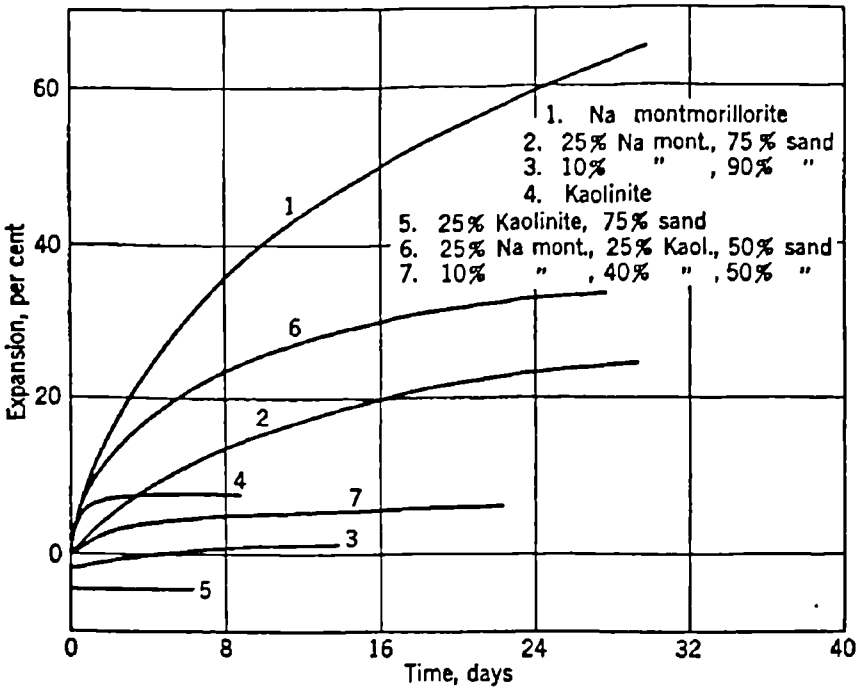

Figure 2.3 Comparison of swelling of reconstituted soils with different clay minerals under a vertical stress of 1 psi. (after Grim, 1962).

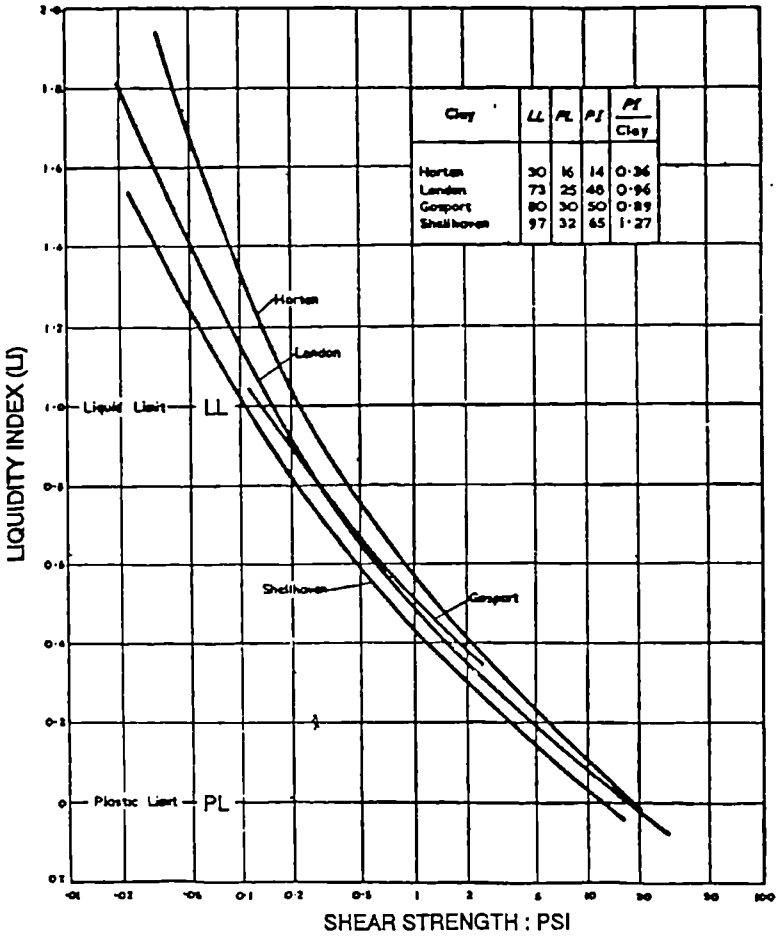

Figure 2.4 Relationship liquidity index and shear strength (after Skempton and Northey, 1953).

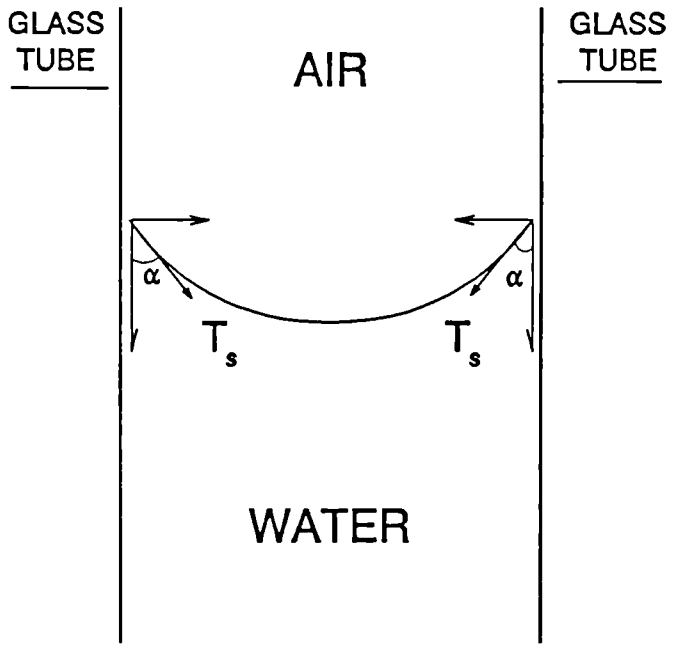

Figure 2.5 Capillary rise in a glass tube.

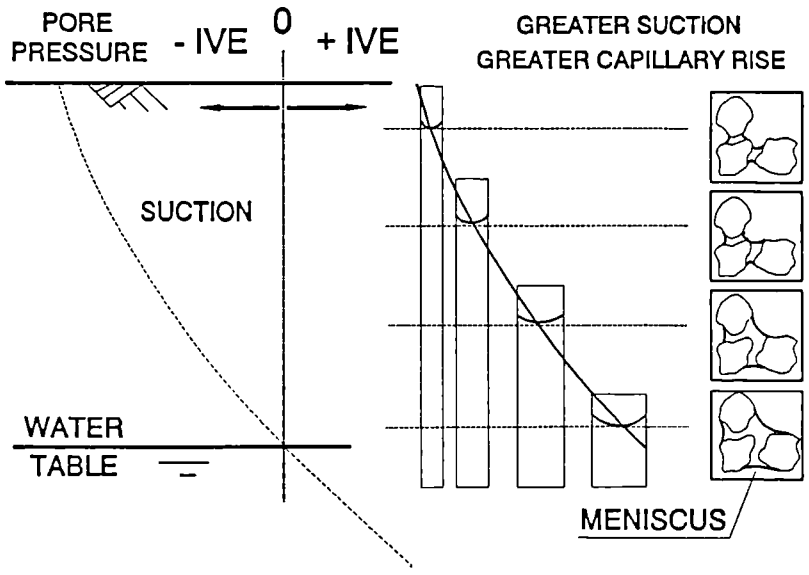

Figure 2.6 Capillary rise compared with soil suction profile in soil.

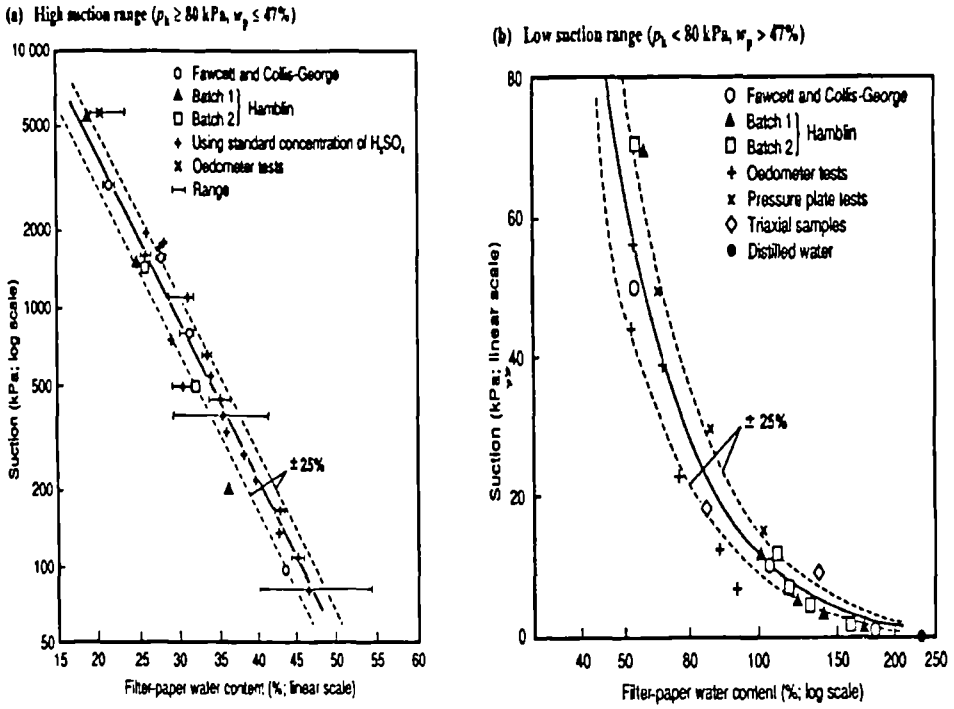

Figure 2.7 Calibration curves for Whatman's Number 42 filter paper (after Crilly et al., 1992).

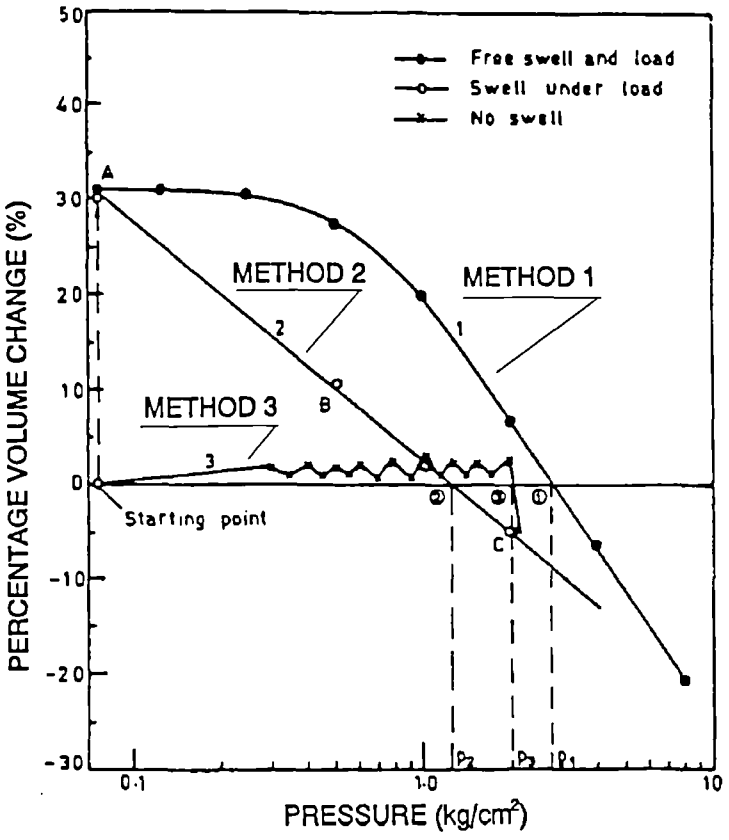

Figure 2.8 Three methods for measuring swelling pressure (after Sridharan et al., 1986).

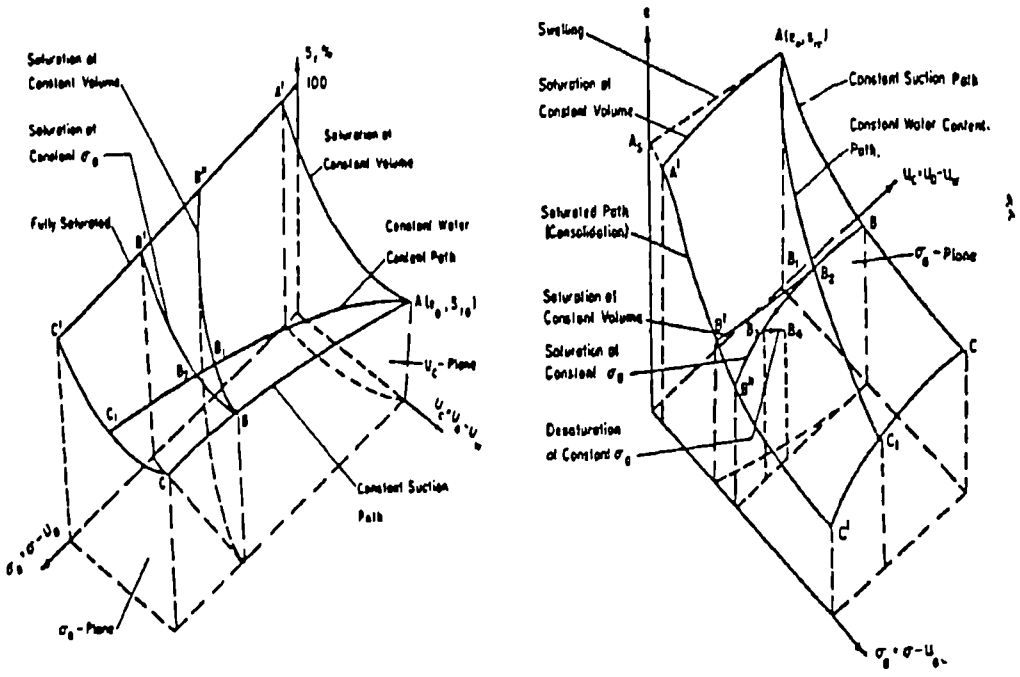

Figure 2.9 Volumetric changes of unsaturated soil described in e, $(\sigma - u_a)$, and $(u_a - u_w)$ space (after Bishop and Blight, 1963).

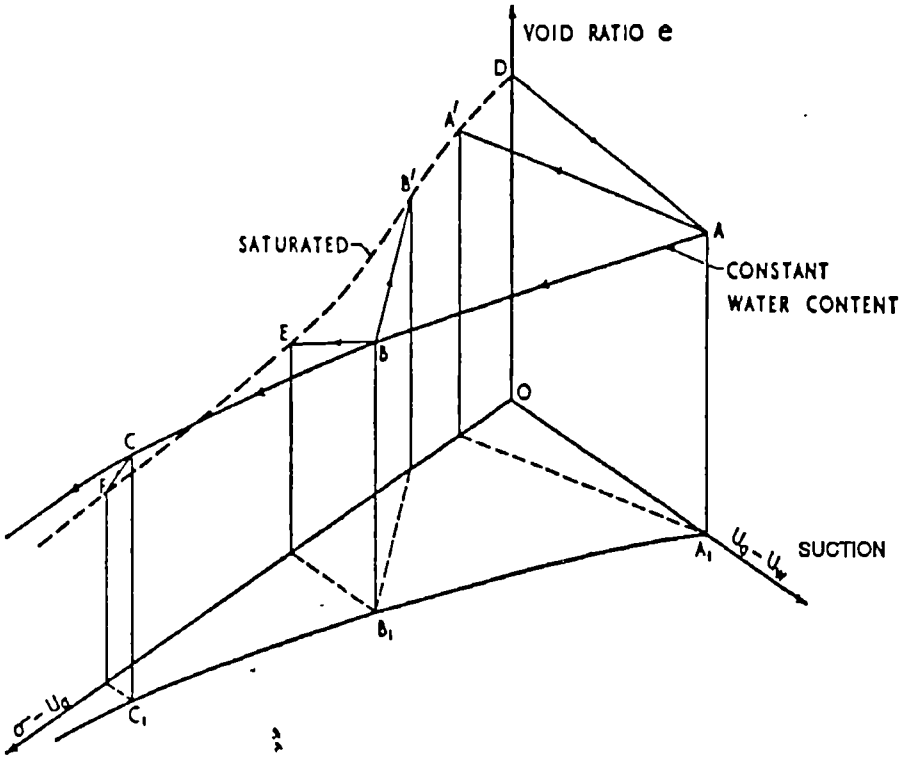

Figure 2.10 State surface in e, $(p - u_a)$ and $(u_a - u_w)$ space and S_r, $(p - u_a)$ and $(u_a - u_w)$ space (after Matyas and Radhakrishna, 1968).

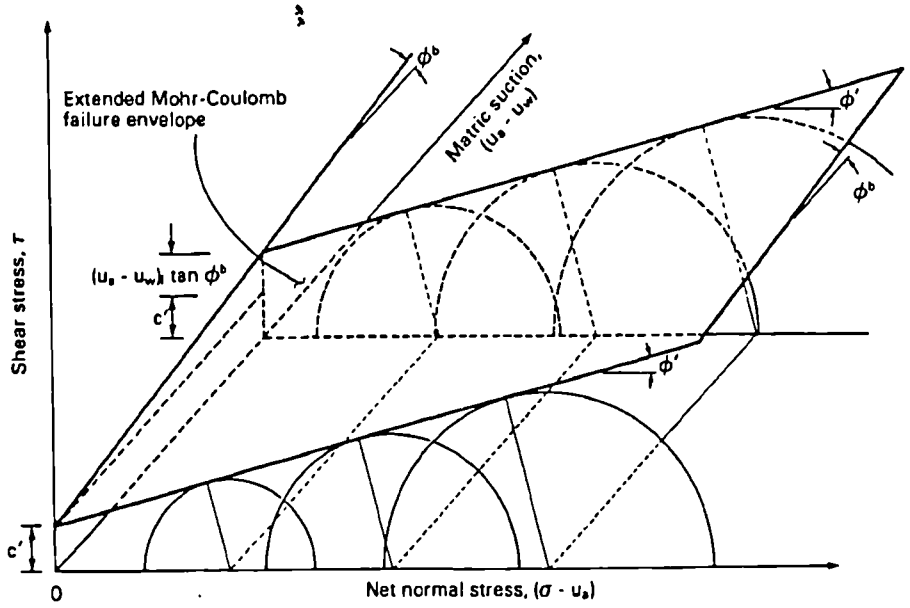

Figure 2.11 Mohr-Coulomb failure envelope extended for unsaturated soil (after Fredlund et al., 1978).

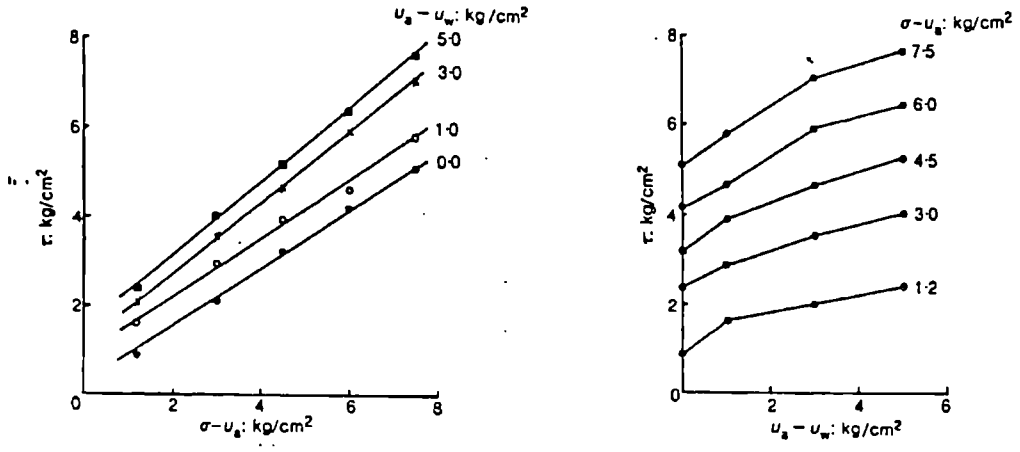

Figure 2.12 Linear relationship between τ and $(\sigma - u_a)$, non linear relationship between τ and $(u_a - u_w)$ (after Escario and Saez, 1986).

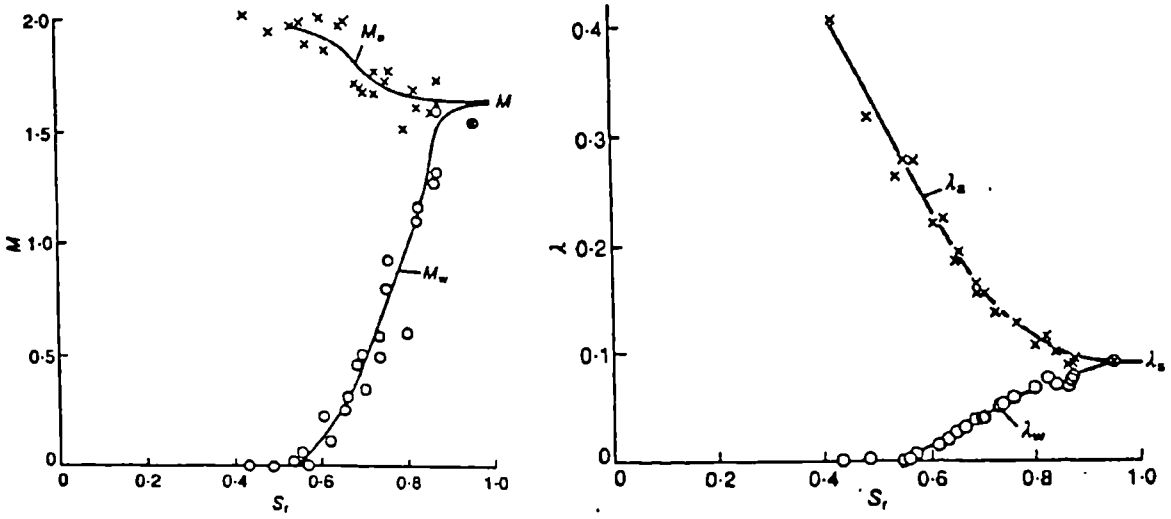

Figure 2.13 Relationships between M and S_r and λ and S_r (after Toll, 1990).

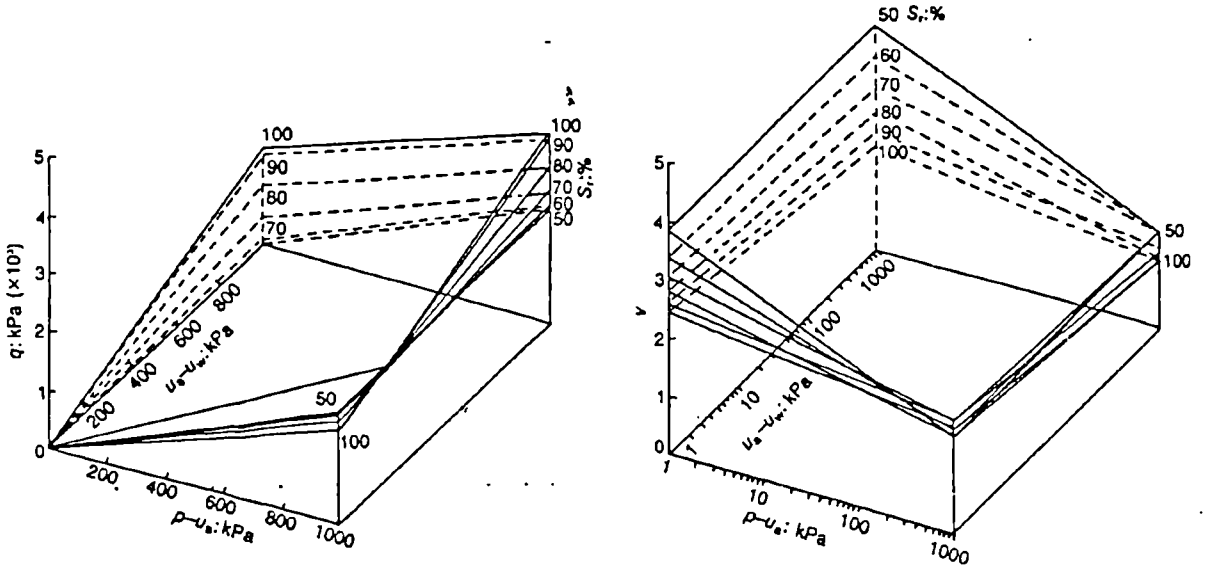

Figure 2.14 State surface in q, $(p - u_a)$ and $(u_a - u_w)$ space and S_r, $(p - u_a)$ and $(u_a - u_w)$ space (after Toll, 1990).

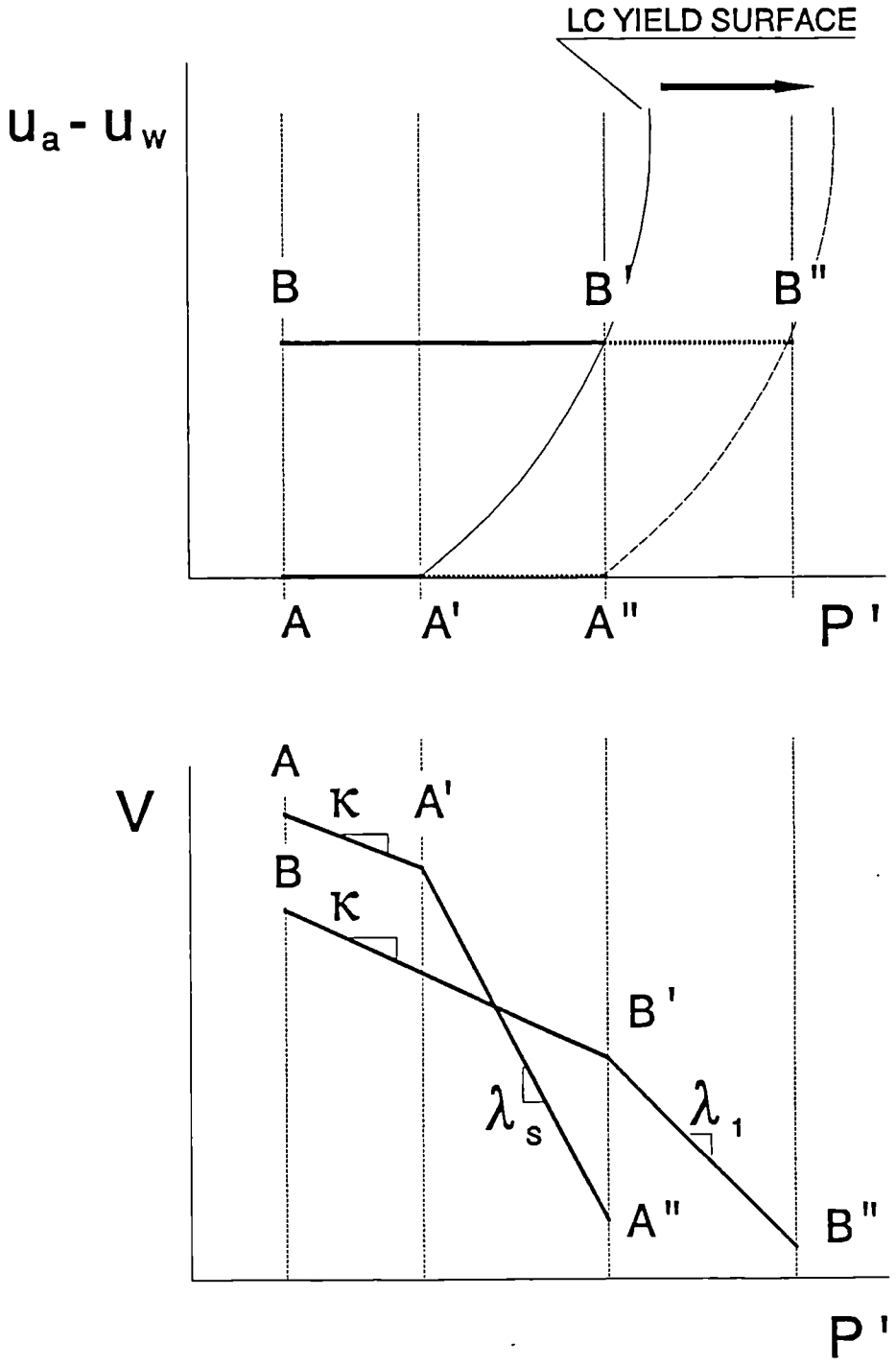

Figure 2.15 Volumetric changes for unsaturated soil at constant suction.

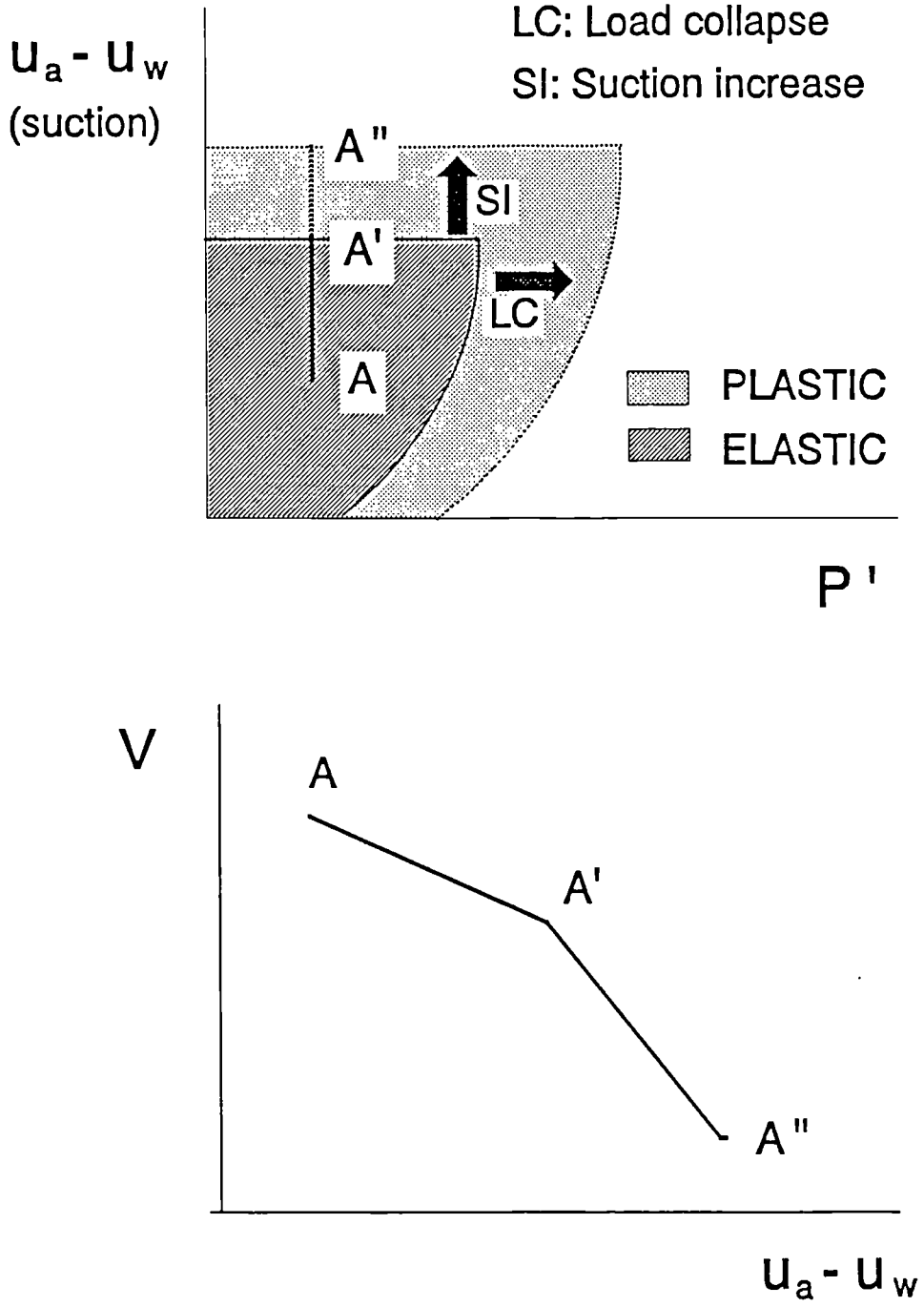

Figure 2.16 Elastic and plastic regions for unsaturated soil.

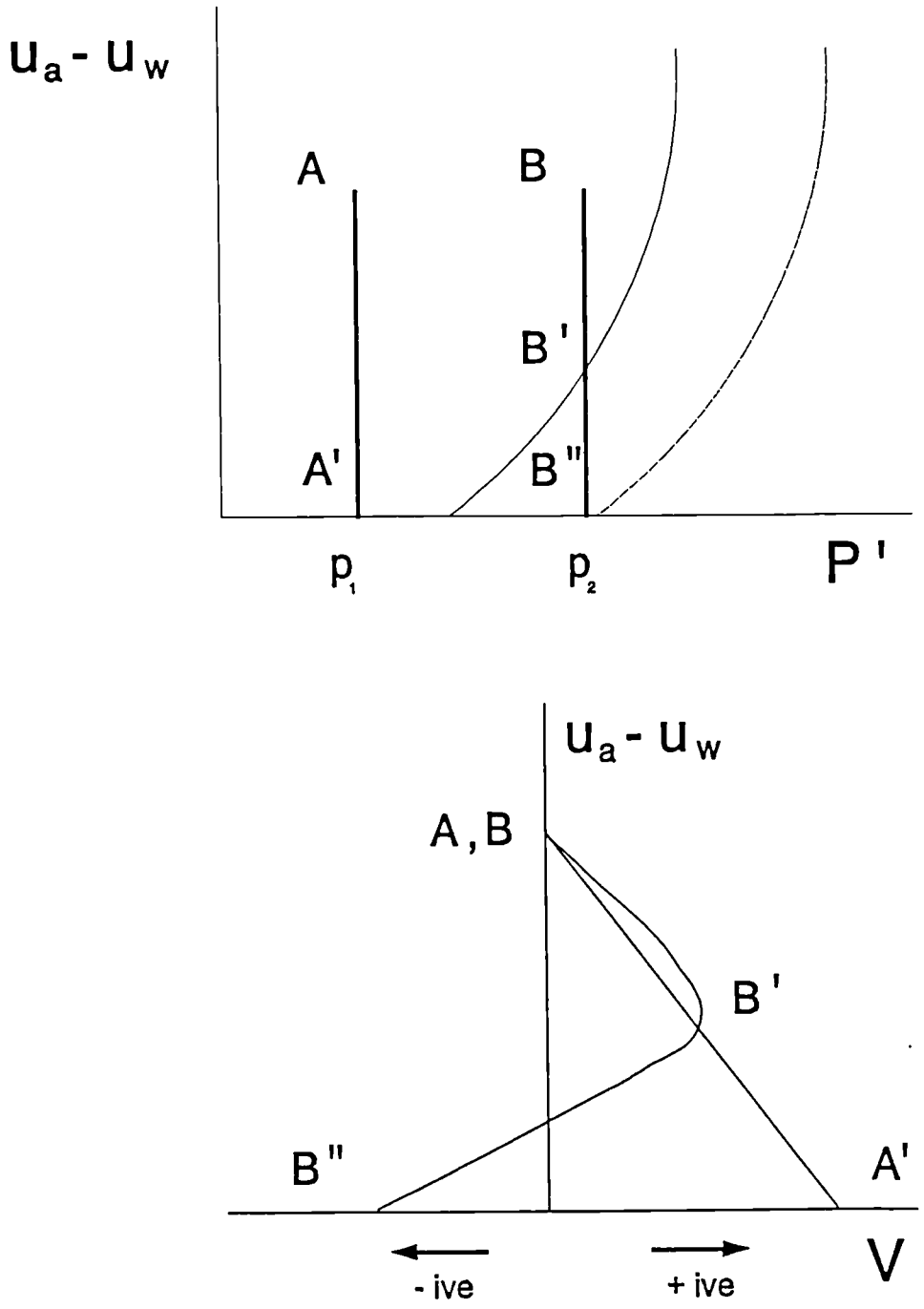

Figure 2.17 Decrease of suction under constant mean net stress.

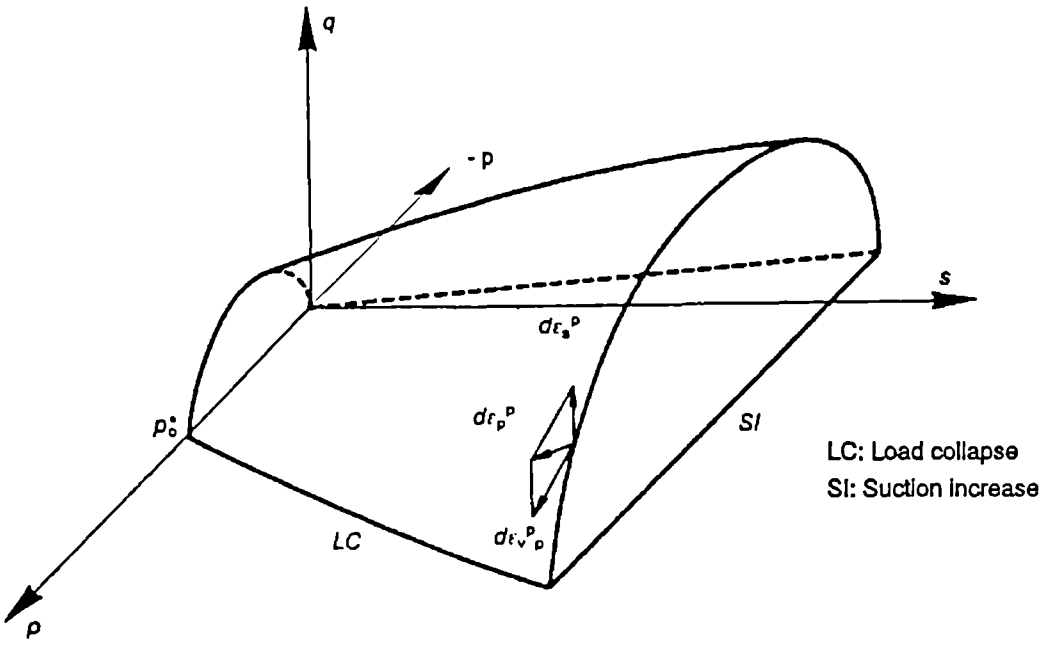

Figure 2.18 Three dimensional yield surface in q, p and s (suction) space (after Alonso et al., 1990).

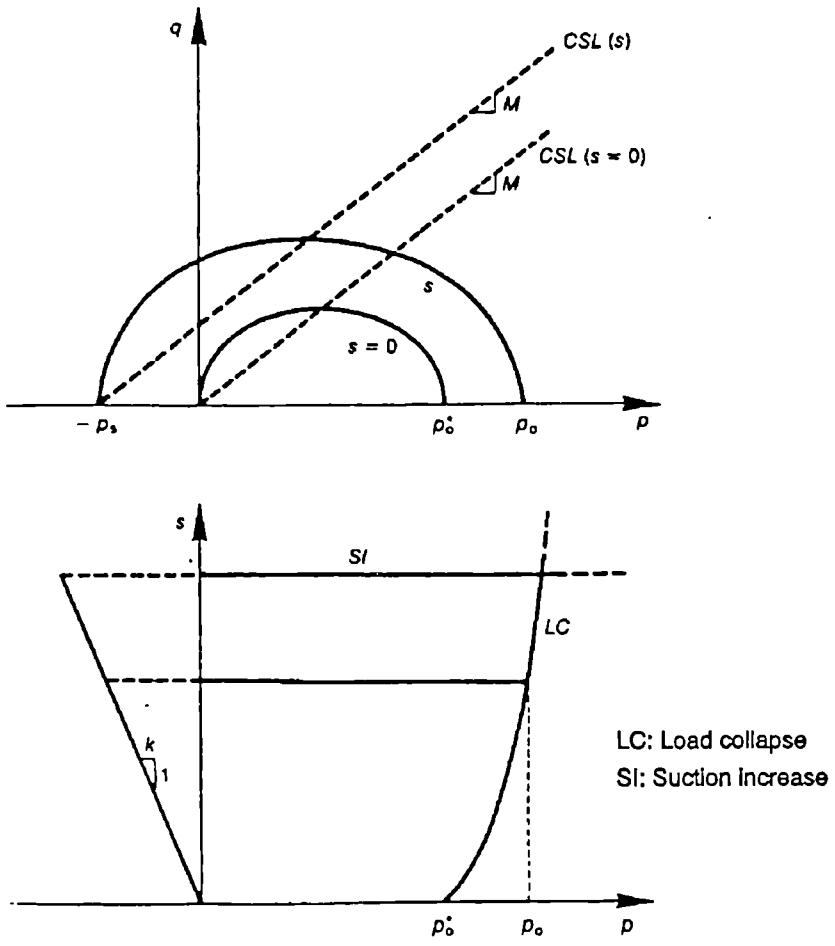

Figure 2.19 Yield surface seen through constant suction surface (after Alonso et al., 1990).

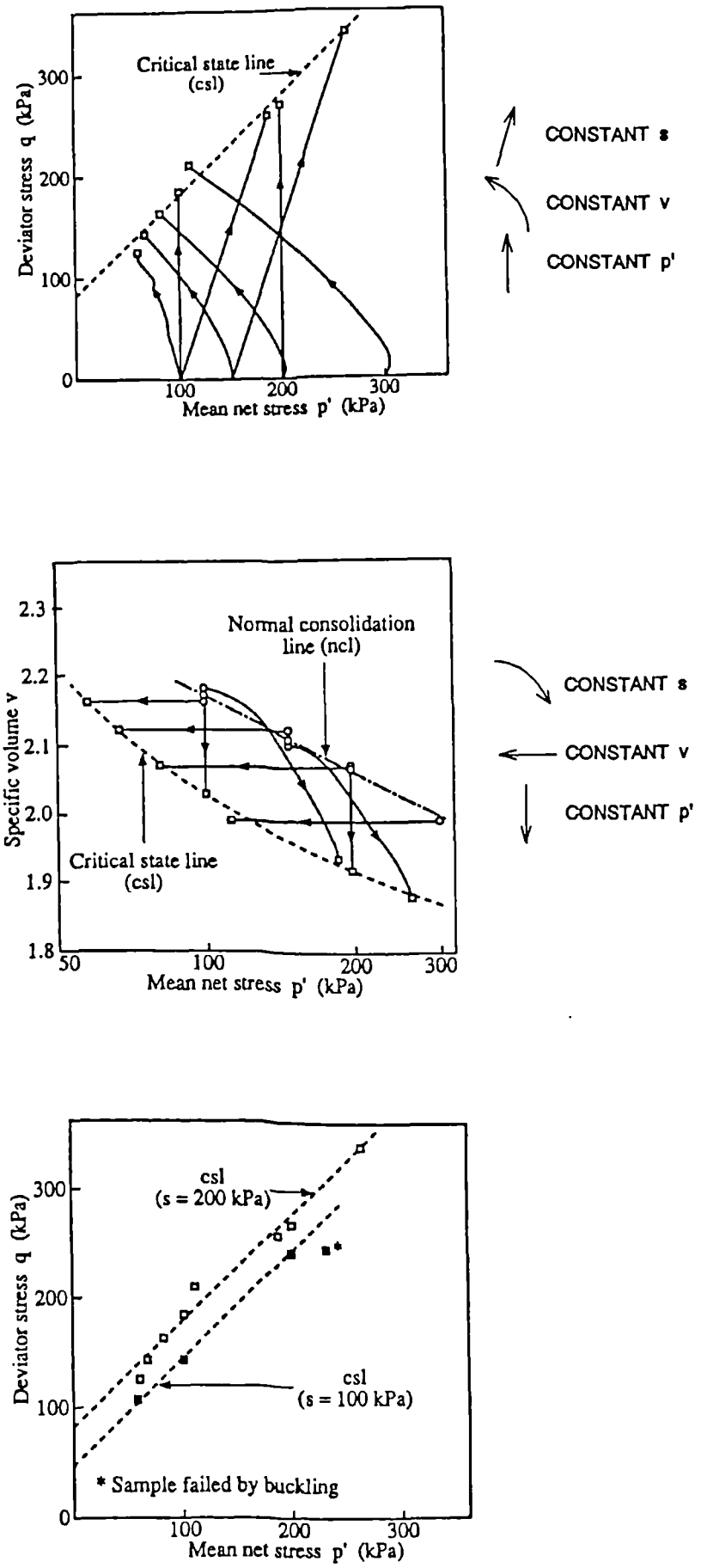

Figure 2.20 Stress paths followed for shearing unsaturated soils (after Sivakumar, 1993).

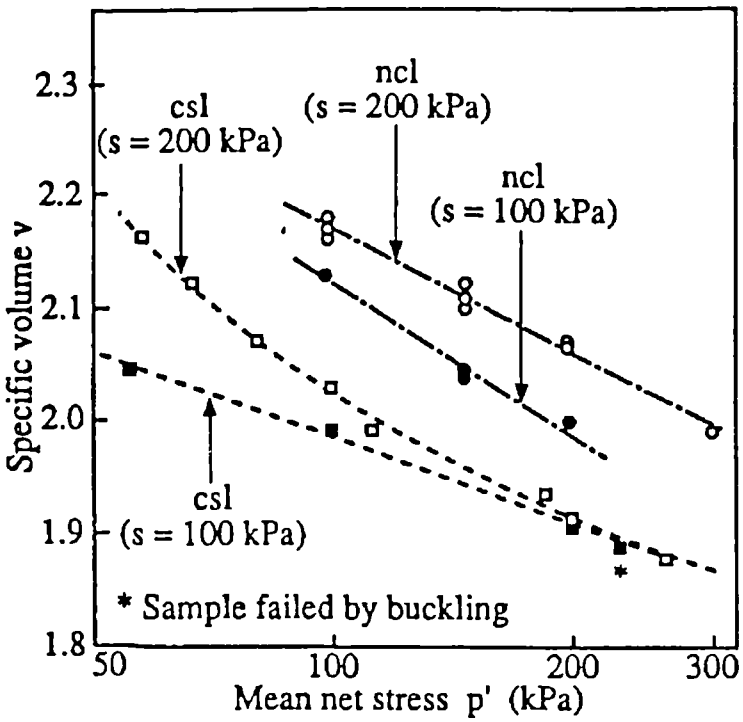

Figure 2.21 Critical state line in terms of specific volume and mean net stress (after Wheeler and Sivakumar, 1992).

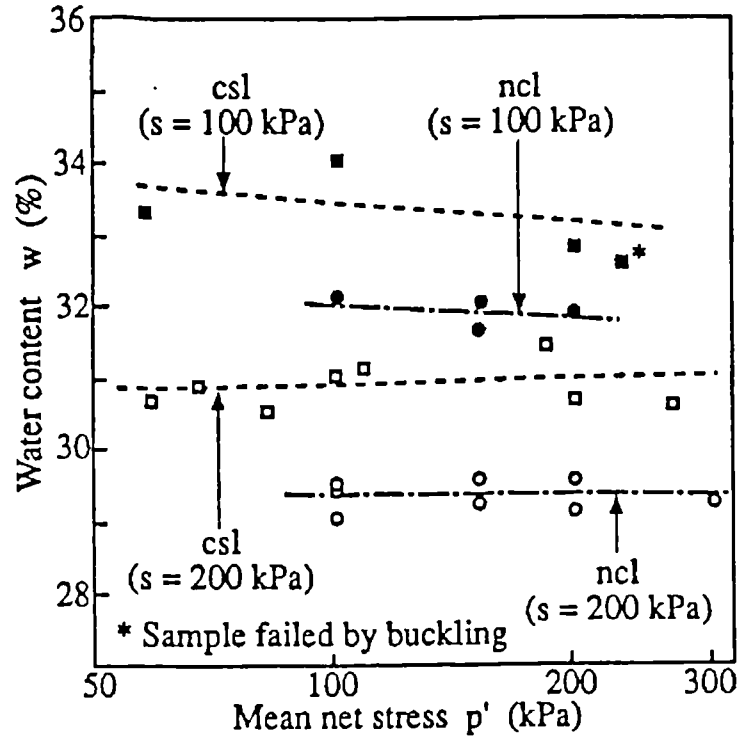

Figure 2.22 Variation of water content with mean net stress (after Wheeler and Sivakumar, 1992).

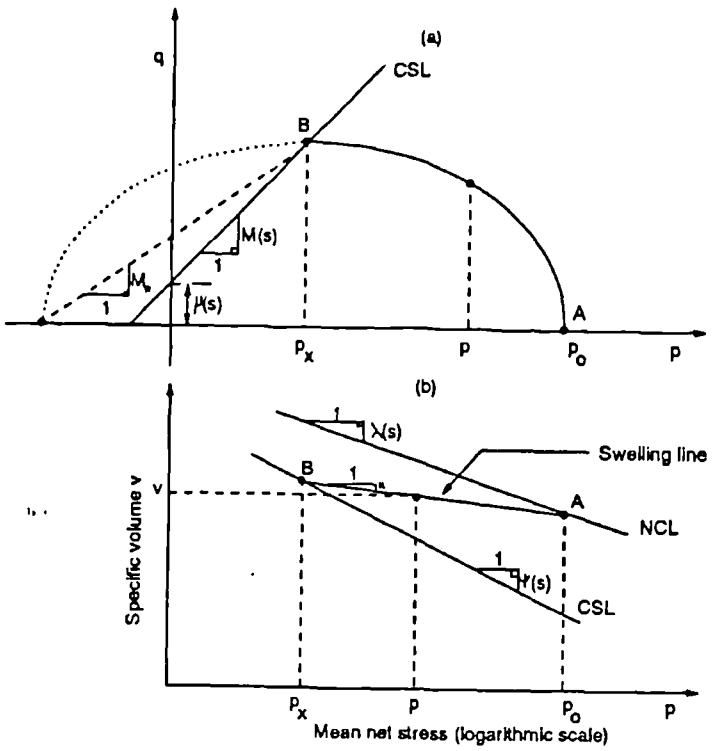

Figure 2.23 Elliptical yield surface for constant suction section (after Wheeler and Sivakumar, 1992).

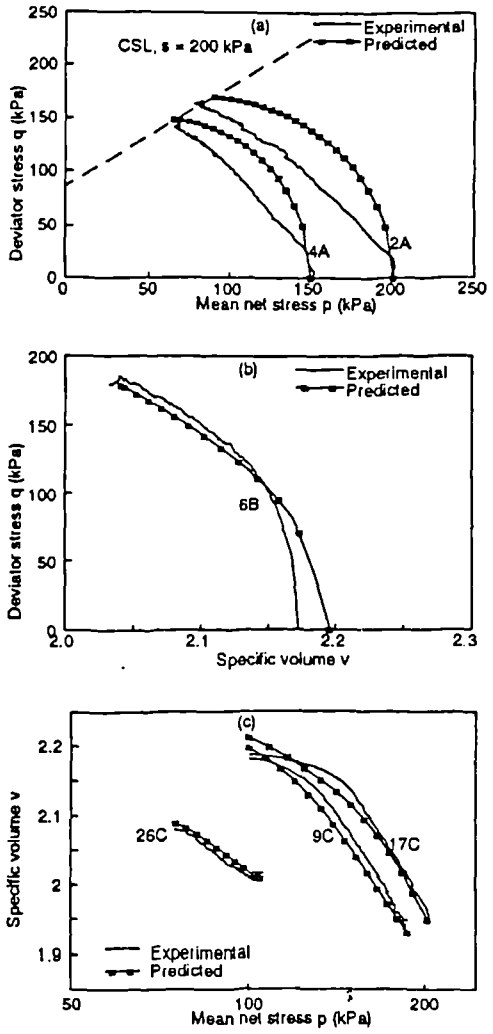

Figure 2.24 Comparison between mathematical model and test results. (after Wheeler and Sivakumar, 1992).

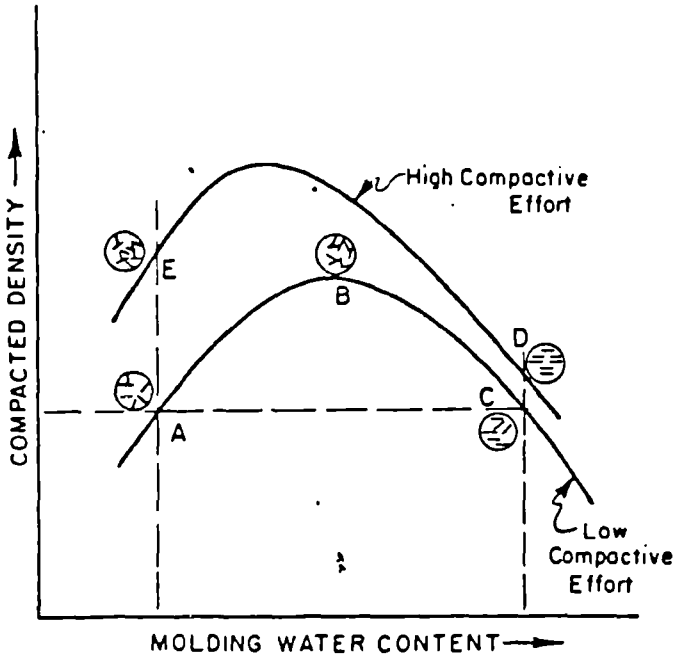

Figure 2.25 Variation of dry density with water content showing "flocculated" and "dispersed" fabric (after Seed and Chan, 1959).

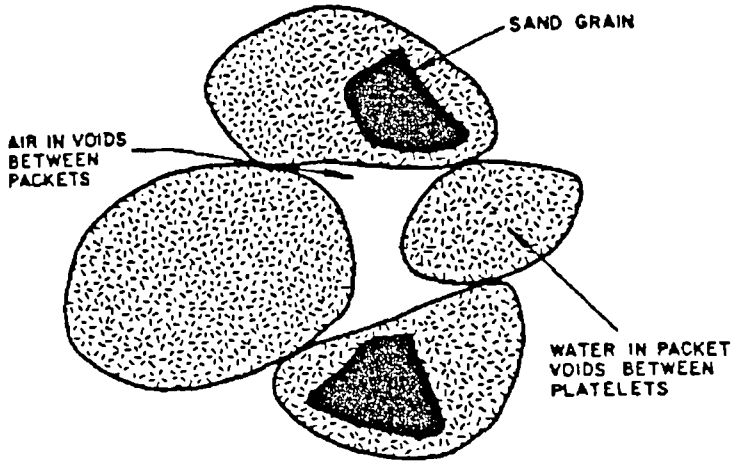

Figure 2.26 Simplified model of unsaturated soil (after Brackley, 1975).

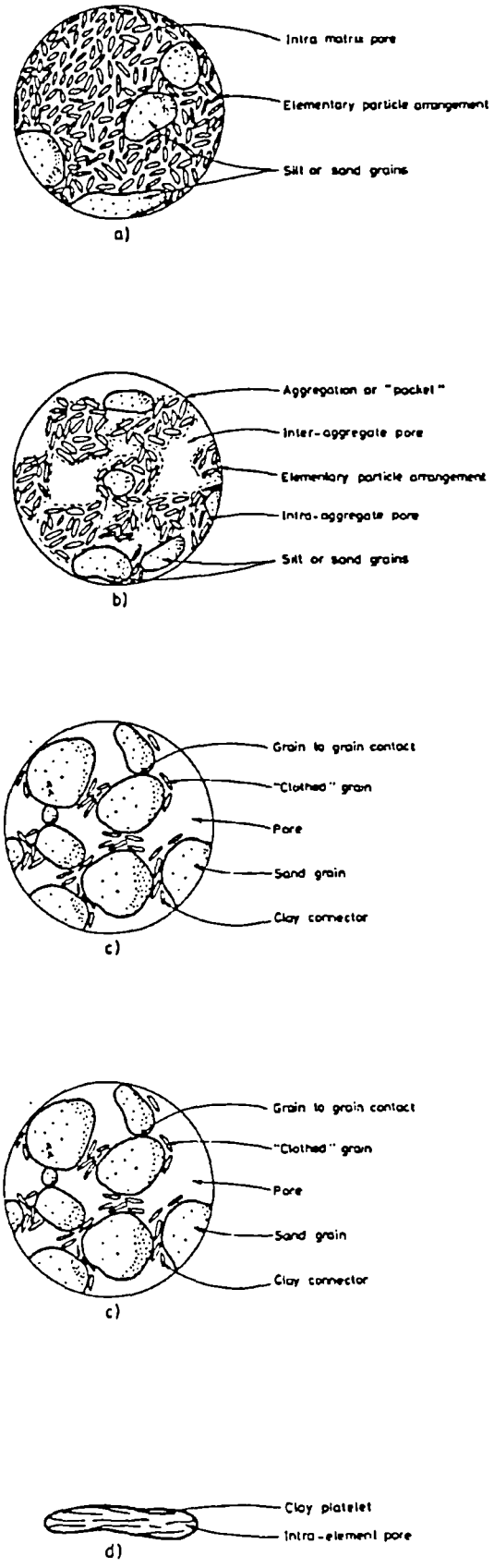

Figure 2.27 Micro – fabric of collapsible and expansive soils (after M^{c}Gown and Collins, 1975).

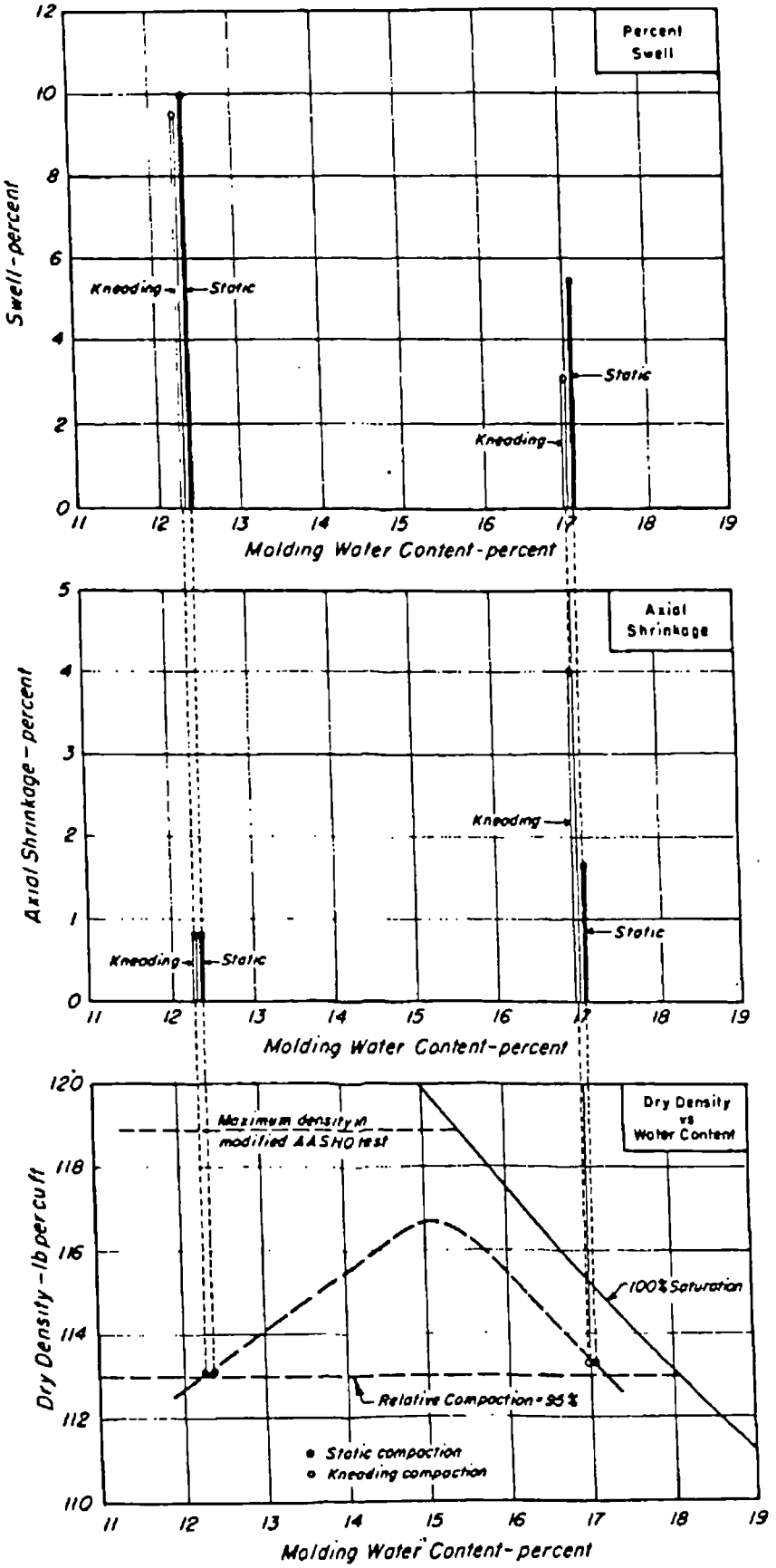

Figure 2.28 Comparison of unsaturated soil compacted using different methods at moisture contents both wet and dry of optimum (after Seed and Chan, 1959).

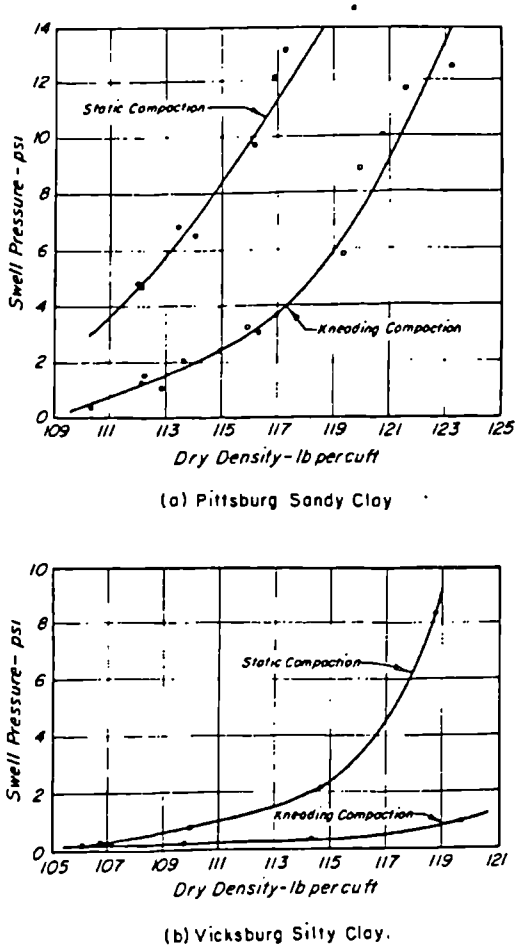

Figure 2.29 Variation in swelling pressure with dry density for different compaction methods (after Seed and Chan, 1959).

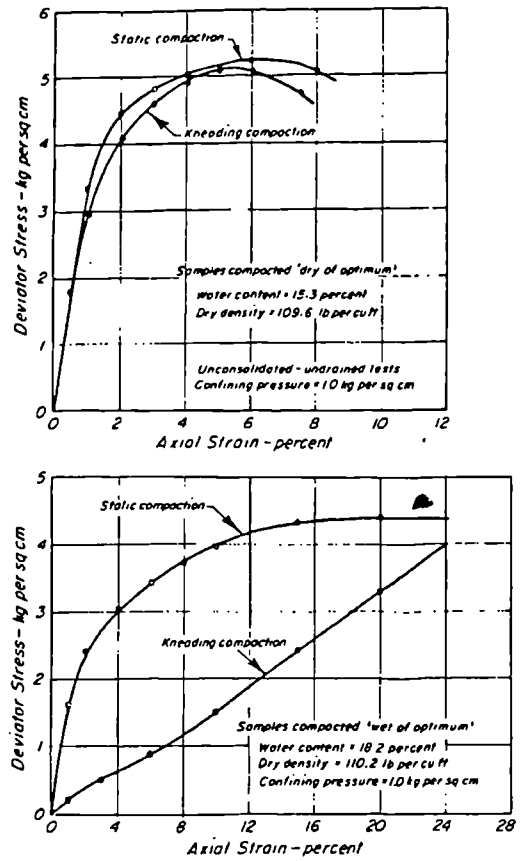

DRY OF OPTIMUM

WET OF OPTIMUM

Figure 2.30 Variation in deviatoric stress with axial strain for different compaction methods (after Seed and Chan, 1959).

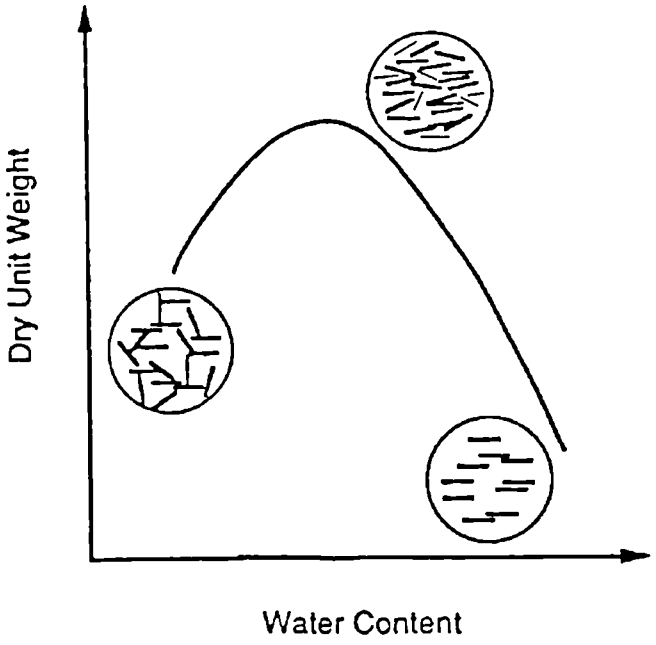

Figure 2.31 Soil structure with respect to dry density and water content (after Benson and Daniel, 1991).

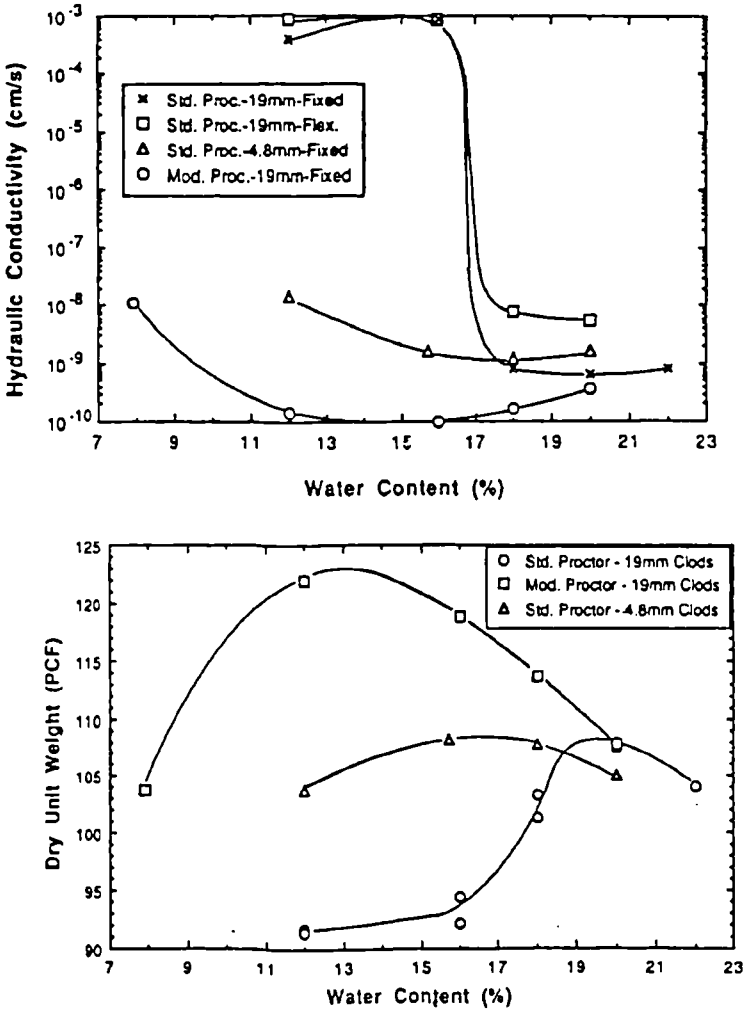

Figure 2.32 Hydraulic conductivity and dry density related to water content. Soils prepared with granules of different nominal sizes (after Benson and Daniel, 1991).

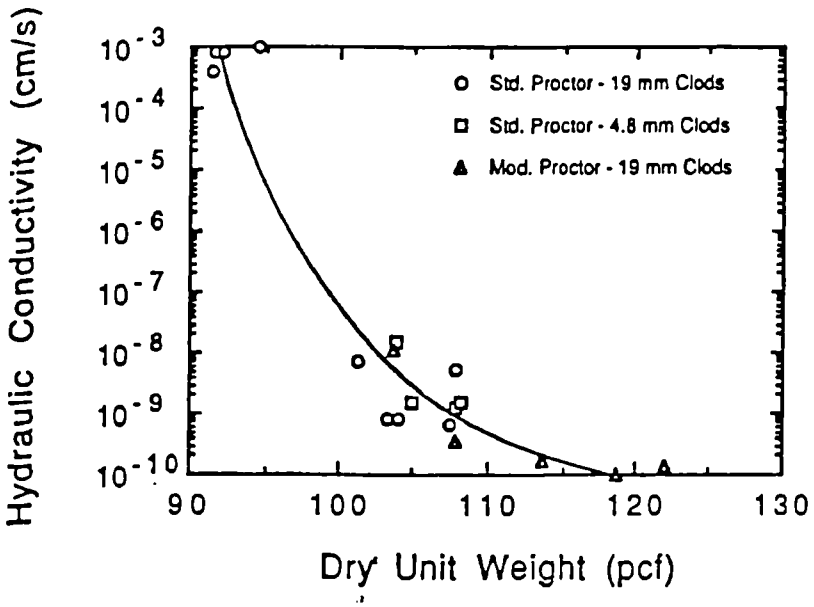

Figure 2.33 Variation of hydraulic conductivity with dry unit weight (after Benson and Daniel, 1991).

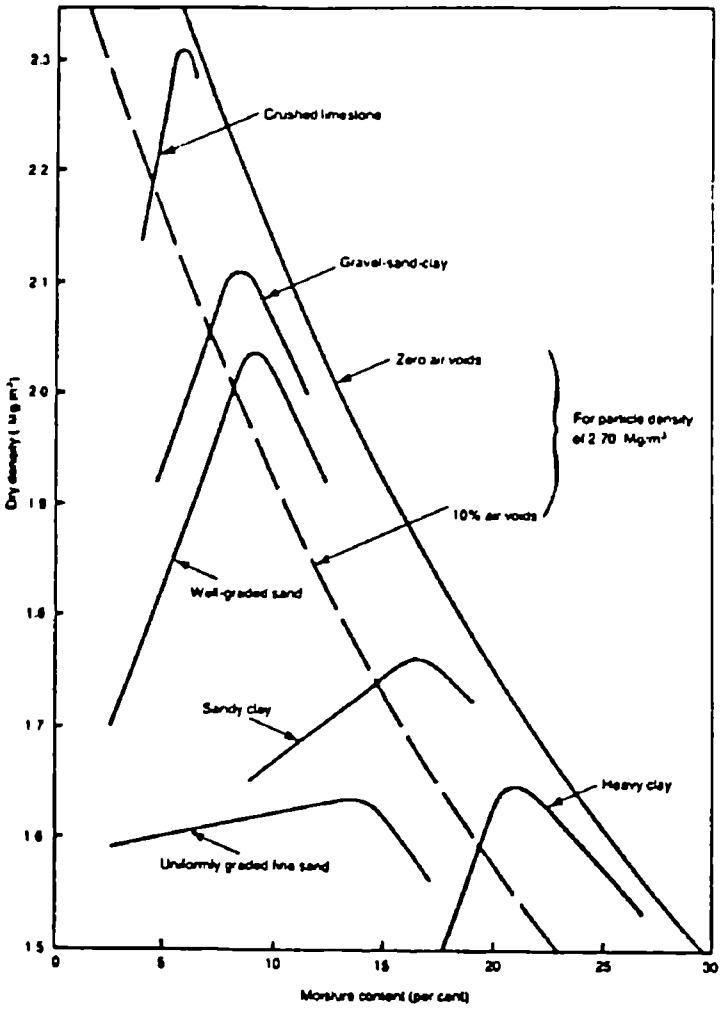

Figure 2.34 Typical compaction curves for different soils (after Parsons, 1992).

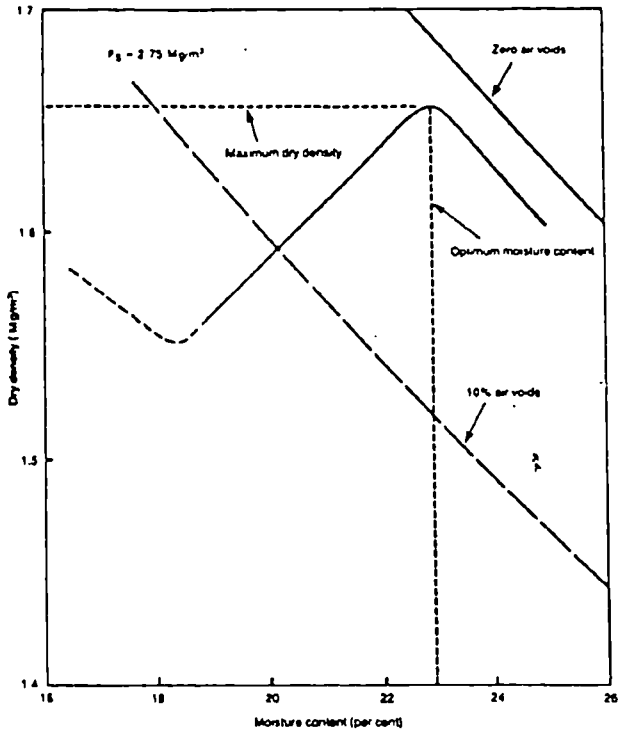

Figure 2.35 Expanded view of compaction curve of soil (after Parsons, 1992).

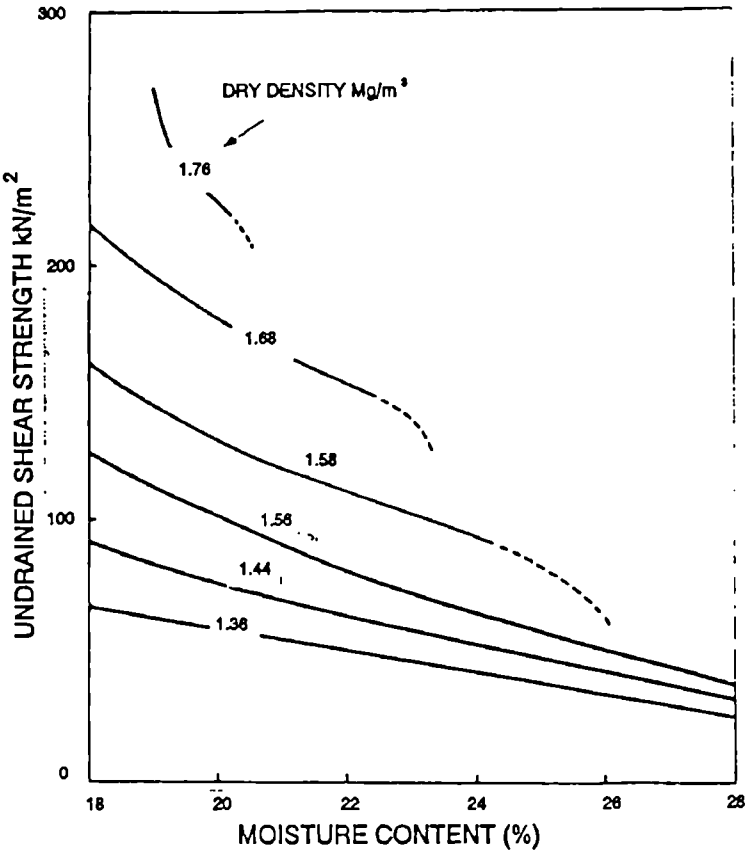

Figure 2.36 Variation of unconfined compression with dry density and moisture content (after Lewis, 1959).

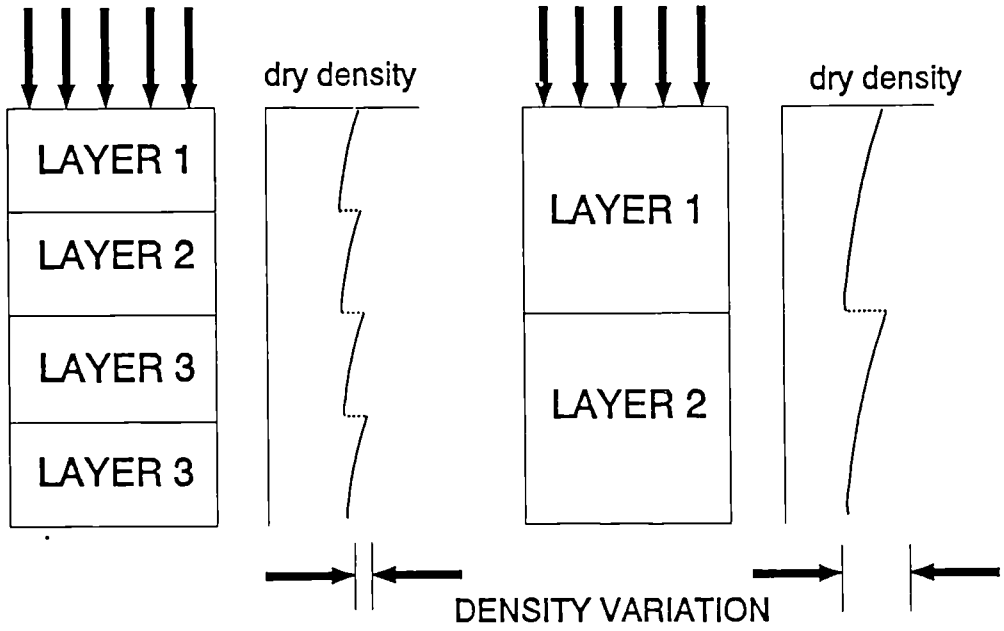

Figure 2.37 Variation of density with layer thickness.

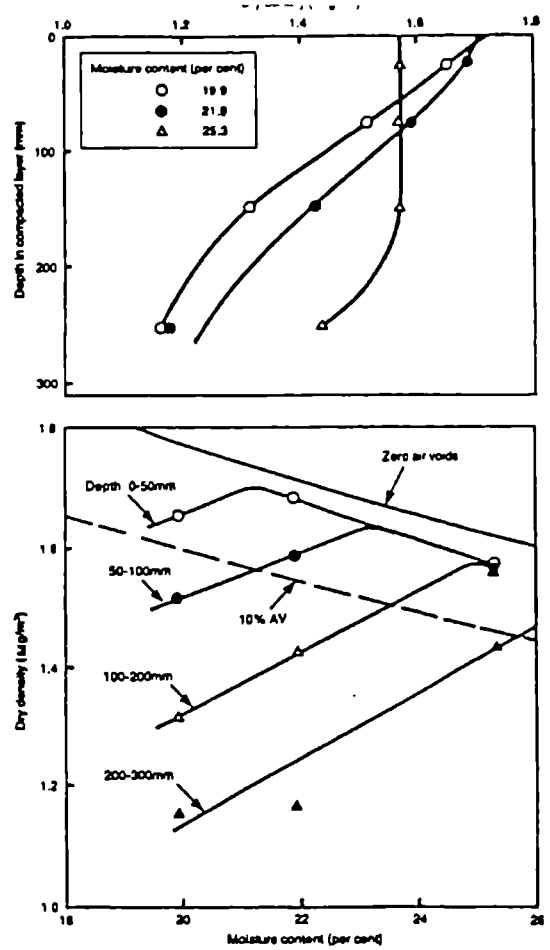

Figure 2.38 Comparison of layer thickness and achieved dry density (after Parsons, 1992).

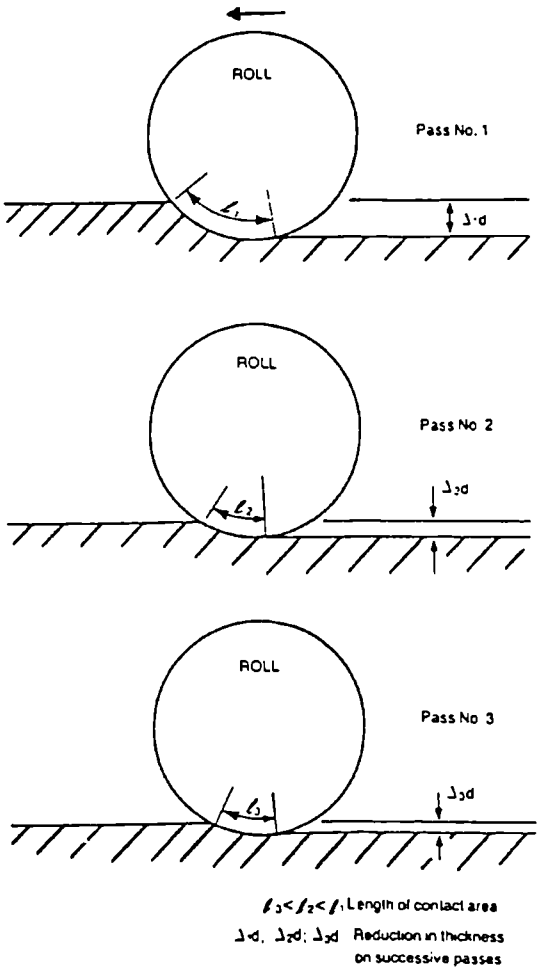

Figure 2.39 The increase in applied stress when compacting with roller (after Parsons, 1992).

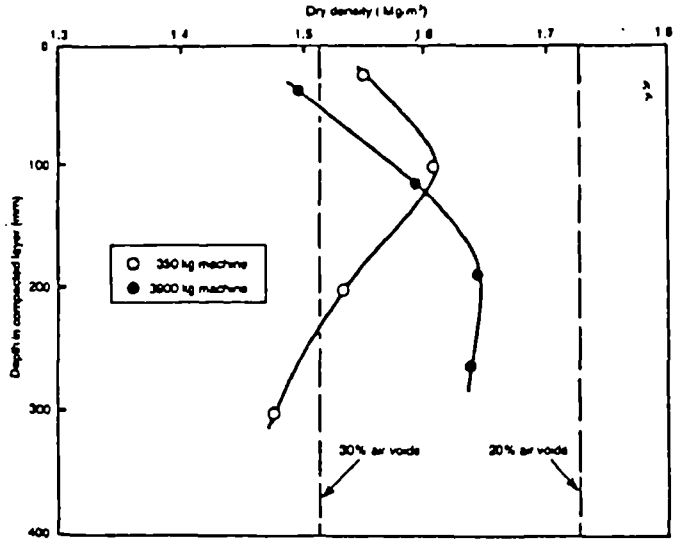

Figure 2.40 Variation in dry density with depth for different compaction stresses (after Parsons, 1992).

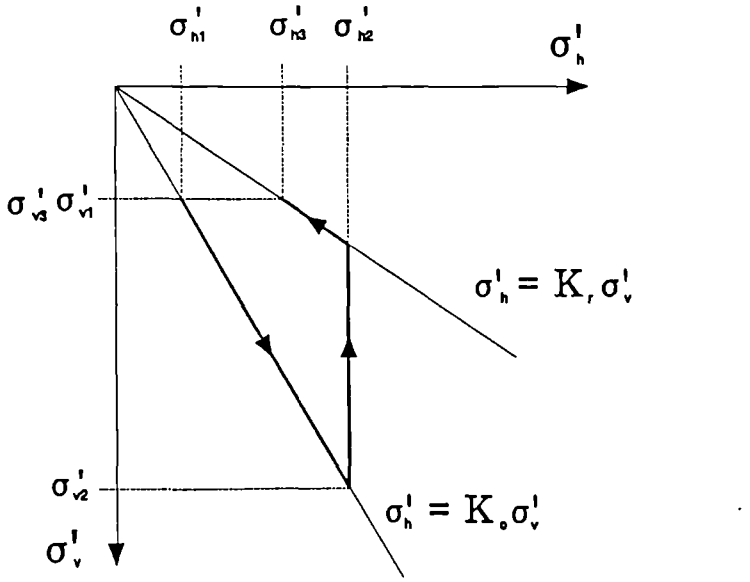

Figure 2.41 Horizontal and vertical stresses on an element of compacted soil.

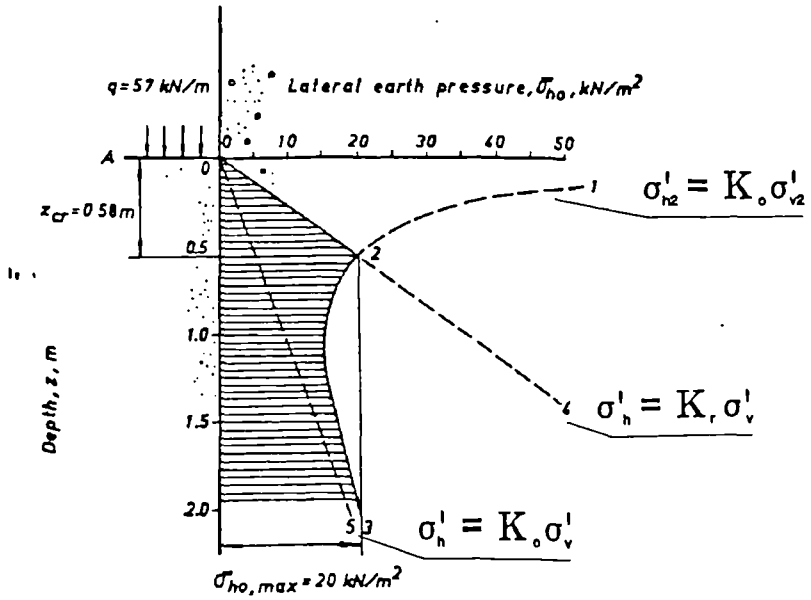

Figure 2.42 Variation of lateral earth pressure with depth for single soil layer (after Broms, 1971).

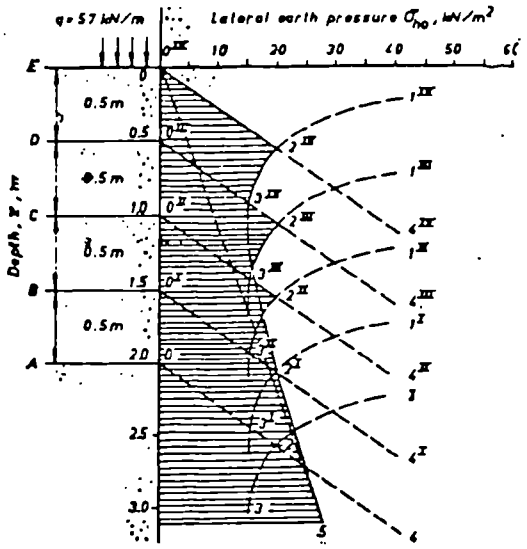

Figure 2.43 Variation of lateral earth pressure with depth for several layers (after Broms, 1971).

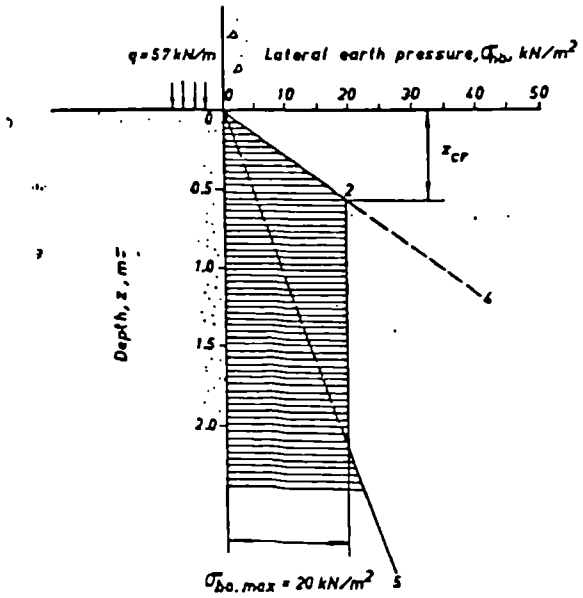

Figure 2.44 Simplified lateral stress distribution (after Broms, 1971).

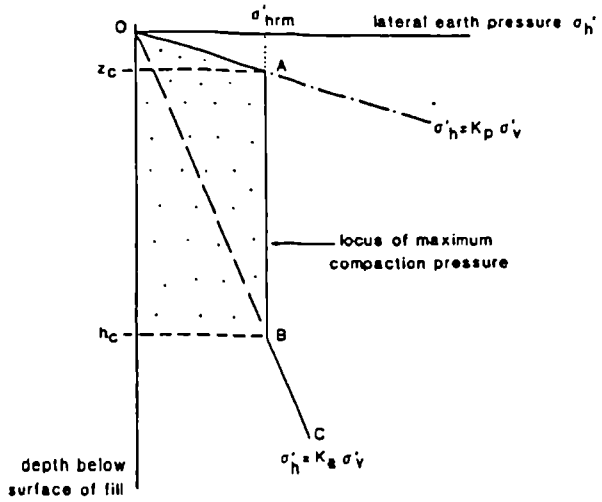

Figure 2.45 Simplified lateral stress distribution (after Ingold, 1979).

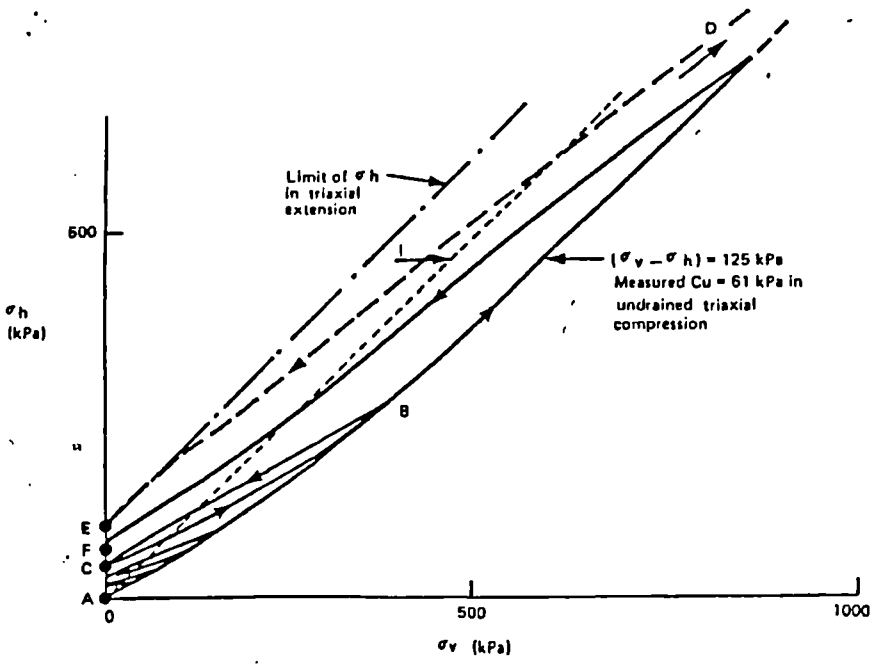

Figure 2.46 Modelling of residual lateral stresses after compaction using a hydraulic oedometer (after Clayton, 1992).

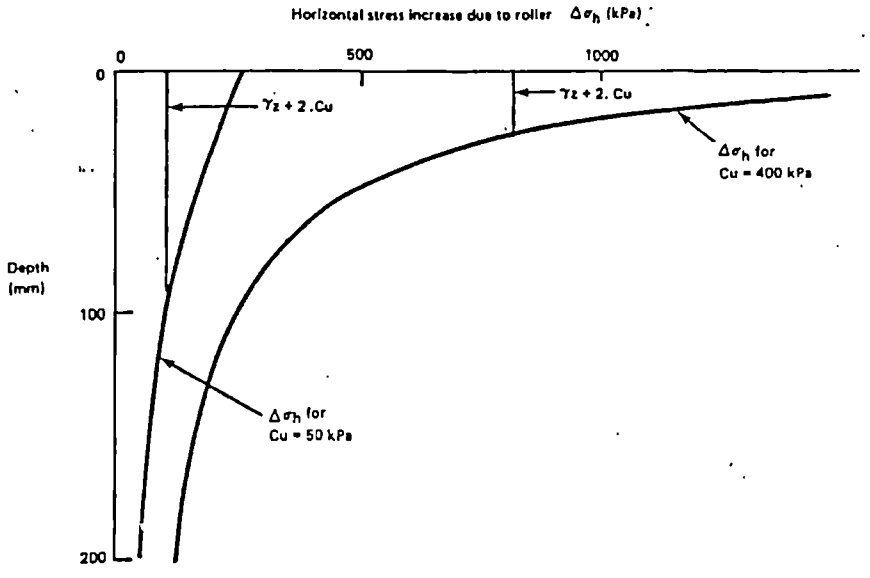

Figure 2.47 Calculated increase of horizontal stress with depth for two value of undrained shear strength (after Clayton, 1992).

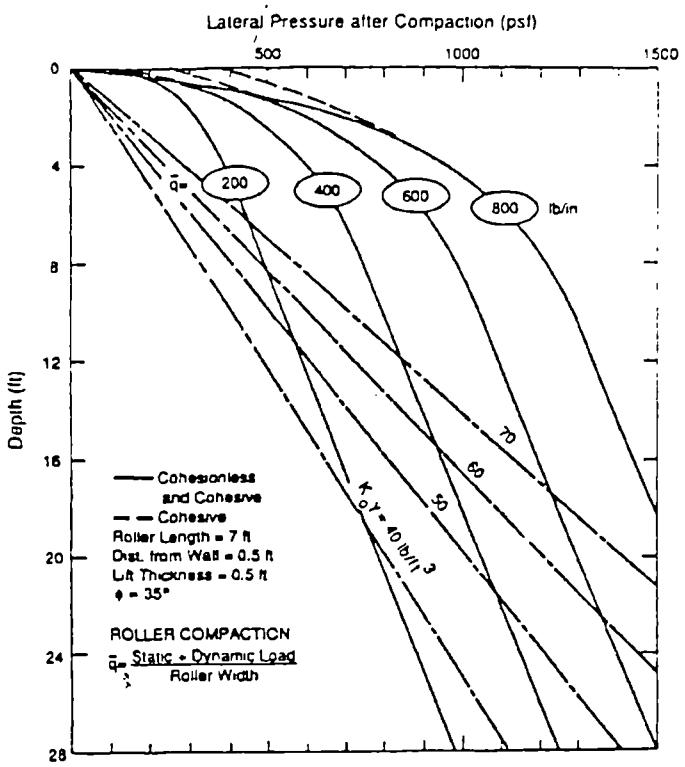

Figure 2.48 Chart relating lateral earth pressure with after compaction for different soil types and loads (after Duncan et al., 1991).

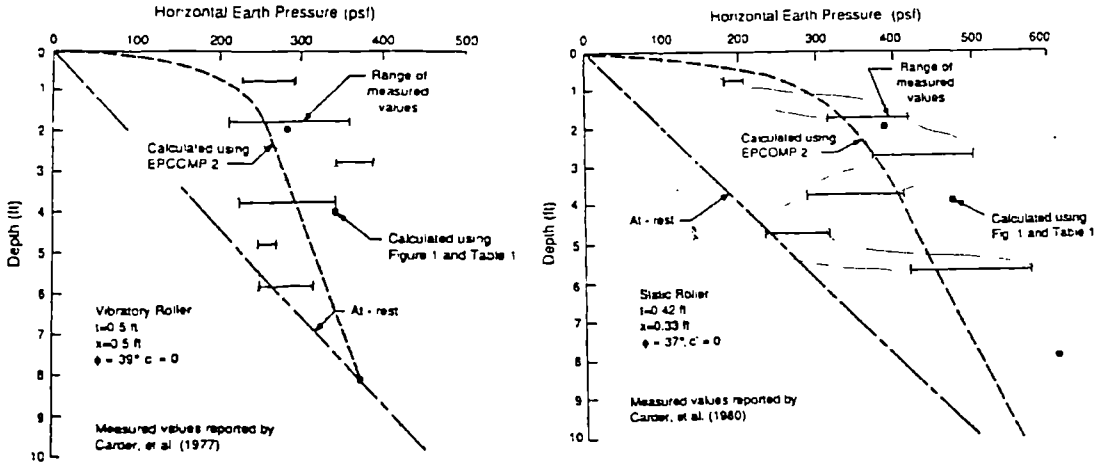

Figure 2.49 Earth pressures from computer model compared with prototype studies (after Duncan et al., 1991).

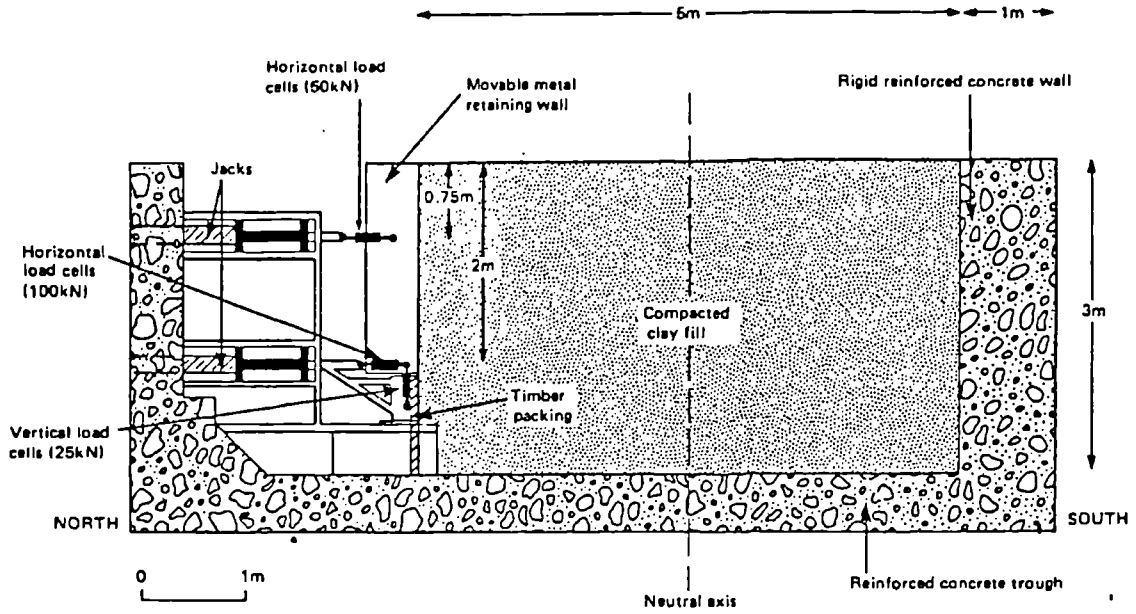

Figure 2.50 Experimental wall facility (after Symons et al., 1986).

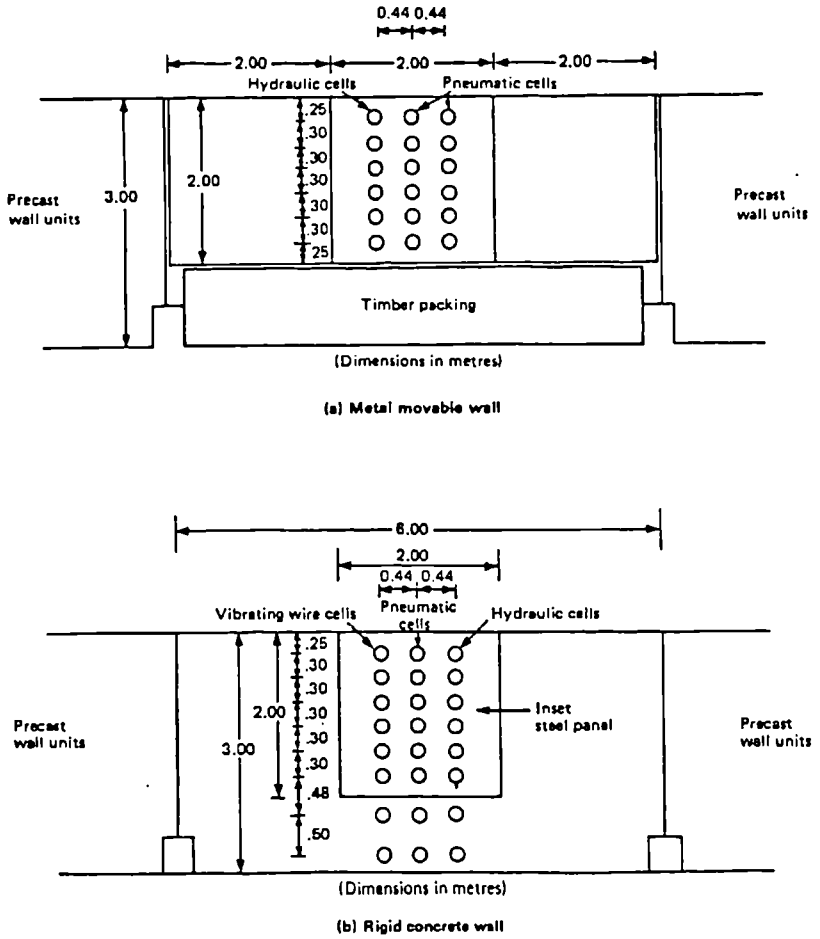

Figure 2.51 Detail of instrumented wall (after Symons et al., 1986).

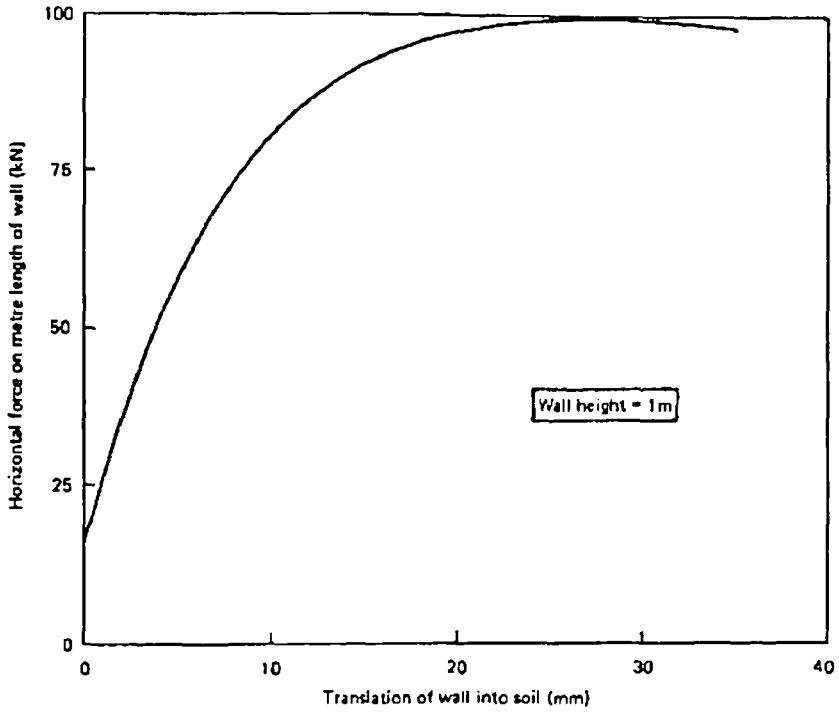

PASSIVE

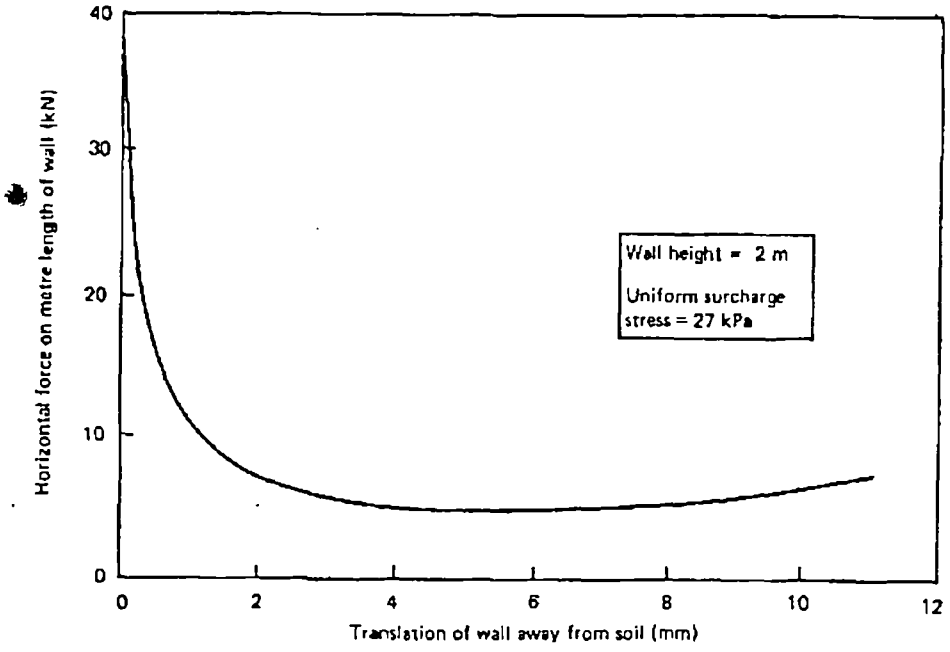

ACTIVE

Figure 2.52 Observed movement of wall in active and passive case (after Carder et al., 1977).

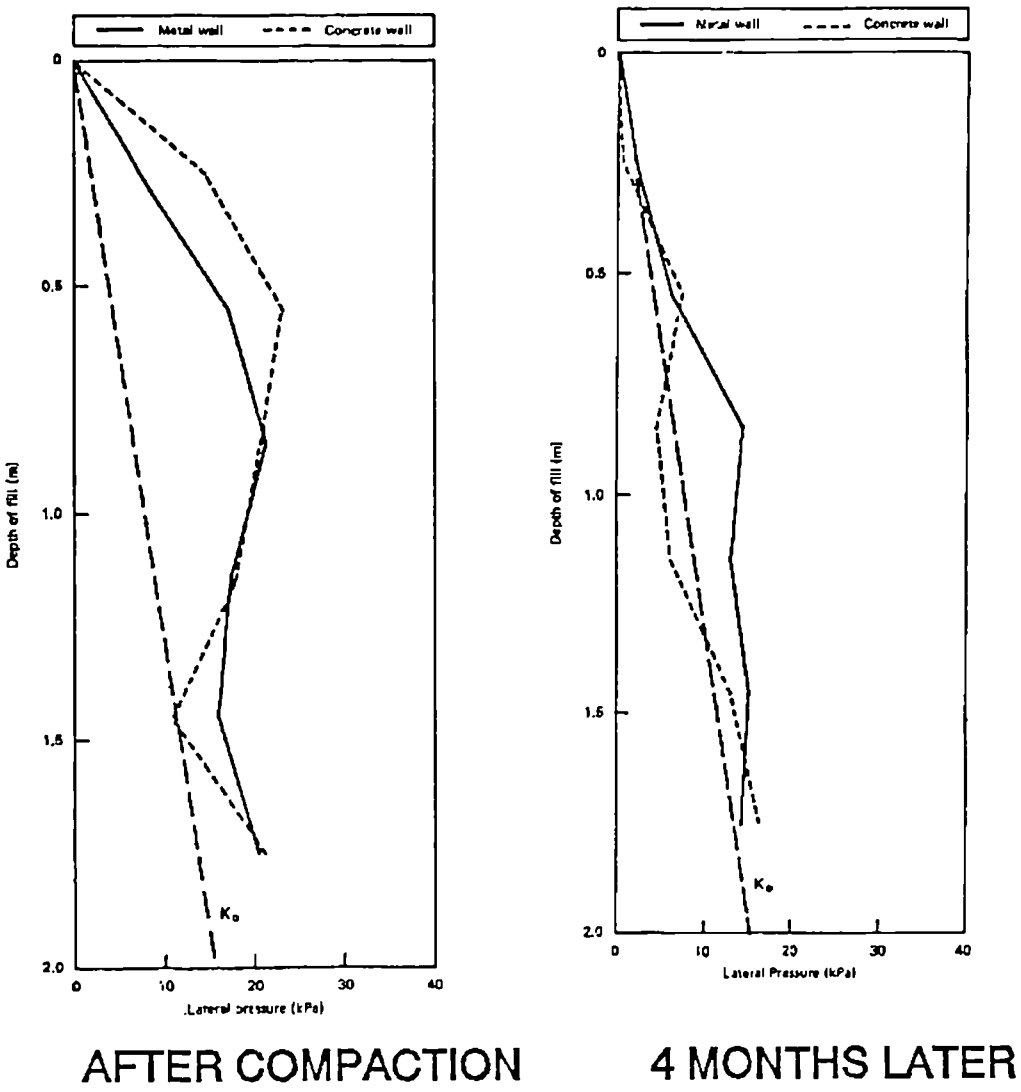

Figure 2.53 Lateral stress on experimental wall immediately after construction and 4 months later (after Carder et al., 1977).

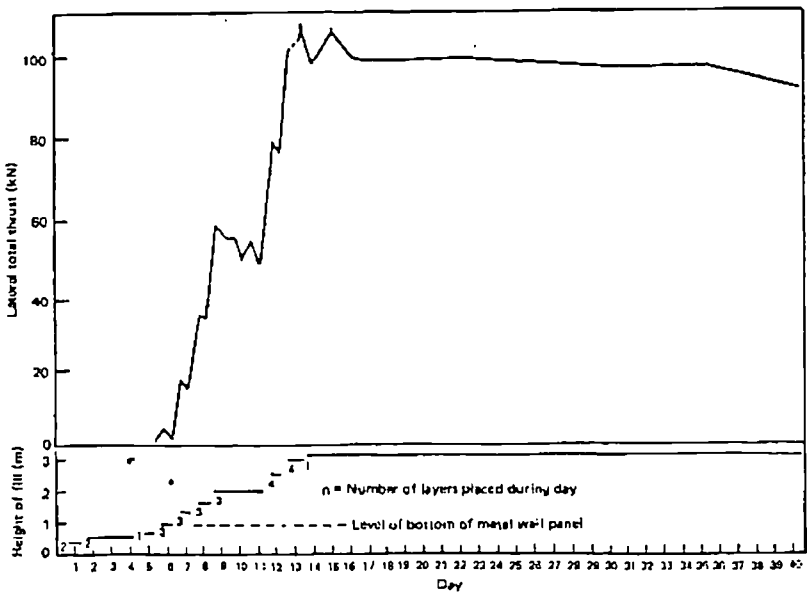

Figure 2.54 Variation of lateral thrust on experimental wall during construction (after Symons et al., 1986).

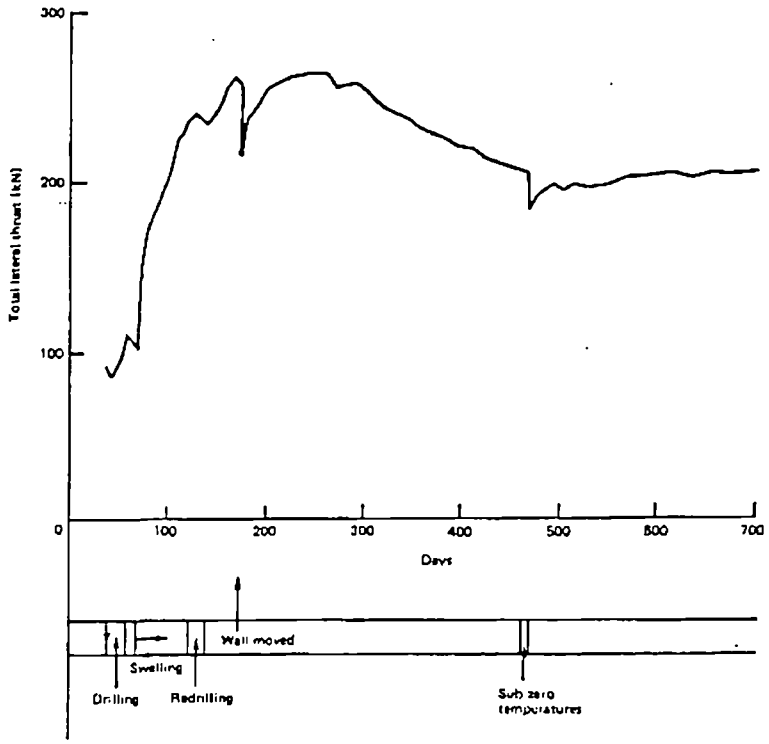

Figure 2.55 Variation of lateral thrust on experimental wall during inundation (after Symons et al., 1986).

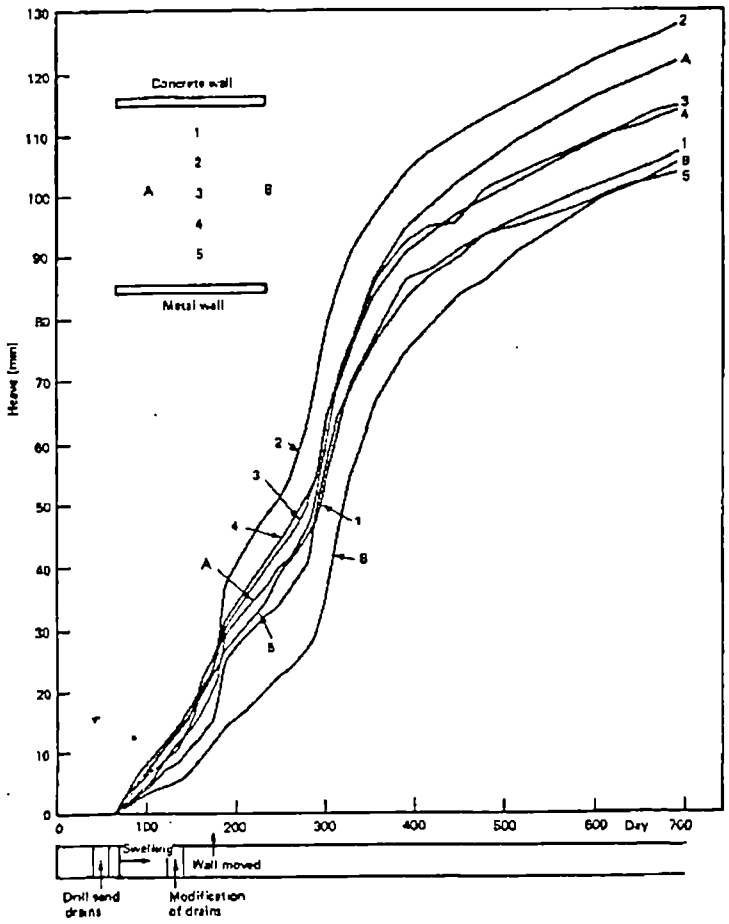

Figure 2.56 Observed surface movement of soil during inundation (after Symons et al., 1986).

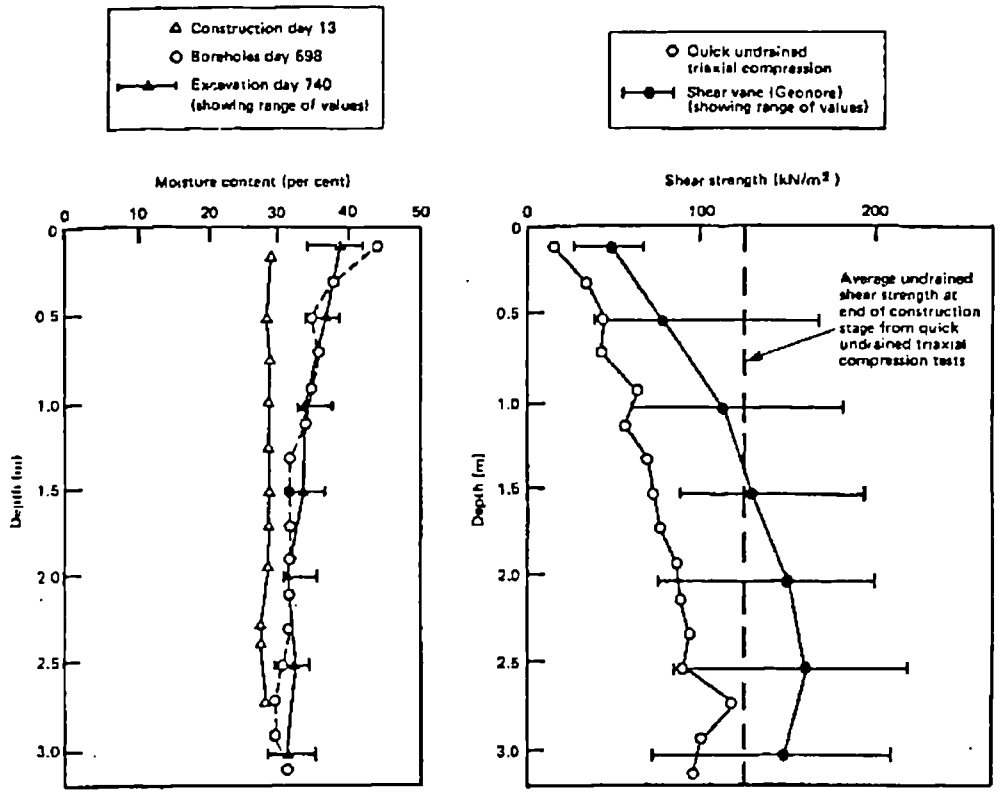

Figure 2.57 Variation of moisture content and undrained shear strength with depth for soil tested in experimental wall facility (after Symons et al., 1986).

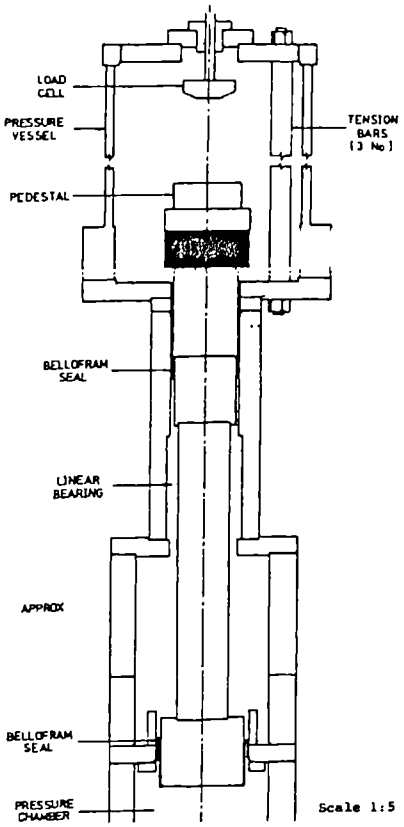

Figure 3.1 Schematic diagram of standard 100 mm stress path triaxial cell.

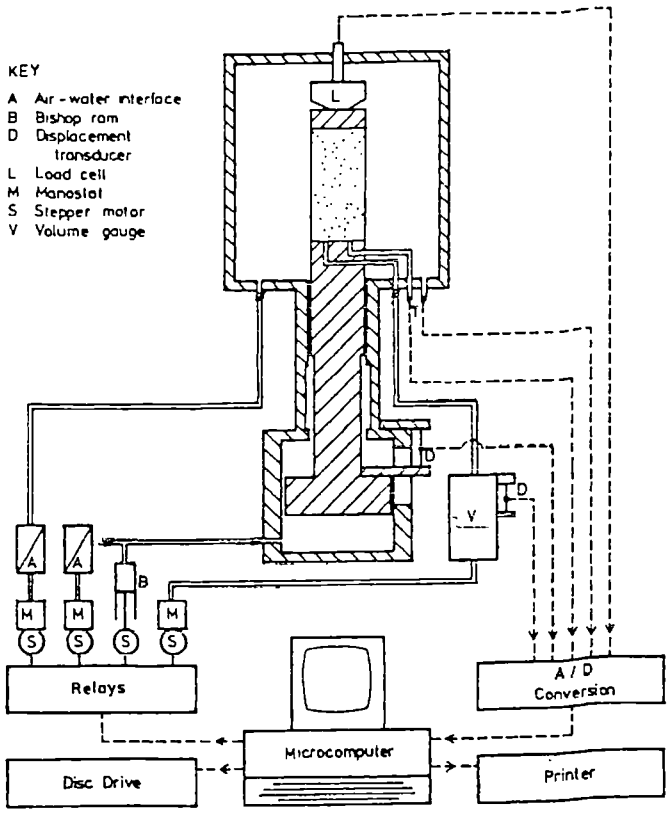

Figure 3.2 Schematic diagram of control system for 100 mm stress path cell

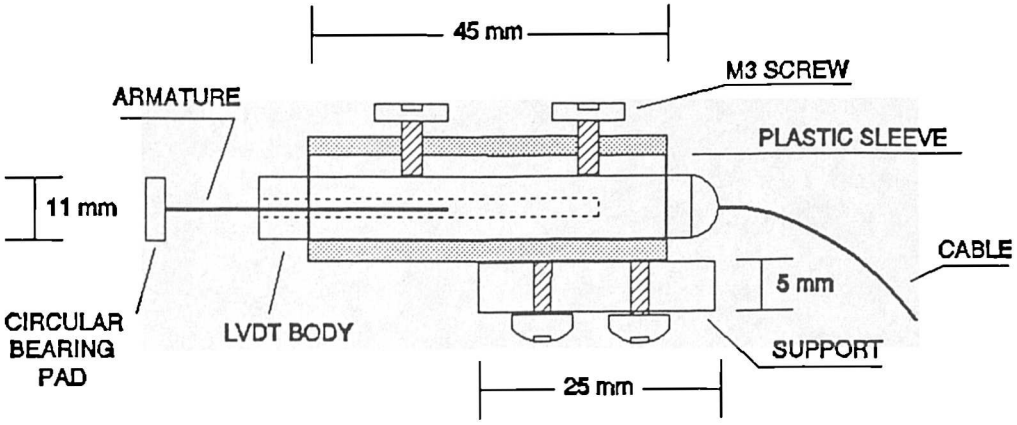

LVDT SENSOR

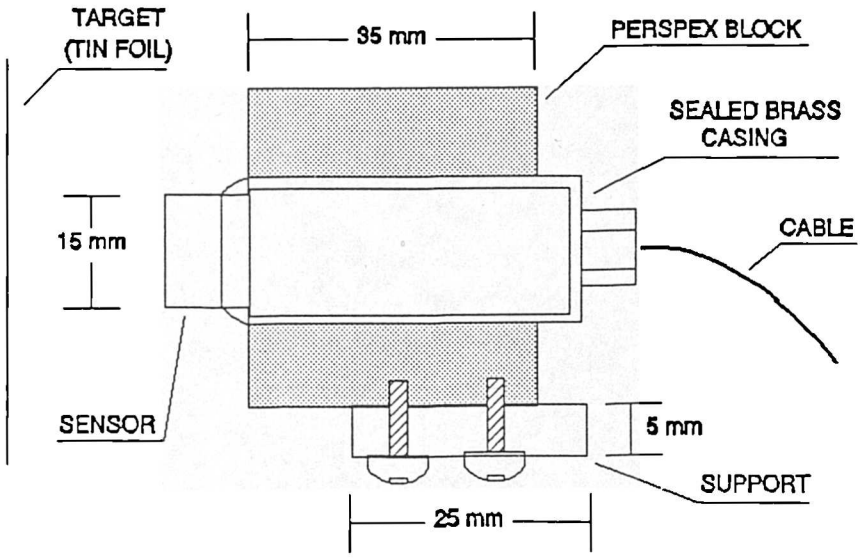

PROXIMITY SENSOR

Figure 3.3 Arrangement of displacement transducers.

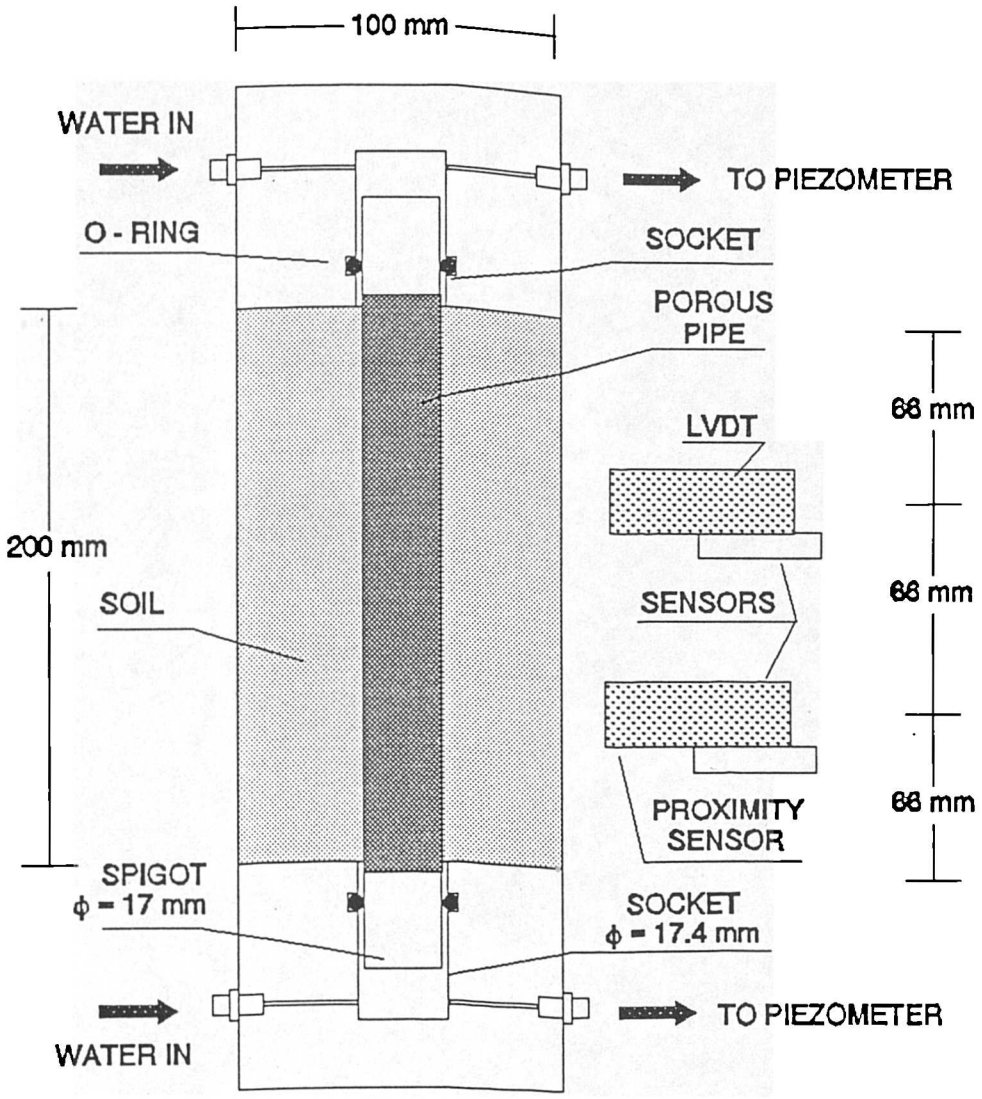

Figure 3.4 100 mm diameter soil sample with internal porous pipe.

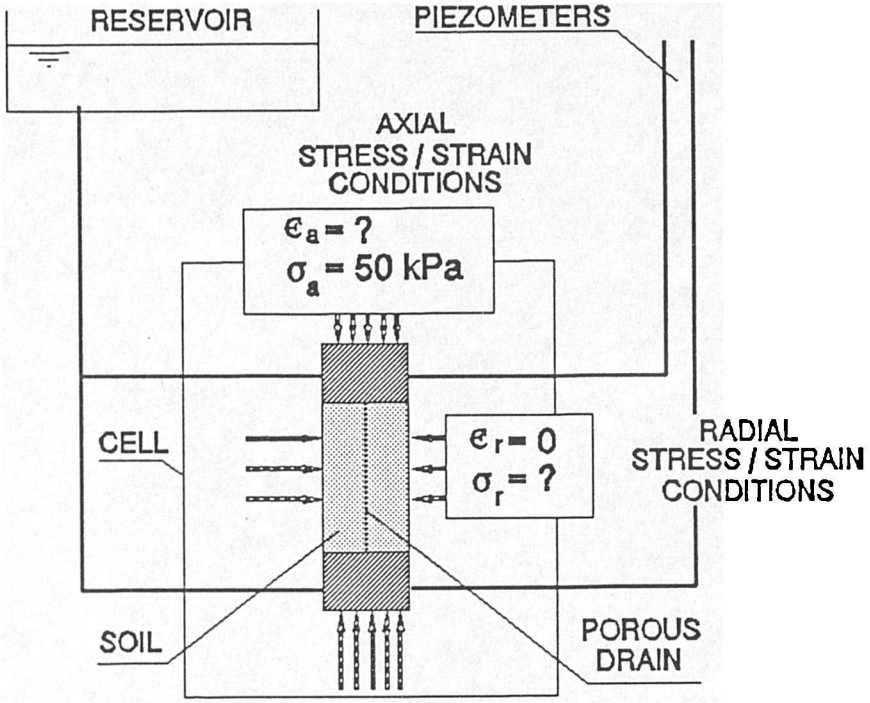

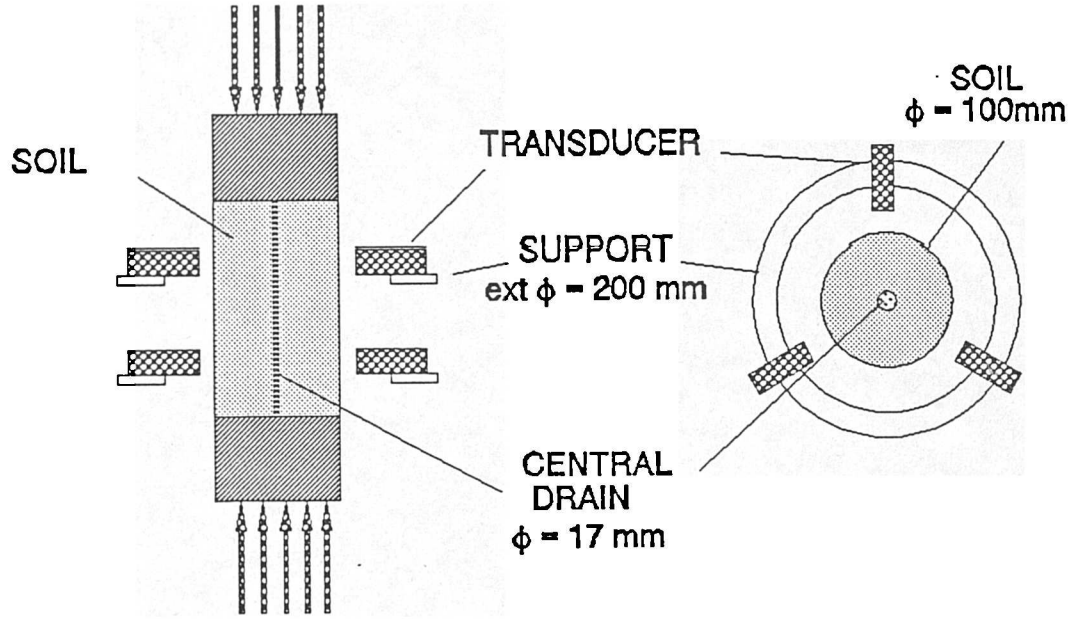

Figure 3.5 Schematic diagram of modified 100 mm stress path cell.

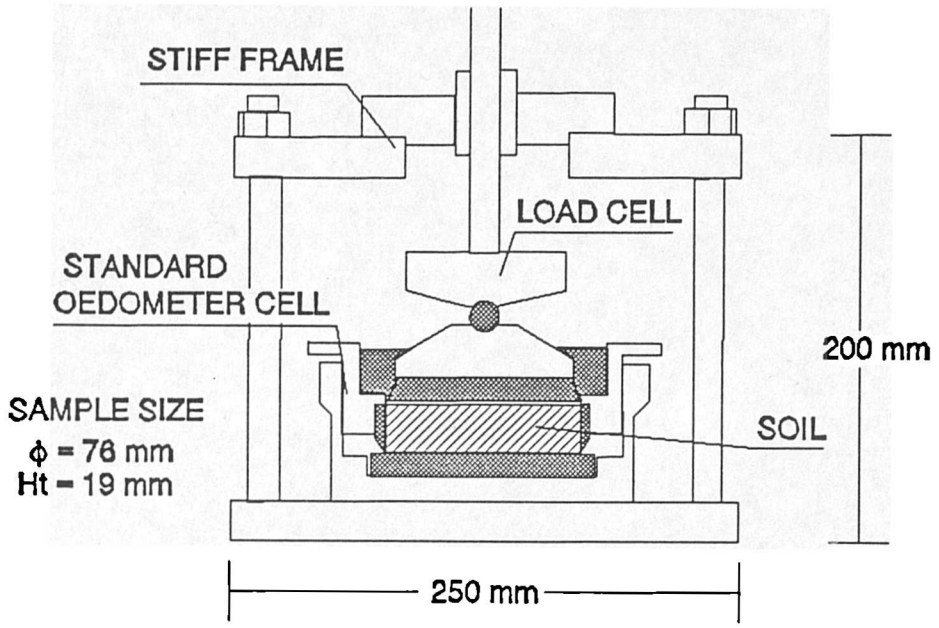

Figure 3.6 Modified oedometer.

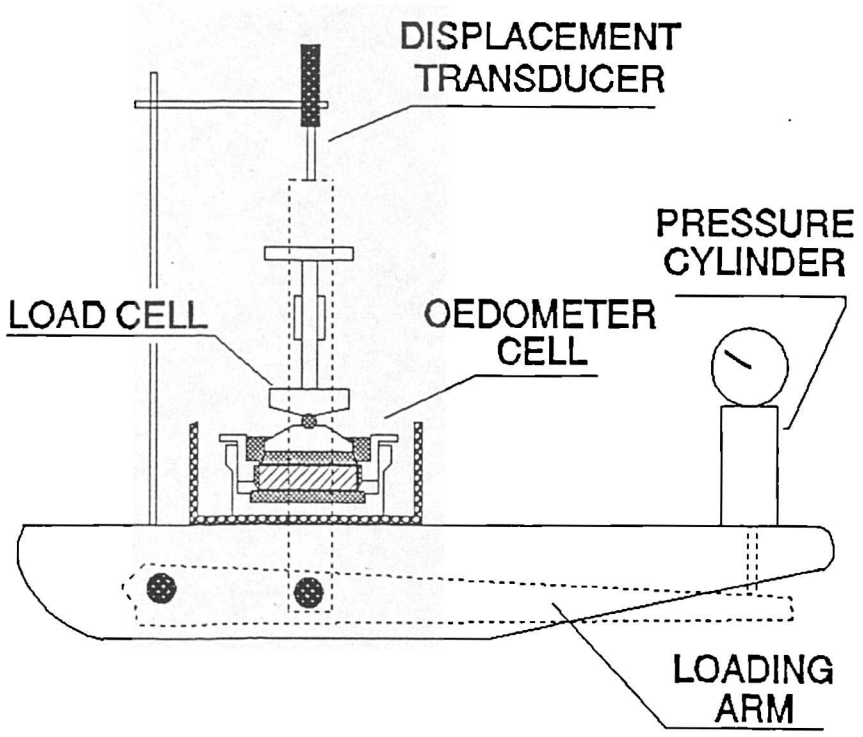

Figure 3.7 Computer controlled oedometer.

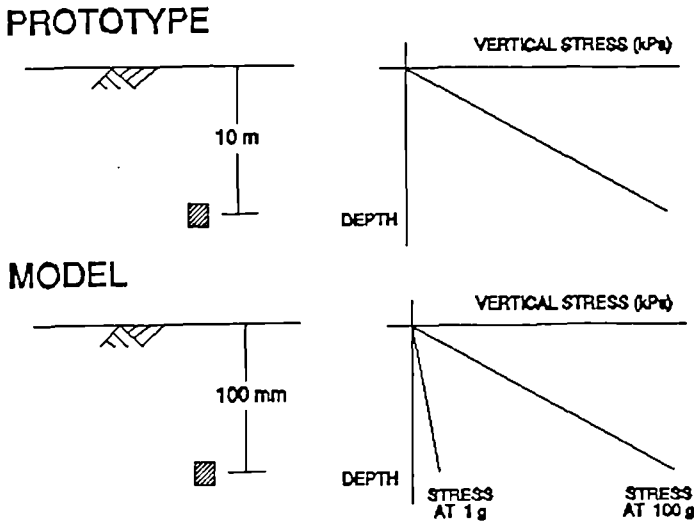

Figure 4.1 Comparison of prototype and model stresses in different acceleration fields.

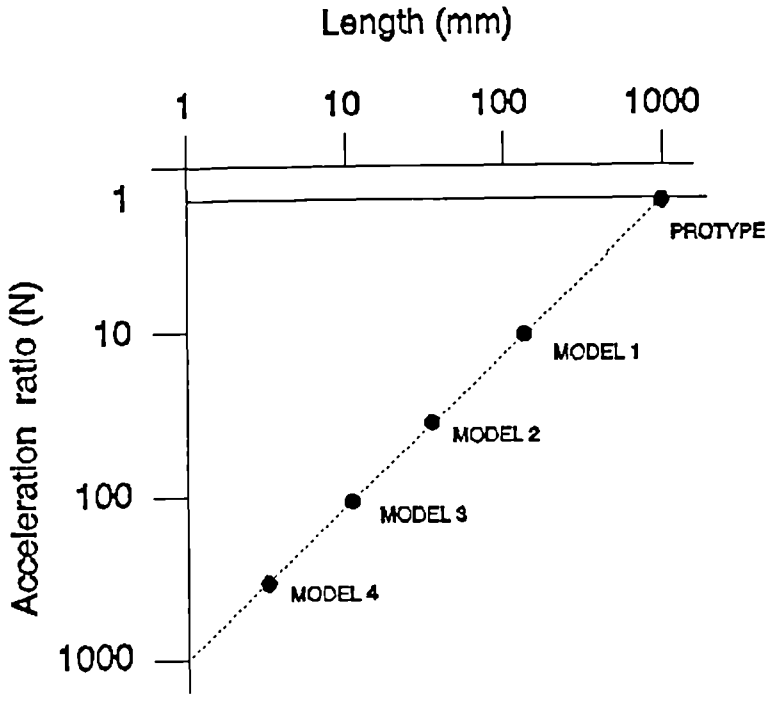

Figure 4.2 Relationship between model scale and acceleration ratio.

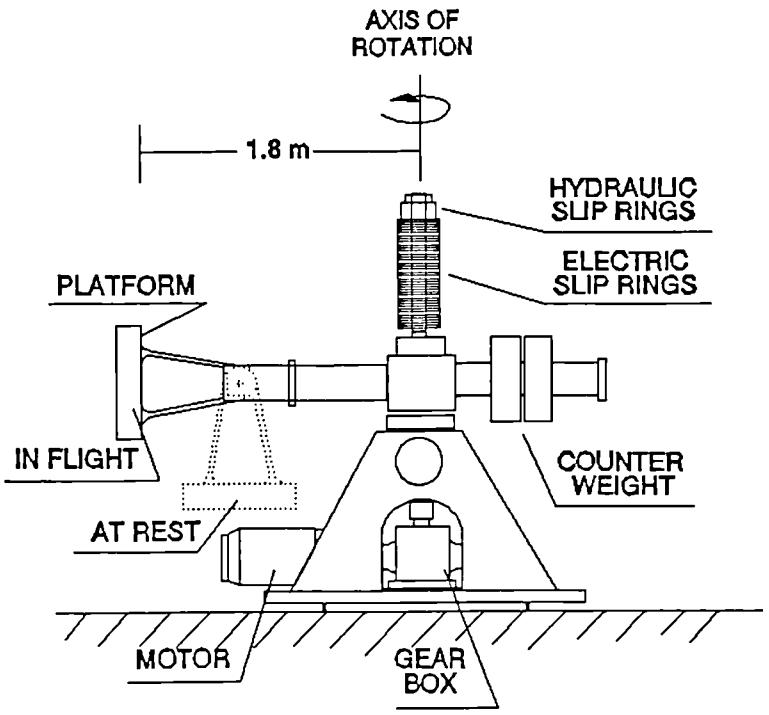

Figure 4.3 Acutronic 661 centrifuge.

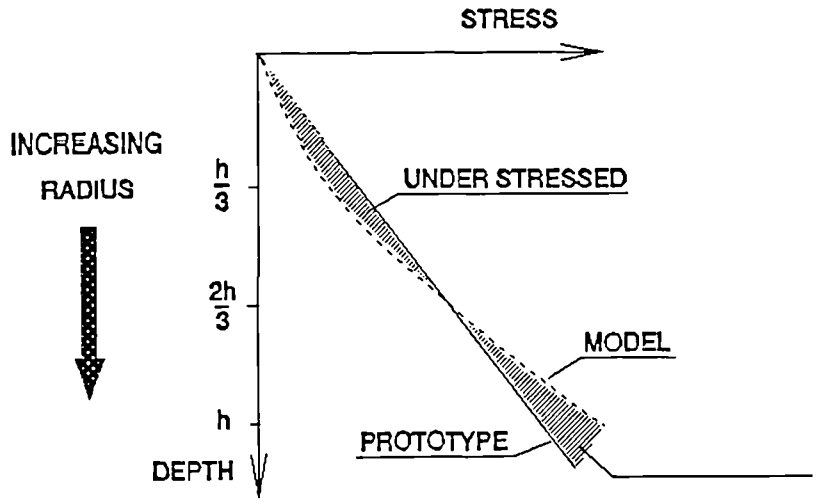

Figure 4.4 Comparison between prototype stress and model stress as centrifuge radius increases.

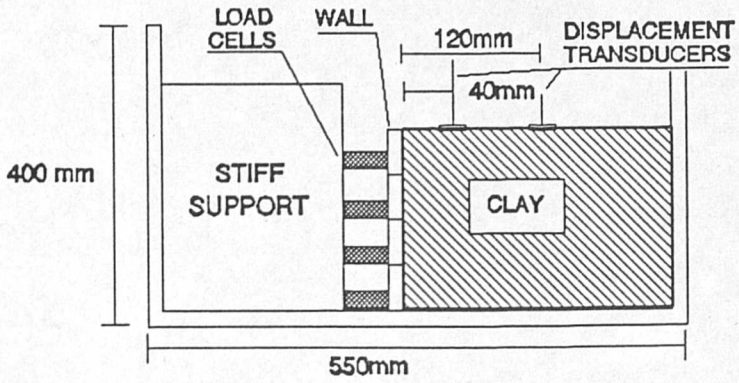

Figure 4.5 Schematic diagram of centrifuge model showing the general arrangement.

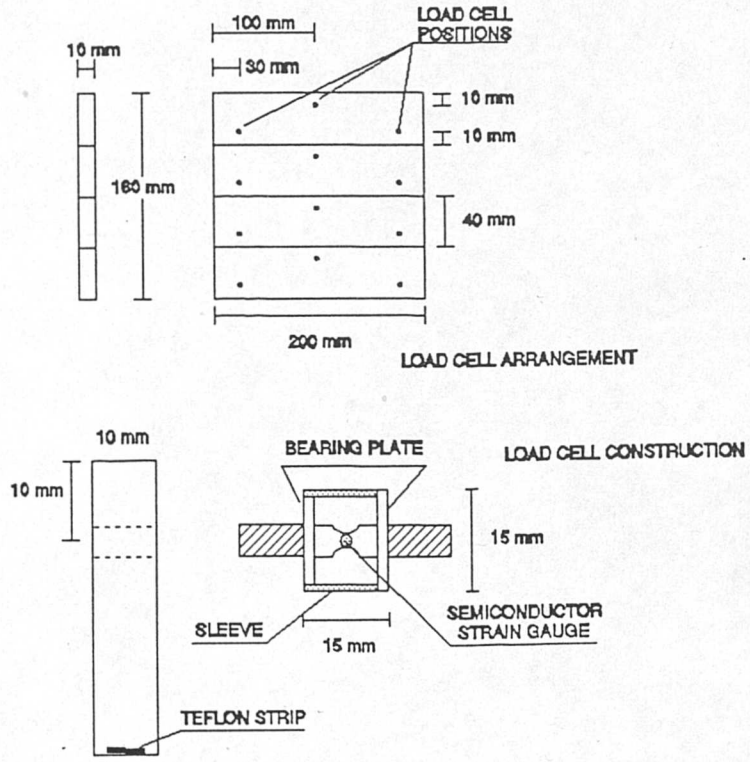

Figure 4.6 Diagram of model retaining wall showing position and construction of load cells.

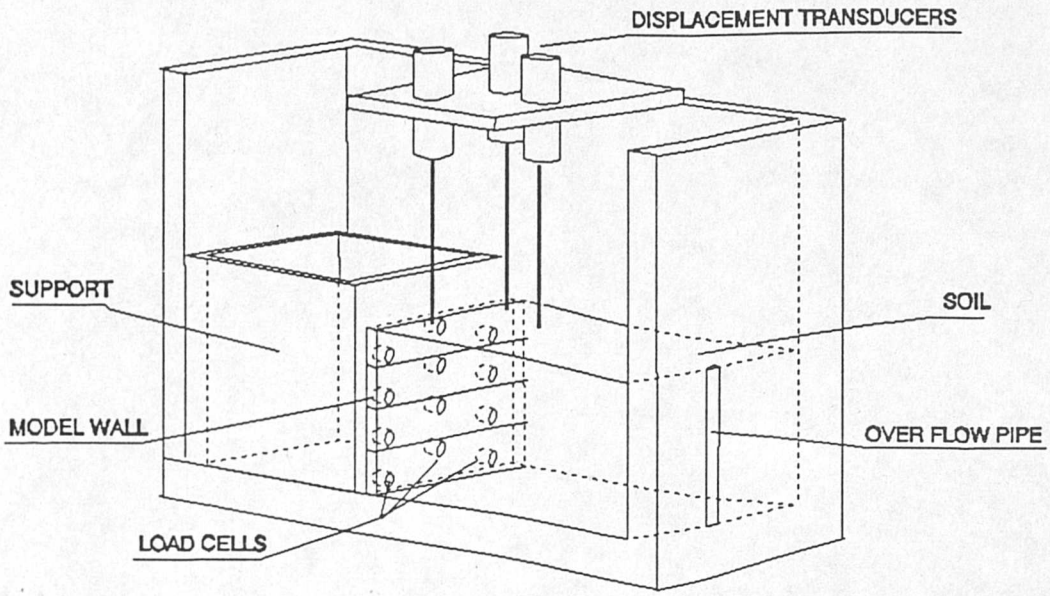

Figure 4.7 Model configuration prior to testing.

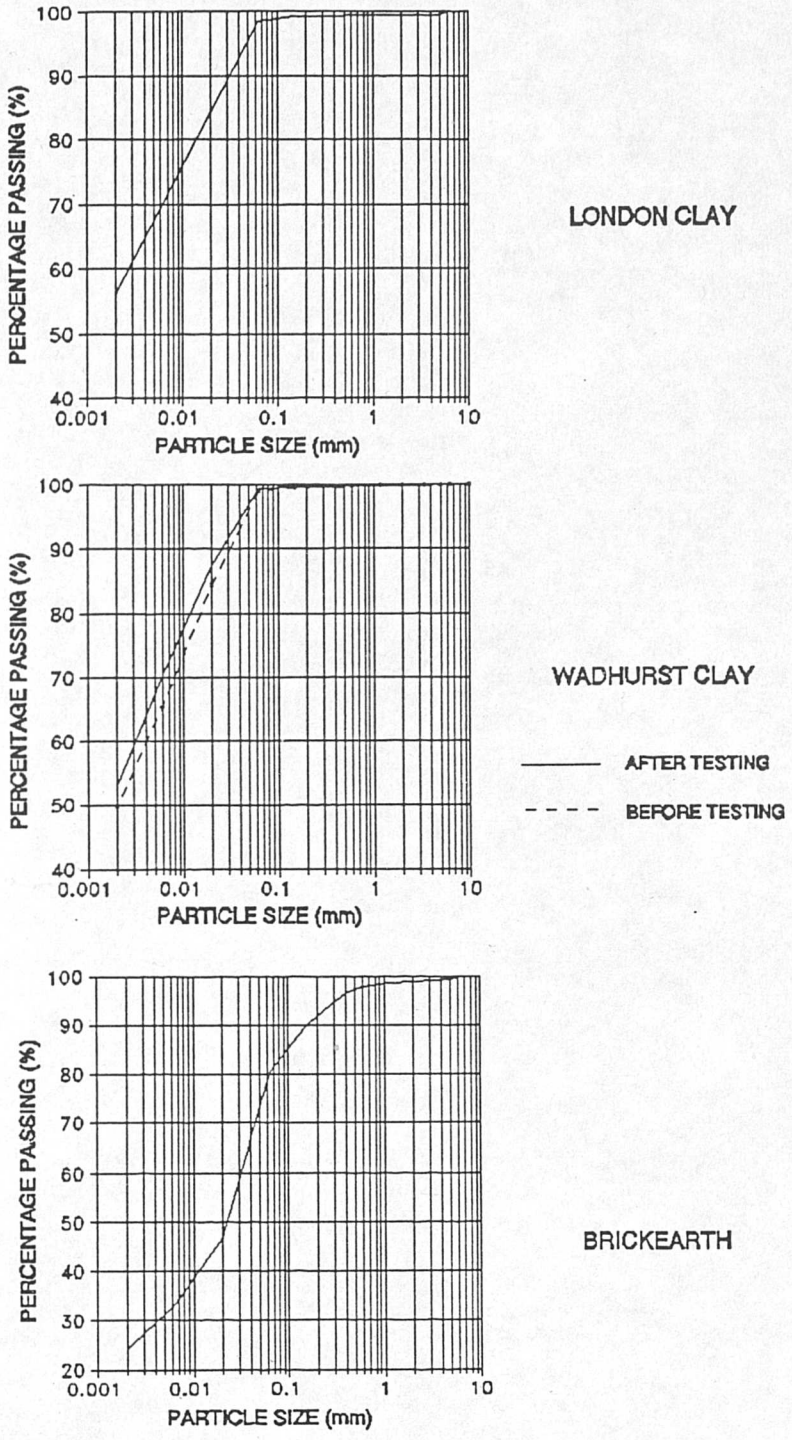

Figure 5.1 Particle size distribution for the three soils tested: London Clay, Wadhurst Clay and Brickearth.

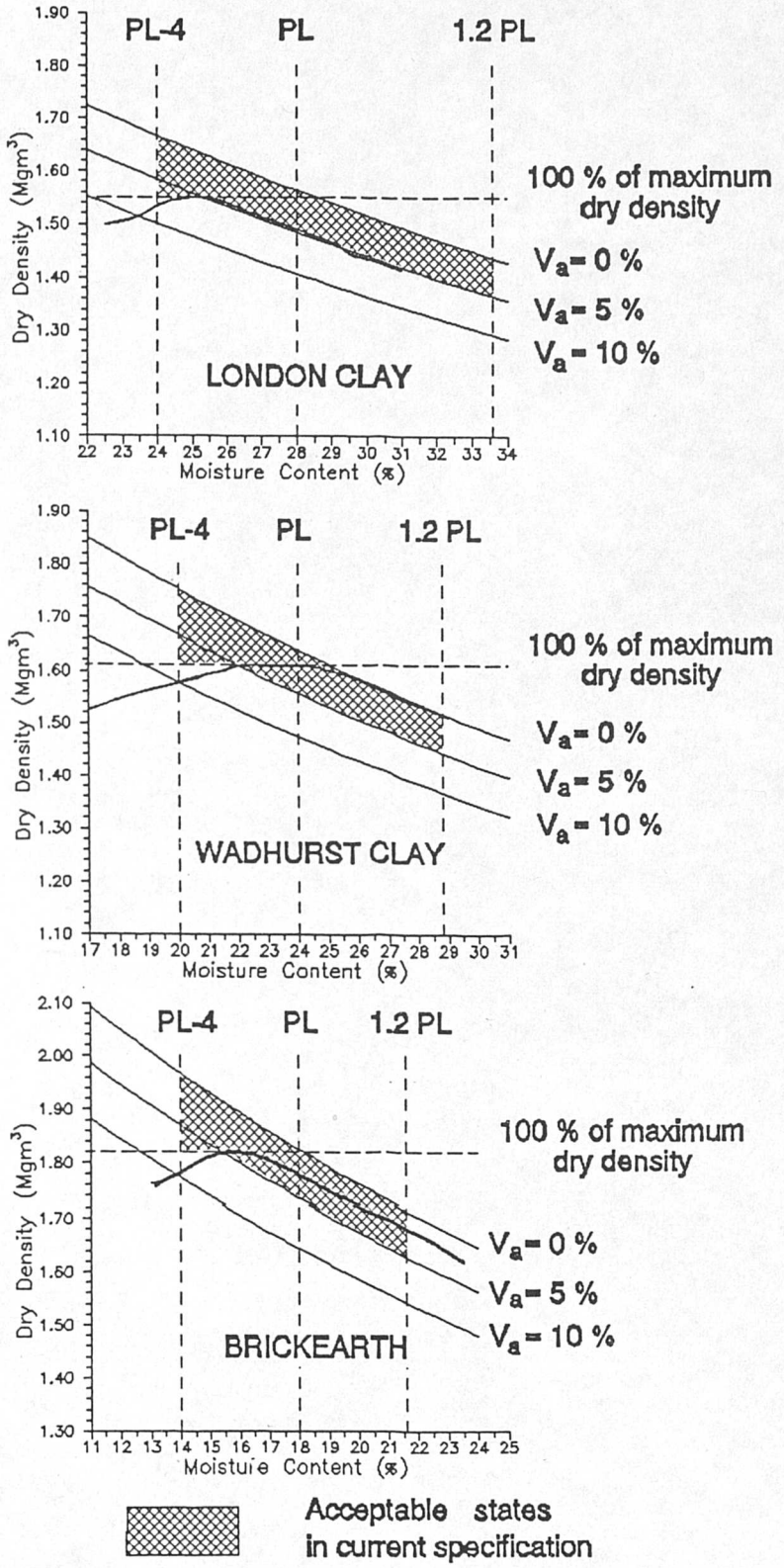

Figure 5.2 Compaction curves for the three soils tested: London Clay, Wadhurst Clay and Brickearth.

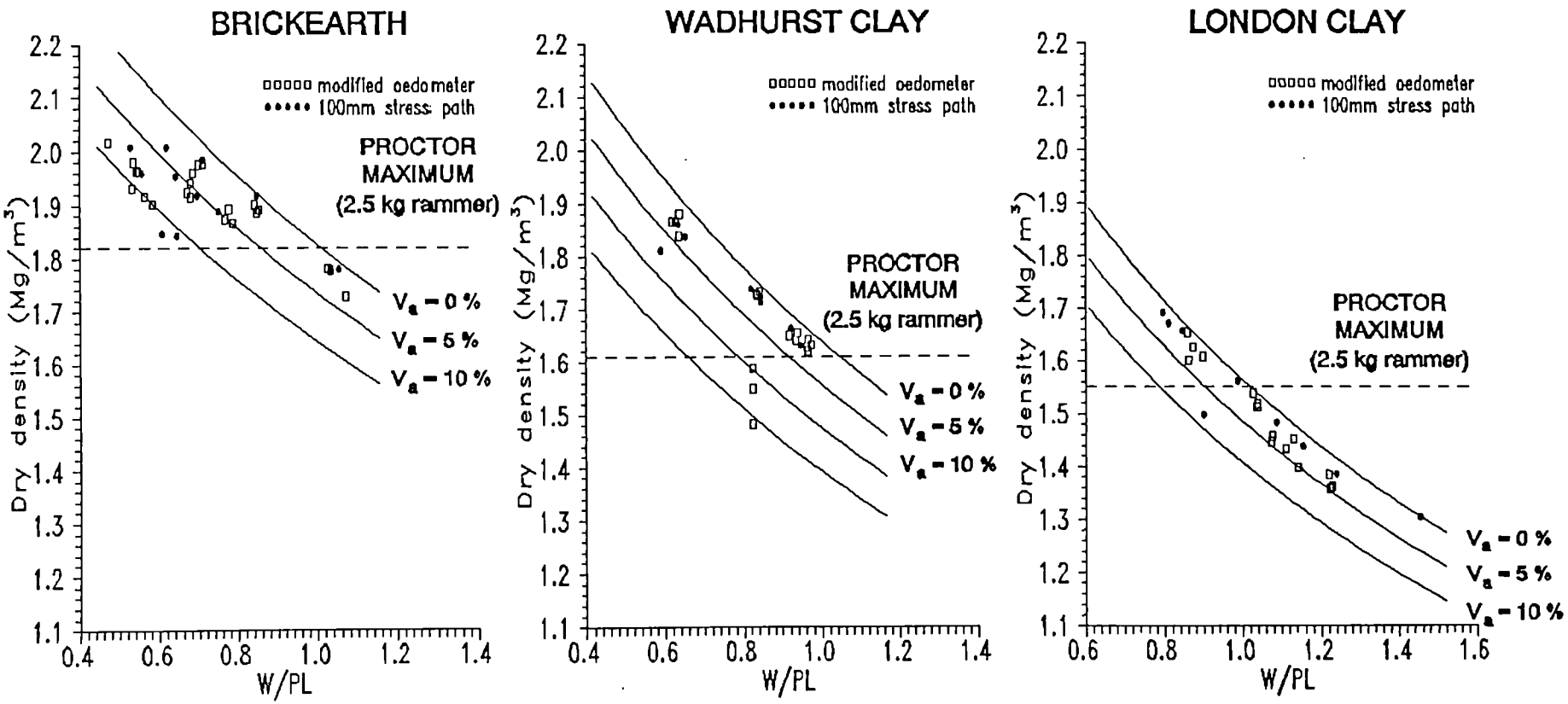

Figure 5.3 Variation of dry density with moisture content (normalised with respect to plastic limit) for soils tested.

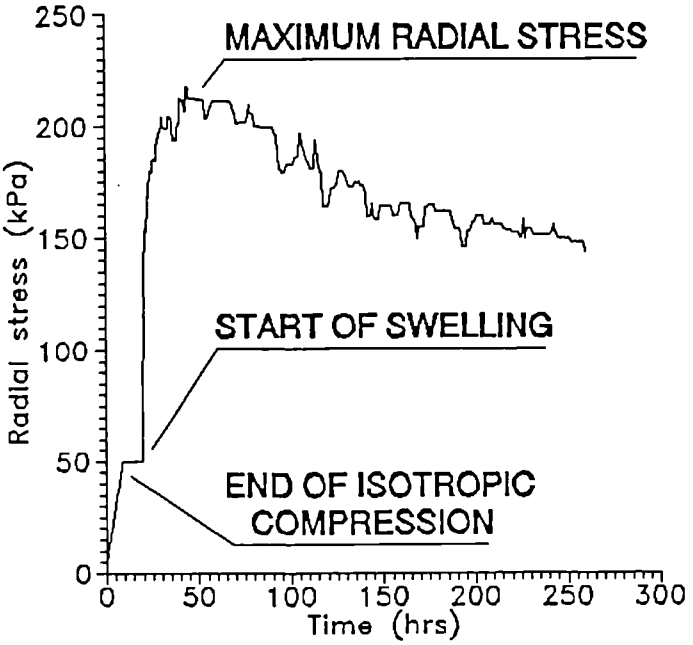

Figure 5.4(a) Change in radial stress with time (London Clay, LC9).

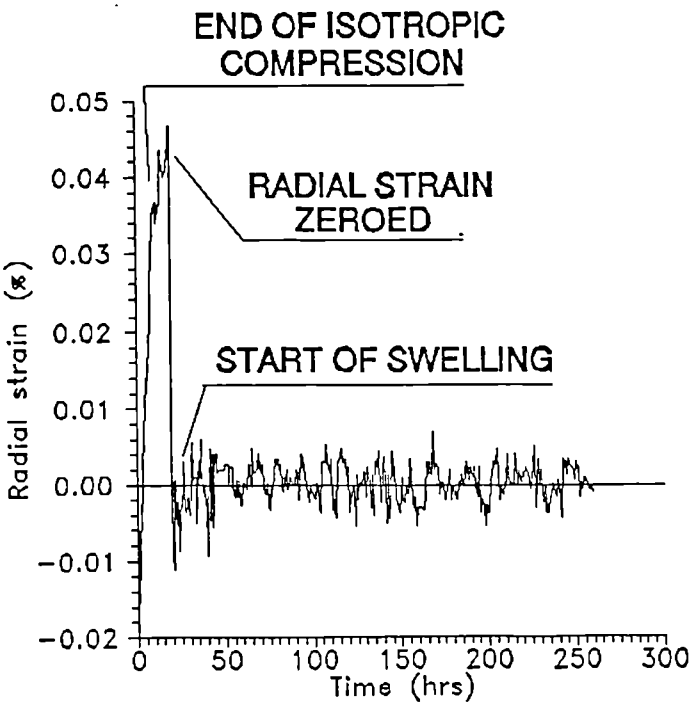

Figure 5.4(b) Change in radial strain with time (London Clay, LC9).

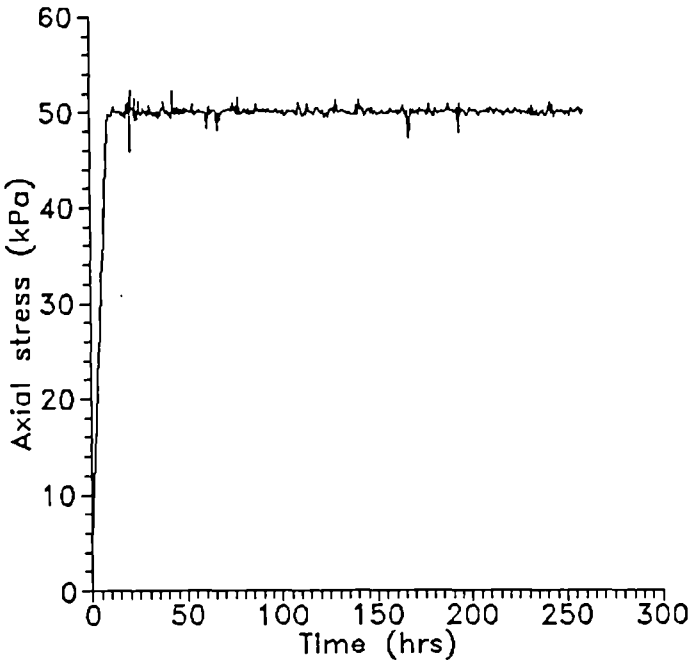

Figure 5.4(c) Change in axial stress with time (London Clay, LC9).

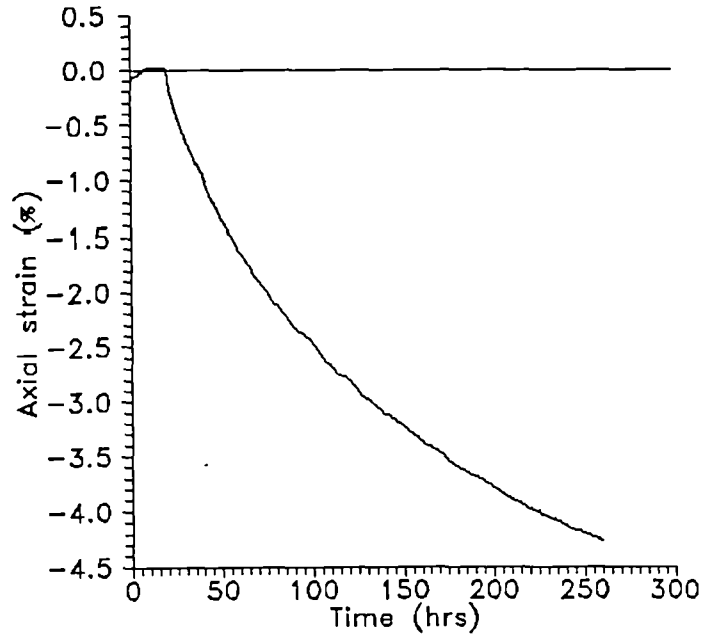

Figure 5.4(d) Change in axial strain with time (London Clay, LC9).

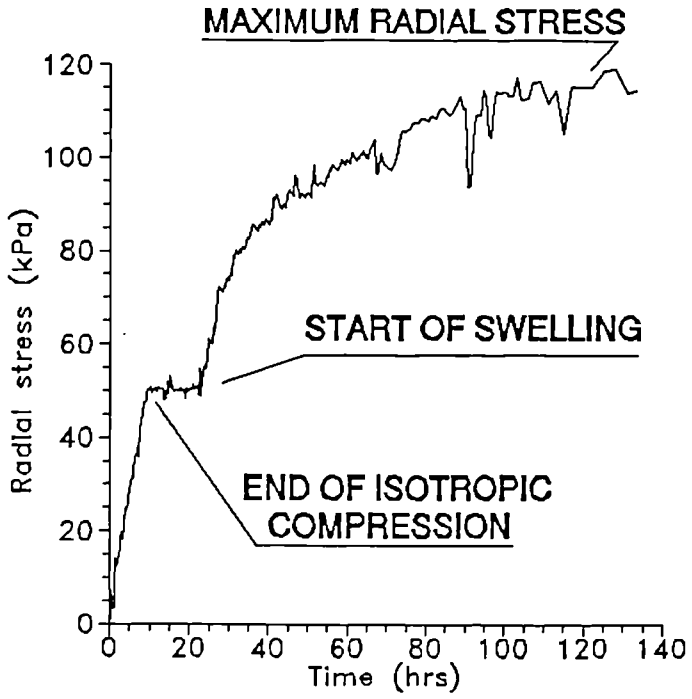

Figure 5.5(a) Change in radial stress with time (Wadhurst Clay, WA1).

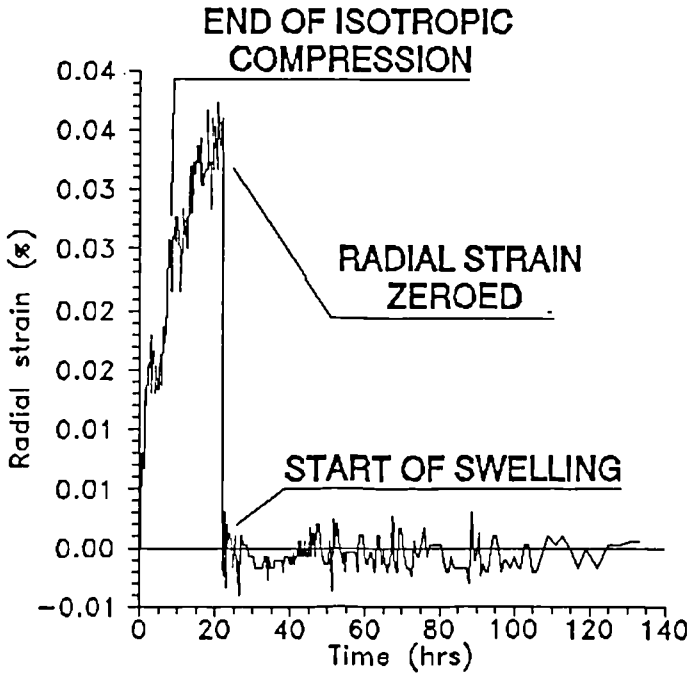

Figure 5.5(b) Change in radial strain with time (Wadhurst Clay, WA1).

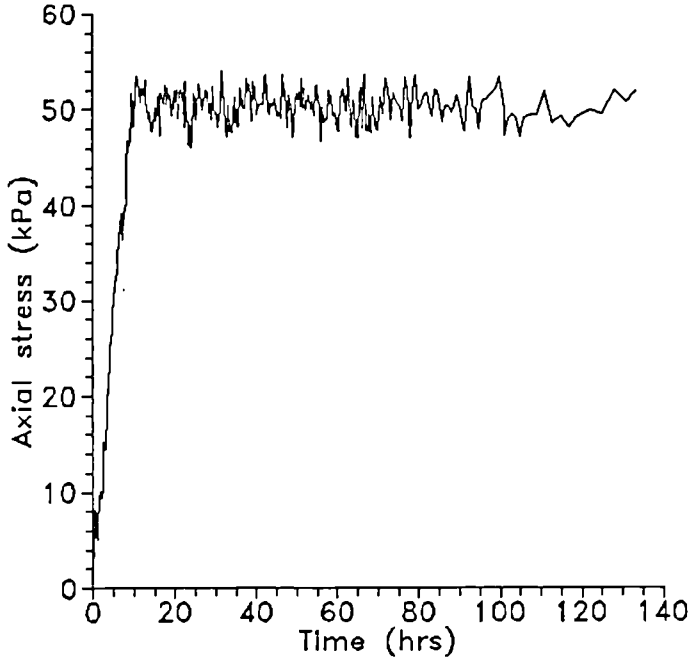

Figure 5.5(c) Change in axial stress with time (Wadhurst Clay, WA1).

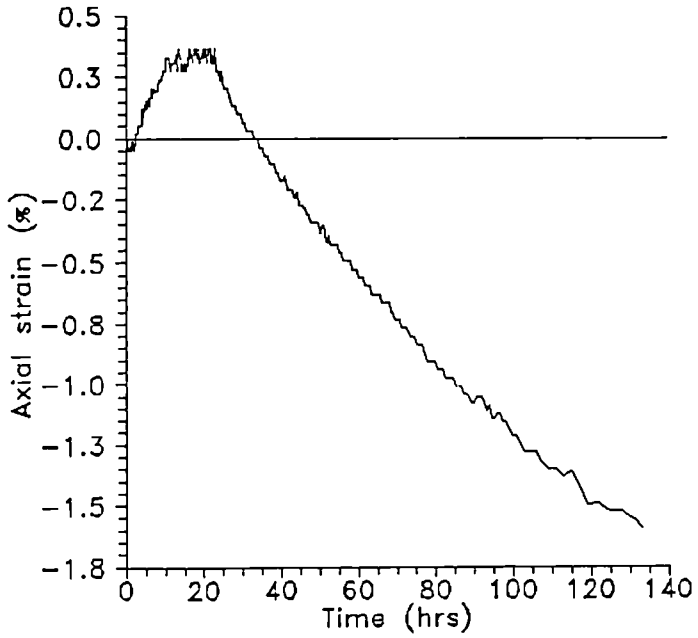

Figure 5.5(d) Change in axial strain with time (Wadhurst Clay, WA1).

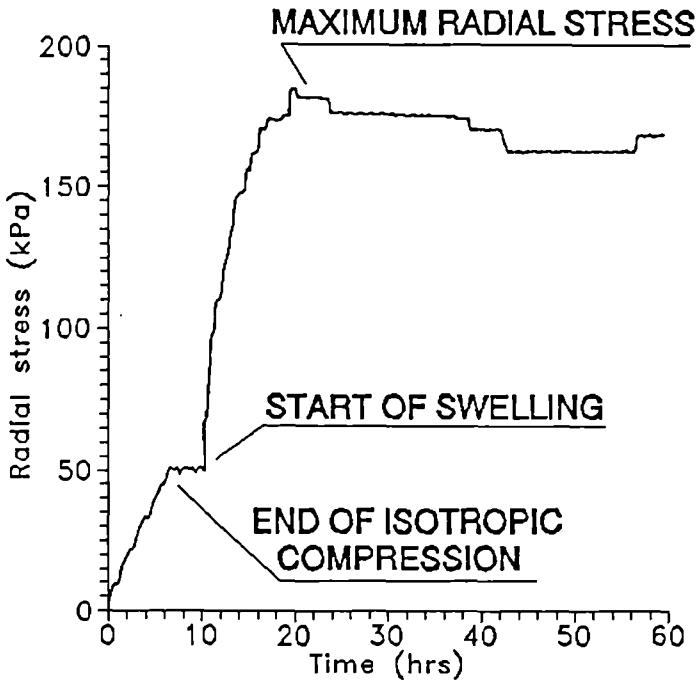

Figure 5.6(a) Change in radial stress with time (Brickearth, BE8).

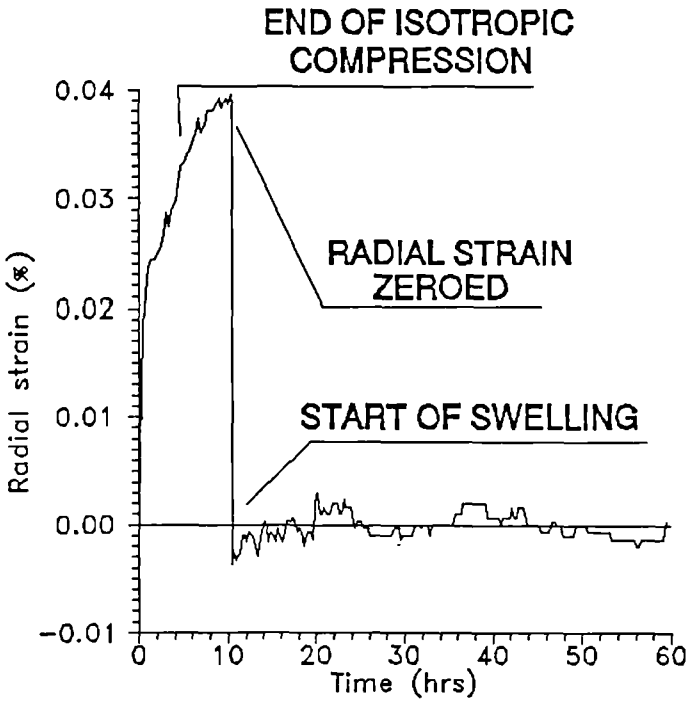

Figure 5.6(b) Change in radial strain with time (Brickearth, BE8).

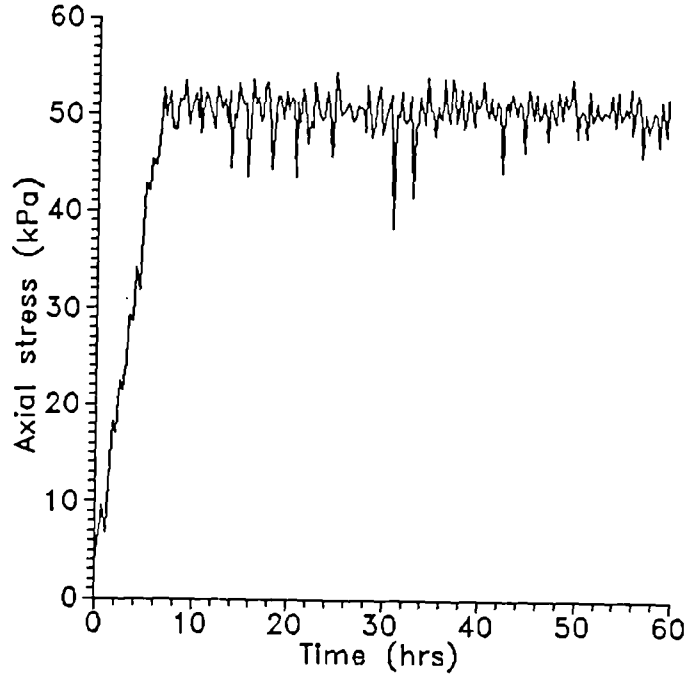

Figure 5.6(c) Change in axial stress with time (Brickearth, BE8).

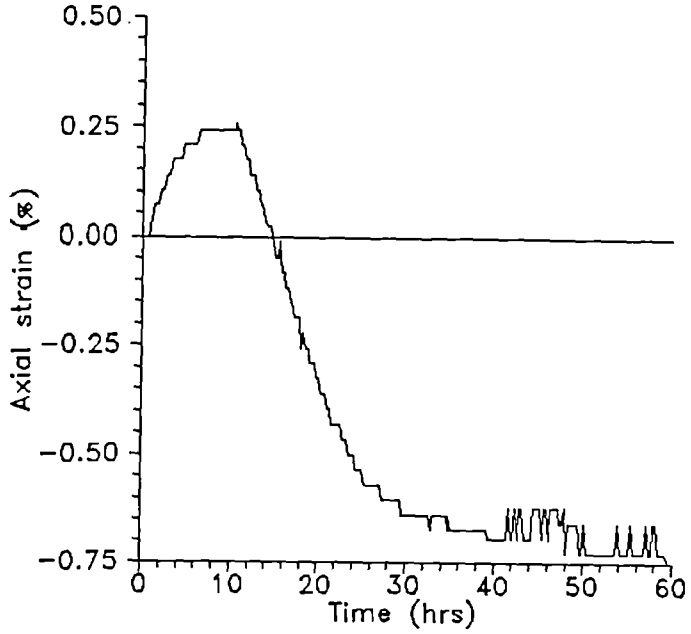

Figure 5.6(d) Change in axial strain with time (Brickearth, BE8).

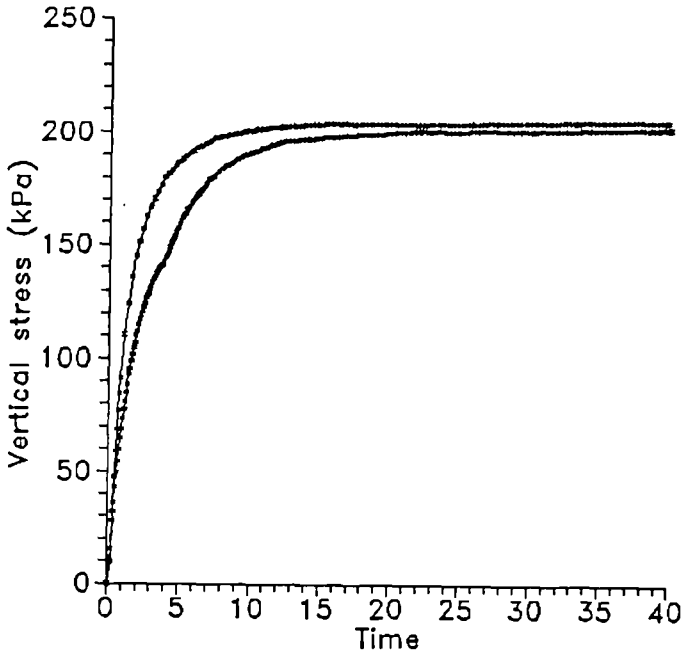

Figure 5.7 Modified oedometer test profile (London Clay, LC7).

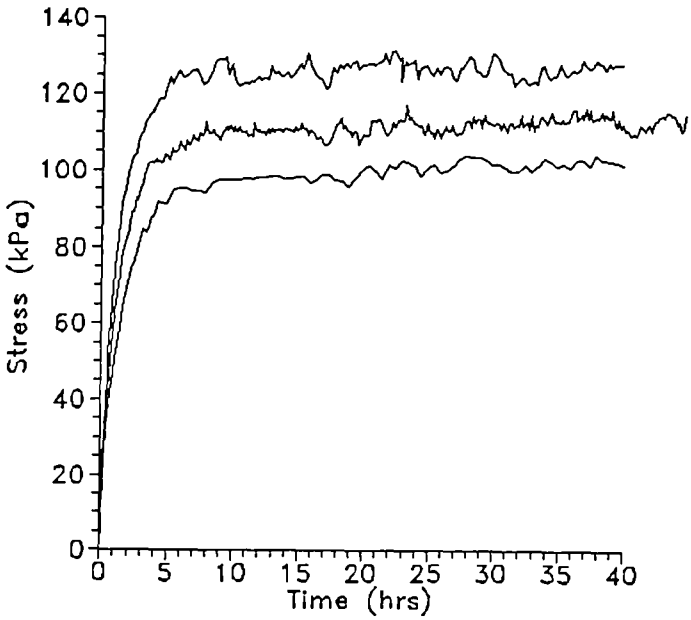

Figure 5.8 Modified oedometer test profile (Wadhurst Clay, WA1).

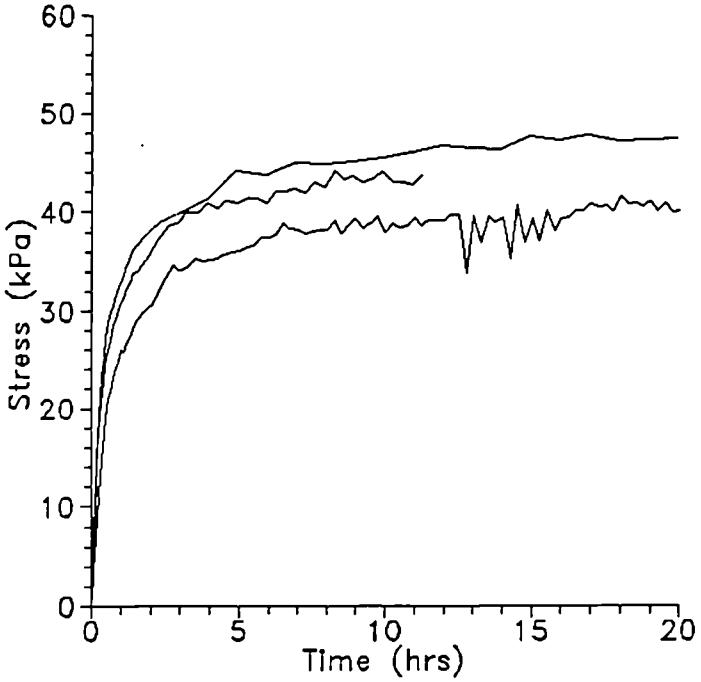

Figure 5.9 Modified oedometer test profile (Brickearth, BE8)

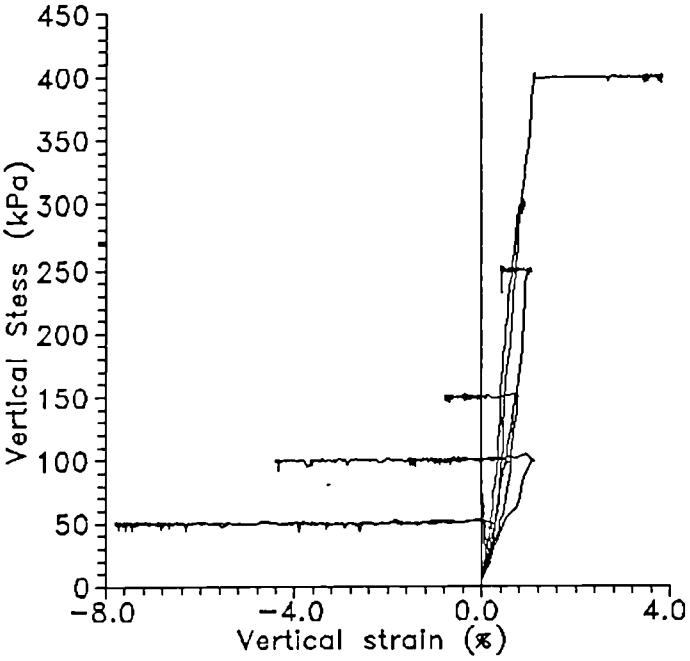

Figure 5.10 Computer controlled oedometer test profiles (London Clay).

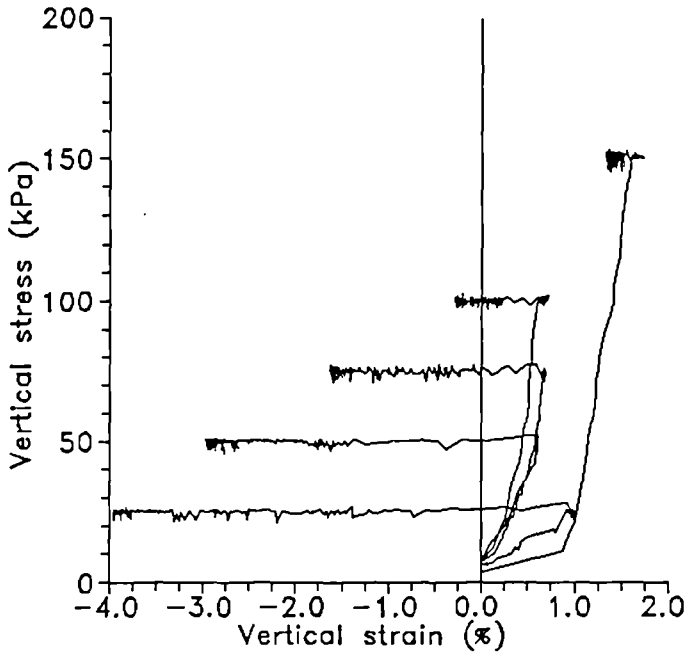

Figure 5.11 Computer controlled oedometer test profiles (Wadhurst Clay).

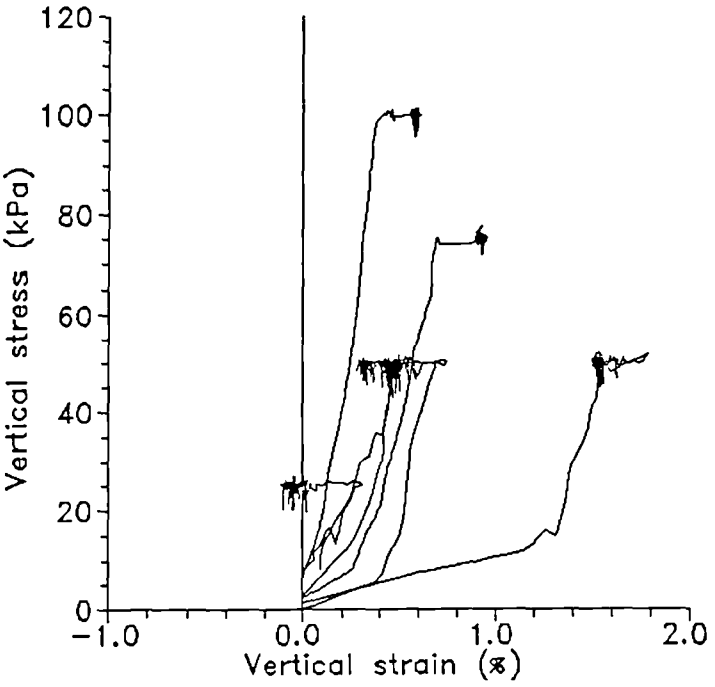

Figure 5.12 Computer controlled oedometer test profiles (Brickearth).

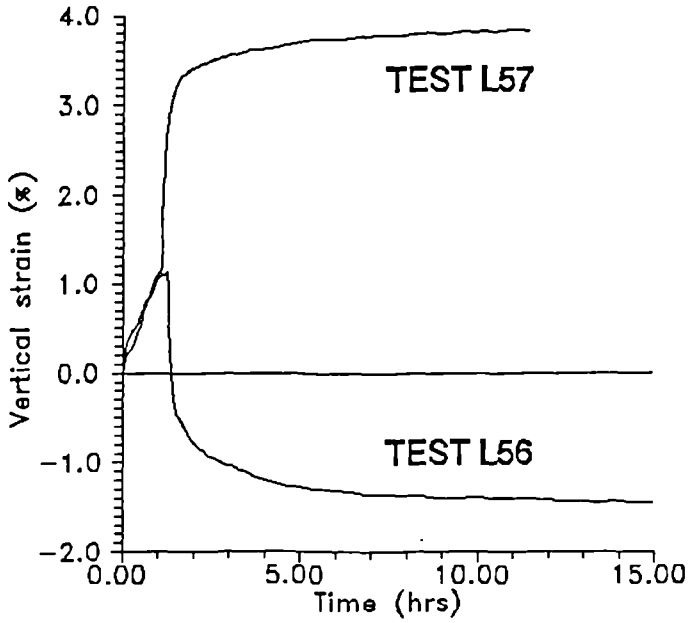

Figure 5.13 Difference in swelling and collapse behaviour of two London Clay samples under constant vertical stresses of 100 kPa and 400 kPa.

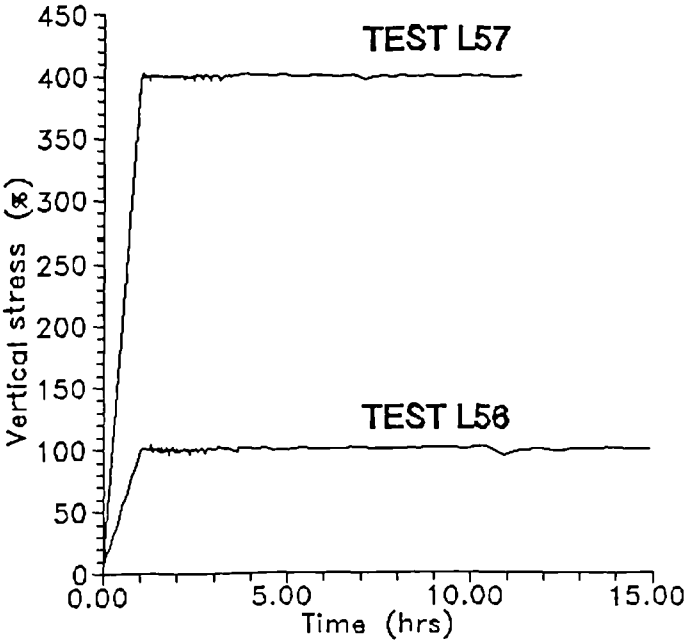

Figure 5.14 Control of vertical stress during computer controlled oedometer test.

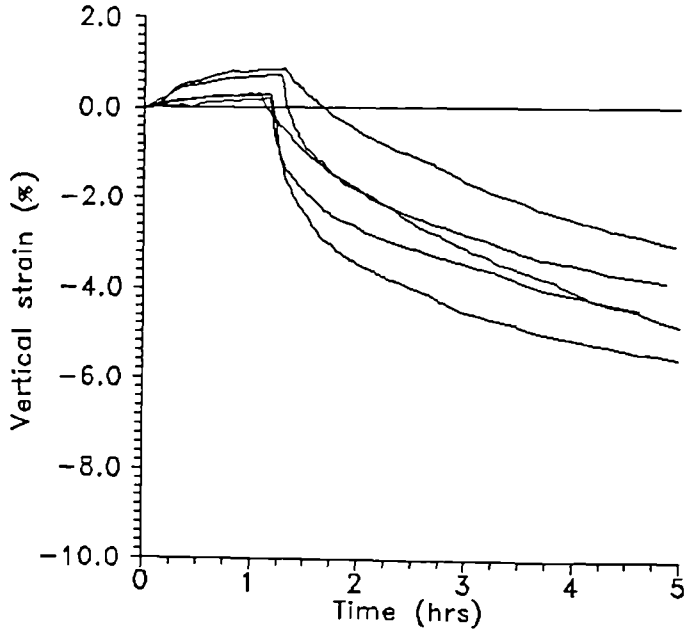

Figure 5.15 Volumetric change of samples compacted to same dry density but different water content (London Clay).

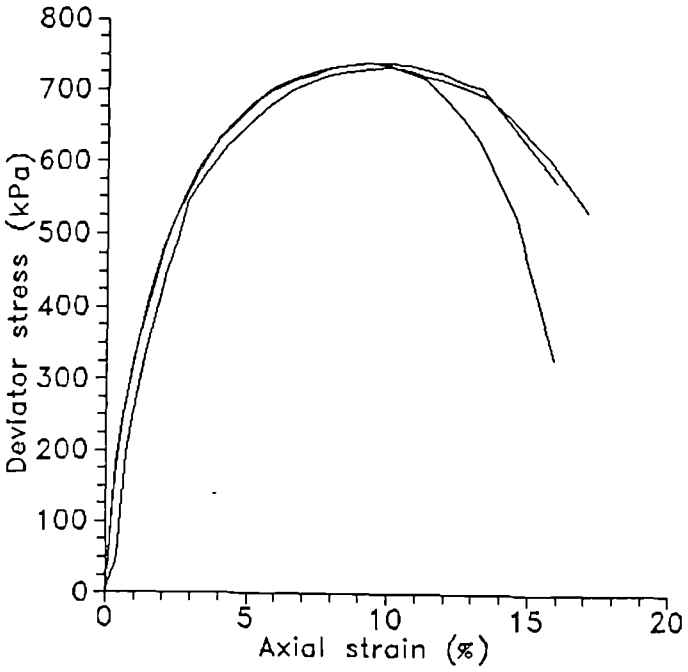

Figure 5.16 Typical response of undrained compression test on 38 mm sample (London Clay, LC8).

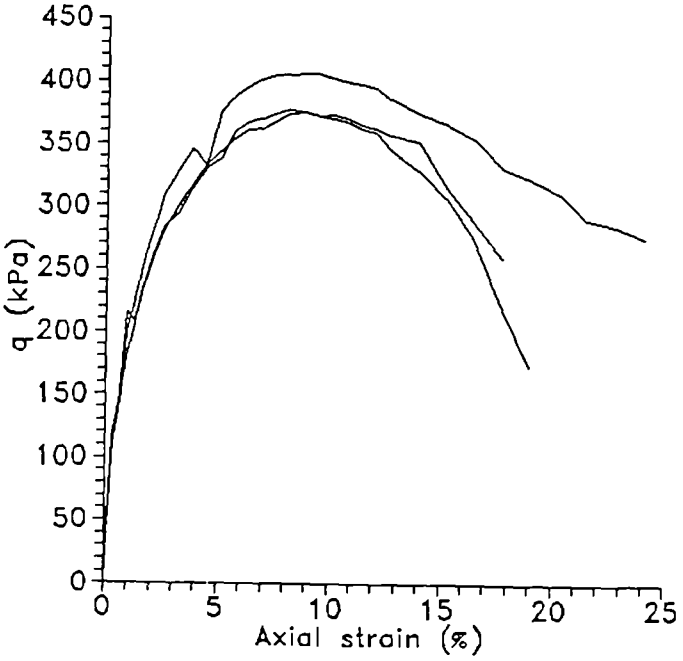

Figure 5.17 Typical response of undrained compression test on 38 mm sample (Wadhurst Clay, WA1).

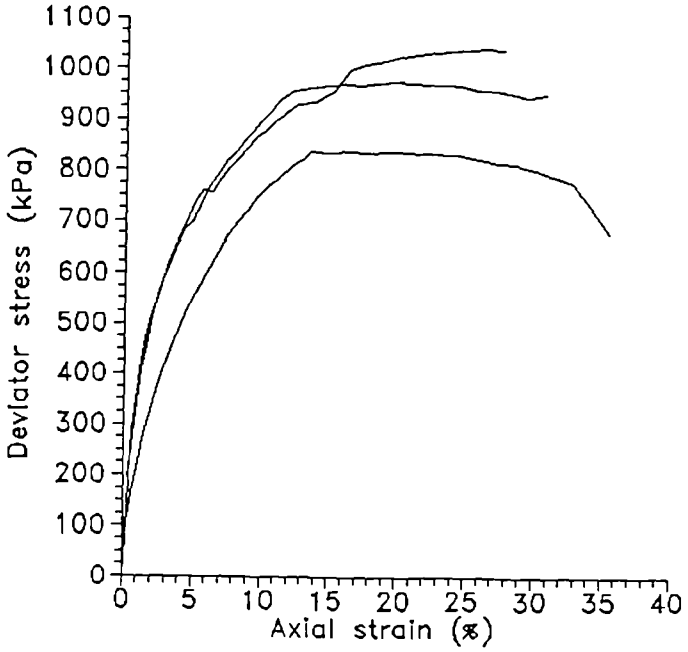

Figure 5.18 Typical response of undrained compression test on 38 mm sample (Brickearth, BE3).

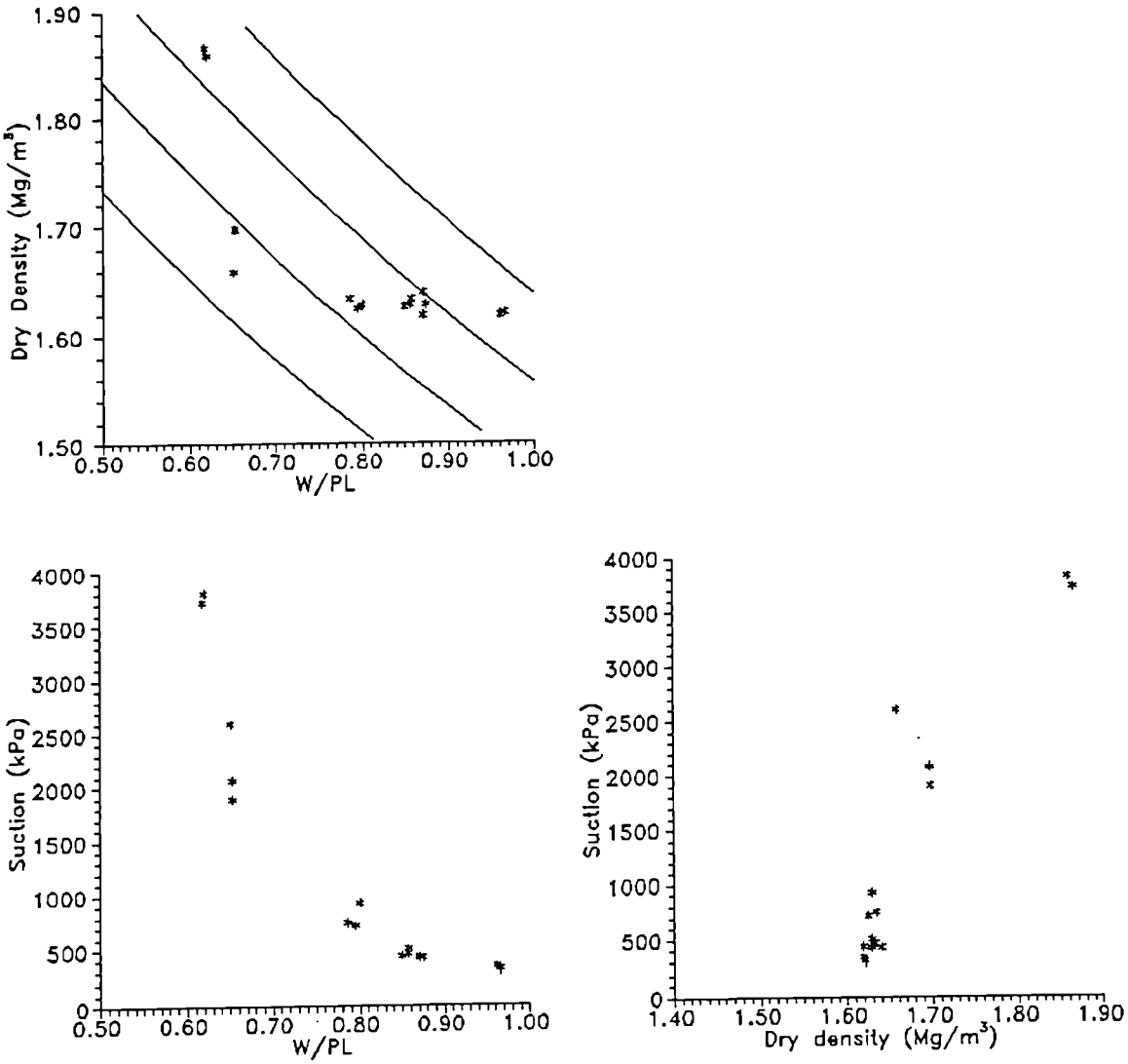

Figure 5.19 Relationship between suction, dry density and water content.

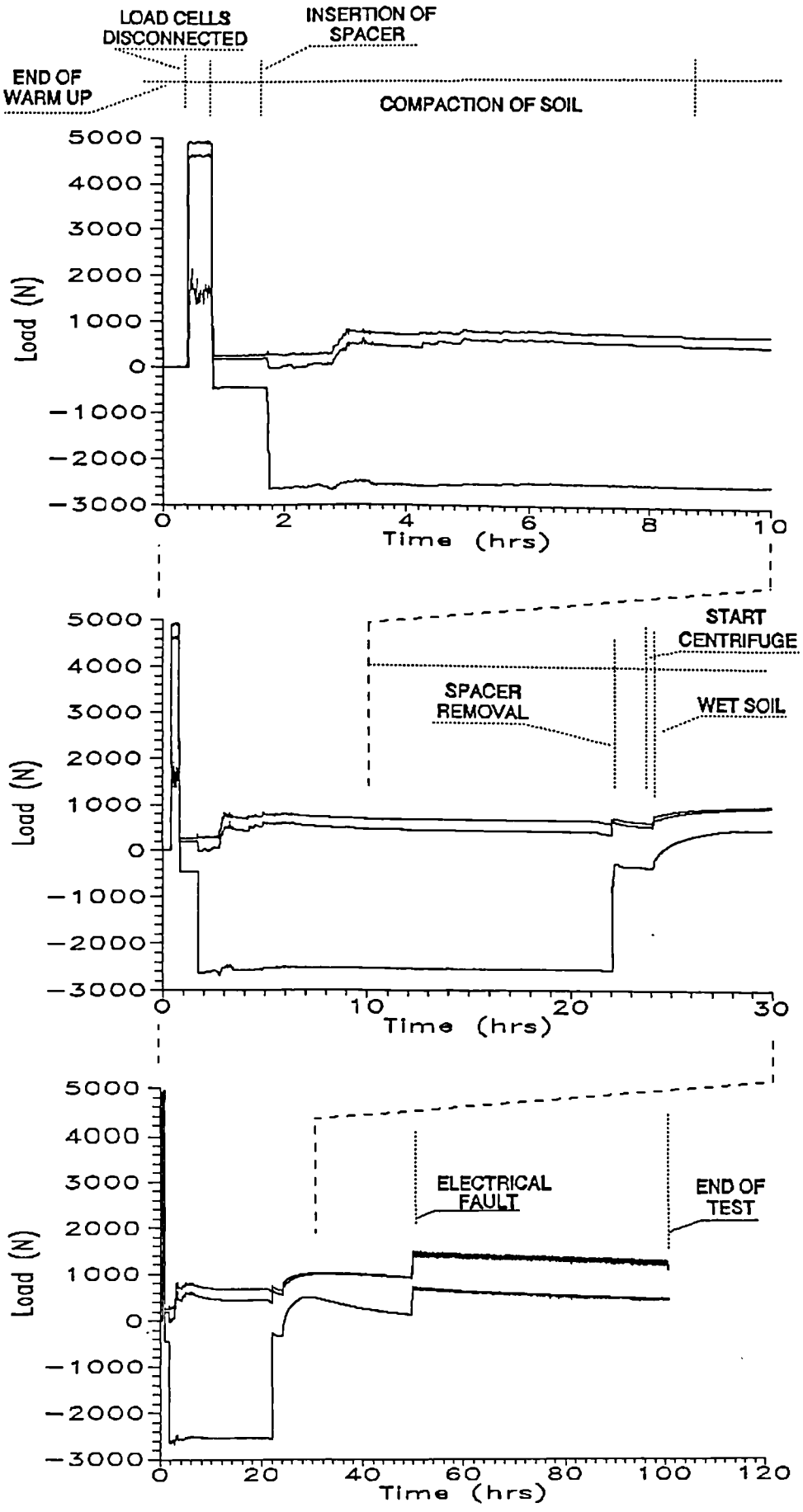

Figure 5.20(a) Load cell outputs during all stages of centrifuge test (CLC3).

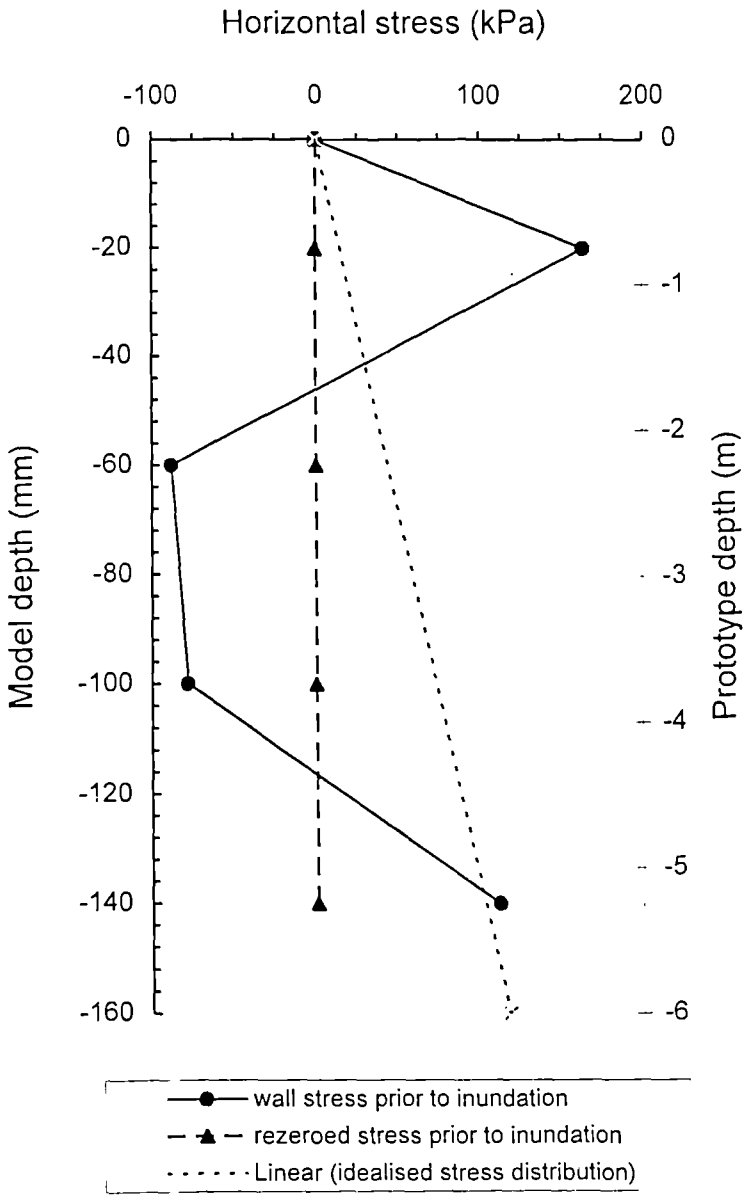

Figure 5.20(b) Variation of stress with depth before inundation (CLC3).

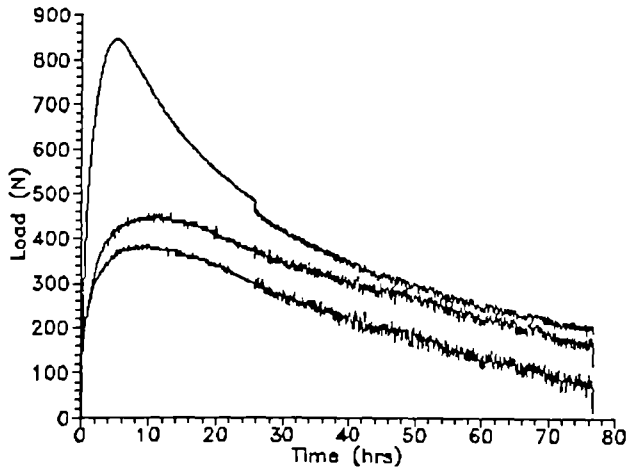

Figure 5.21 Output from load cells in top section of wall during inundation (CLC3).

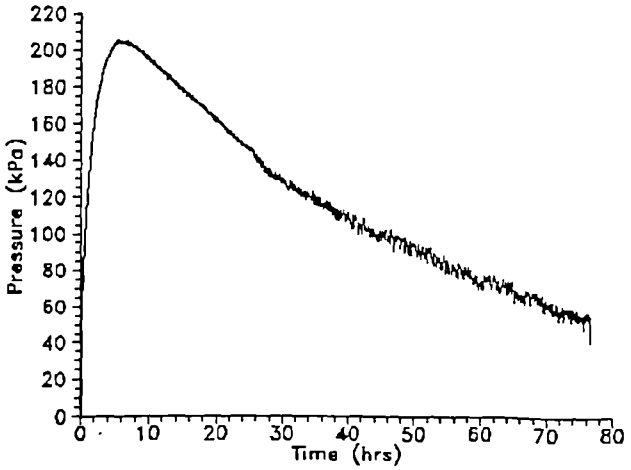

Figure 5.22 Pressure on top wall segment during inundation (CLC3).

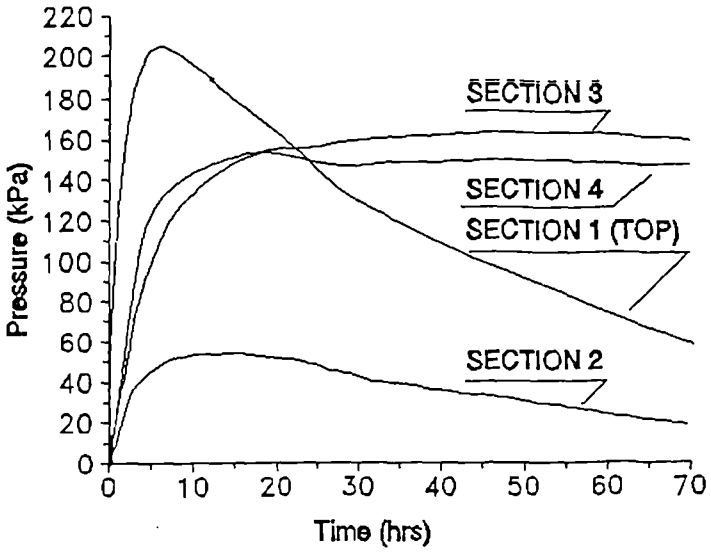

Figure 5.23(a) Variation of pressure with time for all segments of centrifuge model (CLC3).

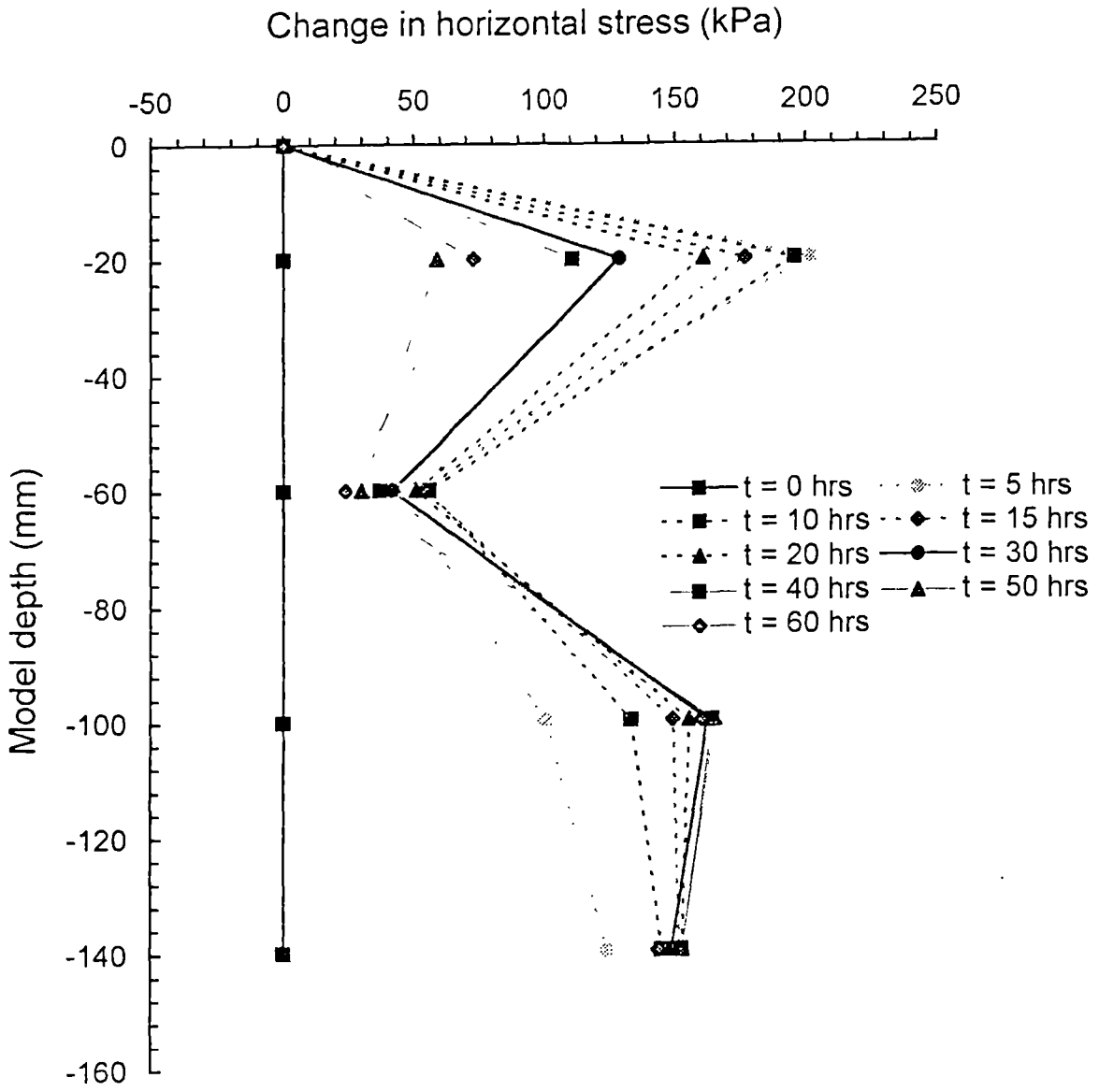

Figure 5.23(b) Variation of stress with depth during inundation (CLC3).

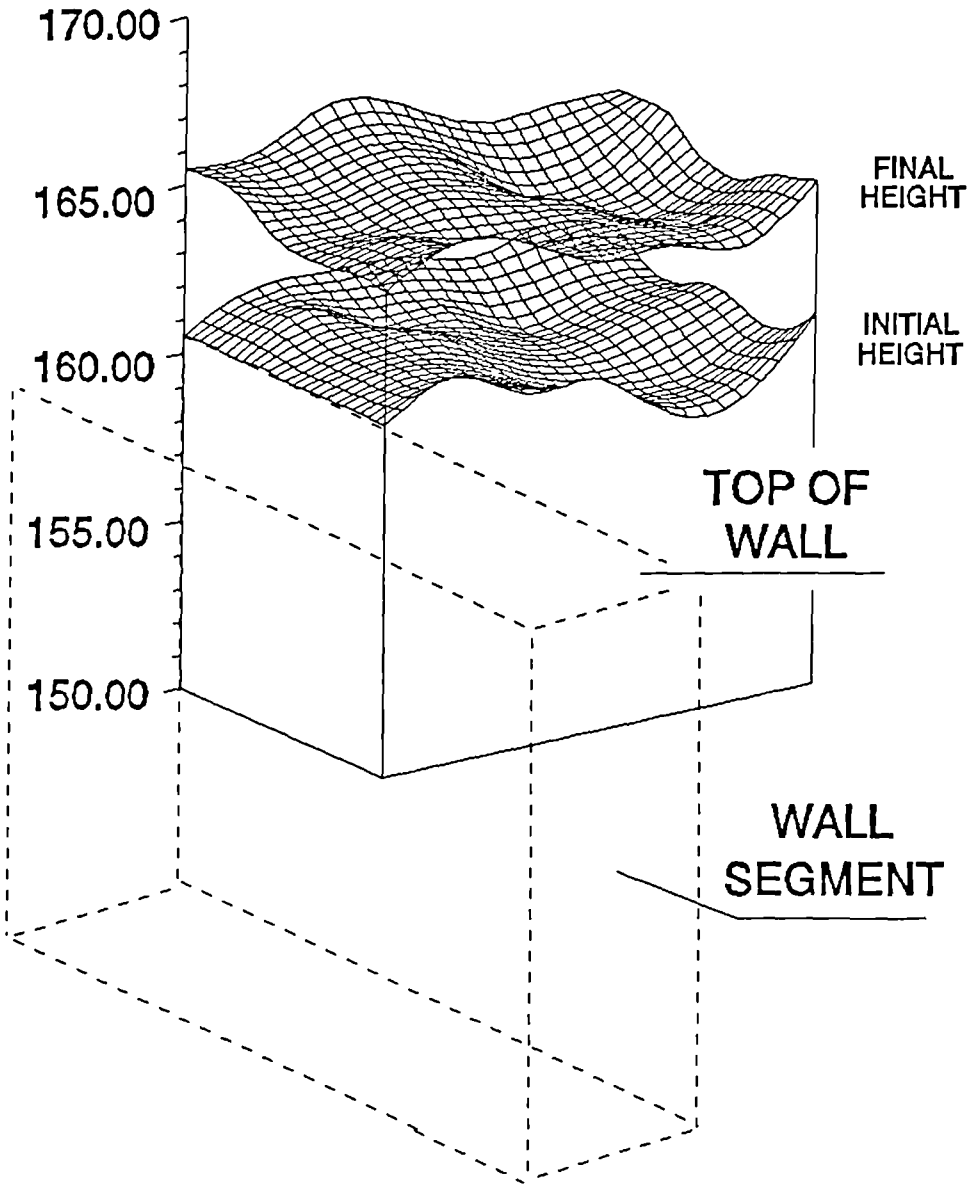

Figure 5.24 Heave in soil behind wall at end of test (CLC3).

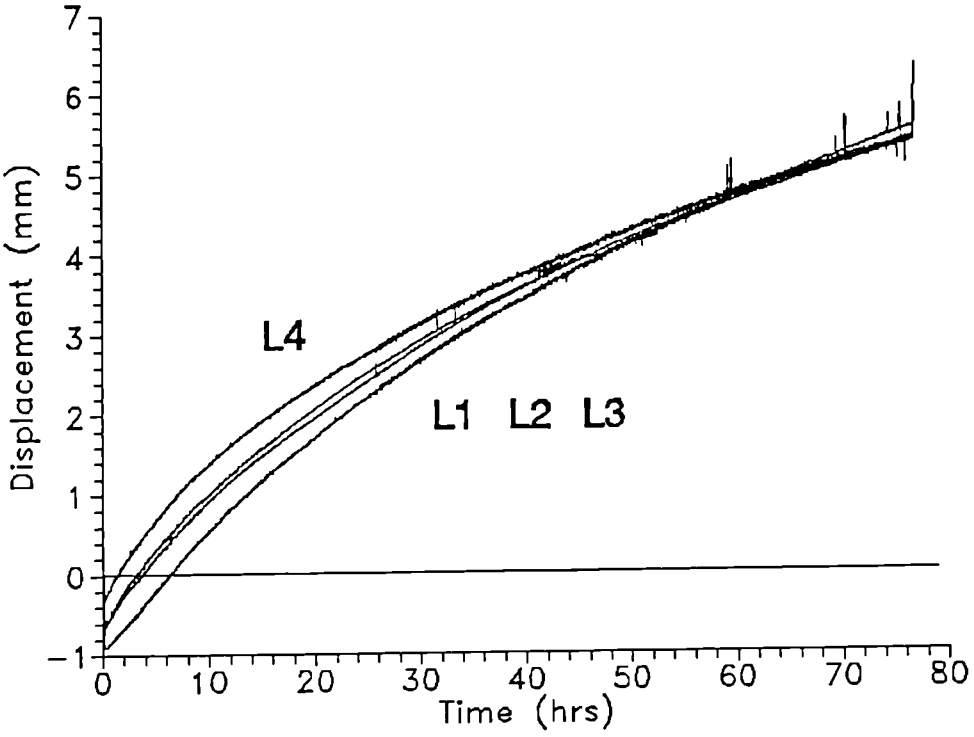

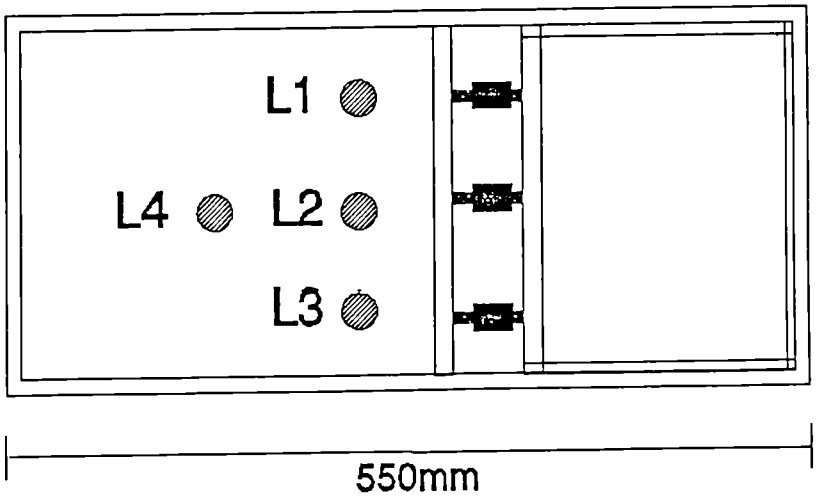

Figure 5.25 Change in vertical stress with time, measured by surface LVDTs (CLC3).

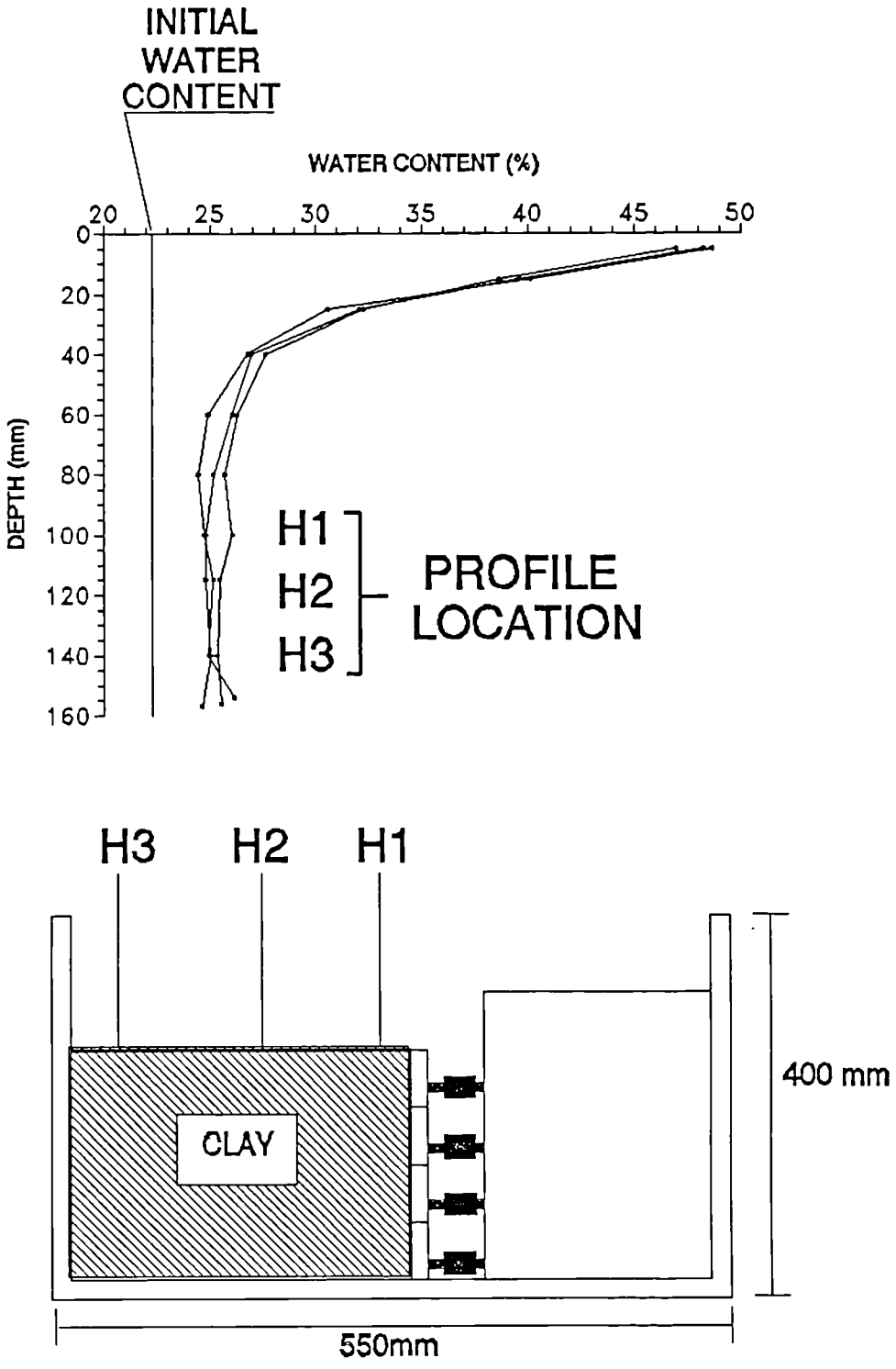

Figure 5.26 Water content profile at end of test (CLC3).

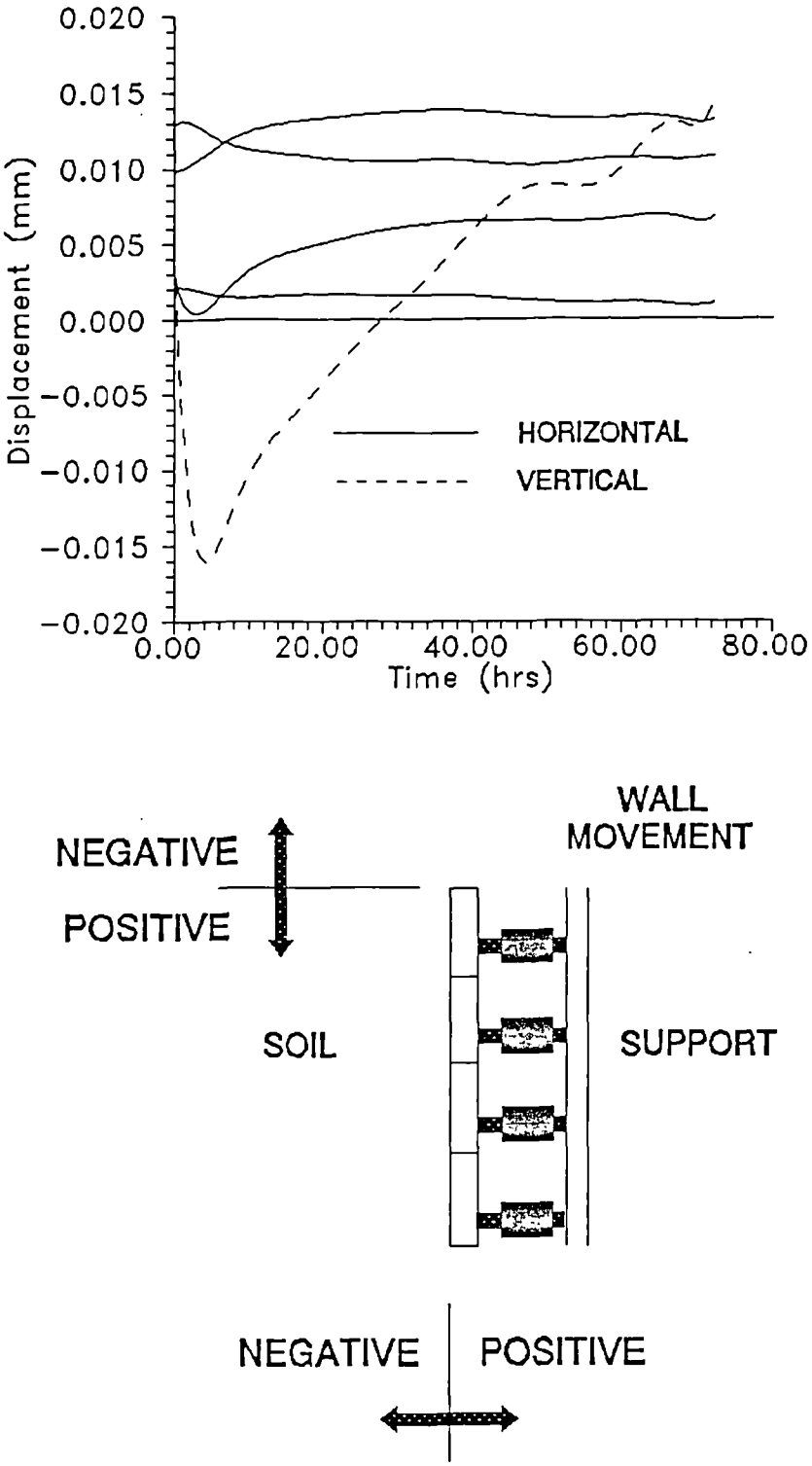

Figure 5.27 Horizontal and vertical wall movement during testing (CWA3).

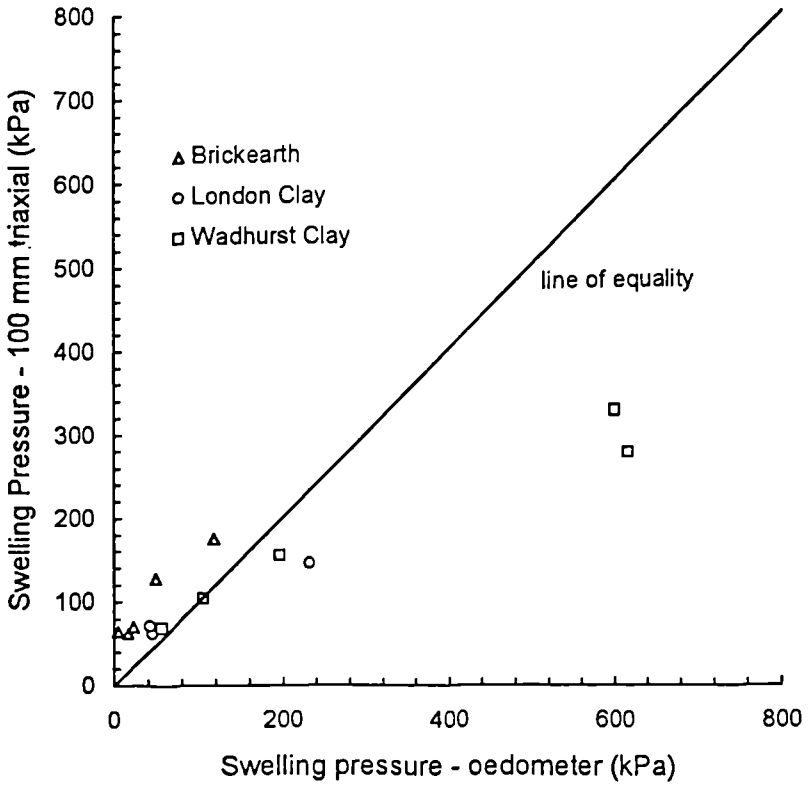

Figure 6.1 Total swelling pressure (100 mm cell) vs. total swelling pressure (modified oedometer).

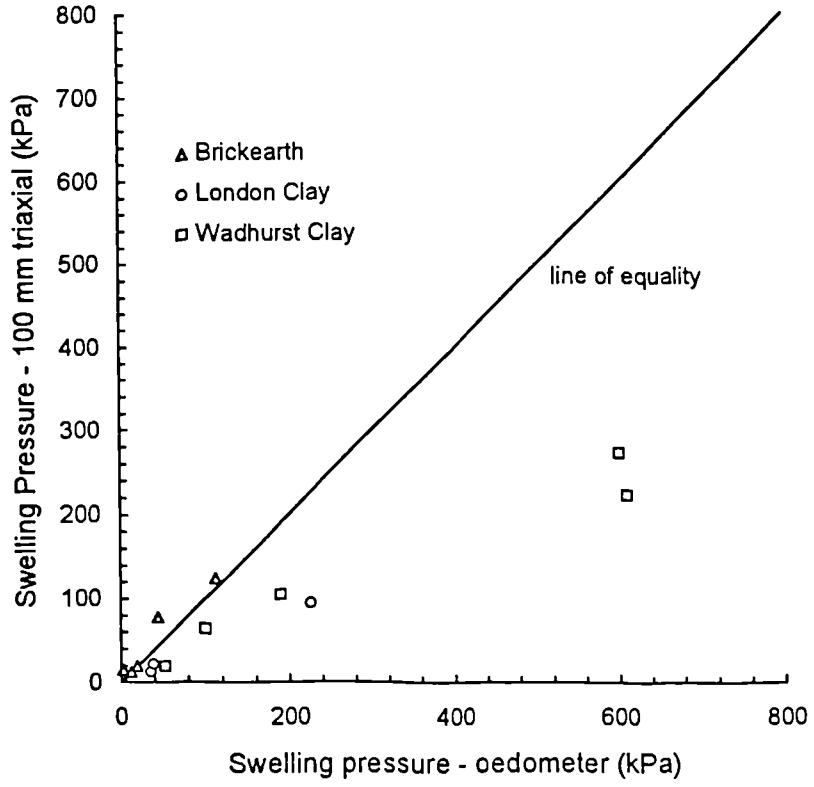

Figure 6.2 Net swelling pressure (100 mm cell) vs. net swelling pressure (modified oedometer).

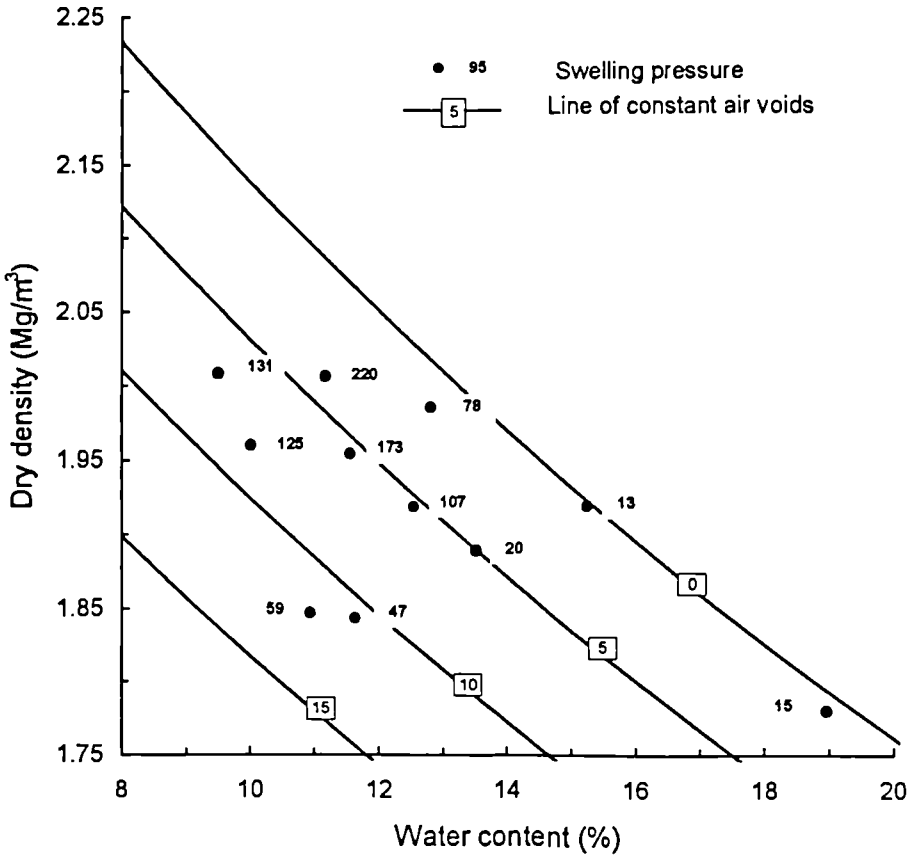

Figure 6.3 Initial state of soil with values of net swelling pressure - Brickearth, 100 mm cell.

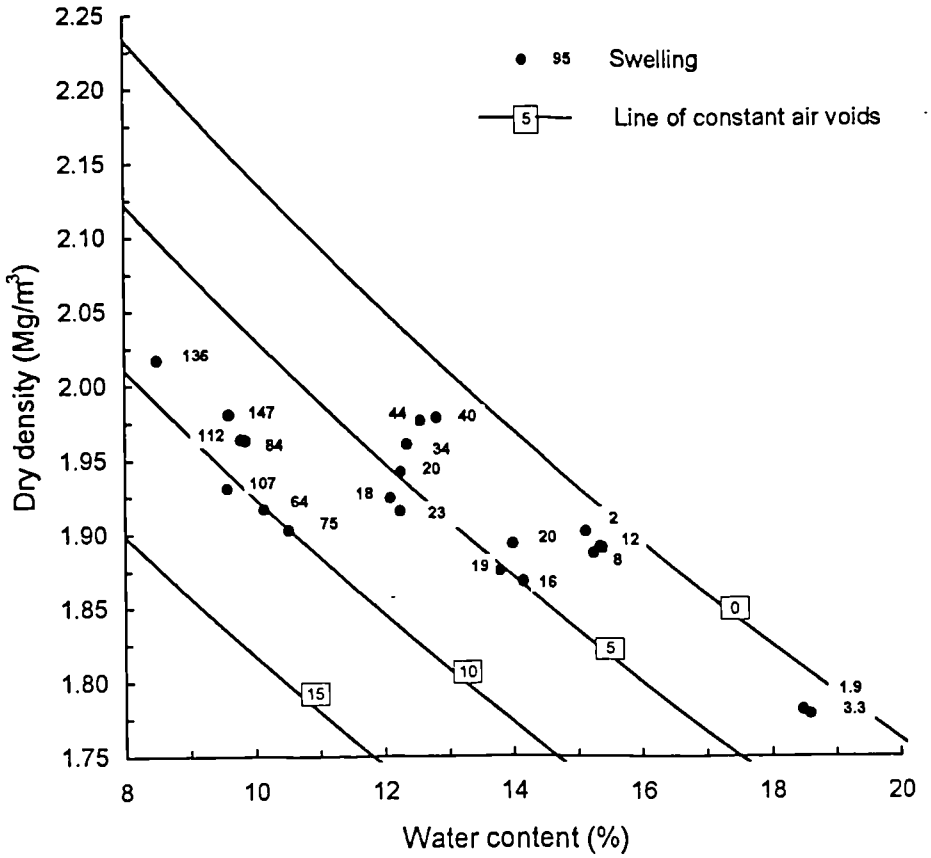

Figure 6.4 state of soil with values of net swelling pressure - Brickearth, modified oedometer.

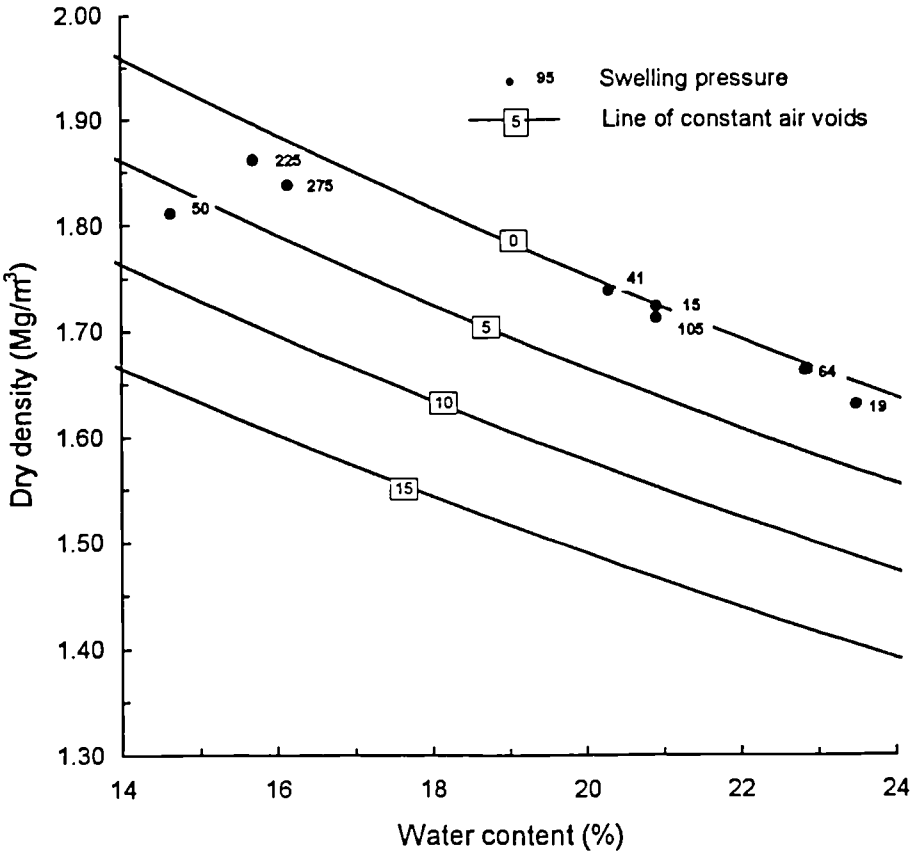

Figure 6.5 Initial state of soil with values of net swelling pressure - Wadhurst Clay, 100 mm cell.

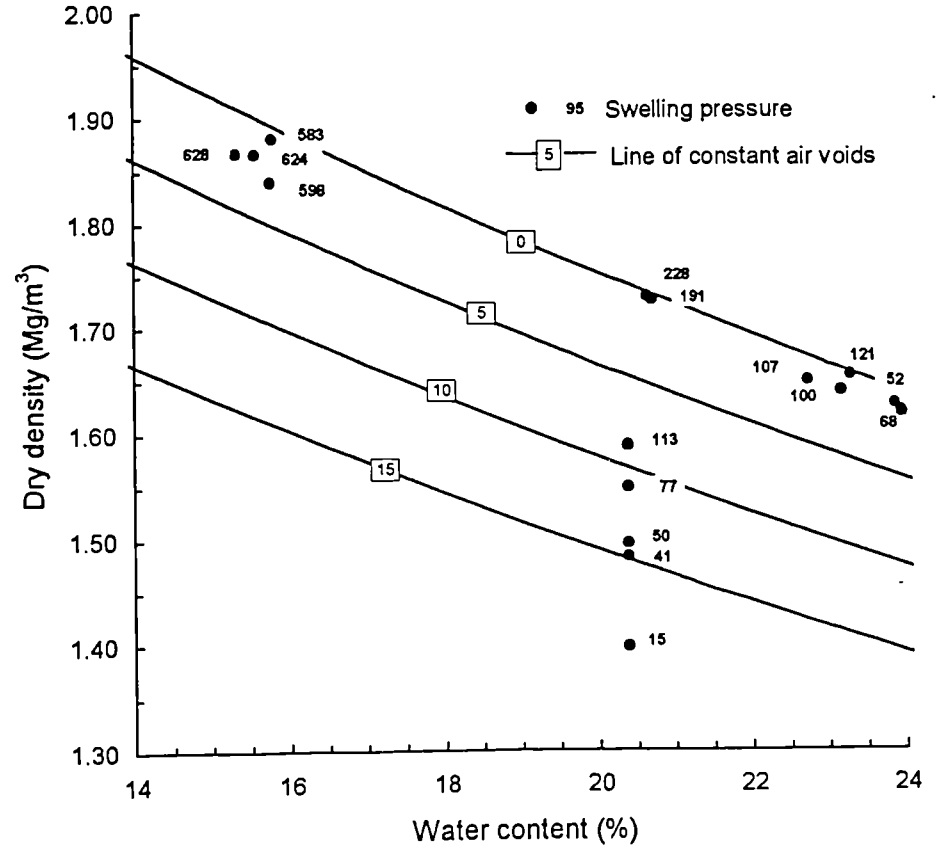

Figure 6.6 Initial state of soil with values of net swelling pressure - Wadhurst Clay, modified oedometer

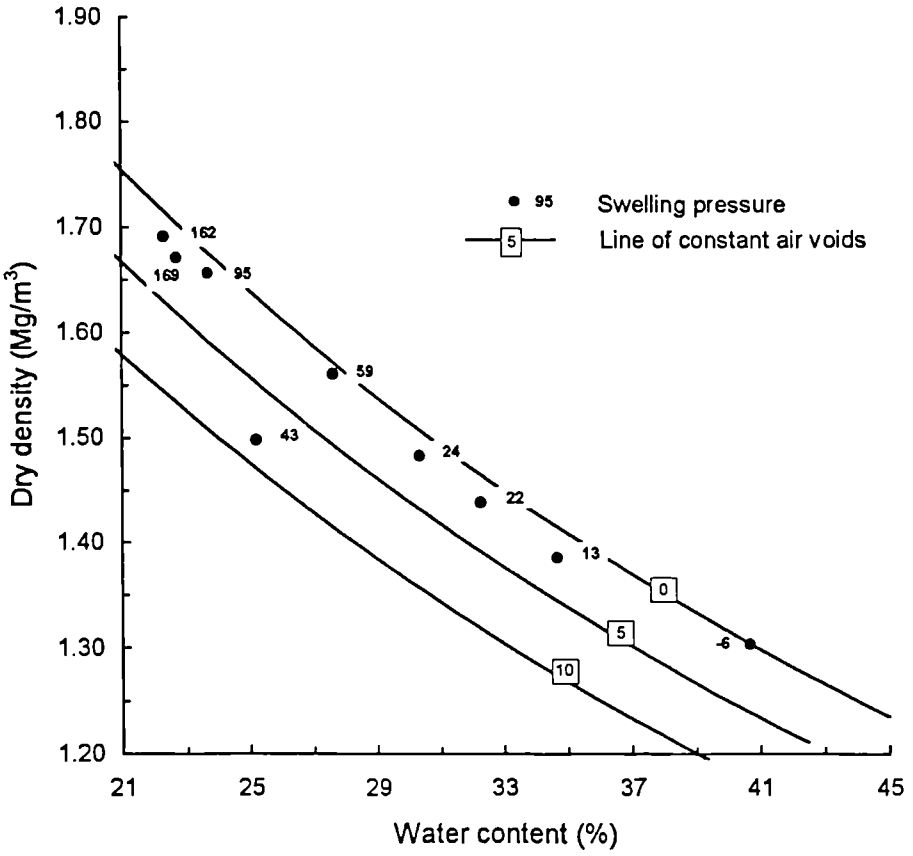

Figure 6.7 Initial state of soil with values of net swelling pressure - London Clay, 100 mm cell.

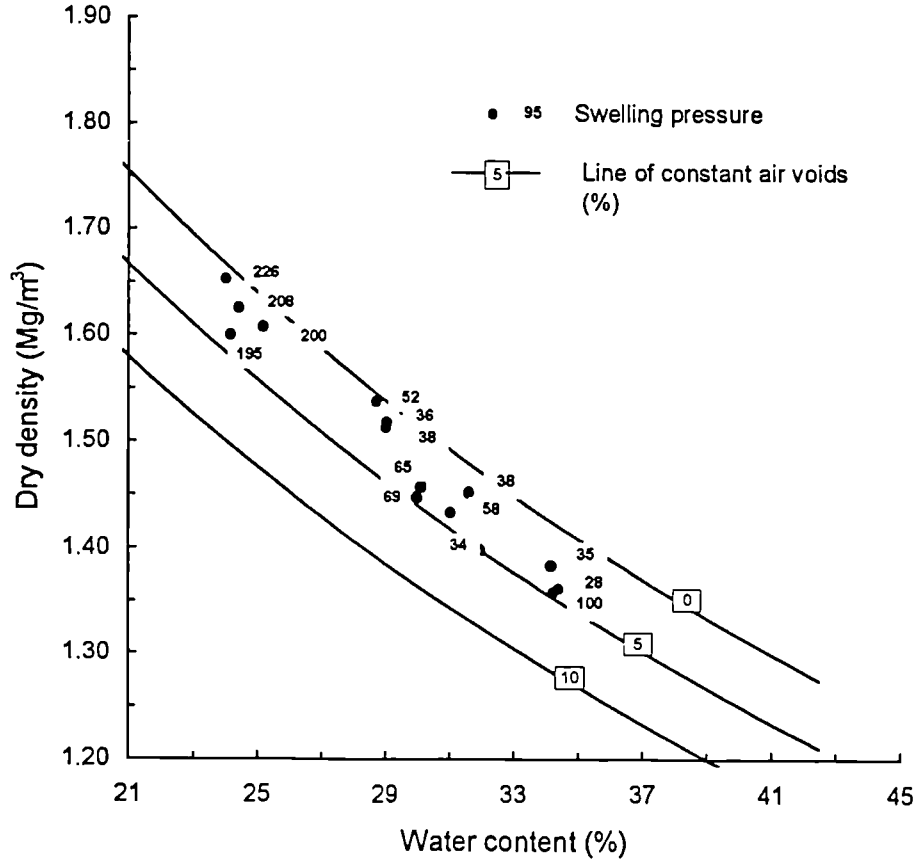

Figure 6.8 Initial state of soil with values of net swelling pressure - London Clay, modified oedometer.

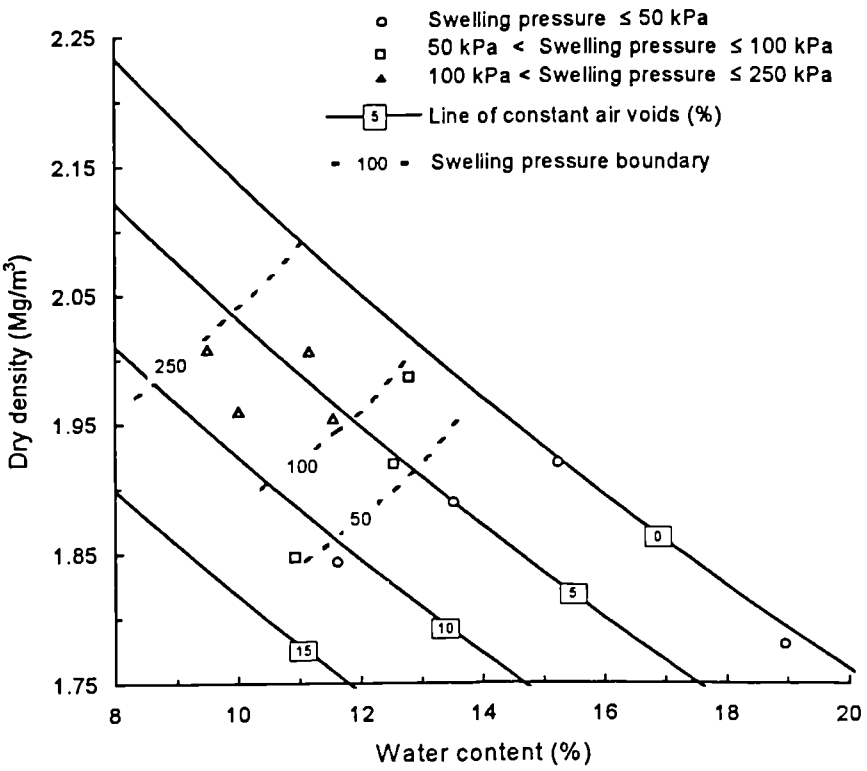

Figure 6.9 Initial state of soil with ranges of net swelling pressure - Brickearth, 100 mm cell.

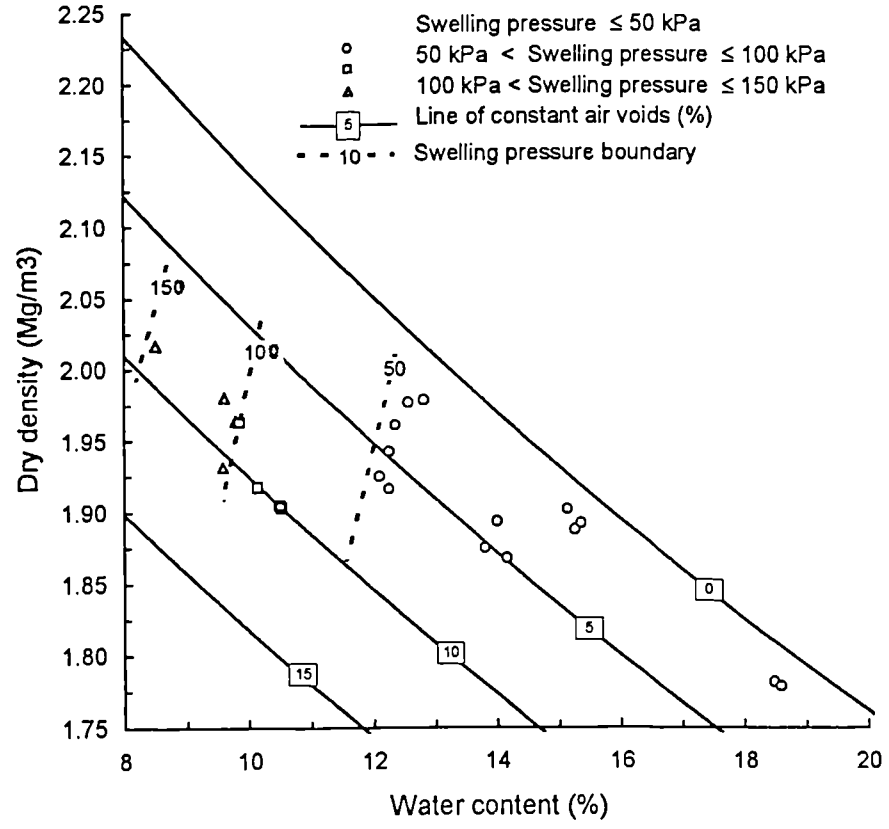

Figure 6.10 Initial state of soil with ranges of net swelling pressure - Brickearth, modified oedometer.

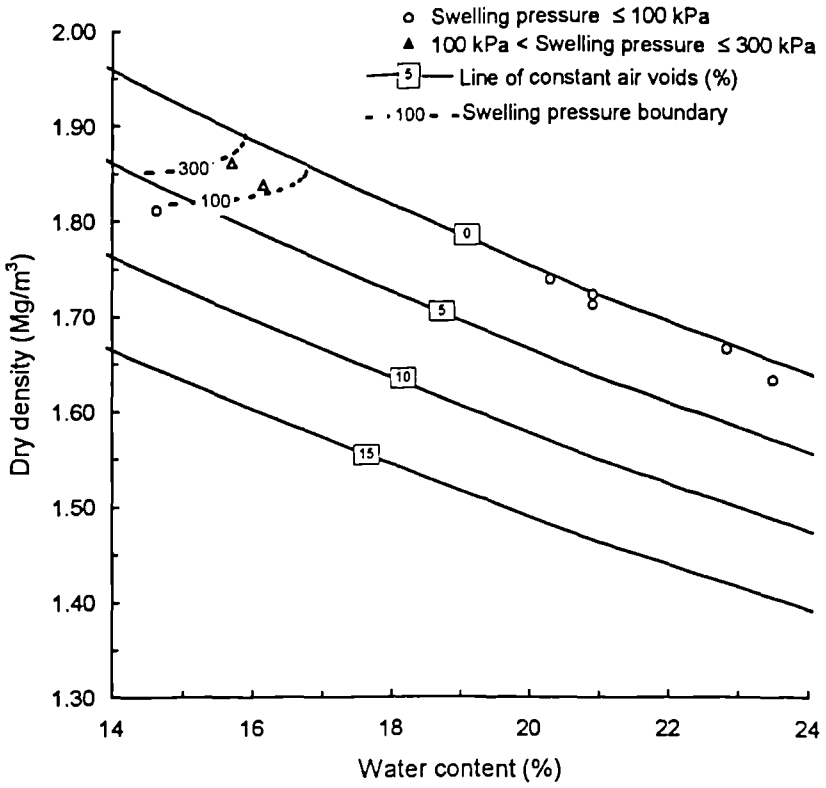

Figure 6.11 Initial state of soil with ranges of net swelling pressure - Wadhurst Clay, 100 mm cell.

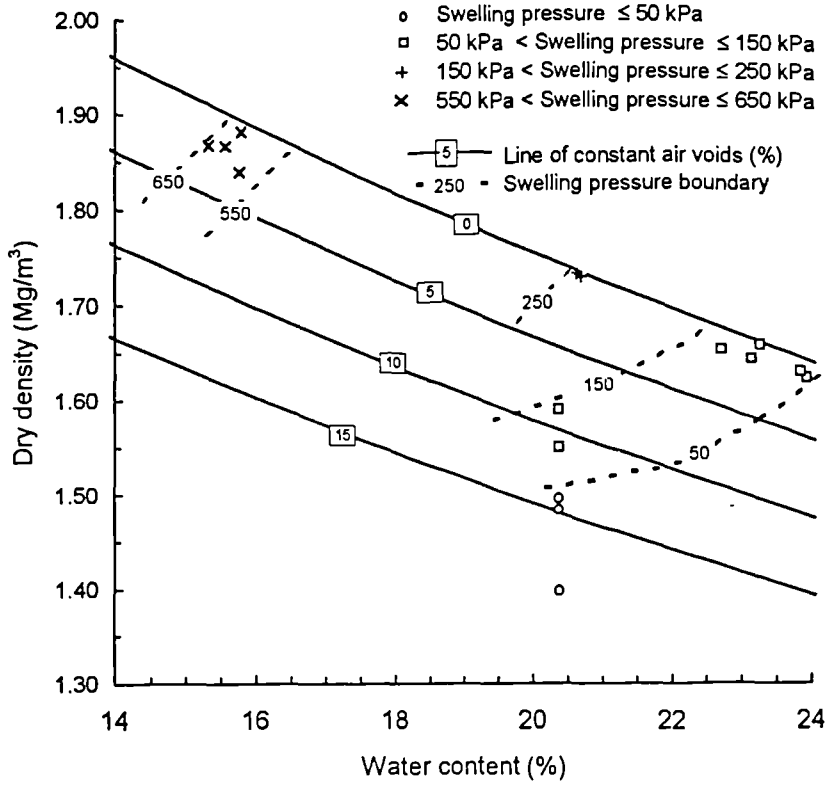

Figure 6.12 Initial state of soil with ranges of net swelling pressure - Wadhurst Clay, modified oedometer.

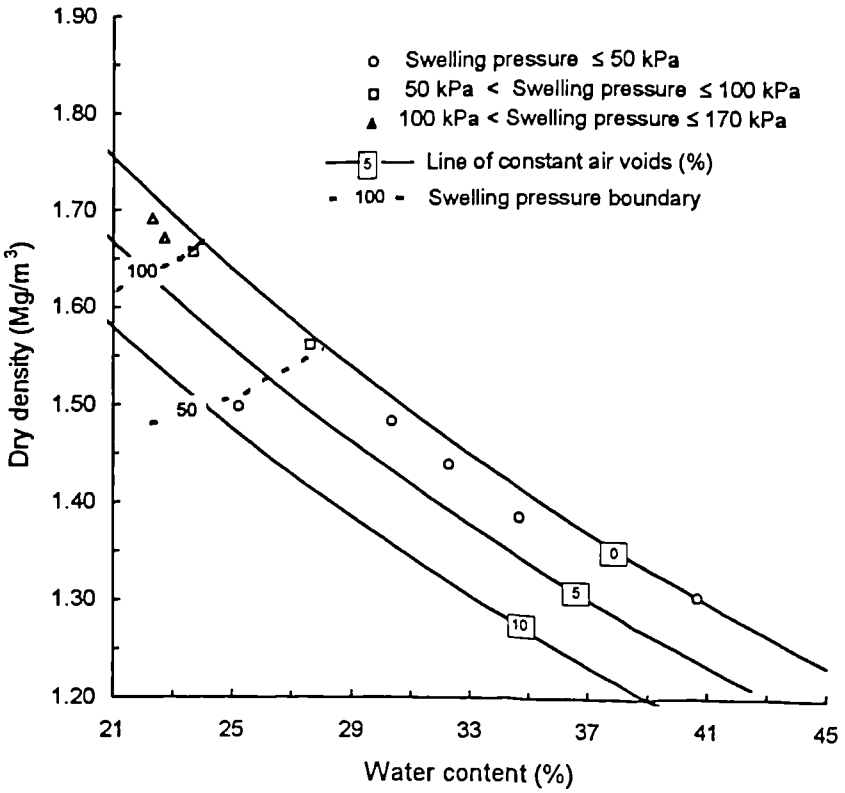

Figure 6.13 Initial state of soil with ranges of net swelling pressure - London Clay, 100 mm cell.

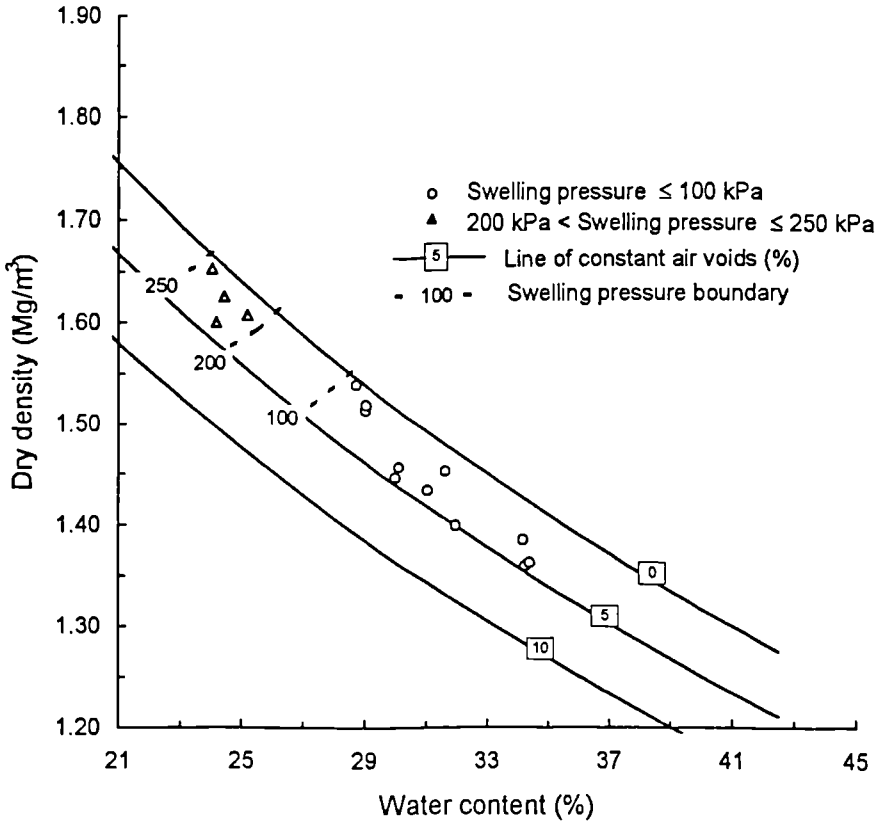

Figure 6.14 Initial state of soil with ranges of net swelling pressure - London Clay, modified oedometer.

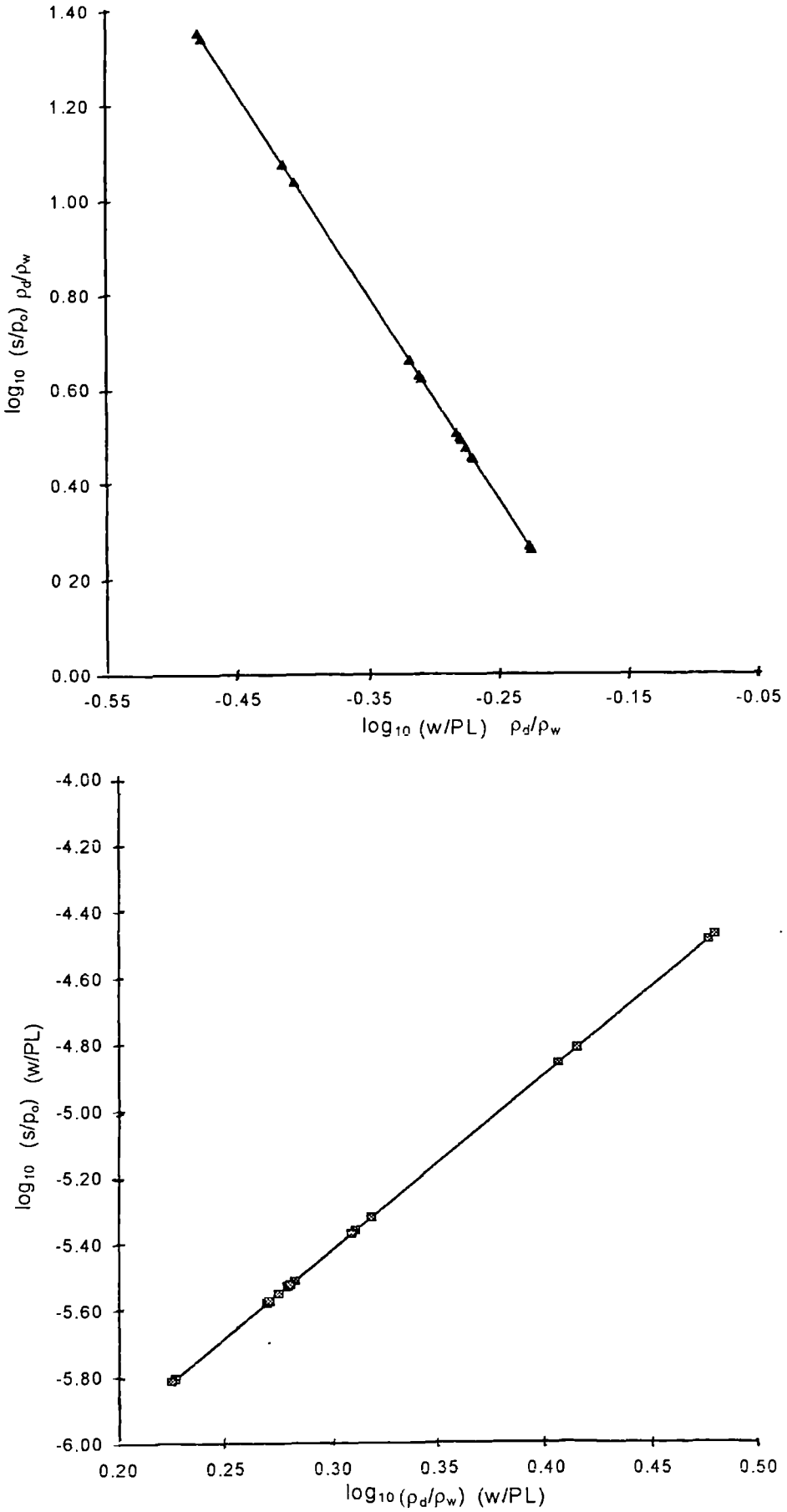

Figure 6.15 Comparison of suction with normalised values of dry density and water content.

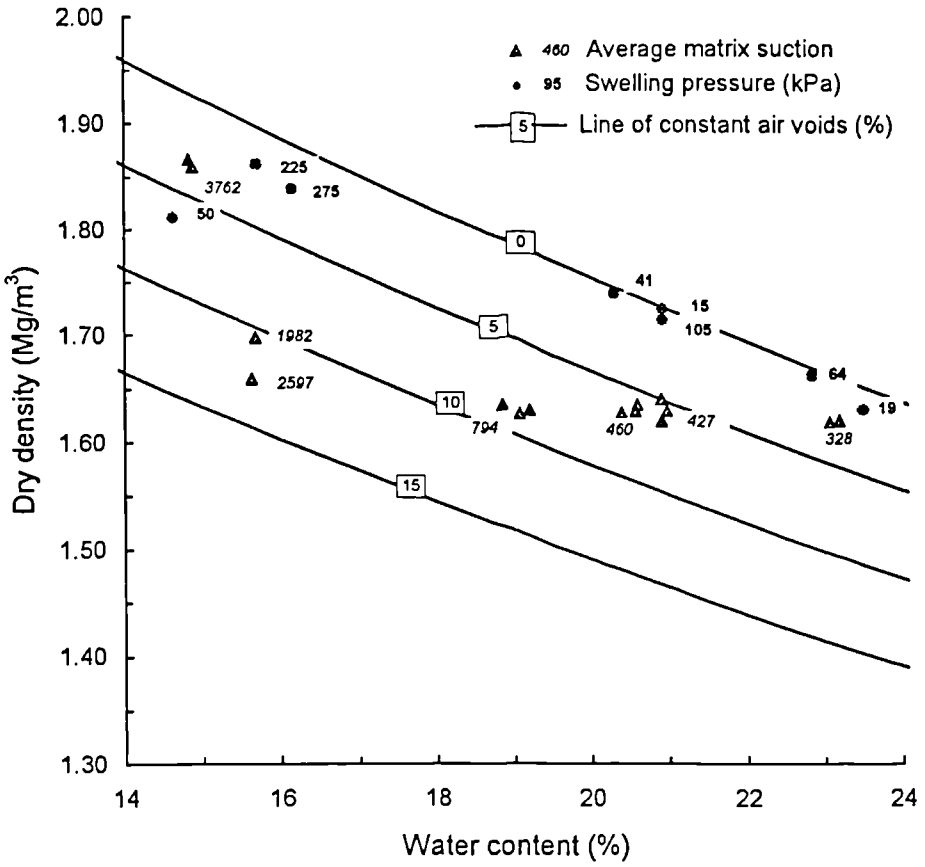

Figure 6.16 Initial state of soil and suction values superimposed on 100 mm cell results - Wadhurst Clay.

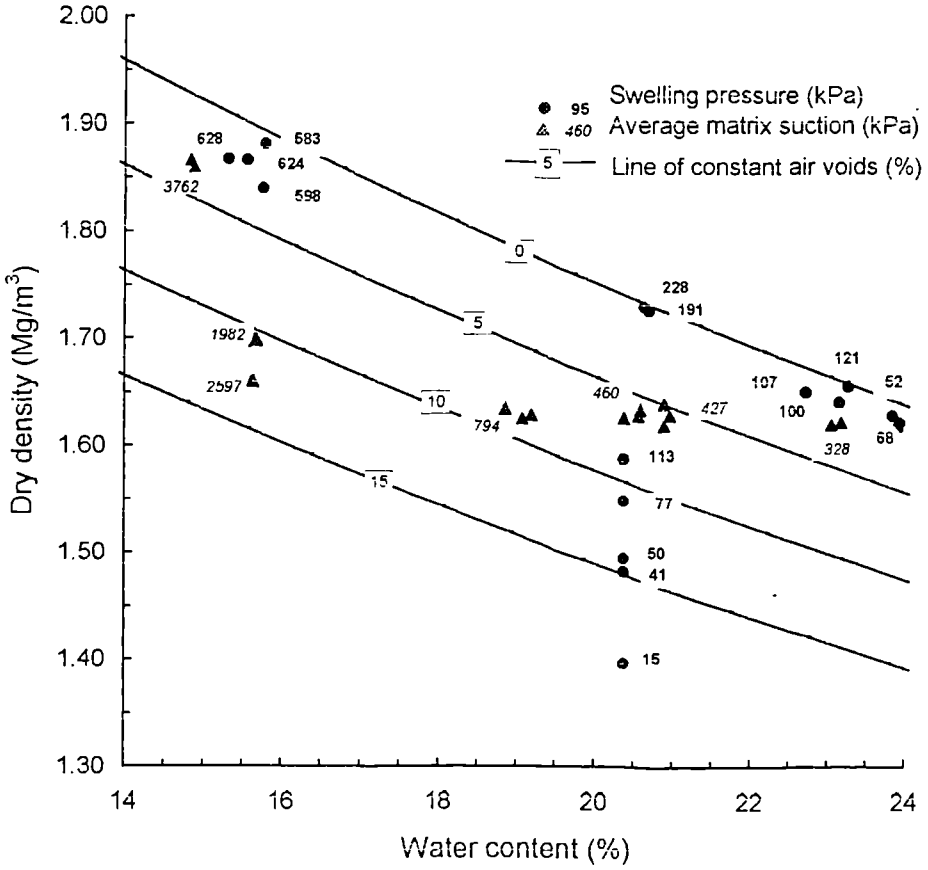

Figure 6.17 Initial state of soil and matrix suction values superimposed on modified oedometer results - Wadhurst Clay.

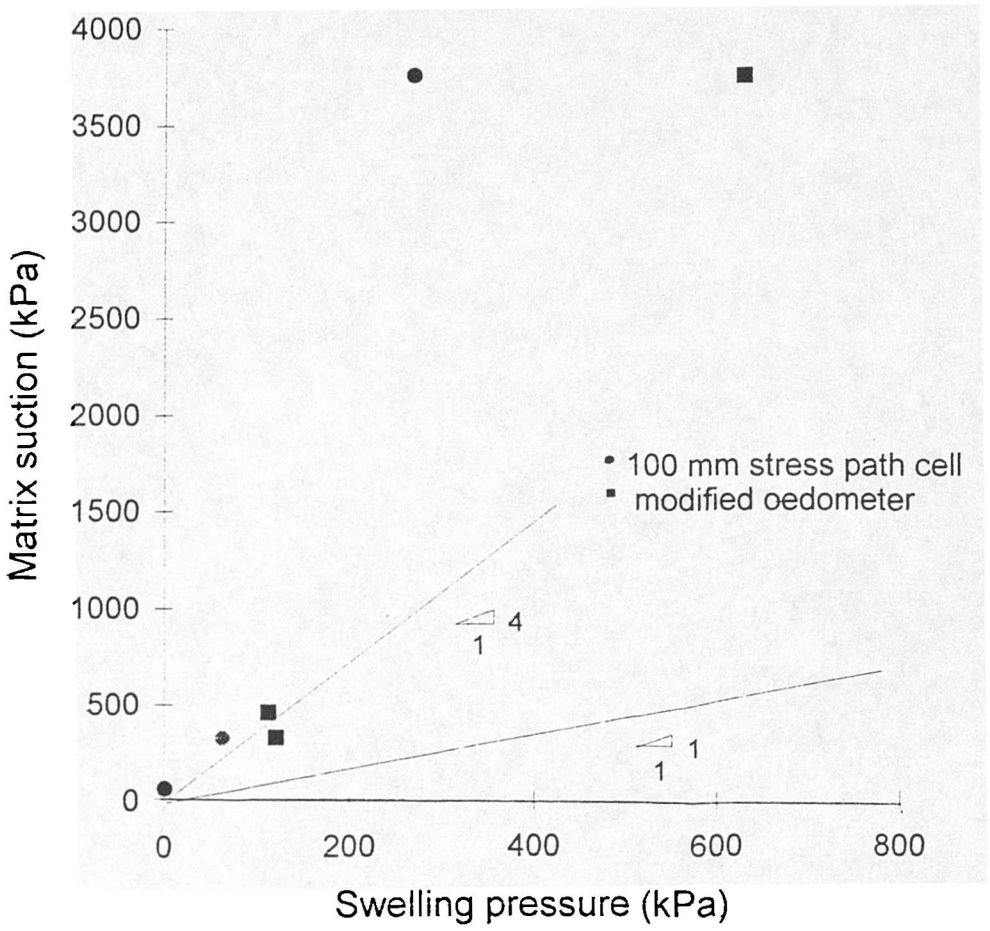

Figure 6.18 Initial state of soil and matrix suction values superimposed on modified oedometer results - Wadhurst Clay.

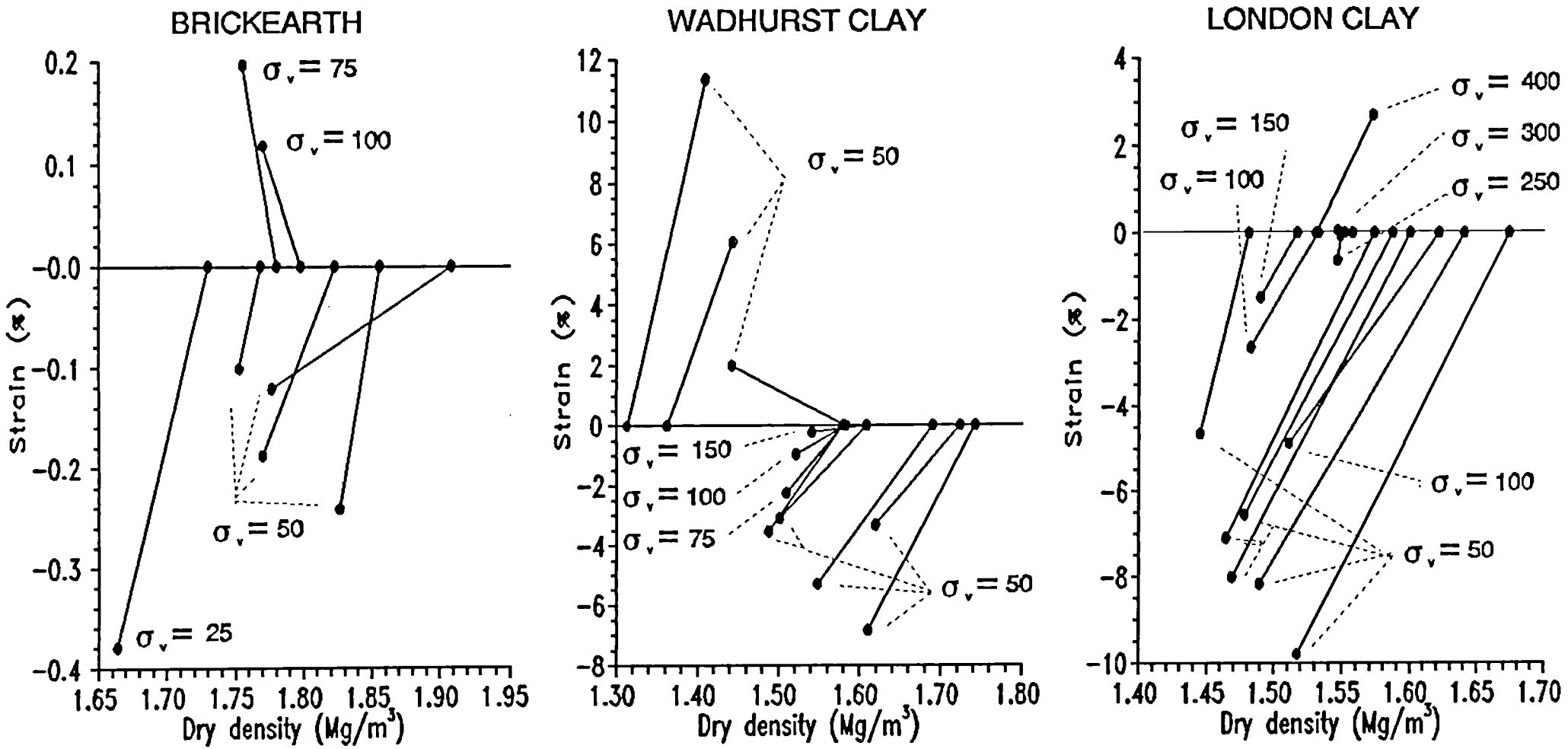

Figure 6.19 Volumetric changes in terms of vertical strains with different initial vertical strains.

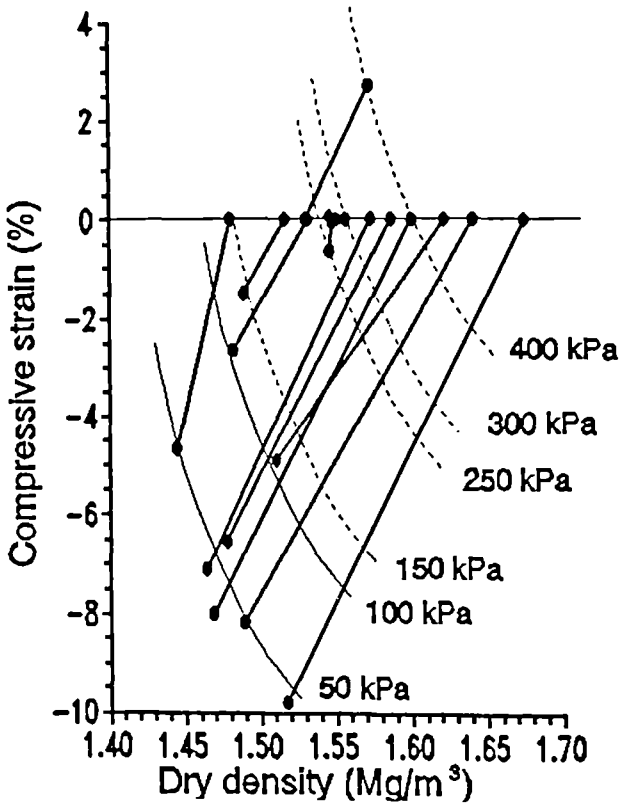

Figure 6.20 Lines of constant vertical stress superimposed on computer controlled oedometer results (London Clay).

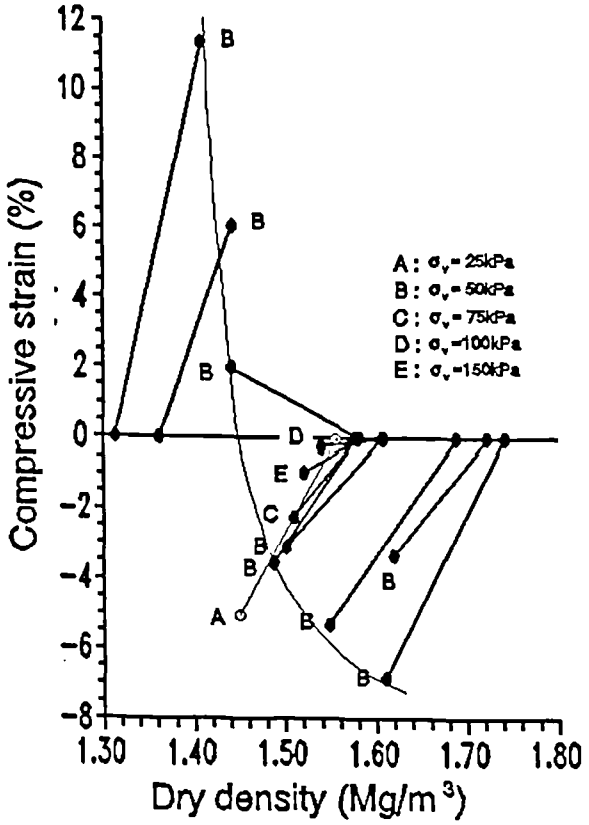

Figure 6.21 Lines of constant vertical stress superimposed on computer controlled oedometer results (Wadhurst Clay).

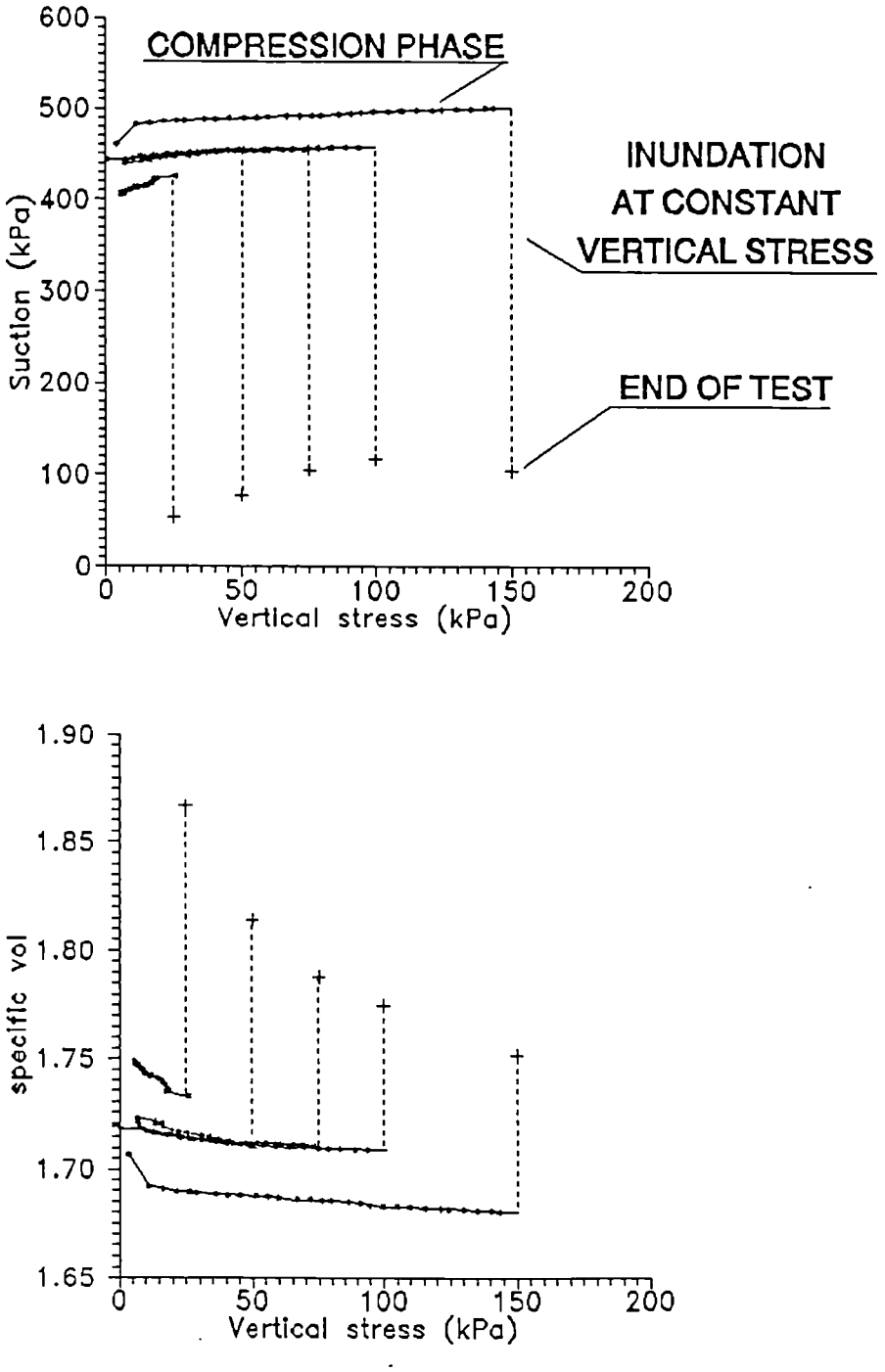

Figure 6.22 Suction changes in computer controlled oedometer tests (Wadhurst Clay).

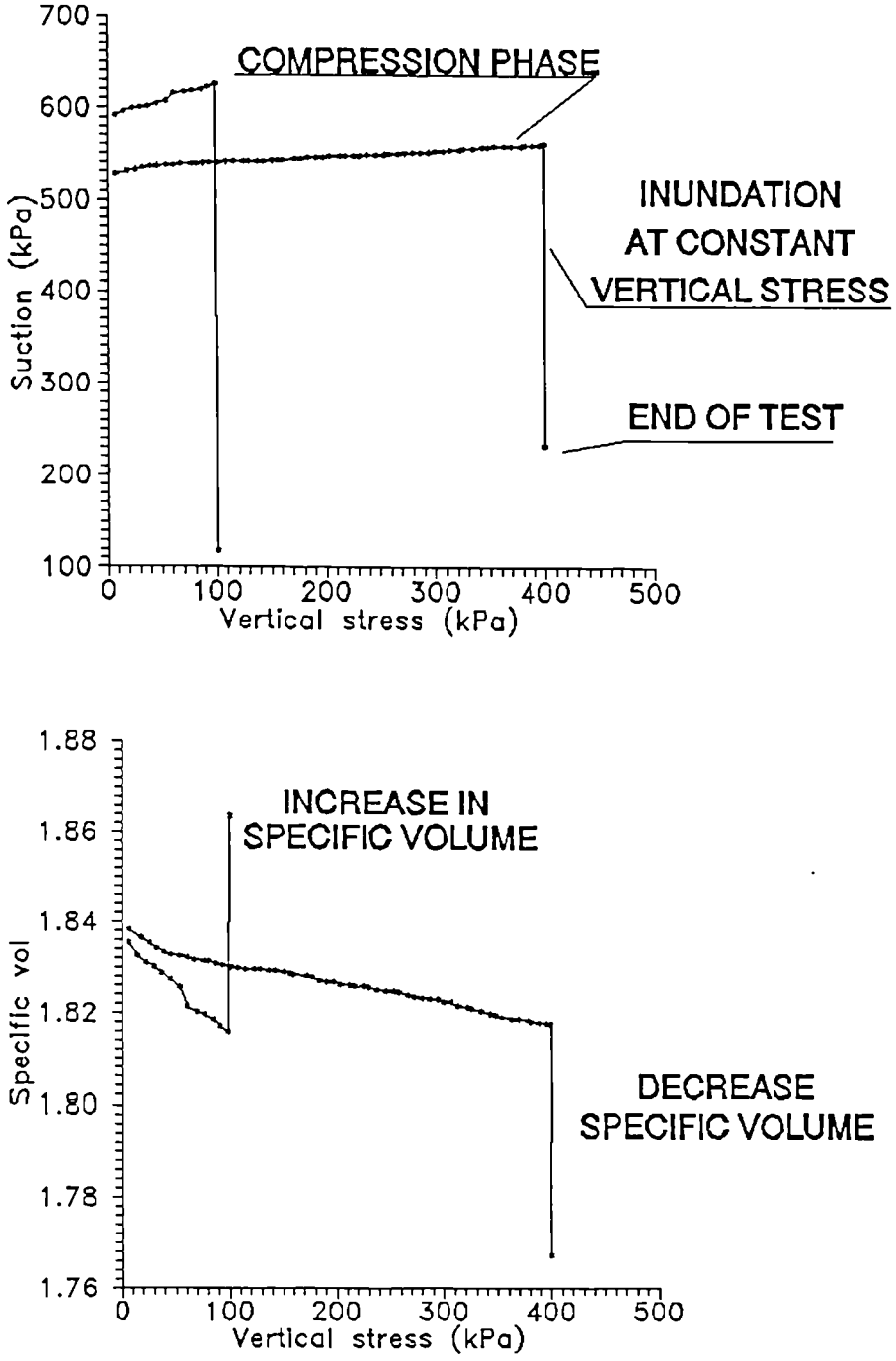

Figure 6.23 Suction changes in computer controlled oedometer tests (London Clay).

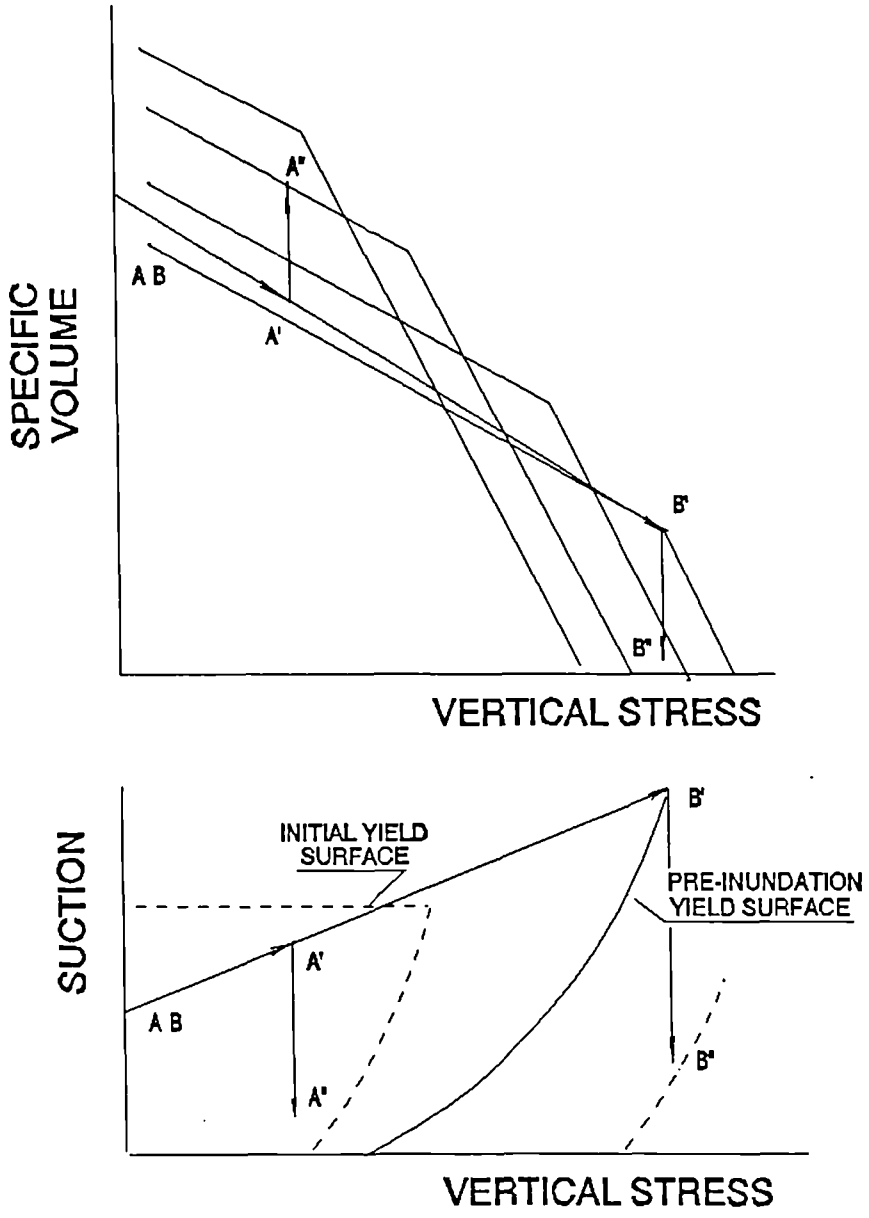

Figure 6.24 Path followed by soil in terms of specific volume, suction and vertical stress.

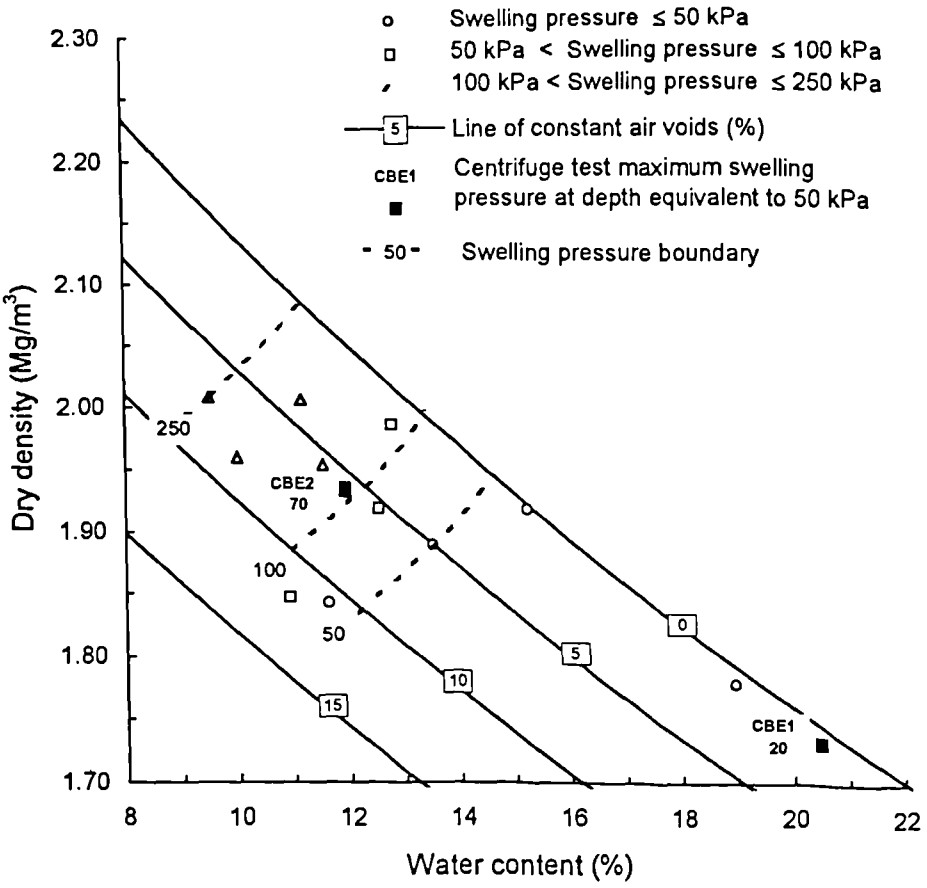

Figure 6.25(a) Comparison of swelling pressure in centrifuge tests with 100 mm cell - Brickearth.

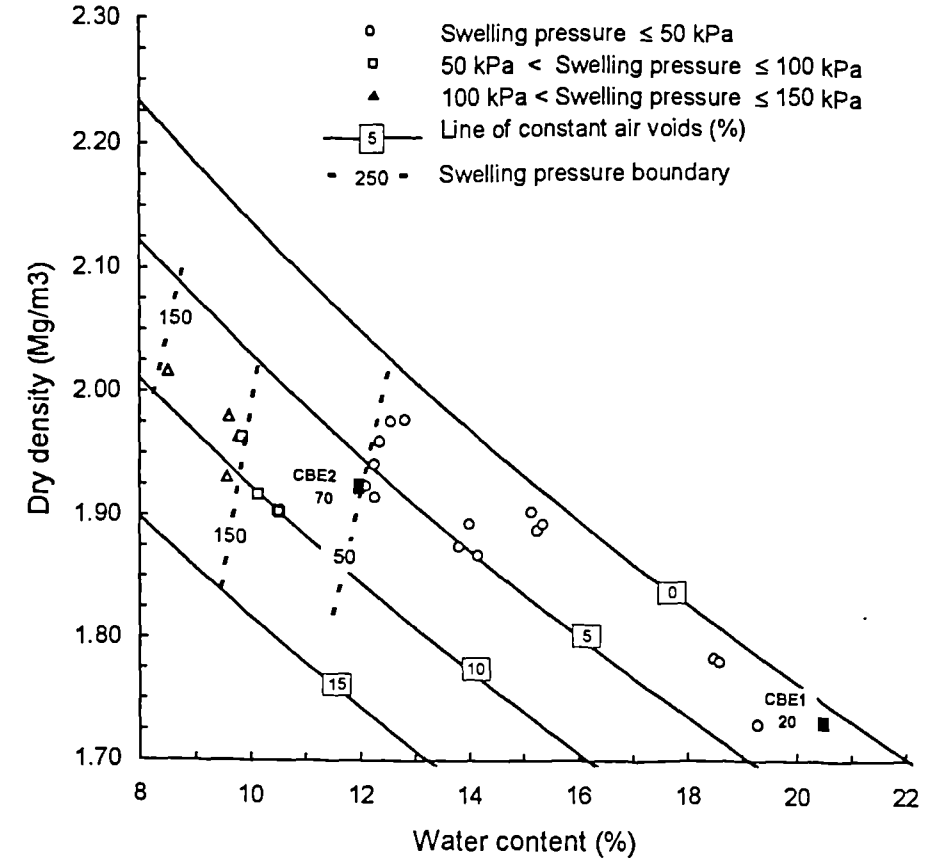

Figure 6.25(b) Comparison of swelling pressure in centrifuge tests with modified oedometer - Brickearth.

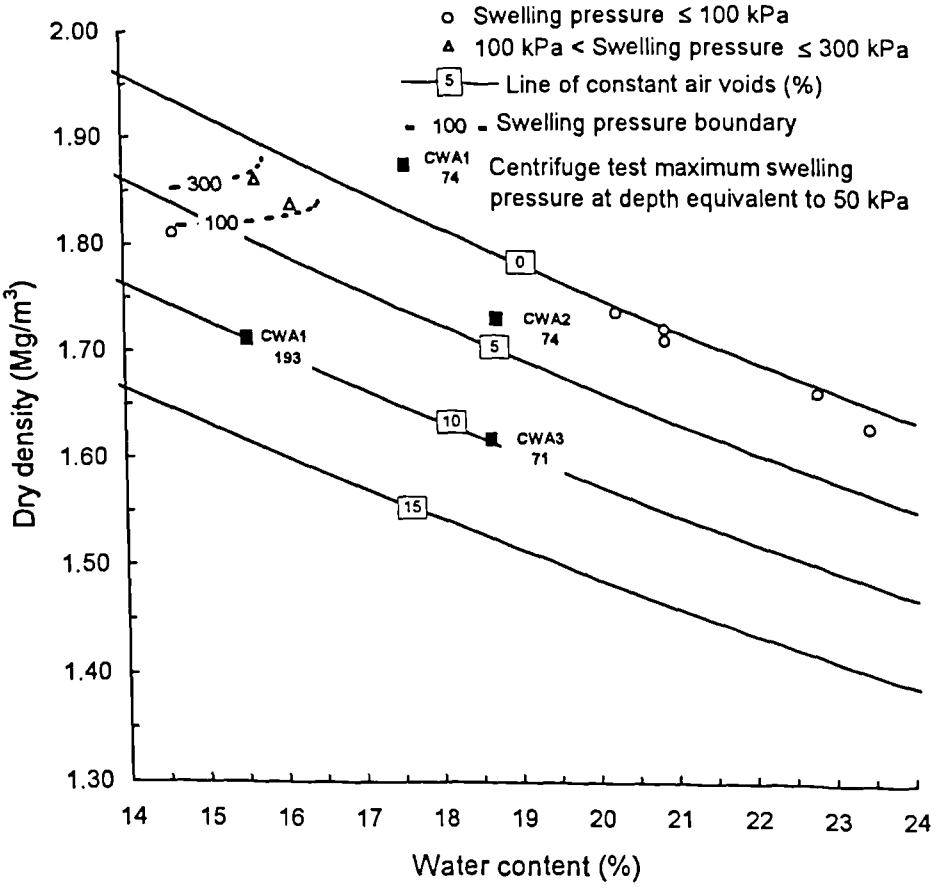

Figure 6.26(a) Comparison of swelling pressure in centrifuge tests with 100 mm cell - Wadhurst Clay.

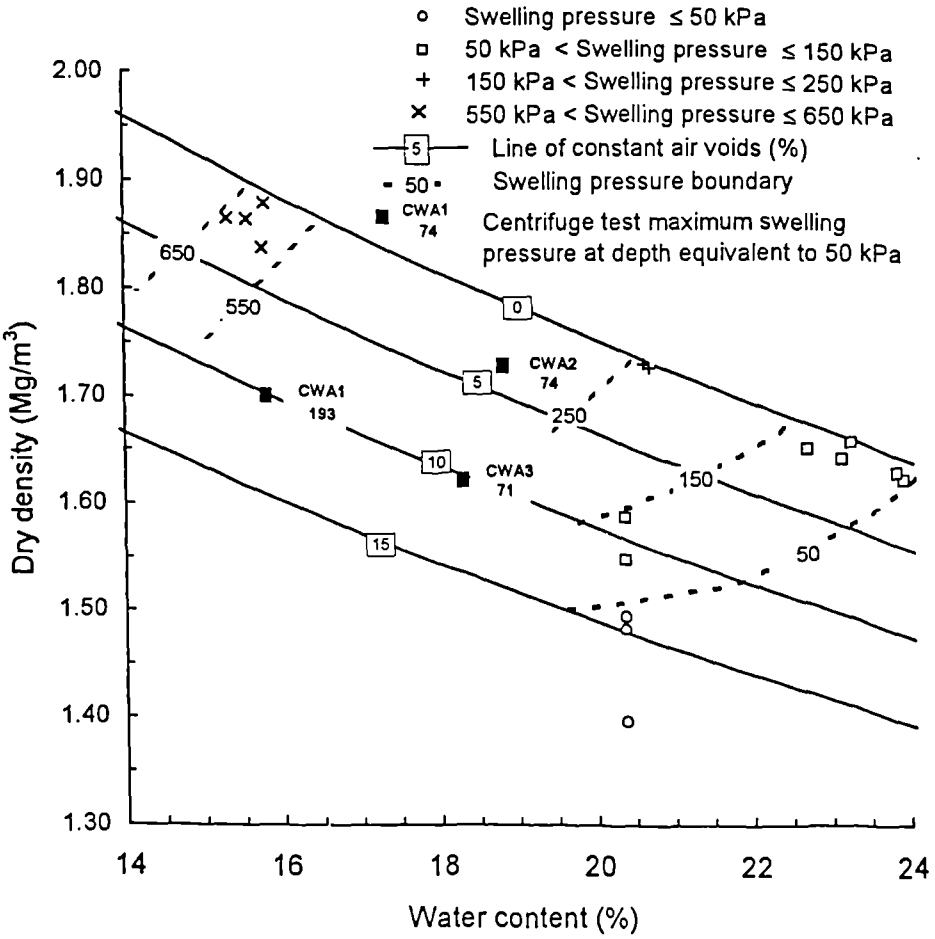

Figure 6.26(b) Comparison of swelling pressure in centrifuge tests with modified oedometer - Wadhurst Clay.

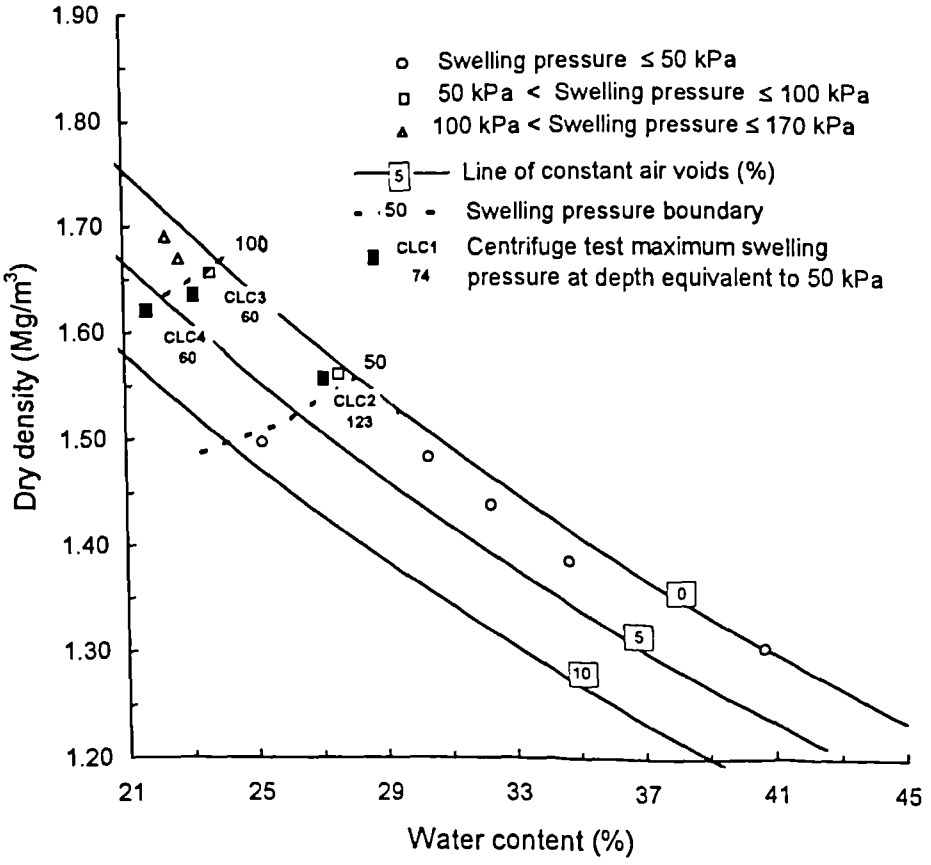

Figure 6.27(a) Comparison of swelling pressure in centrifuge tests with 100 mm cell - London Clay.

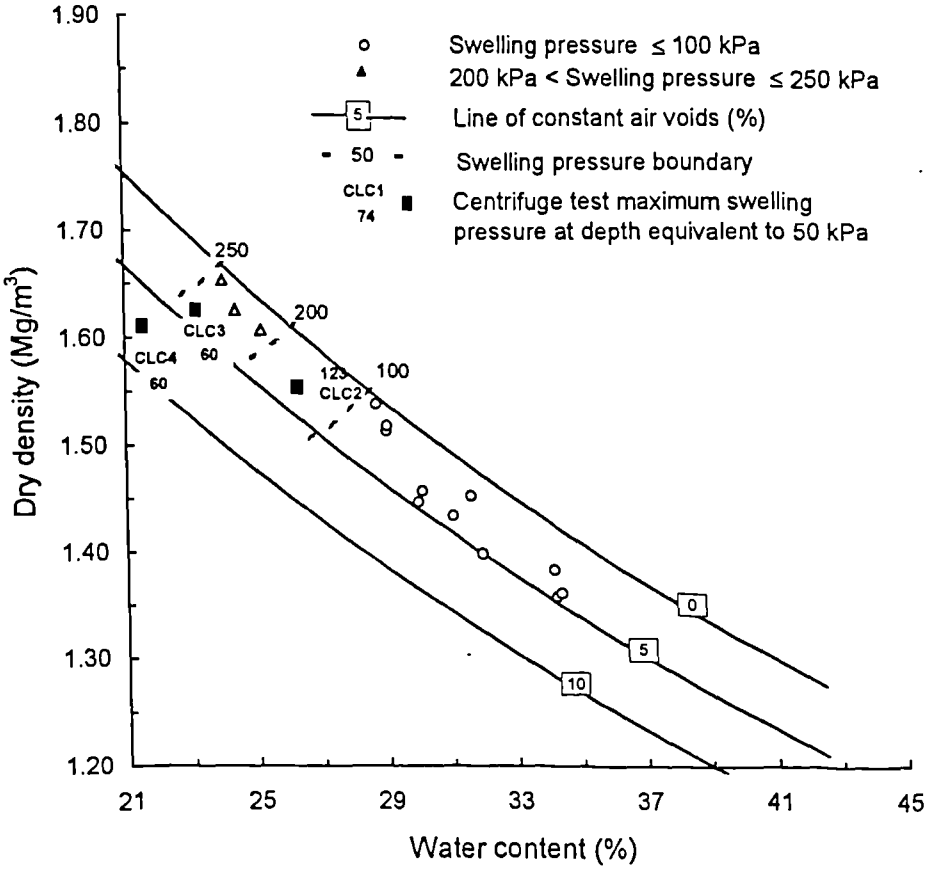

Figure 6.27(b) Comparison of swelling pressure in centrifuge tests with modified oedometer - London Clay.

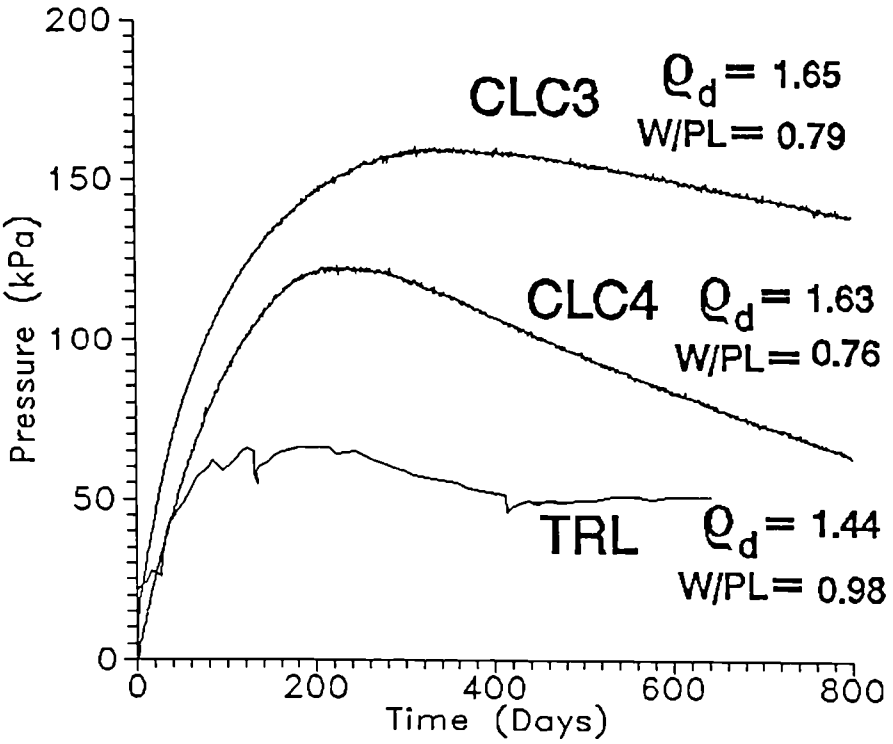

Figure 6.28 Comparison of centrifuge tests with the prototype experimental wall.

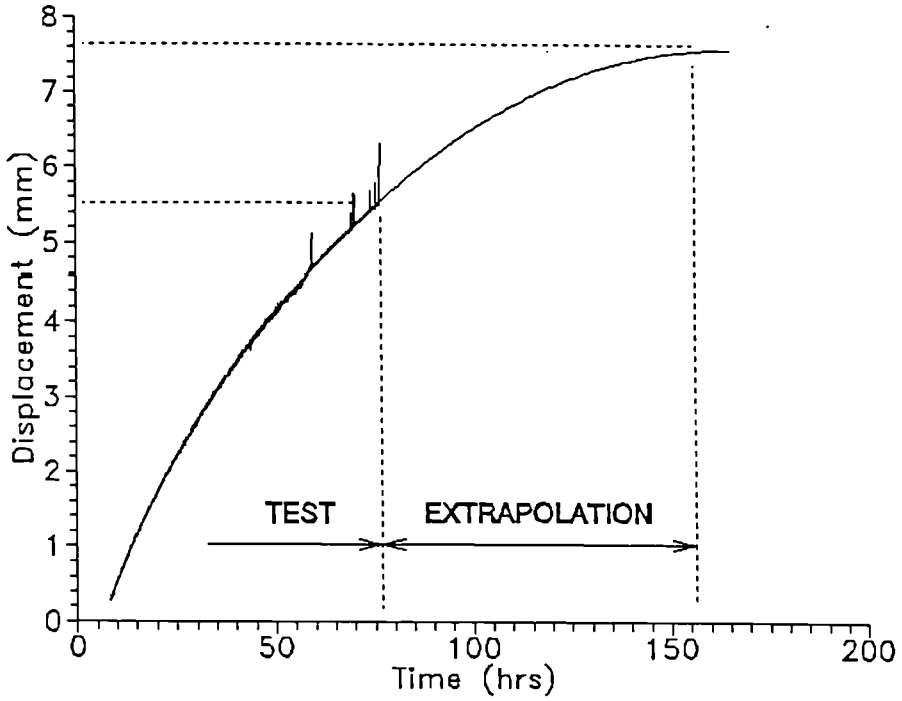

Figure 6.29 Surface displacement of soil in centrifuge test with extrapolation.

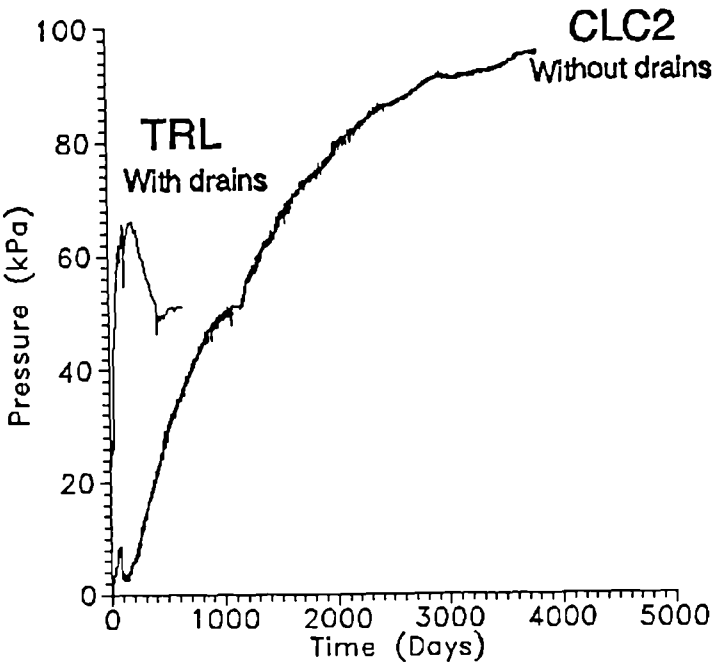

Figure 6.30 Comparison of lateral pressure on wall in centrifuge test (without vertical drains) and prototype (with vertical drains).

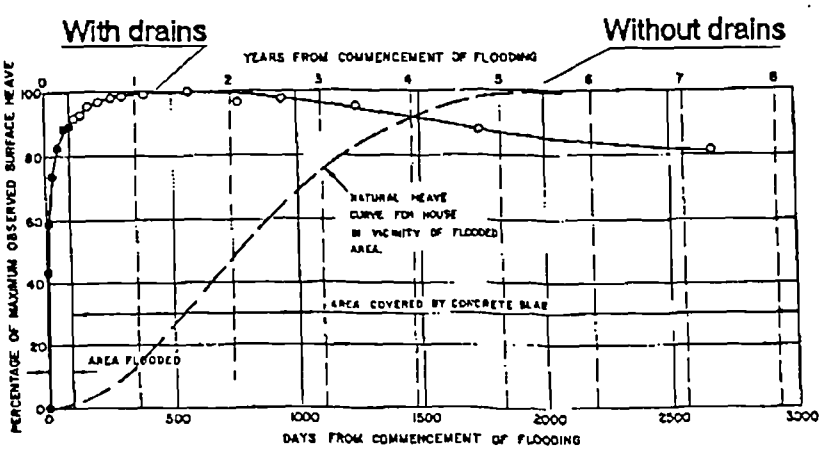

Figure 6.31 Field measurements of heave observed in soil with and without drains (after Blight and De Wet, 1965).

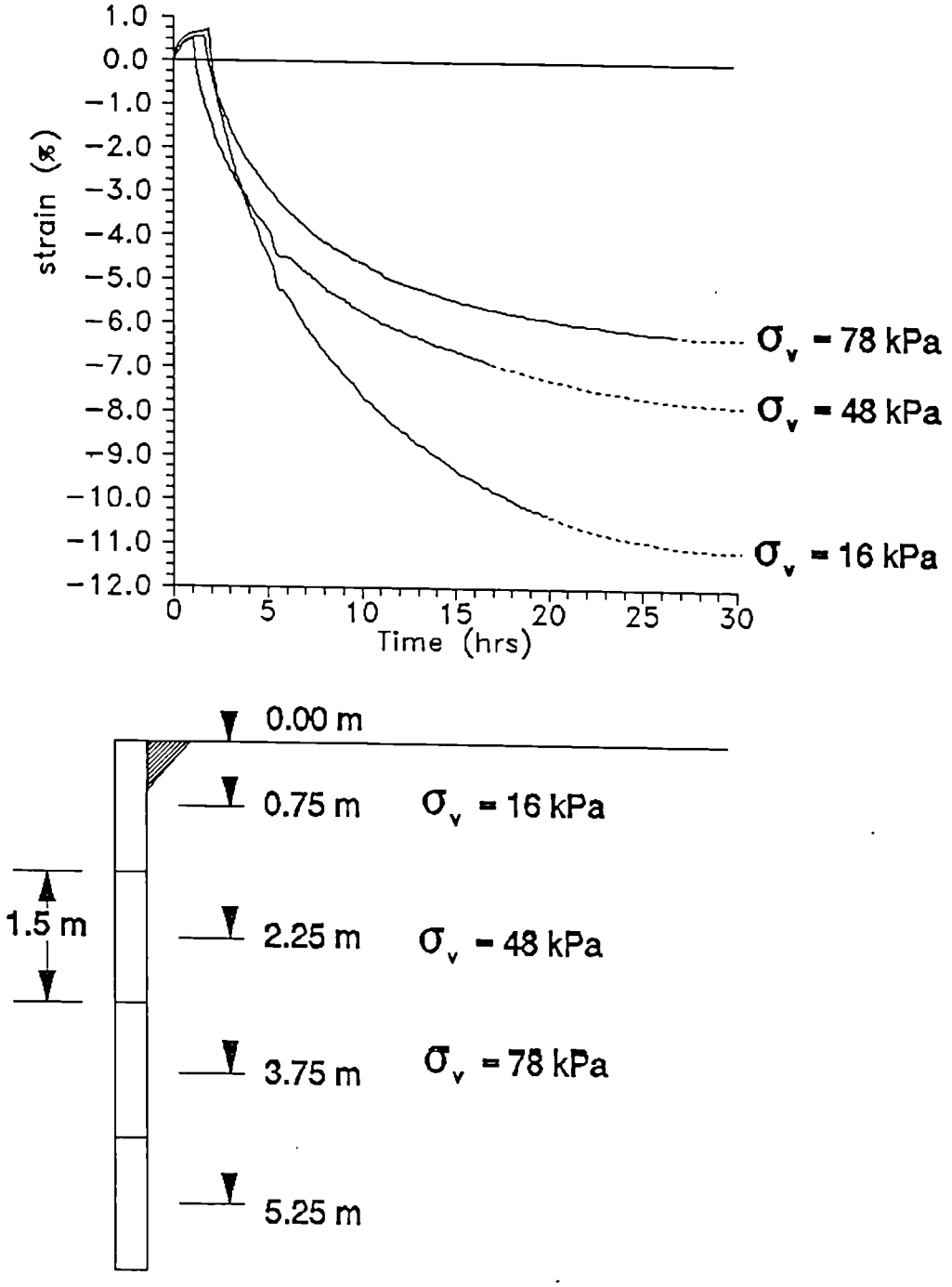

Figure 6.32 Computer controlled oedometer tests with vertical stress comparable to centrifuge model.

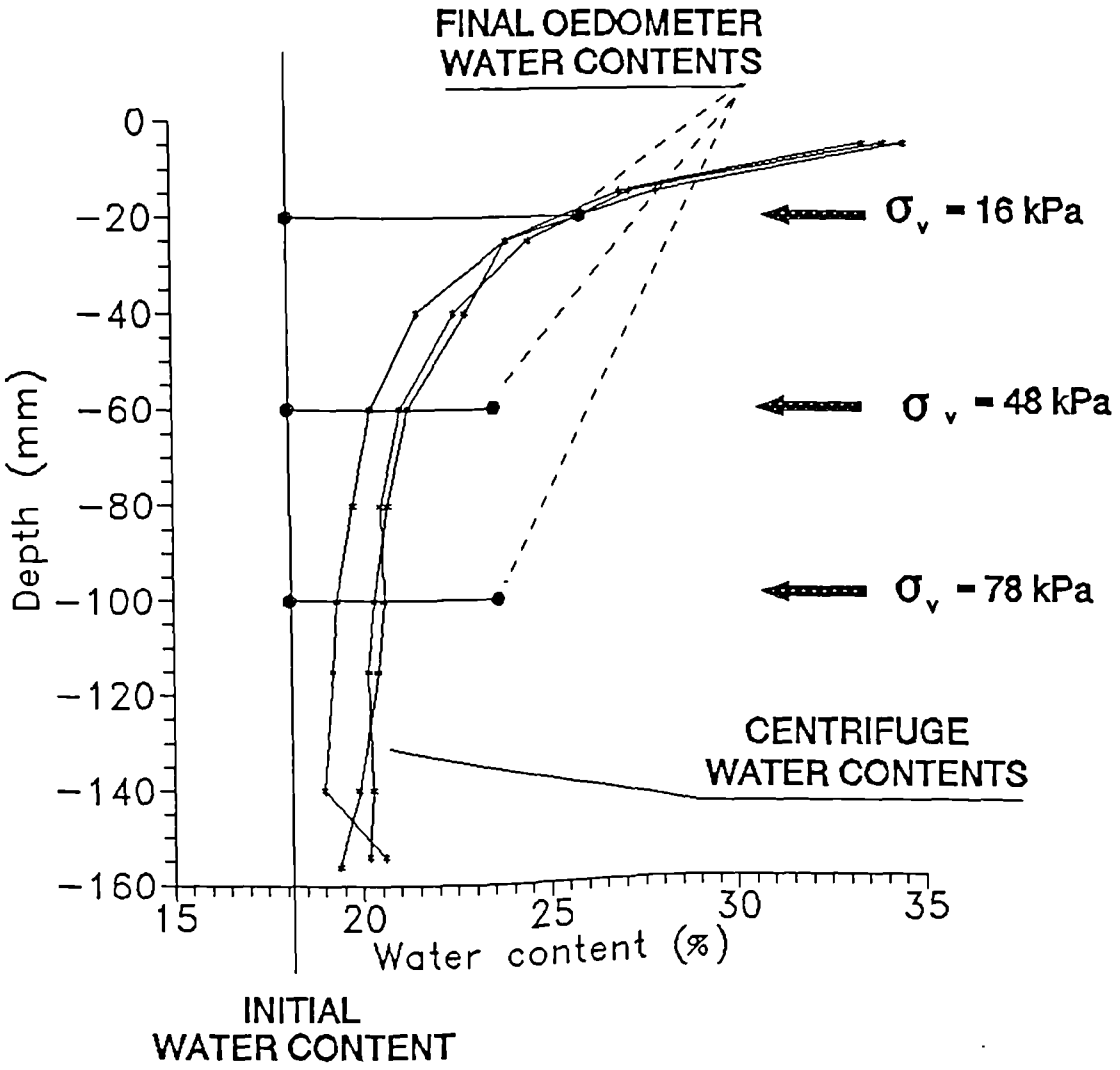

Figure 6.33 Variation in moisture content with depth for samples tested in the computer controlled oedometer and centrifuge model.

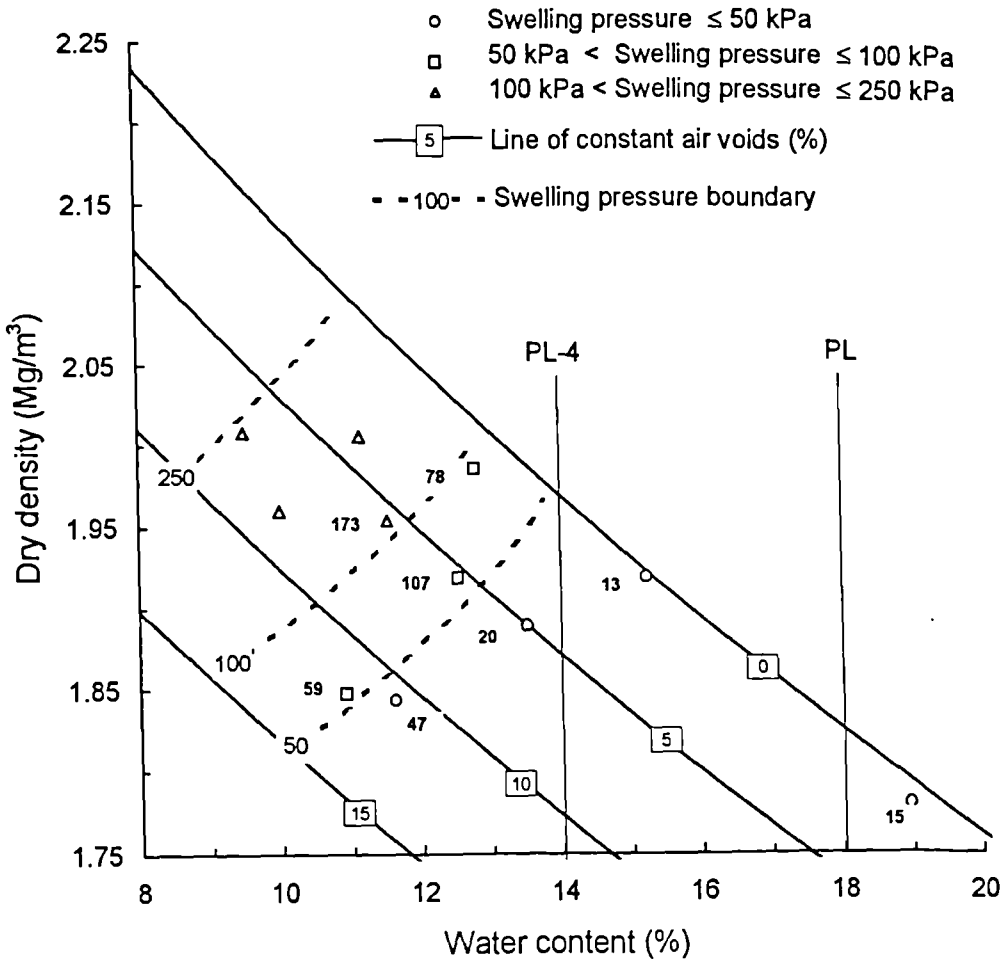

Figure 6.34 Initial conditions of Brickearth samples with associated values of swelling pressure. Also indicated is the lower limit of water content placement (Pl−4).

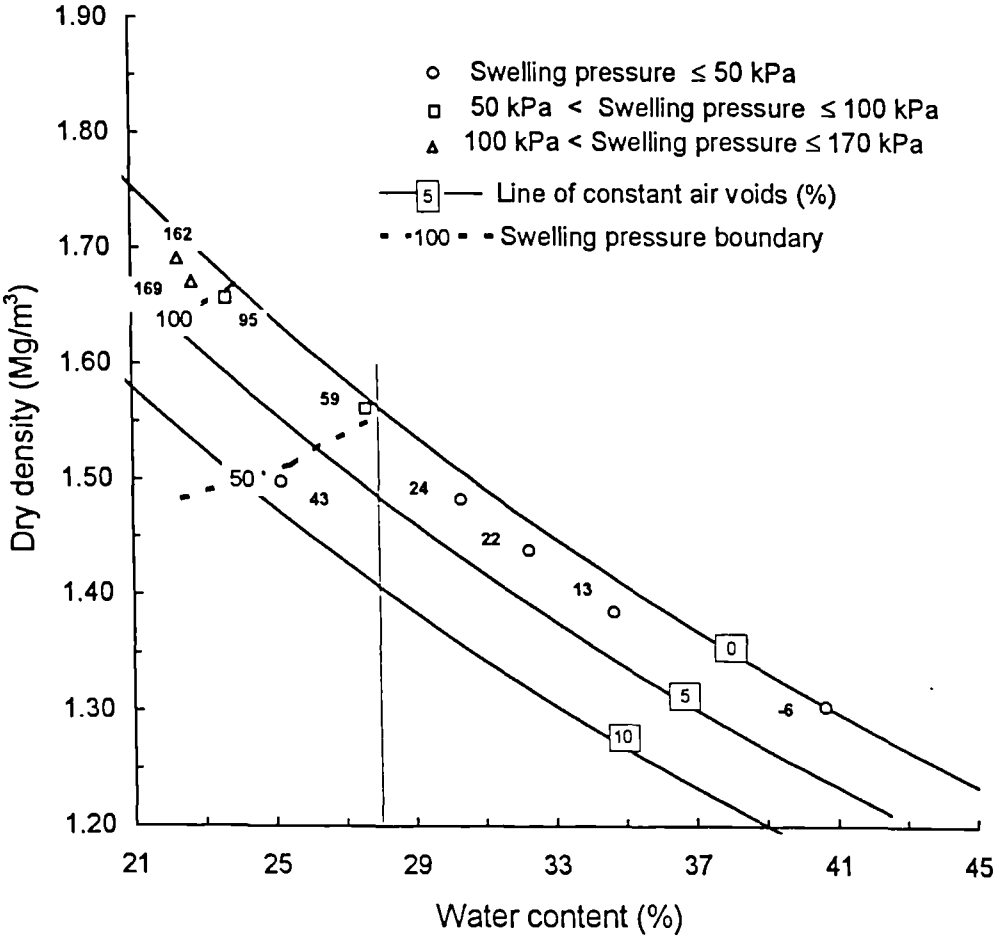

Figure 6.35 Initial conditions of London Clay samples with associated values of swelling pressure.

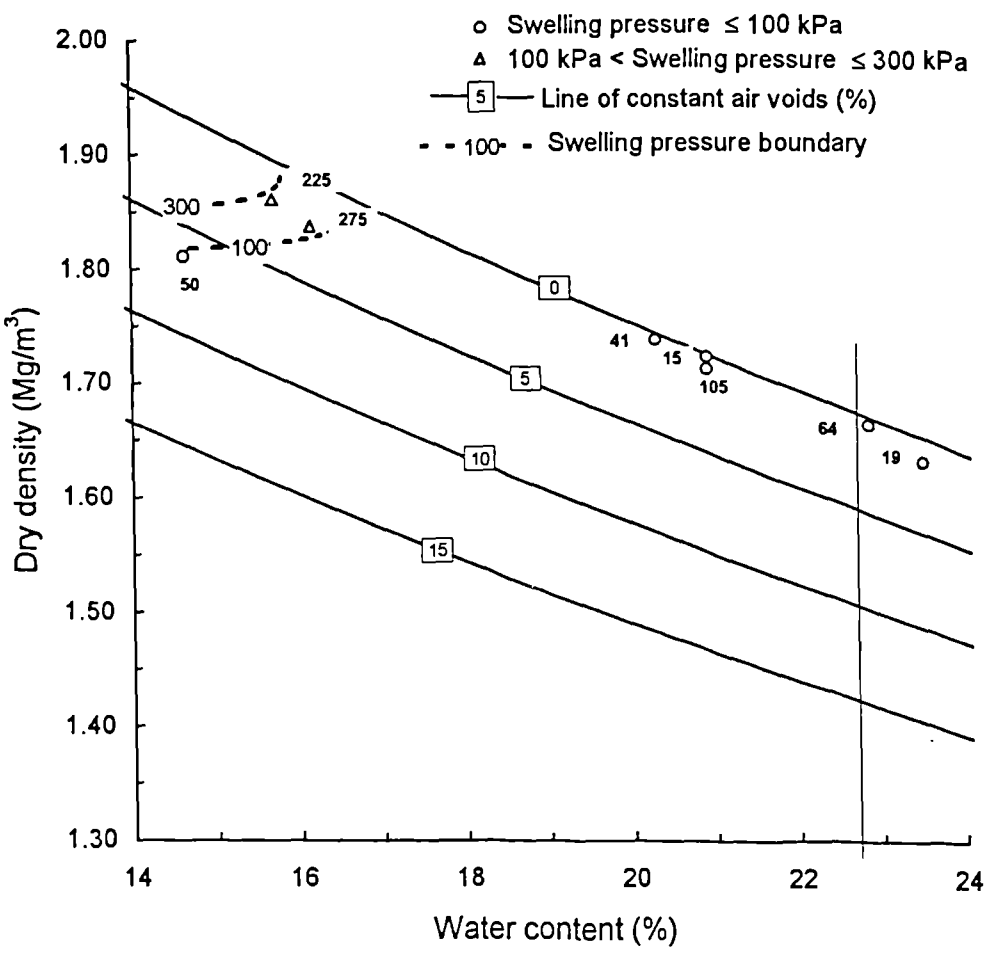

Figure 6.36 Initial conditions of Wadhurst Clay samples with associated values of swelling pressure.

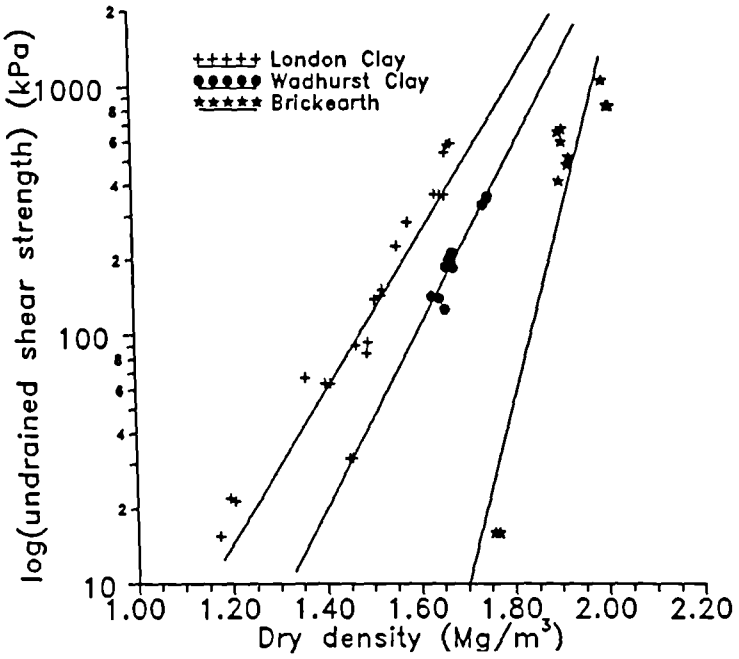

Figure 6.37 Undrained shear strength vs. dry density.

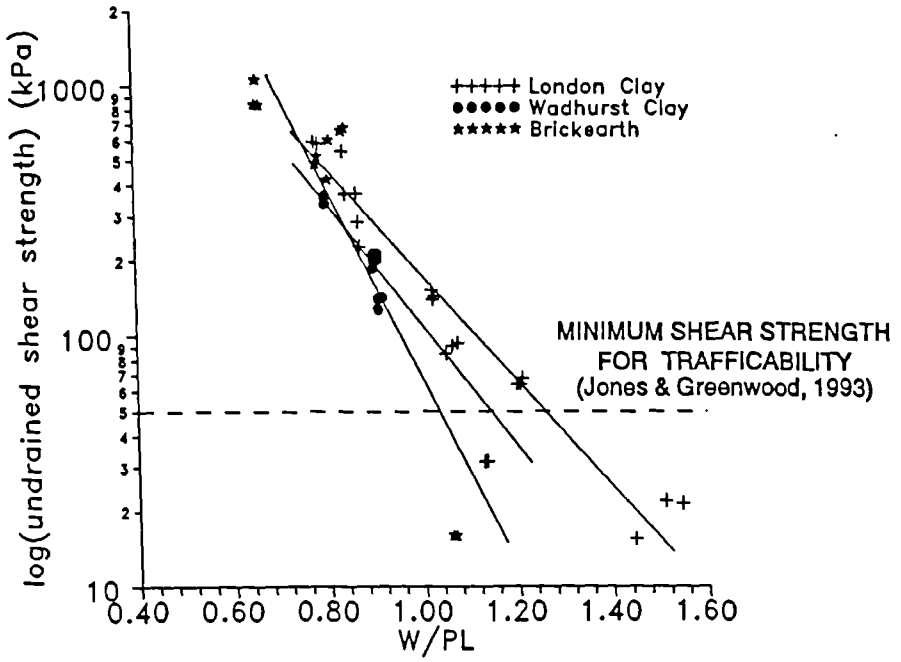

Figure 6.38 Undrained shear strength vs. water content/plastic limit.